



Morrison, Daniel Scott Simpson (2016) *Controlled surface nanotopography and oxygen plasma treatment of PEEK to improve cellular response*. PhD thesis.

<http://theses.gla.ac.uk/7804/>

Copyright and moral rights for this work are retained by the author

A copy can be downloaded for personal non-commercial research or study, without prior permission or charge

This work cannot be reproduced or quoted extensively from without first obtaining permission in writing from the author

The content must not be changed in any way or sold commercially in any format or medium without the formal permission of the author

When referring to this work, full bibliographic details including the author, title, awarding institution and date of the thesis must be given

Glasgow Theses Service
<http://theses.gla.ac.uk/>
theses@gla.ac.uk

Controlled surface nanotopography and oxygen plasma treatment of PEEK to improve cellular response

by

Daniel Scott Simpson Morrison

**Submitted in fulfilment of the requirements
for the Degree of Doctor of Philosophy**

January 2016

Abstract

Poly(aryl-ether-ether-ketone) (PEEK) is a semi crystalline polymer which exhibits properties that make it an attractive choice for use as an implant material. It displays natural radiolucency, and MRI compatibility, as well as good chemical and sterilization resistance, both of which make it of particular interest in orthopaedic implants. However, PEEK has demonstrated poor cellular adhesion both *in vitro* and *in vivo*. This is problematic as implant surfaces that do not develop a layer of adhesive cells are at risk of undergoing fibrous encapsulation, which in turn leads to lack of a strong interface between the implant device and the patient tissue, which can in turn lead to failure of the implant and revision surgery.

As incorporating nanotopography into a polymer surface has been demonstrated to be able to direct the differentiation behaviour of stem cells, a possible solution to PEEKs underlying issues with poor cellular response would be to incorporate specific nanoscale topography into the material surface through injection moulding, and then analysing if this is a viable method for addressing PEEKs issues with cellular response.

In addition to nanoscale topography, the experimental PEEK surfaces were treated with oxygen plasma to address the underlying cytophobicity of the material. As this type of treatment has been documented to be capable of etching the PEEK surface, experiments were carried out to quantify the effect of this treatment, both on the ability of cells to adhere to the PEEK surface, as well as the effect it has upon the nanotopography present at the PEEK surface. The results demonstrated that there were a range of plasma treatments which would significantly improve the ability of cells to adhere to the PEEK surface without causing unacceptable damage to the nanotopography.

Three different types of cells with osteogenic capacity were tested with the PEEK surfaces to gauge the ability of the topography to alter their behaviour: SAOS-2, osteoprogenitors and 271+ MSCs. Due to PEEKs material properties (it is non transparent, exhibits birefringence and is strongly autofluorescent) a number of histological techniques were used to investigate a number of different stages that take place in osteogenesis. The different cell types did

display slightly different responses to the topographies. The SAOS-2 cells cultured on surfaces that had been plasma treated for 2 minutes at 200W had statistically significantly higher levels of von Kossa staining on the NSQ surface compared to the planar surface, and the same experiment employing alizarin red staining, showed a statistically significantly lower level of staining on the SQ surface compared to the planar surface.

Using primary osteoprogenitor cells designed to look into if whether or not the presence of nanotopography effected the osteogenic response of these cells, we saw a lack of statistically significant difference produced by the surfaces investigated. By utilising HRP based immunostaining, we were able to investigate, in a quantitative fashion, the production of the two osteogenic markers osteopontin and osteocalcin by cells. When stained for osteocalcin, the SQ nanotopography had total percentage of the surface with stained material, average area and average perimeter all statistically significantly lower than the planar surface. For the cells that were stained for osteopontin, the SQ nanotopography had a total percentage of the surface with stained material, average area and average perimeter all highly statistically significantly lower than those of the planar surface. Additionally, for this marker the NSQ nanotopography had average areas and average perimeters that were highly significantly higher than those of the planar surface. There were no significant differences for any of the values investigated for the 271⁺ MSC's

When plasma treatment was varied, the SAOS-2 cells demonstrated an overall trend i.e. increasing the energy of plasma treatment in turn leads to an increase in the overall percentage of staining.

A similar experiment employing stem cells isolated from human bone marrow instead of SAOS-2 cells showed that for polycarbonate surfaces, used as a control, mineralization is statistically significantly higher on the NSQ nanopattern compared to the planar surface, whereas on the PEEK surfaces we observe the opposite trend i.e. the NSQ nanotopography having a statistically significantly lower amount of mineralization compared to the planar surface at the 200W 2min and 30W 1min plasma treatments. The standout trend from the PEEK results in this experiment was that the statistically significant differences on the PEEK substrates were clustered around the lower energy plasma

treatments, which could suggest that the plasma treatment disrupted a function of the nanotopography which is why, as the energy increases, there are less statistically significant differences between the NSQ nanotopography and the Planar surface

This thesis documents the response of a number of different types of cells to specific nanoscale topographies incorporated into the PEEK surface which had been treated with oxygen plasma. It outlines the development of a number of histological methods which measure different aspects of osteogenesis, and were selected to both work with PEEK, and produce quantitative results through the use of Cell Profiler. The methods that have been employed in this body of work would be of interest to other researchers working with this material, as well as those working with similarly autofluorescent materials.

1. Table of Contents

1.	Table of Contents	5
2.	List of figures	8
3.	Frequently used Abreviations	16
4.	Introduction	19
4.1.	Biomaterials as a field	19
4.1.1.	Biomaterials development, and what is required of a modern biomaterial	19
4.1.2.	Different properties of a biomaterial which can influence cell response ..	21
4.1.3.	Use of Nanotopography to control stem cell phenotype	23
4.2.	Fabrication of nanotopographies through injection moulding	29
4.3.	PEEK as a biomaterial	31
4.3.1.	Improvements that can be made to PEEK for use in biomaterials applications	33
4.3.2.	The current state of PEEK biomaterials research.	33
4.4.	Reasons for PEEKs use in this thesis	51
4.5.	Initial goals of the PhD project	51
4.5.1.	Key objectives.....	52
5.	Materials and methods	54
5.1.	Substrate fabrication	54
5.2.	Cell culture	55
5.3.	Histological staining.....	58
5.3.1.	Coomassie staining.....	58
5.3.2.	Alizarin staining	58
5.3.3.	Alizarin quantification	58
5.3.4.	Von Kossa staining.....	59
5.3.5.	Alkaline Phosphatase staining	60
5.3.6.	HRP based immunostaining.....	60
5.3.7.	Fluorescence based immunostaining.....	60
5.4.	Microscopy	62
5.4.1.	Whole substrate scans	62
5.4.2.	Polarised light microscopy.....	62
5.4.3.	Scanning Electron Microcopy (S.E.M).....	65
5.5.	Image analysis/quantification	66
5.6.	Plasma treatment	72
5.7.	AFM	72
5.8.	Sessile drop water contact angle measurement	73
5.9.	X-ray photoelectron spectroscopy	73
5.10.	Statistical analysis.....	74
6.	Use of plasma treatment to address poor cell response to PEEK	75
6.1.	Introduction.....	75
6.1.1.	Requirements for PEEK surface modification for use in biomaterials applications	75
6.1.2.	Oxygen plasma treatment for improved biomaterials	75
6.1.3.	Alternative approaches to modifying the PEEK surface	76
6.1.4.	Aims of the chapter	77
6.1.5.	Experimental outline	77
6.2.	Results	78

6.2.1.	Oxygen plasma treatment of PEEK	78
6.2.2.	Wettability	85
6.2.3.	Surface chemistry	87
6.2.4.	Impact of the plasma treatment on osteoprogenitor cells	89
6.3.	Discussion	92
6.4.	Conclusions	94
7.	Interaction between SAOS-2 osteoblast like cells and oxygen plasma treated PEEK nanotopographies	95
7.1.	Introduction	95
7.1.1.	The role of SAOS-2 cells in <i>in vitro</i> PEEK tissue engineering research	95
7.1.2.	SAOS-2 cell line	95
7.1.3.	Our objectives in working with SAOS-2 cells	96
7.1.4.	Experimental outline	97
7.2.	Results	97
7.2.1.	SAOS-2 culture duration experiments	97
7.2.2.	SAOS-2 plasma duration screen	110
7.3.	Discussion	119
7.3.1.	Behaviour of SAOS-2 cells on PEEK nanotopographies	119
7.3.2.	Influence of the energy of plasma treatment on the SAOS-2 cells	120
7.4.	Conclusions	121
8.	Impact of defined nanotopography and controlled surface chemistry in PEEK on the osteogenic behaviour of primary human stem cells	123
8.1.	Introduction	123
8.1.1.	Ability of nanotopography to effect cell activity.	123
8.1.2.	Aims of working with nanotopography	123
8.1.3.	Structure of the experiments	124
8.1.4.	Potential impact of plasma treatment on the activity of the nanotopography	124
8.2.	Results	124
8.2.1.	Plasma treatment screen	133
8.3.	Discussion	140
8.3.1.	Effect of the presence of defined nanoscale topography on stem cell behaviour	140
8.3.2.	The relationship between oxygen plasma treatment and stem cell response	141
8.3.3.	Potential reasons for diversity in the response of stem cells to the same nanotopography in different polymers	142
8.4.	Conclusions	143
9.	The adaptation of chromatic based Immunohistochemistry for use in stem cell research with PEEK	145
9.1.	Introduction	145
9.1.1.	The role of existing fluorescence based immunohistochemistry in biomaterials research	145
9.1.2.	Alternate approaches for immunohistochemistry on PEEK surfaces	149
9.1.3.	Horse radish peroxidase based immunohistochemistry	152
9.2.	Results	154
9.2.1.	Initial testing of the technique	154
9.2.2.	Switch to use of Dako EnVision staining procedure	157
9.3.	Discussion	168

9.3.1.	Effectiveness of horse radish peroxidase based immunostaining as a technique for investigating cell behaviour on PEEK.	168
9.3.2.	Ability of nanotopography at the PEEK surface to influence the osteogenic activity of stem cells.....	169
9.4.	Conclusions.....	170
10.	Discussion.....	172
10.1.	How did our experimental data address the key aims of the project	172
10.1.1.	Alteration of the PEEK surface both in terms of the topography and chemistry to improve the osteogenic response of cells that come into contact with it.	172
10.1.2.	Extent of fidelity of nanopattern effect in different polymers.....	179
10.1.3.	Development of an approach that enables high quality analysis of cell response on PEEK that works around the materials specific difficulties	182
10.2.	Future research avenues with PEEK	183
10.2.1.	Comparison between this work and other approaches to modifying the PEEK surface for use as a biomaterial	183
10.2.2.	Suggested next steps in PEEK research	183
10.2.3.	Continuing relevance of Nanotopography a viable technology for further study with PEEK in the context of the results generated by plasma treatment.....	187
10.3.	Contribution of this thesis to the wider scientific community.	188
10.3.1.	Histological/chromatic methods for investigating osteogenic response on PEEK.....	188
10.4.	Main findings contained within this Thesis	190
10.4.1.	Interaction between PEEK and nanotopography	190
10.4.2.	Development of new approaches for investigating cell behaviour on PEEK.....	190
10.4.3.	Nanotopography may still be a viable approach for modulating cell response to PEEK surfaces	191
10.4.4.	Effects of plasma treatment on PEEK	191
11.	References.....	193

2. List of figures

Figure 1 Results from Yim et al ²⁸ culture of MSCs on their nanopatterned PDMS. Consistently we can see higher expression of the different markers on the nanopatterned surface. In addition, in the presence of a differentiation cue (retinoic acid) the presence of the nanotopography still produces a greater level of staining compared to the unpatterned surface.	26
Figure 2 Results from Dalby et al ³⁵ culture of osteoprogenitor cells on PDMS surfaces with nanopits which have differing spacing between the individual features. We can see that there is an optimum amount of disorder in the spacing of nanofeatures in terms of inducing osteogenic behaviour, where both higher and lower degrees of disorder lead to a reduced level of expression of the two osteogenic markers.	27
Figure 3 Illustration of the significant part of the moulding area of the injection moulding machine used to produce the nanotopographies used in this thesis. Reproduced from Stormonth-Darling ⁶³	30
Figure 4 Visual representation of the different stages involved in injection moulding. Reproduced from Stormonth-Darling ⁶³	30
Figure 5 Demonstration of the radiolucency of PEEK and how it compares to competing metallic implant materials in both X-rays and MRI images. Reproduced from Green et al ⁶⁷	31
Figure 6 Comparison of the elastic modulus between PEEK and other competing biomaterials to that of cortical bone. We can clearly see how much closer PEEK-optima and in particular a CF PEEK-optima compound is to cortical bone compared to other biomaterials. Reproduced from Green et al ⁶⁷	32
Figure 7 In vivo examples of non-surface modified PEEK's poor osseointegration.. In both images it can be observed that there is significant fibrous tissue present between the PEEK implant and the host. In addition, direct comparison with titanium (part A) illustrates PEEKs poor direct bone contact relative to a competing biomaterial. Reproduced from Poulsson ⁸⁵	33
Figure 8 In vivo results from Abu Bakar ⁸⁶ at 6 (labelled A) and 16 weeks (labelled B). At 16 weeks bone has been formed in the pore regions of the composite.	35
Figure 9 Alizarin red staining of MG63 cell on cultured on PEEK, a HA/PEEK composite and a strontium reinforced HA/PEEK composite. Both composites produced significantly greater levels of staining compared to PEEK, with the strontium HA also significantly higher than that of the HA/PEEK composite. Reproduced from Wong ⁸⁷	36
Figure 10 RT-PCR results from human MSCs cultured on bare and HA coated PEEK. The presence of the coating led to a clear enhancement of transcription of the osteogenic markers Runx2 and BSP. Reproduced from Jae Hyup Lee ⁸⁸ ...	37

Figure 11 Quantification of Alizarin staining of human osteoblasts on oxygen plasma treated PEEK. The results demonstrate that 1800s of plasma treatment leads to the greatest mineralisation response from the cells. From Poulsson ⁸⁵	40
Figure 12 Proliferation of foetal osteoblast cells on titanium, untreated PEEK and PEEK treated with an argon beam. The results show that the argon treatment greatly improves the proliferation of cells compared to untreated PEEK, and by day 10 the number of cells present is comparable to that of titanium. Reproduced from Khoudry et al ⁹⁰	42
Figure 13 Adhesion of human osteoblasts to PEEK, PTFE and UHMWPE coated with both gold and titanium. The presence of either metal was shown to significantly increase the degree of osteoblast adhesion compared to the uncoated polymers. From Yao et al ⁹¹	43
Figure 14 Electron micrographs of the different nanotopographies produced via injection moulding used in this thesis. (a) hexagonal nanopattern (HEX). (b) square nanopattern (SQ) (c) disordered square nanopattern (NSQ). Provided by the University of Glasgow bioelectronics research group (BiG)	54
Figure 15 Example of von Kossa staining of osteoprogenitor cells on PEEK viewed via reflected light microscopy without the use of polarized light.	63
Figure 16 Comparison of the same cell prolifer pipeline processing the same area of the surface of a von Kossa stained sample without, and then with polarised light filters. Scale bar = 100um.	64
Figure 17 Comparison of the same cell prolifer pipeline processing the same area of the surface of a von Kossa stained sample without and then with polarised light filters. As we can clearly see the use of polarised light filter allows the accurate identification of only stained mineral (black objects) and not background material or stained cell bodies (pink objects). Scale bar = 100um.	65
Figure 18 Schematic diagram of the stages involved in a Cell Profiler pipeline. Each different stage has differing numbers of operations involved with them. For example “Invert black and white” only has one operation, while “Identify primary objects” has a large number of different parameters to be adjusted in order to correctly identify stained material.	67
Figure 19 Demonstration of the channel splitting stage in a Cell Profiler pipeline. As Cell Profiler cannot process colour images the original image, in this case an example of von Kossa staining, is split into it’s constituent colour channels. As each colour channel has a differing degree of contrast, the operator must decide which image is clearest in order to generate the most accurate results further down the pipeline.	68
Figure 20 Example of the effect that alterations to identification and analysis parameters have on the identification of stained material. Image A has had no modification of the identification parameters in it pipeline outside of what it required to move the image through the pipeline, whereas image B has had extensive modification in order to accurately identify only stained material in the image.	69
Figure 21 Example of different features present on a microscope image analysed by Cell Profiler. The pipeline should be designed to count objects that have been stained black (yellow box) indicating the presence of material containing phosphate. It should not count cell nuclei stained pink/red (green box). This is complicated by the presence of denser areas of nuclear fast red staining which can look black (black box).	70

Figure 22 Comparison of how different analysis algorithms in the “identify primary objects” module of a pipeline can affect how much material on an image is counted as being stained. In each example all of the variables in the pipeline are identical, apart from the method used for thresholding. Global Otsu was the method that we felt gave the best representation of the stained material present in the original image.	71
Figure 23 The impact of different methods for correcting illumination in an image, on the pipelines ability to identify stained material.....	72
Figure 24 SEM images of h-TERT cells cultured on different durations of oxygen plasma treatment between 0 and 10 minutes and cultured for 3 days. The images show that with increaseing energy of plasma treatment we observe an increase in cell spreading and in cell number.	79
Figure 25 SEM images of h-TERT cells culture on machined PEEK surfaces that had benn plasma treated at 200W for 10 minutes after three different time points day 1, day 3 and day 10. These images demonstate that the plasma treatment is suficient to produce an almost complete layer of cells on the PEEK surface by 10 days on culture.	80
Figure 26 SEM images of PEEK nanotopographies that have been treated with plasma treatment for 7 minutes at 200W. The damage to the nanotopogrpahy can be clearly seen.	82
Figure 27 AFM readings of PEEK NSQ nanotopographies that have been treated with 200W of plasma for a range of durations (0, 1, 2, 5, 7, and 10 minutes). These results illustrate that with increasing time of plasma treatmen,t we see an increase in nanopit diameter and a decrease in nanopit depth.....	83
Figure 28 AFM measurements of area between nanopits, nanopit depth and diameter at increasing durations of 200W plasma treatments. The resuts show that as duration of plasma treatment increases, pit diameter and the average roughness of the interpit areas increases and pit depth decreases.	84
Figure 29 Sesile drop water contact angle measurements of PEEK surfaces that have been been exposed to a range of different plasma treatments.....	86
Figure 30 Water contact angle plotted against the energy of the different plasma treatments used.	86
Figure 31 XPS spectra results from PEEK surfaces that had been oxygen plasma treated at 200W between 0 and 600 seconds.	87
Figure 32 Table sumarising the changes in surface chemistry in terms of oxygen and carbon content at the surface after different durations of oxygen plasma treatment . As plasma treatment time increases the percentage carbon falls while the percentage oxygen increases.	88
Figure 33 XPS reuslts for carbon and oxygen at the surface plotted against duration of plasma treatment in seconds.	88
Figure 34 Coomassie blue staining of primary human osteoprigenitor cells cultured for 11 days on PEEK NSQ nanotopographies that have been plasma treated at 200W over a range of different times (0, 2, 5 and 10 minutes). The pattern of staining indicates a definatate increase in cells present at 2 and 5 minutes compared to 0 minutes and a possible decrease at 10 minutes comapred to 5. Scale bar = 100µm.	90
Figure 35 Cell proflier results for the percentage of the surface with stained material . All three durations of plasma treatment result in a statistically significant increase in staining. However 10 minutes is lower than 5 minutes to a highly statistically significant degree.....	91

Figure 36 Representative full substrate high resolution scans of Von Kossa staining of SAOS-2 cells cultured for 28 days on PEEK nanotopographies that had been oxygen plasma treated for 2 minutes at 200W and those which had not receive any treatment. Red staining indicates the presence of cells and.....	98
Figure 37 Polarised light microscope images of Von Kossa staining of SAOS-2 cells cultured for 28 days on PEEK nanotopographies which were treated with oxygen plasma for 2 minutes at 200W. Total number of replicates N=18: 6 Planar, 6 NSQ, 6 SQ. Scale bar = 100µm.	99
Figure 38 Cell Profiler analysis of polarised light microscope images of von Kossa staining of SAOS-2 cells cultured on PEEK substrates that had been oxygen plasma treated for 2 minutes at 200W. The presence of oxygen plasma has produced a strong increase in the level of phosphate produced on the surfaces. Additionally the percentage of the surface with stained material is significantly higher on the NSQ nanotopography compared to the planar surface. Total number of replicates =18: 6 Planar, 6 NSQ, 6 SQ.....	100
Figure 39 Table summarizing both the times increase and fold increase of the percentage of the surface stained via von Kossa, between untreated and plasma treated PEEK nanotopographies.	100
Figure 40 Average area of identified areas of staining calculated by Cell Profiler analysis of von Kossa staining of SAOS-2 cells cultured on PEEK substrates that had been oxygen plasma treated for 2 minutes at 200W. Total number of replicates N=18: 6 Planar, 6 NSQ, 6 SQ.	101
Figure 41 Mean radius of identified areas of staining calculated by Cell Profiler analysis of von Kossa staining of SAOS-2 cells cultured on PEEK substrates that had been oxygen plasma treated for 2 minutes at 200W. Total number of replicates N=18: 6 Planar, 6 NSQ, 6 SQ.	101
Figure 42 Median radius of identified areas of staining calculated by Cell Profiler analysis of von Kossa staining of SAOS-2 cells cultured on PEEK substrates that had been oxygen plasma treated for 2 minutes at 200W. Total number of replicates N=18: 6 Planar, 6 NSQ, 6 SQ.	102
Figure 43 Average perimeter of identified areas of staining calculated by Cell Profiler analysis of von Kossa staining of SAOS-2 cells cultured on PEEK substrates that had been oxygen plasma treated for 2 minutes at 200W. Cells on the NSQ nanotopography displayed a statistically significant higher average perimeter compared to the planar surface Total number of replicates N =18: 6 Planar, 6 NSQ, 6 SQ.	102
Figure 44 A size distribution analysis of the areas of the discrete objects identified by Cell Profiler analysis of SAOS-2 cells cultured for four weeks on PEEK nanotopographies and stained with von Kossa. Total number of replicates N=18: 6 Planar, 6 NSQ, 6 SQ.	103
Figure 45 Polarised light microscope images of Alizarin red staining of SAOS-2 cells cultured for 28 days on PEEK nanotopographies which were treated with oxygen plasma for 2 minutes at 200W. Total number of replicates N=18: 6 Planar, 6 NSQ, 6 SQ. Scale bar = 100µm.....	105
Figure 46 Cell Profiler analysis of polarised light microscope images of alizarin red staining of SAOS-2 cells cultured on PEEK substrates that had been oxygen plasma treated for 2 minutes at 200W. The presence of oxygen plasma has produced a strong increase in the level of phosphate produced on the surfaces. Additionally the percentage of the surface is significantly lower on the SQ nanotopography compared to the planar surface. Total number of replicates N=18: 6 Planar, 6 NSQ, 6 SQ.	106

Figure 47 Table summarizing both the times increase and fold increase of the percentage of the surface stained via Alizarin between untreated and plasma treated PEEK nanotopographies.	106
Figure 48 Average area of identified areas of staining calculated by Cell Profiler analysis of Alizarin red staining of SAOS-2 cells cultured on PEEK substrates that had been oxygen plasma treated for 2 minutes at 200W. Total number of replicates N=18: 6 Planar, 6 NSQ, 6 SQ.	107
Figure 49 Mean radius of identified areas of staining calculated by Cell Profiler analysis of Alizarin red staining of SAOS-2 cells cultured on PEEK substrates that had been oxygen plasma treated for 2 minutes at 200W. Total number of replicates N=18: 6 Planar, 6 NSQ, 6 SQ.	107
Figure 50 Median radius of identified areas of staining calculated by Cell Profiler analysis of Alizarin red staining of SAOS-2 cells cultured on PEEK substrates that had been oxygen plasma treated for 2 minutes at 200W. Total number of replicates N=18: 6 Planar, 6 NSQ, 6 SQ.	108
Figure 51 Average perimeter of identified areas of staining calculated by Cell Profiler analysis of Alizarin red staining of SAOS-2 cells cultured on PEEK substrates that had been oxygen plasma treated for 2 minutes at 200W. Total number of replicates N=18: 6 Planar, 6 NSQ, 6 SQ.	108
Figure 52 Cell Profiler analysis of polarised light microscope images of von Kossa and alizarin red staining of SAOS-2 cells cultured on PEEK substrates that had been oxygen plasma treated for 2 minutes at 200W and cultured for 3 weeks. Total number of replicates N=18: 6 Planar, 6 NSQ, 6 SQ.	110
Figure 53 Polarised light microscope images of Von Kossa staining of SAOS-2 cells cultured for 21 days on PEEK nanoscale topographies that had received varying degrees of plasma treatment. Total number of replicates N=54: 18 Planar, 18 NSQ, 18 SQ. Scale bar =100 μ m.	112
Figure 54 Collected cell percentage of the surface stained results from each of the Oxygen plasma treatments used. The Cell Profiler results were generated from polarised light microscope image of Von Kossa stained SAOS-2 cells. While there is little difference between individual nanotopographies at any of the different plasma treatments, there is however a strong difference in the level of mineralisation between the untreated surfaces and any of the plasma treatments. Total number of replicates N=54: 18 Planar, 18 NSQ, 18 SQ.	113
Figure 55 Percentage of the surface stained results plotted against the power in Watts of the plasma treatment used. Total number of replicates N=54: 18 Planar, 18 NSQ, 18 SQ.	114
Figure 56 Collected average area of identified stained material from each of the Oxygen plasma treatments used The Cell Profiler results were generated from polarised light microscope image of Von Kossa stained SAOS-2 cells. The average area of the SQ nanotopography is statistically significantly lower than the planar surface at both 100W 1min and 200W 6s. Total number of replicates N=54: 18 Planar, 18 NSQ, 18 SQ.	115
Figure 57 Collected mean radius of identified stained material from each of the Oxygen plasma treatments used. The Cell Profiler results were generated from polarised light microscope images of Von Kossa stained SAOS-2 cells. The mean radius of the SQ nanotopography was statistically significantly lower than that of planar surface at 200W 6s and the mean radius of the NSQ nanotopography was also statistically significantly lower than that of the planar surface at 200W 2min. Total number of replicates N=54: 18 Planar, 18 NSQ, 18 SQ.	116

Figure 58 Collected median radius of identified stained material from each of the Oxygen plasma treatments used The Cell Profiler results were generated from polarised light microscope images of Von Kossa stained SAOS-2 cells. The median radius of the SQ nanotopography was statistically significantly lower than that of the planar surface at both 100W 1min and 200W 6s. Additionally the median radius of the NSQ nanotopography was statistically significantly lower than that of the planar surface at 200W 2min. Total number of replicates N=54: 18 Planar, 18 NSQ, 18 SQ.	117
Figure 59 Collected average perimeter of identified stained material from each of the Oxygen plasma treatments used The Cell Profiler results were generated from polarised light microscope image of Von Kossa stained SAOS-2 cells. The average perimeter the SQ nanotopography was statistically significantly lower than that of the planar surface at both 100W 1min and 200W 6s. Total number of replicates N=54: 18 Planar, 18 NSQ, 18 SQ.	118
Figure 60 qPCR experiments measuring the expression of the osteogenesis related genes BMPR2 and RUNX2 by osteoprogenitor cells on PEEK and poly carbonate nanotopogarithies after 11 days of culture. Expression of both genes was naormalised to the expression of GAPDH. For each gene N=81 Planar 27, NSQ 27, SQ 27.	125
Figure 61 Alamar blue measurement of cell density on oxygen plasma treated PEEK nanotopographies with thermanox used as a positive control. We can see the cells rate of proliferation is at its highest between 1 and 7 days and to a lesser extent between 7 and 14 days as there is no statistically significant difference between any of the surfaces.	127
Figure 62 Representative whole substrate scans that have been histologically stained for alkaline phosphatase at 1, 14 and 21 days. In each instance ALP level increases at day 14 compared to day 1 and then declines by day 21 compared to day 14. Total number of replicates N=9 3 Planar, 3 NSQ, 3 SQ.	129
Figure 63 Representative polarised light microscope images of histological staining for alkaline phosphatase at 7, 14 and 21 days. In each instance ALP level increases at day 14 compared to day 7 and then declines by day 21 compared to day 14. Total number of replicates N=9 3 Planar, 3 NSQ, 3 SQ. Scale bar = 100µm	130
Figure 64 Cell Profiler analysis of the percenatge of the surface with ALP staining at 7, 14 and 21 days. The results show that in line with the microscope images, ALP leveld rise at 14 days and decrease again at 21 days. There was no statisticaly signifcant differnces in ALP activity between the surfaces at any of the time points. Total number of replicates N=9 3 Planar, 3 NSQ, 3 SQ.	131
Figure 65 von Kossa staining and Cell Profiler analysis of the percentage of the surface with stained material of primary osteoprogenitor cells cultured for 21 days. Total number of replicates N =9, 3 Planar, 3 NSQ, 3 SQ. Scale bar = 100µm.	132
Figure 66 Total percentage of the microscope image, with stained material analysis of the Cell Profiler results for the experiment. We can see that at 30W 1min and 200W 2min NSQ is statistically significantly lower than the planar control.	134
Figure 67 Average area of identified objects analys, of the Cell Profiler results for the experiment. At 30W 1 min and 30W 15s NSQ is statistically significantly higher than the planar control while at 30W 30s and 50W 15s NSQ is statistically significantly lower than the planar control.	135

Figure 68 Mean diameter of identified objects analysis of the Cell Profiler results for the experiment. 30W 1 min and 30W 15s NSQ was statistically significantly higher than the planar control while 30W 30s and 50W 15s NSQ was lower than the planar control.	136
Figure 69 Median diameter of identified objects analysis of the Cell Profiler results for the experiment. 30W 15s NSQ was statistically significantly higher than the planar control while 30W 30s and 50W 15s NSQ was statistically significantly lower than the planar control.	137
Figure 70 Mean perimeter of identified objects analysis of the Cell Profiler results for the experiment. 30W 1min and 30W 15s NSQ was statistically significantly higher than the planar control while 30W 30s NSQ was statistically significantly lower than the planar control.	138
Figure 71 Microscope images taken with polarised light microscopy of h-tert cells stained with either HRP based immunostaining against β tubulin using Santa Cruz biotech secondary antibodies and haematoxylin or only haematoxylin. In both cases cells were cultured on machined PEEK discs for 3 days. Note the absence of significant additional staining in the presence of the HRP conjugated secondary antibodies compared to the haematoxylin only samples. Scale bar =100 μ m	155
Figure 72 Polarised light microscope images of h-tert cells cultured on machined PEEK surfaces for 14 days and then stained for β tubulin via HRP immunostaining. While it is readily apparent that there is	158
Figure 73 Polarised light microscope images at x20 magnification of h-tert cells cultured on machined PEEK surfaces for 14 days and then stained for β tubulin via HRP immunostaining. Objects enclosed in black rectangles are consistent objects that we believed demonstrated specific staining of β tubulin. Scale bar =100 μ m.	158
Figure 74 A closer look at staining of β tubulin by HRP based immunostaining. A = microscope image of HRP based immunostaining of h-tert cells on PEEK with what we believed to be an example of stained β tubulin enclosed in a yellow rectangle. B = enlarged view of the object. C = example of β tubulin staining using fluorescence based immunostaining. When comparing B and C note the similar shape of the stained area and the round non-stained area in the middle of both (the nucleus).....	159
Figure 75 Examples of fluorescent and HRP based immunostaining of osteopontin in SAOS-2 cells cultured on polycarbonate substrates for 21 days. While the staining is not identical between different types of immunostaining we can see similarities in the overall pattern of staining. Comparison of the immunostaining results generated by two different types of secondary antibody staining for Osteopontin in SAOS-2 cells cultured for 21 days on poly carbonate substrates. In each instance there is a representative example of the type of microscopy used (fluorescence and light respectively) and then a graph generated from the Cell Profiler results based on measuring the percentage of the microscope image containing stained material fluorescence based immunostaining HRP based immunostaining. Cell Profiler analysis of the fluorescent staining indicates that the results for the NSQ nanotopography is highly statistically significant compared to the planar surface.	162

Figure 76 Representative images generated by polarised light microscopy of HRP based immunostaining of stem cells (osteoprogenitors (OPG) and 271+ MSC (271+)) stained for either Osteocalcin or Osteopontin markers cultured on various PEEK nanotopographies for 28 days. In each instance the scale bar is equal to Total number of replicates N=9 Planar=3, NSQ=3, SQ=3. Scale bar =250 μ m.	164
Figure 77 Total percentage of the microscope image with stained material analysis of the Cell Profiler results for the experiment. The osteoprogenitors on the SQ nanotopography produces statistically significantly lower results compared to the planar surface for OCN and highly statistically significantly lower for OPN Total number of replicates N=9 Planar=3, NSQ=3, SQ=3.	165
Figure 78 Average area of identified objects present on the microscope images as generated by Cell Profiler analysis. The osteoprogenitors on the SQ nanotopography produces statistically significantly lower results compared to the planar surface for OCN and highly statistically significantly lower for OPN. These same cells produce statistically significantly higher results for OPN on NSQ. Total number of replicates N=9 Planar=3, NSQ=3, SQ=3.....	165
Figure 79 Average perimeter of identified objects present on the microscope images as generated by Cell Profiler analysis. The osteoprogenitors on the SQ nanotopography produced statistically significantly lower results compared to the planar surface for OCN and highly statistically significantly lower for OPN. These same cells produce statistically significantly higher results for OPN on NSQ. Total number of replicates N=9 Planar=3, NSQ=3, SQ=3.....	166

3. Frequently used Abbreviations

NSQ: The near square or disordered square nanopattern

SQ: The ordered square nanotopography

SEM: scanning electron microscopy

AFM: Atomic force microscopy

OPG: Osteoprogenitors the adherent elements of the mononuclear fraction obtained from human bone marrow

SAOS-2: Human osteosarcoma cell line

h-TERT: immortalised human fibroblast cell line

HRP: Horse radish peroxidase usually used in the context of immunostaining where the chemical reaction replaces the excitation of an attached fluorophore as the mechanism for marking where the antibody complex is bound

PEEK: poly ether ether ketone

MRI: Magnetic resonance imaging

PC: Poly carbonate

271⁺ MSCs: Mesenchymal Stem Cells that have been selected from the osteoprogenitor pool of cells by the presence of the CD271 marker through magnetic sorting

OPN: Osteopontin

OCN: Osteocalcin

QPCR: Quantitative Polymerase Chain Reaction

Acknowledgements

To have got as far as writing this thesis I have a number of people I need to thank.

Firstly my supervisors Nikolaj Gadegaard, Matt Dalby and Alexandra Poulsson for initially offering me a doctoral position, and for all of their help and guidance during my time working on this project.

I would also like to thank all of my colleagues at the University of Glasgow in the Bioelectronics Research Group, the Center for Cell Engineering and the James Watt Nanofabrication Center. In particular, I would like to thank Rasmus Petersen, Johnny Stormonth-Darling, Paul Reynolds, Andrew Greer, Iskander Vasiev, Affar Karimullah, Carol-Anne Smith, Peter Young, Andrew Wilkinson, Dominic Meek, Laura McNamara, Louisa Lee, Ali Khokar, Monica Tsimbouri and William Monaghan.

I would also like to thank the A.O. both for their funding of my project as well as facilitating my work at their institute in Davos. Thanks also go to the colleagues I worked with there, in particular David Eglin, Sandra Thoeny, Nora Goudsouzian, Edward Rochford, Ewa Czekanska and Matteo D'Este.

I would like to thank Invibio Biomaterials for providing us with the PEEK used in the experimental work of this thesis.

Finally I would like to give my heartfelt thanks to my Mum and Dad, for their constant support and encouragement throughout my life, and especially during the writing of this thesis.

Daniel

Author's Declaration

I declare that all the work presented in this thesis has been carried out by me unless otherwise acknowledged or referred to.

Daniel Scott Simpson Morrison

January 2016

4. Introduction

4.1. Biomaterials as a field

4.1.1. Biomaterials development, and what is required of a modern biomaterial

Biomaterials can be defined as “Any substance or combination of substances, other than drugs, synthetic or natural in origin, which can be used for any period of time, which augments or replaces partially or totally any tissue, organ or function of the body, in order to maintain or improve the quality of life of the individual”. Viewed this way the use of biomaterials goes back thousands of years, with gold and ivory used for the repair of cranial defects by the Romans and Egyptians¹. While there were gradual advancements and improvements in the field over time, it was in the 1960’s and 1970’s when we saw a major expansion in the use of these implants and devices. It was at this time we also saw the development and implementation of, amongst others things, artificial joints, dental implants, ocular lenses and vascular stents¹. These devices provided a significant breakthrough in healthcare, improving the quality of life for millions of patients. However, the material for these implants were selected on a trial and error basis, as at the time there was a limited understanding of how the material properties of the implant effected the biological response to the implant, and in turn how this biological response impacted on the performance of the implant. The contemporary requirement for a biomaterial was that it “provided a suitable combination of physical properties to match those of the replaced tissue with a minimal toxic response in the host”²

In an effort to improve biomaterial performance the focus of biomaterials research moved away from producing materials that would not produce an immune response by the host to the implanted foreign body, to producing materials that could “elicit a controlled action and reaction in the physiological environment”². One of the best examples of this second generation of biomaterials is the use of synthetic hydroxyapatite (HA) ceramics in porous

implants and coatings on metal prosthesis to generate bioactive fixation, where the presence of HA induced a tissue response where bone grew along the coating and formed a mechanically strong interface. These improvements are ultimately limited, at least in part by the fact that the materials themselves are man-made, and as such cannot respond to the changing physiological loads or biochemical stimuli in the way living tissues can, ultimately limiting the lifespan of these artificial body parts. The current research focus has now moved to designing materials that can stimulate specific cellular responses at the molecular level in order to produce the desired tissue response at the host biomaterial interface²

Required properties of a biomaterial to be used in orthopaedic implants.

As there is particular interest in adapting PEEK for use in biomaterials applications, and in particular orthopaedic applications, we will consider what is required from these devices. Orthopaedic implants are devices that are implanted into a patient to replace the function of tissue that has become damaged by either age or disease, by providing mechanical and structural support³

There are a number of different properties that are required of what would be considered a successful orthopaedic implant material.

Mechanical properties

A good orthopaedic implant material should demonstrate high fatigue strength to cope with repeated cyclic loads being placed upon it. A good orthopaedic implant material should have a young's modulus as close to that of the bone that it is intended to replace. However, if the implant material has significantly higher stiffness than the surrounding bone it can prevent stress from being loaded onto the surrounding tissue. This results in bone reabsorption around the site of the implant, and in turn, loosening of the implant^{4,5}.

Biocompatibility

Orthopaedic implant materials are required to be highly non-toxic and should not cause any allergic or inflammatory reactions in the body³. The overall success of an implant material in terms of biocompatibility is largely down to

how the human body reacts with the implanted material. These reactions can be split into the following;

- The host response to the material and the degradation of the material in the body.
- Thrombosis, which involves blood coagulation and adhesion of blood platelets to biomaterial surfaces
- Fibrous encapsulation

High corrosion and wear resistance

Implant biomaterials are required to display a high level of resistance to both corrosion and wear, as reaction of the material with fluids in the body can result in the release of non-compatible metal ions. These released ions have been demonstrated to cause allergic and toxic reactions

Osseointegration

It is essential for the implant material to integrate well with the surrounding bone⁶. Factors such as surface chemistry^{7,8}, stiffness^{9,10} and surface topography¹¹⁻¹³ have all been suggested as important factors contributing to the ability of the implant material to form a strong interface with the tissue of the host, by modulating the developmental and behavioural choices of the cells at the surface of the material.

4.1.2. Different properties of a biomaterial which can influence cell response

A critical component of the overall performance of an orthopaedic implant device is how it interacts with the surrounding tissue. The surface of an orthopaedic implant device firstly requires the patient cells to adhere to it, otherwise there is the potential for fibrous encapsulation to occur, which results in a weak interface between implant and host tissue. The strength of the interface between the implant and the tissue of the host has a strong effect on the performance of the implant. Weak bonding between the implant and the

host tissue leads to aseptic loosening, which in turn can lead to the failure of the implant^{4,5}.

To this end, there has been a great deal of research interest into how properties of a material govern cell interaction with the implant, given how significant these interactions are to the performance and lifespan of the device. A number of different material properties have been identified which modulate the cellular response to a material, and from the perspective of trying to design an improved biomaterial surface, each should be considered.

Stiffness

The stiffness of a material has been demonstrated to impact on the behaviour of cells cultured upon it in both two^{9,10} and three^{14,15} dimensional culture. Hydrogels have commonly been used to investigate this phenomenon, as researchers can easily adjust the stiffness of the material by altering the density of crosslinks in the material. Hydrogels can be produced which range from very soft (less than 1 kilopascal which would be a viscous fluid similar to honey) all the way up to stiff (around 500 kilopascals which would be similar to silicone rubber)¹⁶. This stiffness has been demonstrated to play a role in controlling cell differentiation. MSC's cultured on a "soft" matrix (0.1 kPa) differentiated into neuronal like cells. Those cultured on a matrix of "medium" elasticity (11 kPa) differentiated down the myogenic lineage, and cells cultured on a stiff matrix (34 kPa) developed down the osteogenic pathway¹⁰.

Surface topography

It has been long established that the presence of topographical features on a surface which cells are cultured on, can alter cell behaviour^{17,18}. More recently there has been a great deal of interest in the use of features that are on the nanoscale in size^{19,20}, and how they can alter cell behaviour, in particular, that of stem cells. Fabrication methods such as electron-beam lithography^{21,22}, colloidal lithography^{23,24} and polymer demixing²⁵ have allowed different researchers to produce a range of nanofeatures on various material surfaces. A number of different specific nanoscale features have been demonstrated to be capable of directing biological activity, with features such as nanotubes^{26,27}, nanogratings²⁸, nanopillars^{29,30}, nanochannels^{31,32}, matrices of nanofibres^{33,34} and

nanopits^{35,36} all proving capable of influencing the differentiation behaviour of stem cells.

Chemistry

It has been demonstrated that there is a relationship between protein absorption onto a surface, focal contact formation and resulting MSC differentiation, which is related directly to the chemistry of the surface. Attaching specific chemical groups such as -CH₃, -NH₂, -OH and -COOH have been linked to specific MSC responses, such as enhancement of MSC phenotype maintenance, osteogenic differentiation and cartilaginous differentiation. Recent research into the relationship between MSC behaviour and specifically chemically patterned surfaces has demonstrated that the chemistry of the surface can control integrin binding, which feeds into integrin clustering, which in turn is critical in determining the type of adhesion formed, which is subsequently crucial to resulting cell signalling events³⁷⁻⁴⁰. It is interesting to note that the process for how specific patterning of chemical groups on a surface influences MSC behaviour, is very similar to the suggested mechanism for how specific nanoscale topographies impact on MSC behaviour⁴¹. This suggests that it might be possible that surface chemistry and nanotopography act in a synergistic manner to direct MSC behaviour.

4.1.3. Use of Nanotopography to control stem cell phenotype

It has long been understood that cells are capable of responding to the shape of their environment⁴². Since the 1950s there has been in vitro evidence of cells lining both to, and along grooves present on the surfaces they are being cultured on, in a process known as contact guidance¹⁷. The process of interaction between a number of different cell types and different topographies has been demonstrated to lead to specific alterations in a range of cell behaviours, including cell attachment, spreading, nuclear shape, transcript levels and protein abundance¹⁹.

Over time, techniques developed by the electronics industry such as photolithography⁴³ gave researchers access to larger surfaces with more controlled topographies. This led to a range of different cell types being tested, with a library of different micron scale topographies including simple steps⁴⁴,

grooves⁴⁵⁻⁴⁹, spikes⁵⁰, cylinders⁵⁰, mesh⁵¹, films with a honeycomb like structure at the surface⁵² and tunnels and tubes^{53,54}, to look for relationships between the shape of the culture surface and the behaviour of the cells.

Recently there has been a great deal of interest in nanotopography with cells having been demonstrated to be capable of sensing features as small as 10nm⁵⁵. Techniques such as e-beam lithography have led to the production of experimental surfaces with sub 100 nm features on a biologically relevant scale both in terms of surface area and number of replicates^{56,57}. A range of different nanofeatures have been demonstrated to be capable of directing stem cell developmental behaviour. Of these, a number of different nanotopographies have been demonstrated to be capable of encouraging osteogenic differentiation of stem cells including nanotubes^{26,27}, nanofibres⁵⁸, nanopillars³⁰ and nanopits^{35,59,60}.

While the immediate clinical and related commercial application of osteogenic differentiation has led to a greater research focus on this area, nanotopography has proved capable of modulating other developmental behaviour in stem cells as well. Nanogratings have been demonstrated to induce differentiation down the neuronal lineage²⁸, a matrix of nanoscale fibres has proven capable of inducing myogenic differentiation⁶¹ and nanofibres can encourage the differentiation of MSCs into cartilage⁶²

*Yim et al*²⁸ looked at the effect 350nm wide nanogratings fabricated on poly(dimethylsiloxan) (PDMS) had on the differentiation of human MSC's isolated from bone marrow. They found that both the cell bodies and nuclei of the cells were elongated and aligned along the axis of the grating on the nanopatterned surfaces, while there was no elongation or specific orientation from cells on the non-patterned control surface. They found that mature neuronal markers such as MAP2 and β tubulin 3 (Tuj1) expression was found in hMSCs on the nanopatterned samples, both with, and without neuronal differentiation medium, whereas on the non-patterned samples the cells expressed these markers only in the presences of the differentiation medium. Additionally, Synaptophysin again was shown to be expressed by the cells cultured on the nanopattern both in the presence and absence of the differentiation media, but not by those cells on the non-patterned surface, which indicated that the cells being cultured on the topography were directed to form synapses. Furthermore,

qPCR experiments showed up-regulation of neuronal markers such as Tuj1, MAP2 and GFAP by cell cultured on the nanopatterned surface.

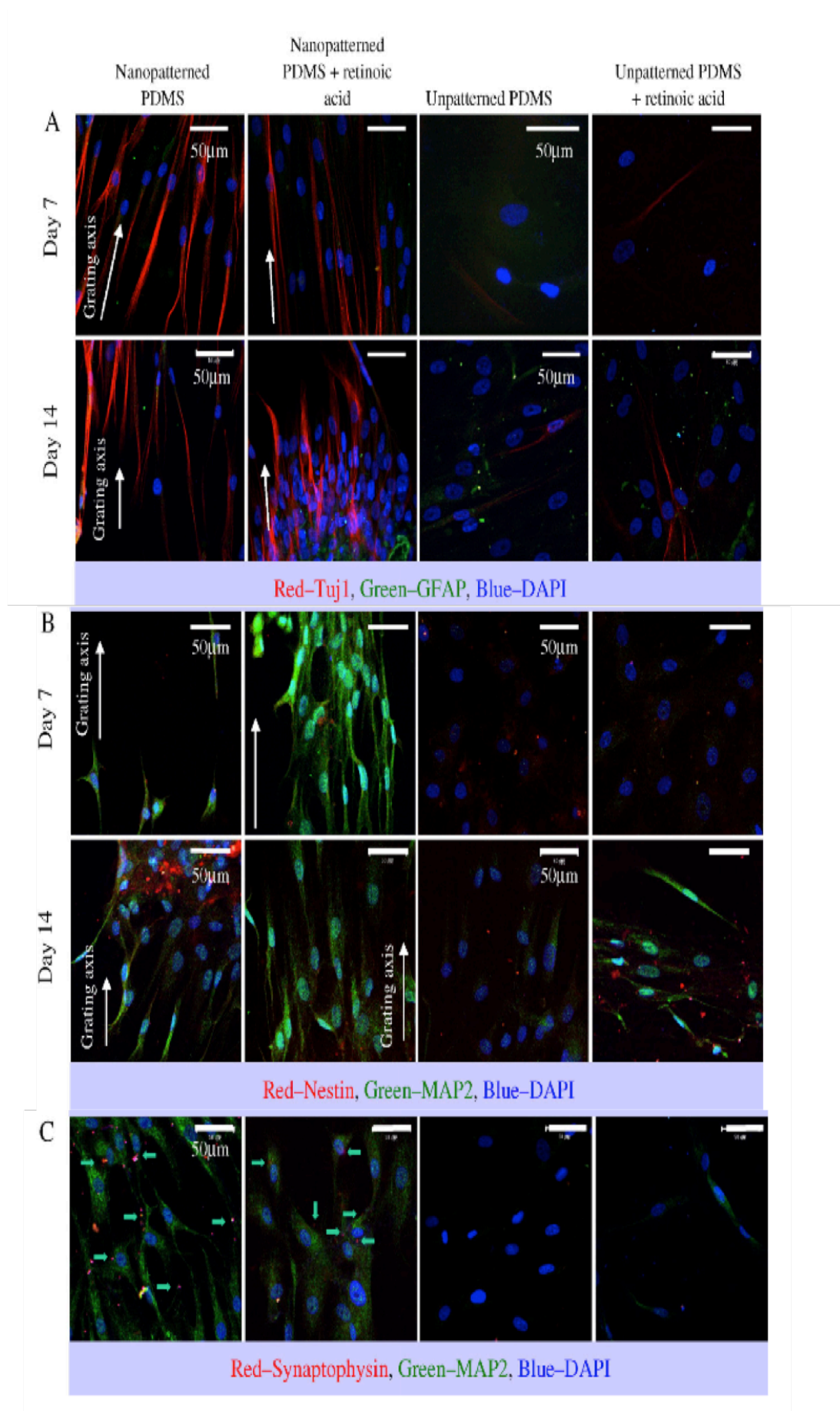


Figure 1 Results from Yim et al²⁸ culture of MSCs on their nanopatterned PDMS. Consistently we can see higher expression of the different markers on the nanopatterned surface. In addition, in the presence of a differentiation cue (retinoic acid) the presence of the nanotopography still produces a greater level of staining compared to the unpatterned surface.

Finally, Yim et al²⁸ investigated whether or not the behaviour they had observed was specifically down to the presence of nano-scale topography, or if features on the micron scale were capable of eliciting these results. To do this they compared the behaviour of MSCs on gratings with widths of 350nm, 1µm and 10µm and found a significant width dependency for proliferation and differentiation on the nanoscale topography, compared to the two micron scale topographies.

*Dalby et al*³⁵ used surfaces fabricated from polymethylmethacrylate (PMMA) with 120 nm diameter, 100 nm deep nano-features with varying degrees of disorder to try to stimulate osteogenic behaviour from human osteoprogenitors and specifically isolated MSC populations. Immunostaining for osteopontin and osteocalcin with primary osteoprogenitors cultured for 21 days showed that on the non nanopatterned planar surface the cells were largely fibroblastic in appearance. Cells cultured on the completely random topography displayed more dense growth compared to the planar surface, but there was little expression of either marker. However, on the DSQ50 topography they observed cells forming dense accumulations that were similar in appearance to bone nodules that had raised levels of both markers.

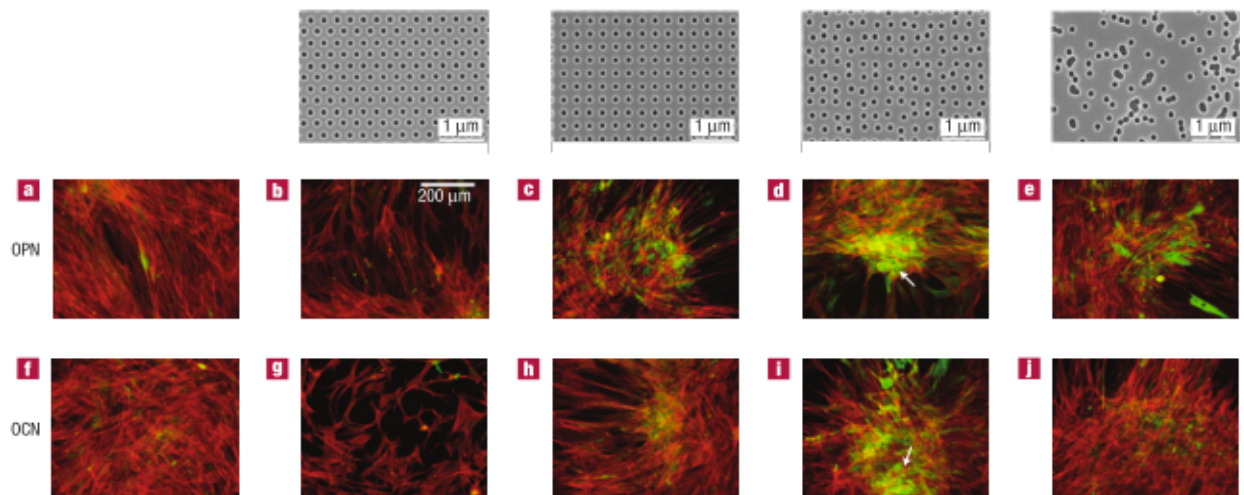


Figure 2 Results from Dalby et al³⁵ culture of osteoprogenitor cells on PDMS surfaces with nanopits which have differing spacing between the individual features. We can see that there is an optimum amount of disorder in the spacing of nanofeatures in terms of inducing osteogenic behaviour, where both higher and lower degrees of disorder lead to a reduced level of expression of the two osteogenic markers.

To follow up on this result they then cultured primary human MSCs on the surfaces for 21 days and again stained for osteopontin and osteocalcin, and also cultured cells for 28 days, staining them with alizarin red to look for the presence of calcium. On the planar surface at 21 days, MSCs had a characteristic fibroblastic appearance whereas the cells on DSQ20 appeared more typically osteoblastic and shown some osteopontin staining though no osteocalcin. However, cells cultured on the DSQ50 topography had results that were similar to the results observed for the osteoprogenitor cells, namely that they had formed into nodule like structures which were positive for both osteopontin and osteocalcin. Additionally, after 28 days of culture, MSCs on DSQ50 showed alizarin staining which demonstrates that the cells are mineralising, while this behaviour was not observed by the MSCs on any of the other surfaces. To look at the osteogenic capacity of the DSQ50 nanotopography in more depth, osteospecific microarrays were used to compare the differentiation behaviour of MSCs cultured on DSQ50, a planar surface where the cells were cultured in the presence of dexamethasone and a planar surface where the cells were cultured only in standard culture media. The cells with dexamethasone showed the largest osteogenic up-regulation with 24 gene hits, MSCs on DSQ50 had 11 gene hits while cells without dexamethasone on the planar surface had 3 gene hits. qPCR carried out with primers for OCN, ALP, ICAM1 and TGF β R1 showed that both cells on the planar surface cultured with dexamethasone and cells on the DSQ50 topography had significantly higher expression of these genes.

Given this demonstrated ability of topography alone to direct stem/progenitor cell differentiation there is an obvious application for this type of technology in orthopaedics/regenerative medicine, as the “correct” topography would be capable of directing the cells that adhered to the surface of an implant with this type of topography at its surface, down the osteogenic lineage to greater osteogenic behaviour, leading to a significantly stronger interface between native bone and the implant. In turn, stronger bone implant interface in the past has signalled implants that last longer with improved performance for the patient

4.2. Fabrication of nanotopographies through injection moulding

While in this PhD project the authors did not fabricate the PEEK nanotopographies used in the experiments themselves, the use of injection moulding to produce PEEK surfaces does have an impact on how this work could lead to technology suitable for use in the clinic, and so, is covered here.

Injection moulding is an industrial process for the manufacture of plastic objects. This process revolutionised manufacturing in the second half of the twentieth century by allowing for the rapid replication of identical parts made from thermoplastic materials from a single machine mould. The reason this process had such a profound effect on the production of plastic parts is due to the fact that while there are significant costs associated with initiating the process (the cost of the equipment in general, and in particular, production of precisely constructed moulds are high). Once production is in full swing the ability to produce large numbers of parts quickly and with high fidelity of replication, made injection moulding stand out compared to other methods of plastics manufacture⁶³.

Injection moulding has been used for producing surfaces with precisely ordered topographies in industry for some time, beginning with the production of compact discs in the 1980s. Injection moulding was employed for the production of compact discs as it permitted the cheap, accurate replication of micron scale features on a much larger scale than had previously been seen. Currently, the production of Blu-Ray Discs involves injection moulding of features below 150nm. There is potential for further development in this area with researchers demonstrating the possibility of producing distinct structures as small as 25, 20 and 5 nm in size⁶³.

The injection moulding process consists of heating a thermoplastic polymer to around 100°C above its glass transition temperature. The molten plastic is then injected into the mould cavity, which is typically kept at 30-50°C below the particular polymers glass transition temperature. In the mould cavity the polymer rapidly cools and the moulded part is ejected before the process starts

over again in a fully automated and unsupervised process. It is due to the separation of the heating and cooling parts of the process which leads to injection moulding being such a high throughput process compared to competing methods, such as hot embossing. In an optimised industrial process it takes only 4s to produce a compact disc⁶³.

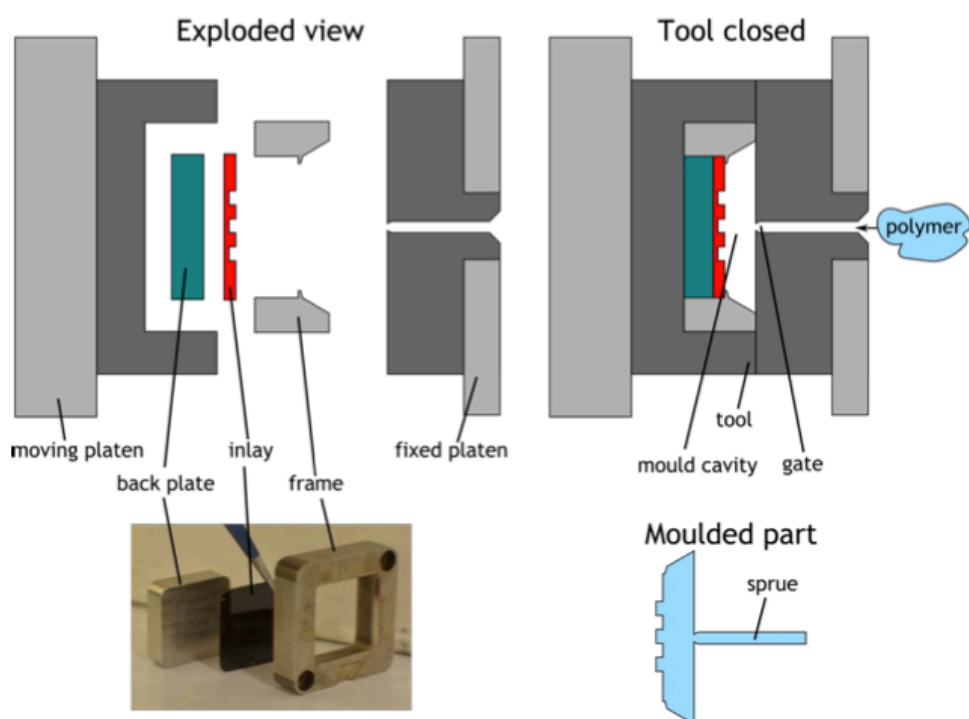


Figure 3 Illustration of the significant part of the moulding area of the injection moulding machine used to produce the nanotopographies used in this thesis. Reproduced from Stormonth-Darling⁶³

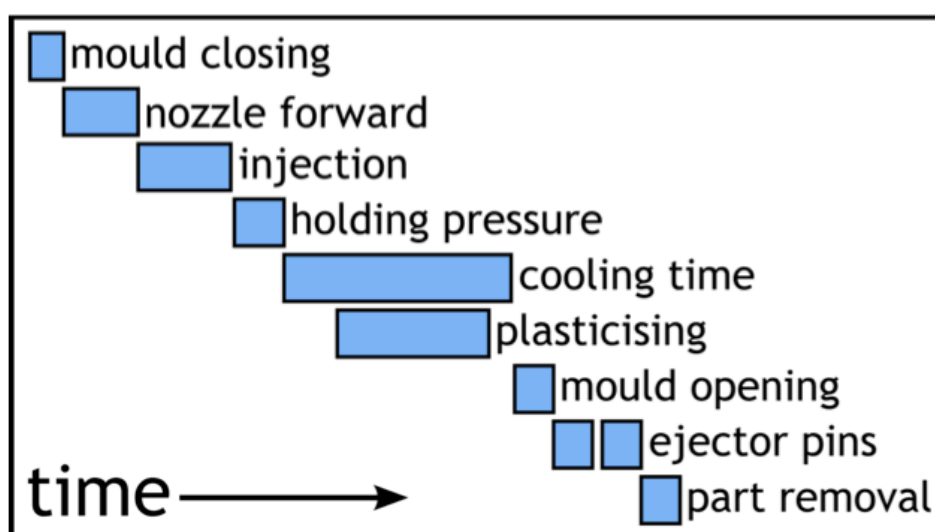


Figure 4 Visual representation of the different stages involved in injection moulding. Reproduced from Stormonth-Darling⁶³

From the perspective of carrying out biological research, using injection moulding to produce experimental surfaces makes a great deal of sense. Given that in our opinion the two most important factors are; obtaining a sufficient number of substrates, and ensuring the highest degree possible of fidelity of topography replication between surfaces, injection moulding provides an excellent method for fulfilling both of these objectives.

4.3. PEEK as a biomaterial

Poly(aryl-ether-ether-ketone) (PEEK) is a semi crystalline polymer which exhibits properties that make it an attractive choice for use as an implant material⁶⁴. It displays natural radiolucency and MRI compatibility, as well as good chemical and sterilization resistance⁶⁵, These properties make it of particular interest for use in biomaterials applications⁶⁶.

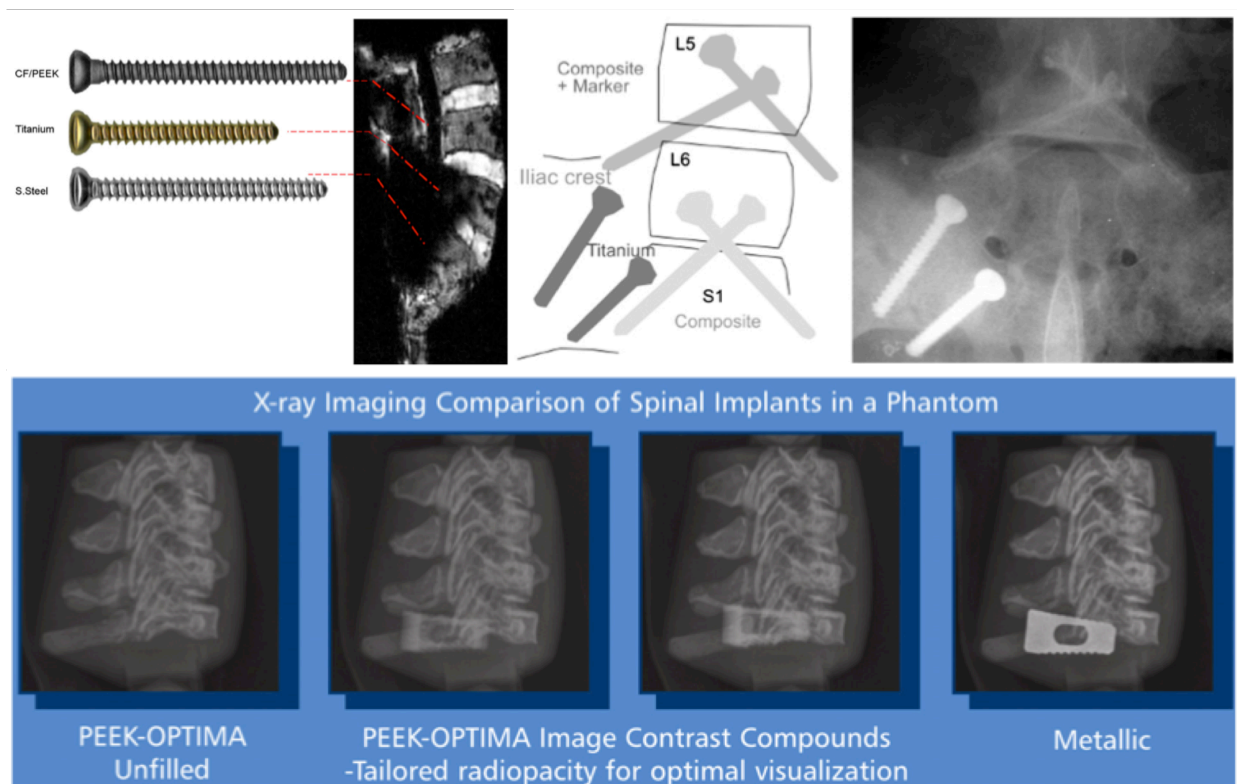


Figure 5 Demonstration of the radiolucency of PEEK and how it compares to competing metallic implant materials in both X-rays and MRI images. Reproduced from Green et al⁶⁷

Implant devices fabricated from PEEK have been demonstrated to have mechanical characteristics such as stiffness and modulus that match those of bone and is better than competing biomaterials such as Titanium and stainless

steel⁶⁸. The elastic modulus can be made even closer to that of cortical bone through the addition of carbon fibres⁶⁹

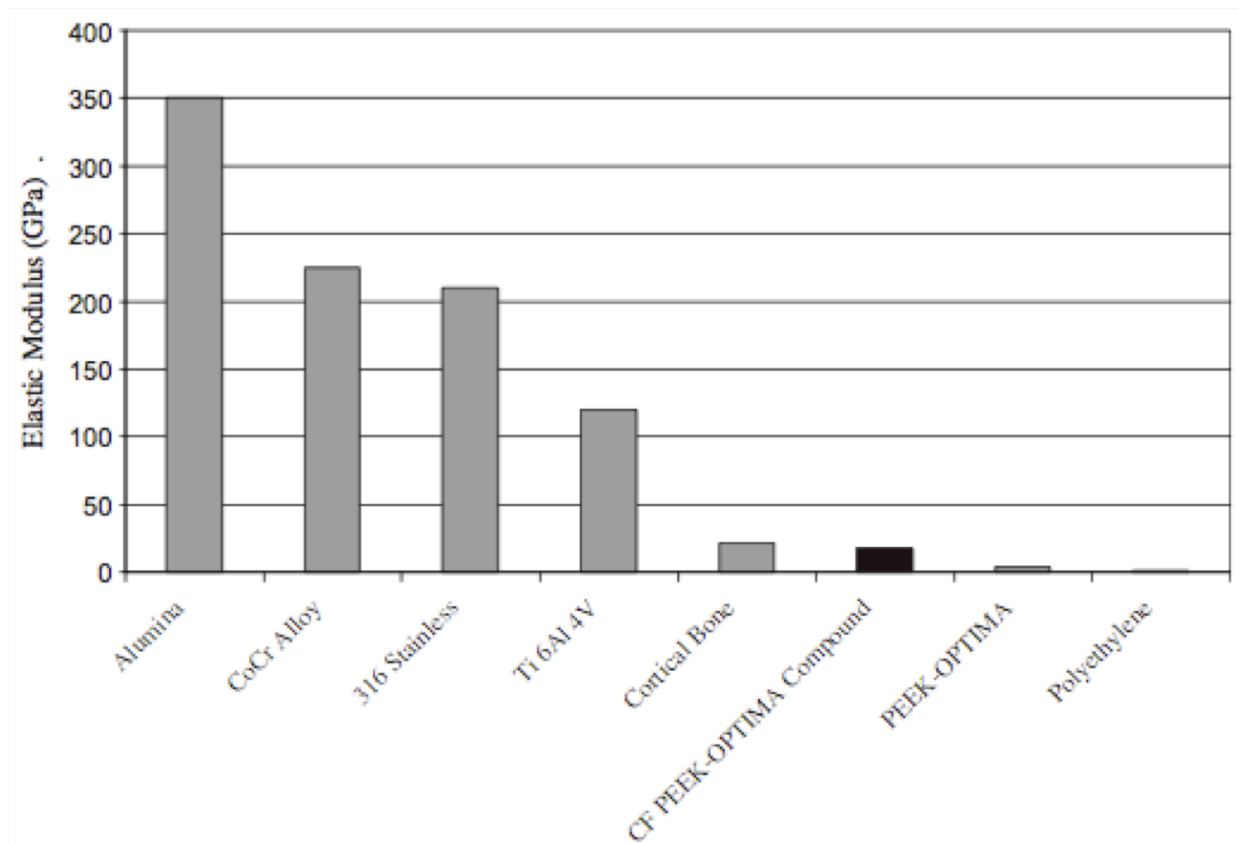


Figure 6 Comparison of the elastic modulus between PEEK and other competing biomaterials to that of cortical bone. We can clearly see how much closer PEEK-optima and in particular a CF PEEK-optima compound is to cortical bone compared to other biomaterials. Reproduced from Green et al⁶⁷

A close match between the elastic modulus of bone and that of the implant is highly desirable, as too great a gap between the two leads to a phenomenon known as stress shielding, where the bone next to the implant is shielded from the load normally placed on the bone. This in turn leads to re-absorption of the proximal bone and eventual loosening of the implant⁷⁰. There is a body of research testifying to PEEKs biocompatibility⁷¹⁻⁷⁵ and further to this the material has a FDA master file and as a result has undergone extensive studies on intracutaneous toxicity and intramuscular implantation, sensitization and gene toxicity⁶⁴. Using plastics technologies offers a range of different methods for the mass production of PEEK substrates and the material has a reproducible, pure and traceable supply route⁶⁵. PEEK has been used in a number commercially available implant devices including spine cages, craniomaxillo facial implants like skull plates and arthroscopic suture anchors^{64,76-81}

4.3.1. Improvements that can be made to PEEK for use in biomaterials applications

PEEKs main drawback as a biomaterial is that it demonstrates a low level of cell adhesion both *in vivo*^{64,82,83} and *in vitro*^{65,84}. This is problematic, as implant surfaces that do not develop a layer of adhesive cells are at risk of undergoing fibrous encapsulation. This in turn leads to the lack of a strong interface between the implant device and the patient tissue, which in turn can lead to failure of the implant and revision surgery³.

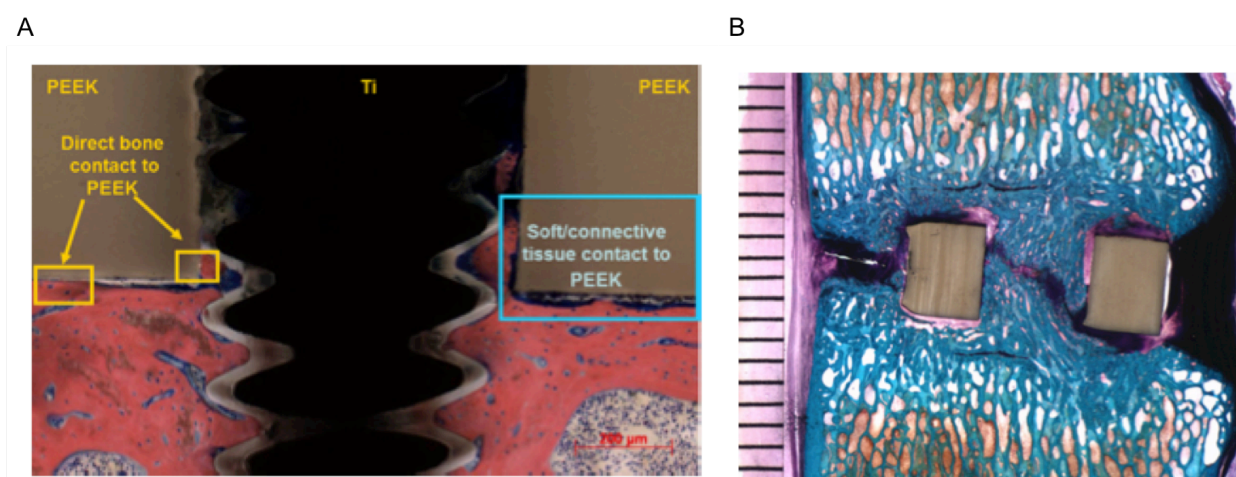


Figure 7 *In vivo* examples of non-surface modified PEEK's poor osseointegration.. In both images it can be observed that there is significant fibrous tissue present between the PEEK implant and the host. In addition, direct comparison with titanium (part A) illustrates PEEKs poor direct bone contact relative to a competing biomaterial. Reproduced from Poulsson⁸⁵

4.3.2. The current state of PEEK biomaterials research.

The main focus of tissue engineering research done with PEEK has been focused on improving the materials ability to permit cell adhesion/proliferation at its surface. Due to this, much of the research work done in PEEK can be split into either producing PEEK composites or modifying the surface of PEEK, in each case trying to improve cellular response of the material.

PEEK composites

While a number of different PEEK composite materials have been fabricated, the most widely studied have been PEEK hydroxyapatite composites.

*MS Abu Bakar et al*⁸⁶ produced a series of PEEK hydroxyapatite composite materials with percentage by volume of HA particles up to 40% and with spherical HA particles with a mean size of 25.68 micron. They produced their experimental surfaces through a series of processes consisting of compounding, granulating and then injection moulding. They found that as the percentage of HA increases the composite experiences a reduction in ductility. Additionally the tensile properties of the composites is also dependent on the HA content, with tensile strength decreasing as HA content increases.

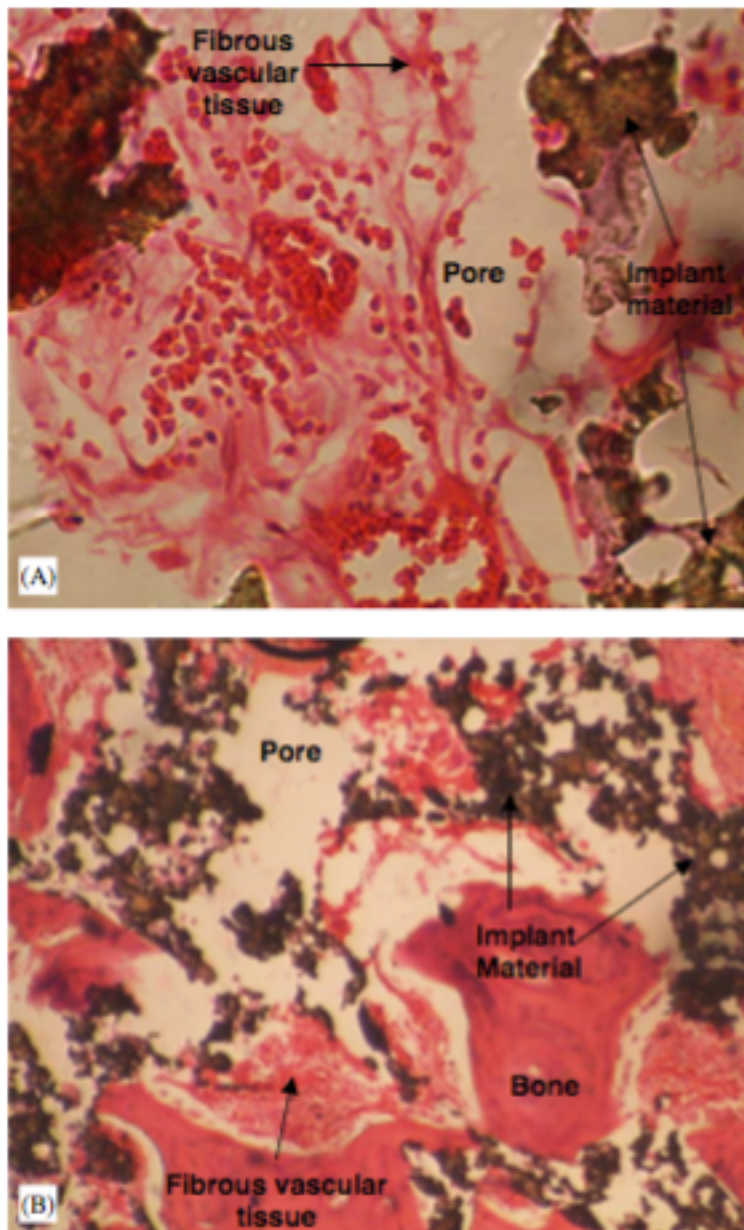


Figure 8 In vivo results from Abu Bakar⁸⁶ at 6 (labelled A) and 16 weeks (labelled B). At 16 weeks bone has been formed in the pore regions of the composite.

KL Wong *et al*⁸⁷ used hydroxyapatite that had strontium salts added to it to make a composite with PEEK, as strontium salts have been demonstrated, both in vivo and in vitro to stimulate bone formation and inhibit bone reabsorption. SrHA-PEEK composite substrates were produced with the SrHA filler making up 0, 15, 20, 25 and 30 % of total volume through compression moulding. The bending modulus of the composites was shown to increase with the volume of SrHA filler. They decided that 25% of volume filler had the best combination of mechanical properties, and as such was used for biological testing in order to investigate the response of osteoblasts to the SrHA composite, by measuring the proliferation, ALP activity and calcium production (via alizarin staining) of MG63 cells. There

was no significant difference in proliferation or ALP activity between PEEK, HA-PEEK or SrHA-PEEK. There was however a reported significantly higher level of alizarin staining on the SrHA-PEEK composite compared to both PEEK and HA-PEEK composite.

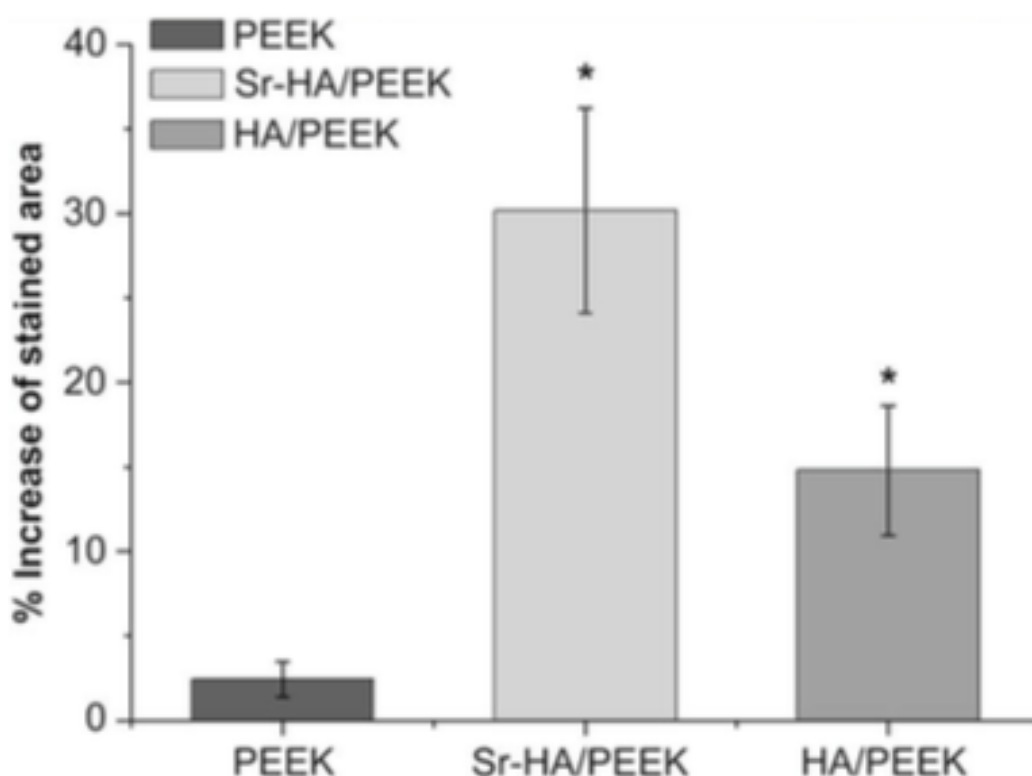


Figure 9 Alizarin red staining of MG63 cell on cultured on PEEK, a HA/PEEK composite and a strontium reinforced HA/PEEK composite. Both composites produced significantly greater levels of staining compared to PEEK, with the strontium HA also significantly higher than that of the HA/PEEK composite. Reproduced from Wong⁸⁷

*Jae Hyup Lee et al*⁸⁸ coated commercial PEEK substrates with HA particles via a cold spray method. The cold spray method was employed as the use of high temperature spraying techniques can result in polymer deformation. They demonstrated that the presence of the HA coating was shown to decrease the water contact angle by almost half (94.9 to 48.83)

The biological impact of the HA coating was investigated using human bone marrow mesenchymal stem cells. Using these cells, a number of different aspects of cellular response were investigated including proliferation, ALP activity, calcium concentration and transcriptional activity of osteogenesis related genes. The MTT cell proliferation assay showed that until a confluent layer of cells was formed on the surfaces the rate of proliferation was significantly higher on the HA coated surface than on the bare PEEK. ALP activity

was shown to be significantly higher on the HA coated samples at both one and three weeks when compared to the bare PEEK. Calcium concentration was shown to be significantly higher at one and three weeks compared to the bare PEEK. The RT-PCR results showed that there was no significance in ALP expression between the two surfaces, both Runx2 and BSP expression was markedly enhanced on the HA coated surface.

For the in vivo work, microCT showed the contact ratio between surrounding bone and implant was higher for the HA coated samples but not to a statistically significant degree.

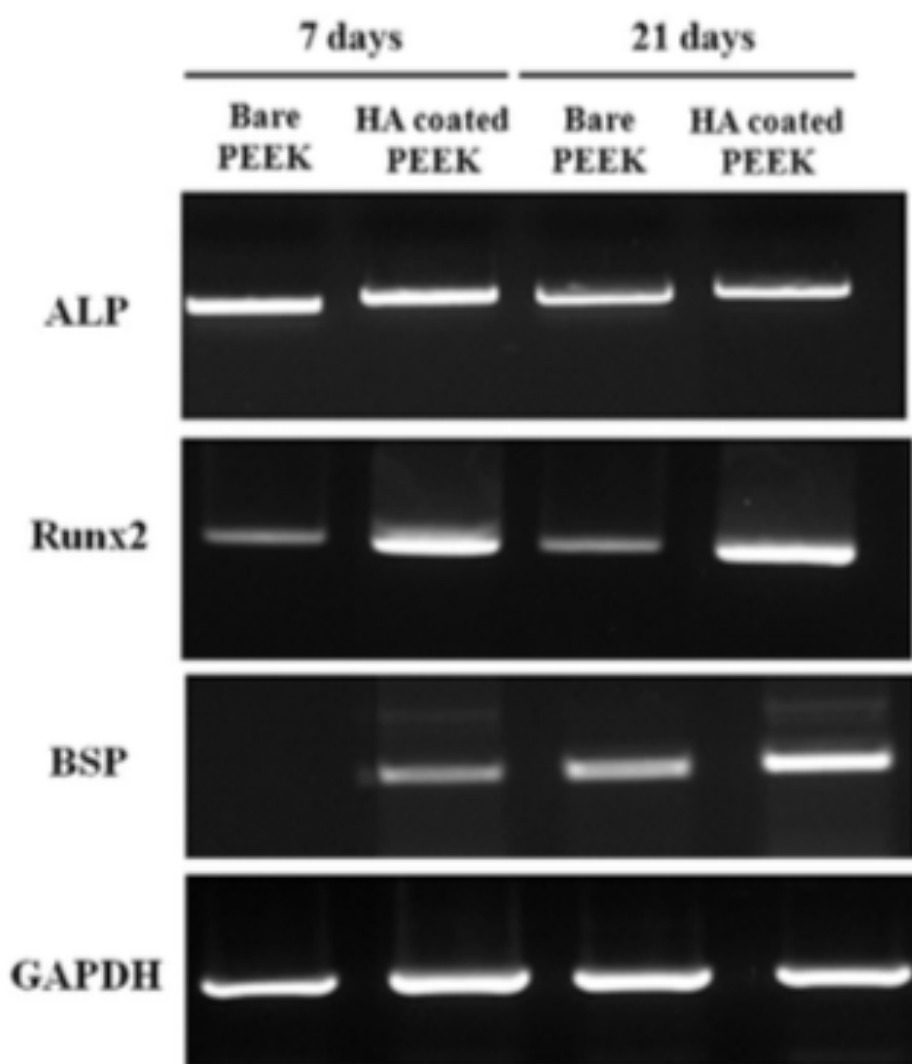


Figure 10 RT-PCR results from human MSCs cultured on bare and HA coated PEEK. The presence of the coating led to a clear enhancement of transcription of the osteogenic markers Runx2 and BSP. Reproduced from Jae Hyup Lee⁸⁸.

PEEK surface modification

Plasma treatment

The most widely used, and in our opinion most successful, approach to PEEK surface modification has been through the treatment of the surface with different types of plasma treatment.

*Briem et al*⁸⁹ treated PEEK foils with microwave plasma using ammonia/argon gas, a power of 500W and 0.1 mbar pressure in a specially designed UHV reactor system. They then looked at the response of primary human fibroblasts and primary osteoblasts derived from new-born CD-1 mice. Comparing the proliferation rate of primary fibroblasts on both the plasma treated PEEK and TCPS showed that the rate was significantly higher on the PEEK surface compared to the TCPS, with the cells on both surfaces capable of producing a confluent layer of cells. Additionally, toxicity testing was negative for the plasma treatment. Primary osteoblasts were stained for alkaline phosphatase, collagen type 1 and bone nodules to assess the impact of the plasma treatment on osteogenic response. After 30 days of culture, cells on the plasma treated PEEK surfaces tested positive for all three stains and there was no observed difference between cells cultured on the plasma treated PEEK and TCPS.

*Awaja et al*⁸⁴ treated 500 micron thick PEEK films with a methane oxygen gas mixture employing a range of bias voltage and plasma treatment times and looked at the impact this had on the level of attachment and degree of spreading of MG63 cells. They found that the presence of methane oxygen plasma treatment had a pronounced effect on cell attachment with the untreated PEEK surface exhibiting 2.9% cell attachment, whereas after plasma treatment it ranged from 38 to 75%. However, when the samples were plasma treated with just methane gas the improvement in cell attachment was much smaller, with all but one of the screened treatments having a cell attachment rate of between 4-8% (the exception was one sample that had an attachment rate of 31.6% - this was still lower than any of the methane oxygen plasma treated samples). Cells cultured on the methane oxygen plasma treated surfaces were reported to display a much greater degree of spreading and a flattened morphology compared to cells on the untreated PEEK surface, where the cells appeared very rounded. Cells on the methane only plasma treated

surfaces however showed similar morphology to the cells on the untreated surface. Overall the authors reported that “cell adhesion increases as both time and voltage increase reaching a maximum of 90% cell adhesion at the highest voltage of 10kv and time of 100s”. They also postulated that “Cell adhesion increased linearly with decreasing water contact angle and increasing of polar components of water contact angle”.

*Schroeder et al*⁶⁸ treated 250 micron thick peek foils in a low pressure microwave (2.54 GHz) reactor using pure ammonia. The treatment was carried out at a microwave power of 500W at a pressure of 0.2 mbar and treatment duration was varied up to 600s. MG63 cells were used to look at cell adhesion, actin cytoskeleton organisation and integrin organisation, at the early phase of cell culture. The results showed that on the plasma treated PEEK adhesion was comparable to that seen on the collagen type 1 coated TCPS positive control. There was no observed difference in integrin expression between any of the plasma treatments used.

*Poulsion*⁸⁵ investigated the impact of oxygen plasma treatment on PEEKs surface chemistry and how the treatment impacts the adhesion and osteogenic behaviour of human osteoblasts. PEEK surfaces were treated with a range of oxygen plasma treatments from 10s up to 2400s. They monitored the surface energy and wettability of their plasma treated surfaces, which had been cleaned after treatment, and found that both were found to be stable after 26 months. The XPS analysis showed that the plasma treatment led to increase in surface oxygen, with the formation of polar functional groups such as carbonyl and carboxyl at the surface.

AFM analysis of the PEEK surfaces which had been plasma treated showed that while the plasma treatment did etch the surface, overall this was not found to be significant, with the PEEK surfaces appearing relatively smooth compared to standard microrough commercially pure titanium. Biological response to the treatment was assessed by investigating cellular attachment, proliferation, morphology, ALP activity and calcium production through alizarin red staining. The presence of plasma treatment led to greater cell spreading and proliferation compared to that of the cells on the untreated surface, to the point where the untreated surface cells had not formed a confluent monolayer by 28 days. The

alizarin red staining results showed that mineralisation was occurring earlier than the other surfaces and that 1800s plasma treated surface demonstrated the most abundant staining.

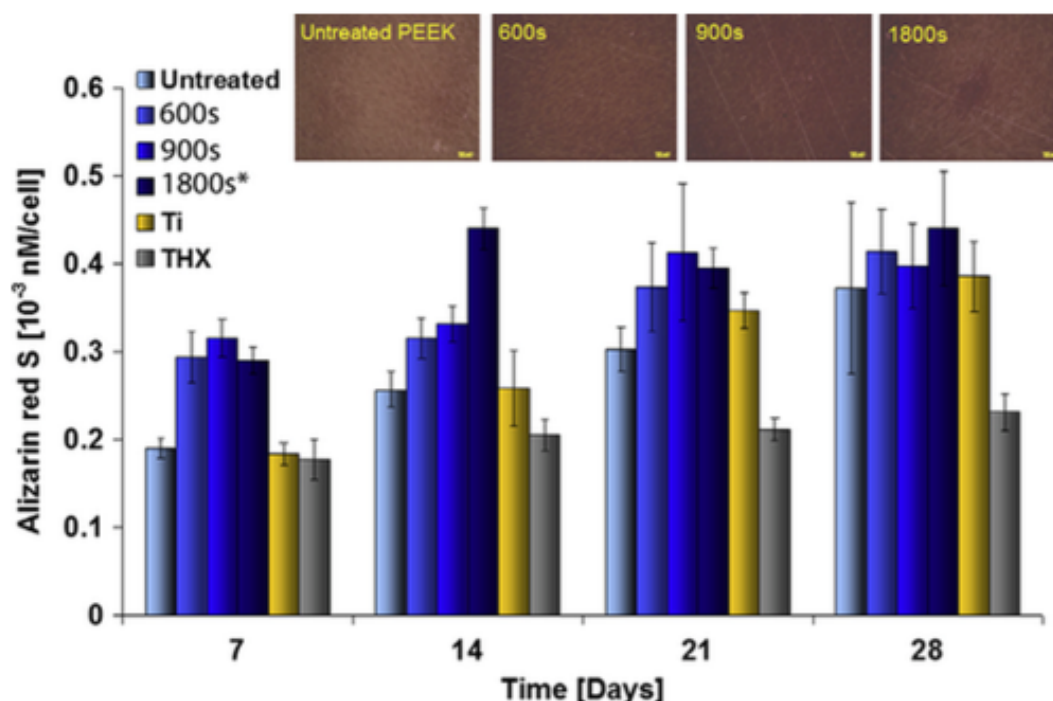


Figure 11 Quantification of Alizarin staining of human osteoblasts on oxygen plasma treated PEEK. The results demonstrate that 1800s of plasma treatment leads to the greatest mineralisation response from the cells. From Poulsson⁸⁵

In addition to this Poulsson *et al*⁷⁶ carried out an *in vivo* investigation on the plasma treatment that was tested in the previous *in vitro* experiment. Here they implanted injection moulded and machined PEEK rod shaped devices that were 4mm diameter and 12 and 15mm long and had been oxygen plasma treated for 1800s at 45W, into 24 skeletally mature sheep (16 implants per sheep: 8 implants were used in biomechanical push out tests and the other 8 were prepared for histology). The devices were implanted in both cancellous and cortical bone. Direct bone contact to the PEEK surface and the bonding strength of the implants to the bone were assessed at 4, 12 and 26 weeks after implantation. Before implantation XPS was used to assess surface chemistry and AFM and white light profilometry were employed to investigate the topography of the implants. Intra vital fluorochrome injection of calcein green and xylenol was utilised at 3 and 1 weeks before the end of the experiment, to label new bone. The plasma treated samples had higher bone to implant contact ratios but these were not found to be statistically significant. There was a reported trend for improved PEEK to bone interfacial strength for the plasma treated

samples compared to the untreated samples which was demonstrated to be statistically significant. In the devices implanted into cancellous bone the bone to implant contact ratio showed a clear trend of higher bone apposition on the plasma treated samples compared to the untreated, but this was not found to be statistically significant.

Argon gas beam

*Khoury et al*⁹⁰ used an intense directed beam of neutral gas atoms (argon gas was used in this instance) to treat 0.2mm thick PEEK films and 3mm diameter PEEK rods cut into 1mm discs. The treatment reduced the sessile drop water contact angle from 76.4° to 36.1° and AFM showed nanometer scale texturing when compared to the non-treated control. Human foetal osteoblast cells were used to look at the impact of the treatment on cell adhesion and proliferation, the cells being cultured on the surfaces for 14 days and then cell number calculated using MTS and crystal violet assays. The results showed very few cells adhering to the untreated PEEK and the cells had either delaminated or failed to proliferate by day fourteen. Cells on the treated surfaces showed very good attachment and proliferation over the fourteen days. To look at the in vivo impact of the accelerated neutral atom beam treatment, a rat calvarial defect model was used. The results showed the non-treated implant had no bone growth with only fibrous tissue around the implant, while the treated implant had a bone ledge on top of the implant covering approximately fifty percent of the implant.

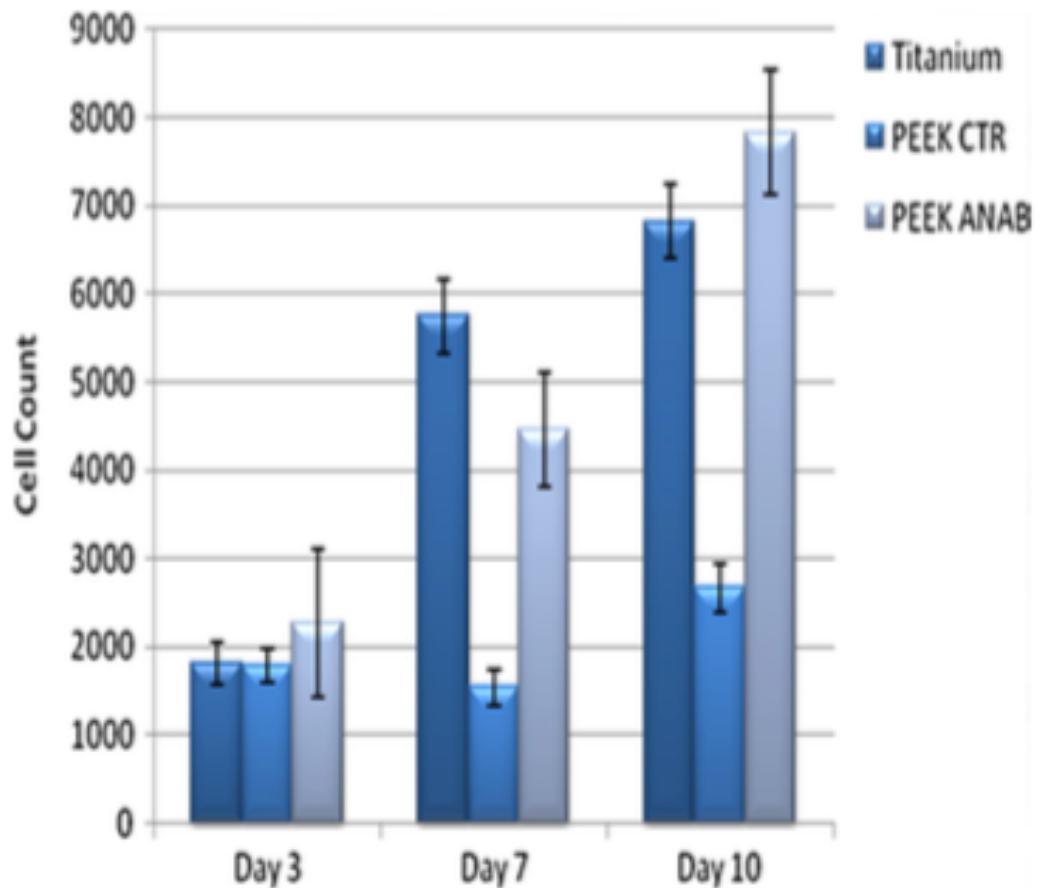


Figure 12 Proliferation of foetal osteoblast cells on titanium, untreated PEEK and PEEK treated with an argon beam. The results show that the argon treatment greatly improves the proliferation of cells compared to untreated PEEK, and by day 10 the number of cells present is comparable to that of titanium. Reproduced from Khoudry et al⁹⁰

Surface deposition

Yao et al⁹¹ used the IPD deposition process (a process carried out in a vacuum that allows the creation of controllable nanometer sized features) to deposit titanium and gold on the surfaces of PEEK, UHMWPE and PTF. They reported that the deposited particles were mostly less than 100 nm in diameter. They then used human osteoblasts to look at how these metal coatings impacted on the cells ability to adhere to the surfaces, and then looked at the spreading behaviour of the cells on the surfaces. They reported that compared to the uncoated polymers, the presence of either a titanium or gold coating significantly increased the level of osteoblast adhesion. They also noted that osteoblast adhesion was greater on surfaces that had nanoscale titanium particles compared to micron sized titanium particles. Cells on the uncoated surfaces were reported to display a more rounded shape whereas they were

more spread on the polymer surfaces that were coated with either gold or titanium.

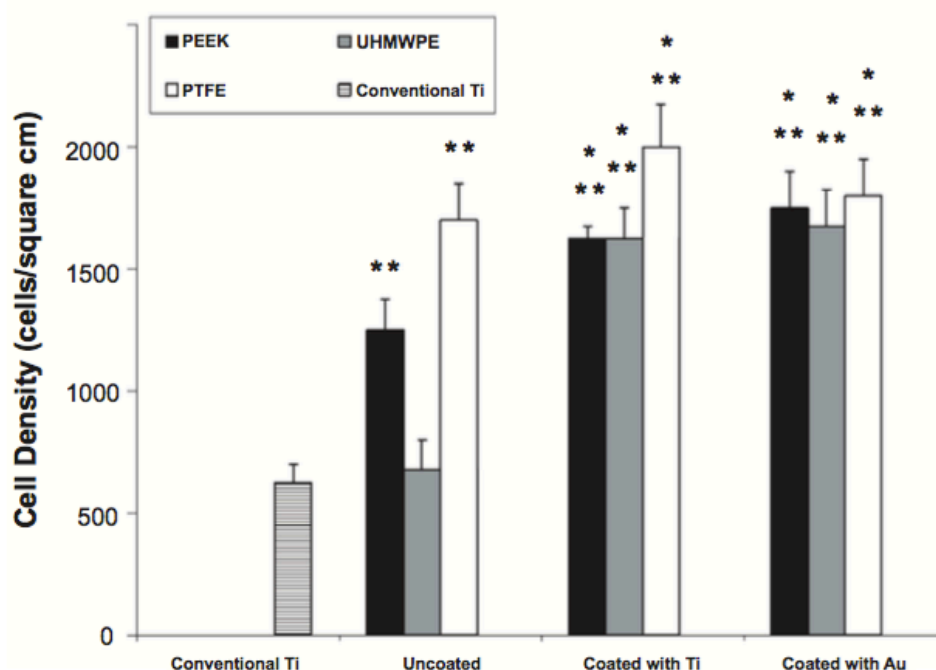


Figure 13 Adhesion of human osteoblasts to PEEK, PTFE and UHMWPE coated with both gold and titanium. The presence of either metal was shown to significantly increase the degree of osteoblast adhesion compared to the uncoated polymers. From Yao et al⁹¹

Han et al⁹² used e-beam deposition to coat a layer of titanium onto PEEK. They coated a 1 micron thick titanium film onto 15mm diameter, 2mm thick PEEK discs. They found that the e-beam deposition method deposited a dense uniform titanium film on the PEEK surfaces which did not have defects like cracks or voids, and had a thickness of 1 micron across the surface. The presence of the titanium film reduced the sessile drop water contact angle from 71° to 54°. The impact of the deposited titanium film on cell attachment, proliferation and osteoblastic differentiation was investigated *in vitro* using MC3T3-E1 cells. In terms of initial attachment (cells were seeded on to the surfaces and surfaces were inspected for cell attachment after three hours) there appeared to be a similar number of cells on both the titanium coated and non-coated surfaces, although the cells on the titanium coated surface were reported to show a more spread morphology. The rate of proliferation (measured via the MTT method) however showed that there was double the number of living cells on the titanium coated surface compared to bare PEEK

after five days of culture. Osteogenic differentiation (as measured by ALP activity at seven and fourteen days) showed differentiation to be significantly higher on the titanium coated PEEK compared to bare PEEK, at both seven and fourteen days. In fact the titanium coated surface had higher ALP activity at day seven than the bare PEEK did at day fourteen. The *in vivo* response to titanium coated PEEK was investigated by implanting 3.4mm diameter, 6mm long PEEK screws with a thread length of 4.5mm which had been half coated with titanium film, into the tibia of five rabbits. Both the bare and titanium coated sides of the screws showed similar bone regeneration between the screw threads, but the bare PEEK sides showed gaps between new bone and the implant surface, whereas on the titanium coated sides there was tight contact between the bone and the implant surface. The bone to implant contact ratios were calculated using a image analysis programme which showed that the titanium coated side had a significantly higher bone to implant contact ratio compared to the bare PEEK side.

A M Rust-Dawicki *et al*⁹³ implanted 40 titanium coated and bare PEEK cylinders into the femurs of four mongrel dogs and then assessed the implants histologically and mechanically at four and eight weeks. The PEEK cylinders had a diameter of 4.0mm and a length of 10.0mm. The experimental surfaces were coated with a 2000 Angstrom thick layer of titanium through plasma vapour deposition. Three sections from each femur were used for pull out testing while the remaining two sections were used for histological testing. From the pull out testing, interface shear strength was determined by dividing load to failure by the bone implant contact area, determined from direct measurement with a calliper micrometer. This measurement showed that at four weeks the uncoated surfaces had a higher mean shear strength than the titanium coated surfaces, and there was no significant difference between the two at eight weeks. There was no significant increase in bone contact between four and eight weeks for either the coated or uncoated PEEK. At both four and eight weeks there were significantly higher percentages of bone contact for the titanium coated surfaces compared to the uncoated. They found that there was no severe inflammatory response seen for any of the specimens used, and no interpositionary fibrous tissue was found among any of the specimens.

*Barkarmo et al*⁹⁴ spin coated PEEK surfaces with precipitated HA particles then heat treated them at 300°C. Nine of these samples along with nine uncoated samples were implanted into nine rabbits at the femur, and were kept in place for six weeks. After removal and histological staining, the implants underwent histological analysis where an image software analysis programme was used to measure the percentage of bone to implant contact. Of the eighteen implants used, seven failed to integrate into the bone tissue (six were coated samples the other five were left uncoated) and were excluded from the study. The remaining samples showed a general trend for higher mean values for the coated samples, but these differences were not statistically significant. The titanium coated implants had a higher mean value for both bone to implant contact and bone area compared to the uncoated implants, although these differences were not statistically significant.

Author	Modification type	Material aspects investigated	Cells used	Biological behaviour investigated	In vivo work	Key findings
Abu Bakar et al	PEEK hydroxyapatite composite	Bending behaviour of composites investigated			Yes	Increasing the % of the composite made up of HA results in loss of ductility. After 16 weeks mature bone being formed within pores of the implant
KL Wong et al	Hydroxyapatite with strontium salts added made into a composite with PEEK via compression moulding	Tested bending modulus	MG63	Proliferation, ALP activity and calcium production	No	Significantly higher level of staining on the SrHA-PEEK composite compared to PEEK and HA -PEEK composite
Jae Hyup Lee et al	PEEK coated with HA particles through cold spray method	Water contact angle measured	Human bone marrow mesenchymal stem cells	Proliferation, ALP activity, calcium conc. and transcription of osteogenic markers through RT-PCR	Yes	HA coating leads to higher proliferation, ALP activity, calcium concentration and RUNX2 and BSP expression. In vivo higher bone implant contact for HA coated samples but not statistically significant

Author	Modification type	Material aspects investigated	Cells used	Biological behaviour investigated	In vivo work	Key findings
Briem et al	Microwave plasma treatment with ammonia/argon gas	none	Primary fibroblasts from newborn CD-1 mice and primary human fibroblasts	Proliferation rate, toxicity testing, ALP staining, collagen type 1 staining and von Kossa staining	No	Result of the plasma treatment was similar biological response to PEEK as to the TCPS positive control
Awaja et al	Plasma treatment with oxygen/methane gas	Water contact angle measure and XPS used to investigate surface chemistry	MG63	Cell adhesion and cell spreading	No	Much better adhesion with methane/oxygen mix opposed to just methane (38-75% compared to 4-8%) Cell adhesion increases as both time and voltage of treatment increases.
Schroder et al	Reaction of PEEK in low pressure microwave reactor with ammonia	XPS used to assess surface chemistry	MG63	Cell adhesion and actin cytoskeleton and integrin organisation	No	Different plasma treatments did not lead to changes in integrin expression. Plasma treatment brought cell adhesion to the same level as the collagen type 1 coated positive control.

Author	Modification type	Material aspect investigated	Cells used	Biological behaviour investigated	In vivo work	Key findings
Poulsson et al	Oxygen plasma treatment ranging from 10s to 2400s at 45W	XPS to asses surface chemistry and measurement of water contact angle	Human osteoblasts	Adhesion, proliferation, cell morphology, ALP activity and alizarin red staining	No	Plasma treatment shown to be stable in terms of chemistry and wettability for 26 months if washed after treatment. Plasma treatment increases adhesion and spreading as well as leading to earlier presence of alizarin red staining
Poulsson et al	Oxygen plasma treated for 1800s at 45W	XPS AFM white light profilometry			Yes	
Khoudry et al	PEEK treated with accelerated neutral atom beam	AFM used to investigate nanoscale changes to topography, and water contact angle measured	Human foetal osteoblasts	Cell adhesion and proliferation	Yes	Improved adhesion and proliferation on treated PEEK compared to untreated. In vivo untreated implant had no bone growth while the treated implant had 50% bone coverage.

Author	Modification type	Material aspects investigated	Cells used	Biological behaviour investigated	In vivo work	Key findings
Yao et al	Titanium and gold particles of less than 100nm deposited onto PEEK via IPD process	Field emission scanning electron microscopy used to investigate deposited particles	Human osteoblasts	Cell adhesion and spreading behaviour	No	Much improved osteoblast adhesion on both gold and titanium coated surfaces compared to the uncoated. Osteoblast adhesion greater on surfaces with nanoscale titanium particles compared to micron scale particles
Han et al	E beam deposition used to deposited 1 micron thick layer of Titanium	Water contact angle measured and AFM used to investigate topography of deposited layer of titanium	MC3T3-E1 cells	Cell adhesion, morphology, proliferation and ALP activity	Yes -	Higher proliferation and ALP activity on titanium coated PEEK. In vivo titanium coated side of screws had significantly higher bone to implant contact ratio compared to bare PEEK

Author	Modification type	Material aspects investigated	Cells used	Biological behaviour investigated	In vivo work	Key findings
AM Rust-Dawicki et al	2000 Angstrom thick layer of titanium coated onto PEEK via plasma vapour deposition				Yes -	Both 4 and 8 weeks significantly higher % of bone contact for the titanium coated surfaces. No severe inflammatory response to any of the surfaces
Barkarmo et al	PEEK surface coated with HA nano particles				Yes -	Samples showed a general trend for higher mean values for coated surfaces but were not statistically significant.

4.4. Reasons for PEEKs use in this thesis

Given the material advantages PEEK has over competing biomaterials for orthopaedic device manufacture, we believe that it has the capacity to become the first choice biomaterial for a wide range of orthopaedic applications once a surface modification can be found which can improve the materials interaction with cells at its surface. Since PEEK can be injection moulded, it is possible to produce large numbers of identical nanopatterned substrates in a short space of time with equipment we already have. Due to this, we believed that PEEK was a natural choice to replicate biological results that had been derived from specific nanotopographies that were fabricated from other polymers.

Injection moulding, while providing an excellent method for producing the experimental surfaces required to test whether or not PEEK nanotopographies are capable of directing cell behaviour, also has the potential to be used to fabricate whole orthopaedic implants.

4.5. Initial goals of the PhD project

The broad idea for the project was to take the nanotopographies that had been developed at Glasgow (of particular interest was the NSQ nanopattern that had demonstrated the ability to direct stem cell behaviour in other polymers e.g. polycarbonate, PMMA), and see if they have the same effect when fabricated from PEEK. Given PEEK's potential as an implant material and its current shortcomings in terms of cellular response when compared to competing biomaterials, it was felt that if specific nanoscale topography incorporated into the PEEK surface could have a similar impact on cell response as that previously observed with other polymers, there would be a substantial potential market for nanostructured PEEK orthopaedic implants. It was also felt that as nanotopographical surface texturing does not require additional compatibility and toxicity testing in a way say a novel surface chemical treatment would, this type of technology would have a substantially shorter and cheaper lead time into clinic, and as a consequence,

would stand a good chance of becoming the standard surface modification for PEEK orthopaedic implant devices.

How does this thesis contribute to the field

The primary contribution that this PhD project will make to the use of PEEK in biomaterials applications, is to investigate if the incorporation of specific nanotopographies into its surface can alter how stem cells respond to the material. In addition to this, we also aim to further investigate the relationship between plasma treatment and the osteogenic response of stem cells, and the effect, if any, of using a combination of nanotopography and plasma treatments on cellular response.

4.5.1. Key objectives

- Can we use plasma treatment to address poor cellular response at the PEEK surface?
 - Poor cell response in terms of adhesion and proliferation is a major hindrance to working with PEEK both in vitro and in vivo. A surface treatment that can ameliorate the effects of this, without altering the bulk properties, would be of great use. There has been previous work in this area with positive results. We wanted to explore how different energies of plasma treatment effect the response of cells in order to find the most suitable treatment.
- Can we use plasma treatment and surface nanotopography to improve PEEK for use in orthopaedic implants?
 - PEEKs excellent material properties make it a natural choice for biomaterial applications, however poor cell response to the material provides an impediment to its wider use. A combination of plasma treatment to improve initial cell attachment and proliferation, as well as nanoscale topography to direct the behaviour of the cells once attached, could provide a mechanism for improving this.. So, the primary aim of this thesis is to try to identify a combination of plasma

modification and nanotopography to produce an improved cell response to the PEEK surface.

- Do the same nanotopographies fabricated from different polymers still have the same biological response?
 - Previous work carried out with the nanotopographies used in this thesis demonstrated consistency of nanotopography effect on cells across different polymers. If this also proved to be true of--for PEEK, it would offer the possibility of identifying other nanopatterns of interest in other cheaper and easier to handle polymers, which would then have the same effect when fabricated from PEEK
- Is Oxygen plasma treatment compatible with surface nanotopography?
 - As plasma treatment has been demonstrated to cause etching at material surface, we aimed to find a plasma treatment which could address poor cell response to the material without causing unacceptable damage to the nanotopography.

5. Materials and methods

5.1. Substrate fabrication

The following is a description of the parameters for the injection moulding process used to produce the nanotopographies used in this PhD thesis. For a description of how the process of injection moulding works, please consult the appropriate section in the “Introduction” chapter of this thesis. The substrates used in this thesis were provided by member of the University of Glasgow bioelectronics research group.

Both PEEK and Polycarbonate substrates were produced by an Engel Victory 28 ton injection moulder. For PEEK, processing parameters were set as prescribed by the polymer manufacturer. The nozzle temperature was 375°C, (dropping 5°C per zone towards the hopper), the tool temperature was 180°C and the injection speed was moderate (ca. 20-30 cm³/sec). Polycarbonate was used as a control material, as it has been used previously in this field and has already been optimized for biological work.

Nickel shims for embossing were made directly from the patterned PMMA resist. A thin (50nm) seeding layer of Ni-V (7% vanadium) was sputter coated on both of the samples. The layer acted as an electrode in the galvanic bath where nickel was plated electrochemically on the Ni-V to a thickness of ca. 300µm. Once returned from galvanic plating, the nickel shims were cleaned by firstly stripping the polyurethane coating using chloroform in an ultrasound bath for 10-15 minutes, rinsed thoroughly in ROH₂O, dried in a stream of nitrogen and then checked by AFM.

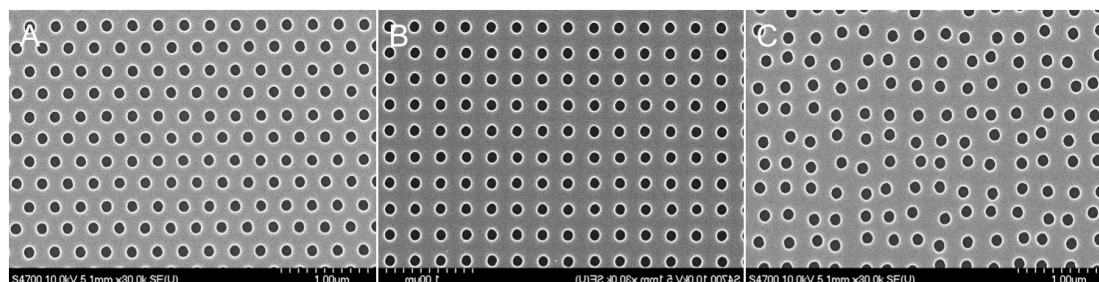


Figure 14 Electron micrographs of the different nanotopographies produced via injection moulding used in this thesis. (a) hexagonal nanopattern (HEX). (b) square nanopattern (SQ) (c) disordered square nanopattern (NSQ). Provided by the University of Glasgow bioelectronics research group (BiG)

5.2. Cell culture

Over the course of the PhD project a number of different cell types were used in different experiments. In each instance the cell type used was chosen based on the requirements of the experiment and the properties of the cells themselves. For example, the osteoprogenitor cells provide by far the more accurate representation of how cells in the human body would respond to one of our experiment surfaces when implanted in the femoral cavity (the source of the osteoprogenitor cells). However these cells have to be extracted from human bone marrow in a process that takes considerable time and practice to perfect, and yields a relatively small number of cells which divide slowly. Osteoblasts from a cell line (for examples the SAOS-2 osteosarcoma cell line) provide a large number of cells very quickly, and are also commercially available. However, as a consequence their behaviour shows less similarity to that of cells in the human body than that of primary cells. Due to the different practicalities of handling, and nature of the data provided by these different cell types, the most appropriate cell type for the goals of the given experiment was used in each instance

Cells were seeded on substrates at varying cell densities calculated using a haemocytometer. Substrates were sterilized by washing in ethanol for a minimum of 30 minutes, then washed in HEPES or PBS and finally washed in the appropriate media. The substrates were then placed in six well plates and left to dry in the laminar flow hood. A 0.3 ml droplet was then deposited and spread across the surface of each substrates and left for 30 minutes in order to give cells sufficient time to settle on the surface. 3ml of the appropriate media was added per well and the samples were then incubated at 37° C in a 5% CO₂ atmosphere. The medium was changed the day after seeding and subsequently on Mondays, Wednesdays and Fridays. .

h-TERT cells

Infinity telomerase immortalized human fibroblasts (hTERT-BJ1, Clontech, USA) were cultured in complete medium. The medium used was 71% Dulbecco's modified eagles medium (DMEM) (Sigma, UK), 17.5% medium 199 (Sigma, UK), 9% foetal calf serum (FCS) (Life Technologies, UK), and 0.9% 100mM sodium pyruvate (Life Technologies, UK)

Complete culture medium

DMEM 400ml

Medium 199 100ml

Foetal calf serum 50ml

Antibiotics 10ml

Sodium pyruvate 5ml

SAOS-2 cells

The Osteosarcoma cell line SAOS-2 cells were cultured in complete medium. The medium used was 71% Dulbecco's modified eagles medium (DMEM) (Sigma, UK), 17.5% medium 199 (Sigma, UK), 9% foetal calf serum (FCS) (Life Technologies, UK), and 0.9% 100mM sodium pyruvate (Life Technologies, UK)

Osteoprogenitor cells

Marrow was donated from waste femoral heads from total hip replacement, with NHS and local ethical approval. Bone marrow samples were taken from haematologically normal patients undergoing routine hip replacement surgery. Bone marrow was divided equally into two sterile universals and was centrifuged for 10 minutes at 1400 RPM. The supernatant was then removed to waste, the pellet re-suspended in 10ml of media and then centrifuged at 1400 RPM for ten minutes. After centrifugation, the supernatant was removed to waste and the pellet was re-suspended in 10ml of media and was overlaid on a 7.5ml Ficoll gradient and centrifuged for 45 minutes at 1513 RPM. After being allowed to stand for 10 minutes, cells were harvested from the interface to a fresh universal and made up to 10ml with media, and then centrifuged for 10 minutes at 1400 RPM. This was done twice. The pellet was then re-suspended in 10ml of media and transferred to a t25 vented flask and cultured in a 37°C incubator. Cells were

cultured in complete medium. The medium used was 87.71% (500ml) Dulbecco's modified eagles medium (DMEM) (Sigma, UK), 8.77% (50ml) foetal calf serum (FCS) (Life Technologies, UK), 3.70%(10ml) antibiotics, 0.87%(5ml) 100mM sodium pyruvate (Life Technologies, UK) and 0.87%(5ml) MEM Non-essential amino acids 100X (Gibco Invitrogen).

271⁺ MSCs

271⁺ MSCs were extracted from primary osteoprogenitors through a process of magnetic sorting using the Easysep human CD271⁺ cell selection kit produced by Stem Cell Technology. Osteoprogenitor cells were cultured until 70 - 80% confluent. They were then trypsonised with trypsin/versine to detach the cells from the culture flask. Once the cells had been removed, they were centrifuged at 1400 RPM for 10 minutes and all media removed. The cells were then re-suspended in 500µl volume of 1xPBS with 2% FBS and transferred to plastic tubes for use with the sorting magnet. 12.5µl of human FcR receptor blocker was then added to the solution and mixed several times before the addition of 25µl positive selection cocktail, and mixed again by pipetting. The solution was incubated at room temperature for 15 minutes before adding 25µl of magnetic nanoparticles and the sample again mixed by pipetting and incubated for 15 minutes at room temperature. The solution was made up to 2.5ml through the addition of PBS/FBS and then placed inside the selection magnet without the plastic cap. The solution was incubated in the magnetic field for 5 minutes and then inverted in a continuous motion for 2-3 seconds to remove unselected cells and then returned to an upright position. The tube was removed and 2.5ml PBS/FBS added and mixed again and the plastic tube returned to the selection magnet for a further 5 minutes. This process was repeated a further 3 times to ensure unselected cells were removed from the suspension. The cells remaining within the plastic tube were CD271⁺ MSCs, as they had been positively selected by the magnetic sorting protocol.

5.3. Histological staining

5.3.1. Coomassie staining

After the specified period of cell culture, the cells on the test substrates were fixed in 2ml of 4% formaldehyde/PBS fixative at 37°C for 30 minutes. The cells were then stained for 2 minutes in 0.5% Coomassie blue in a methanol/acetic acid aqueous solution and washed with water to remove excess dye.

Coomassie blue

1g Coomassie brilliant blue (BioRad) in 1L of methanol - 50%, glacial acetic acid - 10% and H₂O - 40%

Fixative

10ml of formaldehyde in 90ml of PBS

2g of sucrose

5.3.2. Alizarin staining

The cells on the test substrates were fixed in 2ml of 4% formaldehyde/PBS fixative at 37°C for 30 minutes. The substrates were washed three times in milliequ water and then stained with 3ml of 40mM Alizarin red and then incubated on an orbital shaker for 1 hour. After staining, the cells were then washed five times in milliequ water then washed for fifteen minutes on an orbital shaker in PBS, and finally washed in milliequ water to remove salts.

Alizarin red s 40mM

1.369g Alizarin red s made up in 100ml milliequ water

pH is brought up to 4.2 from around 3.5 with sodium hydroxide.

Fixative

10ml of formaldehyde in 90ml of PBS

2g of sucrose

5.3.3. Alizarin quantification

After drying the stained substrates the Alizarin was dissolved off the surface with 10% Cetyl Pyridinium Chloride Monohydrate and incubated on an orbital shaker for

one hour in a fume hood. 200µl of each sample was loaded into a 96 well plate along with appropriate standards, and absorbance was measured at 550nm.

5.3.4. Von Kossa staining

The cells on the test substrates were fixed in 2ml of 4% formaldehyde/PBS fixative at 37°C for 30 minutes. Silver Nitrate was added to the substrates which were then exposed to strong light for 30 minutes and washed with milleque water. 5% Sodium Thiosulfate was added for 10 minutes then the substrates were rinsed with tepid tap water for 10 minutes before being washed with milleque water. The substrates were then counterstained with nuclear fast red, washed in milleque water and finally washed in 70% ethanol.

5% silver nitrate

5g silver nitrate

100ml milique water

stir together

5% sodium thiosulphate

5g sodium thiosulphate

100ml millique water

stir together

nuclear fast red

0.1g nuclear fast red

5g aluminium sulphate

100ml millique water

boil for 5-10 minutes while stirring, cool down and then filter.

Fixative

10ml of formaldehyde in 90ml of PBS

2g of sucrose

5.3.5. Alkaline Phosphatase staining

The cells on the test substrates were fixed in 2ml of 4% formaldehyde/PBS fixative at 37°C for 30 minutes. The cells were then stained with the alkaline-dye mixture wrapped in tinfoil and left for one hour. After the incubation period the stain was removed to waste and the substrates were washed in distilled water to remove non-adherent stain.

5.3.6. HRP based immunostaining

Staining was carried out using the Dako Envision AEC staining kit (Product K4004)

The cells on the test substrates were fixed in 2ml of 4% formaldehyde/PBS fixative at 37°C for 30 - 45 minutes. The fixative was removed, and peroxidase block solution was added to the samples, which were then incubated at room temperature for 5 minutes. The peroxidase block was then removed and replaced with permeability buffer, and the samples were incubated at 5°C for 5 minutes. The permeability buffer was removed and replaced with PBS/BSA and incubated at 37°C for 5 minutes. The PBS/BSA was removed and replaced with the primary antibody, after which the samples were wrapped in tinfoil and incubated at 37°C for 1 hour. The primary antibody was removed, and the samples were washed 3 times for 5 minutes each with the last wash taking place on an orbital shaker. The PBS/Tween was removed and replaced with the peroxidase labelled polymer and incubated at room temperature for 10 minutes. The peroxide labelled polymer was then removed and the AEC substrate chromagen added to the samples and then incubated at room temperature for 10 minutes. The AEC chromagen was then removed and samples thoroughly washed and allowed to dry.

5.3.7. Fluorescence based immunostaining

The cells on the test substrates were fixed in 2ml of 4% formaldehyde/PBS fixative at 37°C for 30 - 45 minutes. The fixative was removed, permeability buffer was added to each of the samples and they were then incubated at 5°C for 5 minutes. The permeability buffer was then removed and PBS/BSA was added to each of the samples and they were then incubated at 37°C for 5 minutes. The PBS/BSA was then removed and the primary antibody with phalloidin was added and the samples wrapped in tinfoil and incubated at 37°C for 1 hour. The primary antibody was

then removed and samples washed 3 times for 5 minutes each with PBS/Tween, with the last wash taking place on an orbital shaker. The PBS/Tween was removed and replaced with the secondary antibody, and the samples wrapped in tinfoil and then incubated at 37°C for 1 hour. The secondary antibody was then removed and samples washed 3 times for 5 minutes each with PBS/Tween, with the last wash taking place on an orbital shaker. The PBS/Tween was removed and replaced with Streptavidin-FITC and the samples wrapped in tin foil and incubated at 5°C for 30 minutes. The Streptavidin-FITC was removed and samples washed 3 times for 5 minutes each with PBS/Tween, with the last wash taking place on an orbital shaker. The samples were then mounted with a coverslip with a drop of vectroschild-DAPI.

Fixative

10ml of formaldehyde in 90ml of PBS

2g of sucrose

PBS/BSA

1g Bovine serum albumin in 100ml PBS

PBS/Tween

0.5ml Tween20 in 100ml PBS

Permeability buffer

10.3g sucrose

0.292g NaCl

0.06g MgCl₂

0.476g HEPES

100ml PBS

TritonX 0.5ml

qPCR

After the appropriate culture period (11 days), the Osteoprogenitor cells were harvested from substrates, lysed and total RNA was extracted using a Qiagen

RNeasy kit. The RNA samples were treated with DNase and reverse-transcribed using the SuperScript first-strand synthesis system for real-time PCR (Invitrogen). Real-time qPCR was carried out using the 7500 Real Time PCR system from Applied Biosystems for analyzing expression of GAPDH, RUNX2 and BMP2. GAPDH served as the house-keeping gene, and expression for the genes of interest was normalized to GAPDH expression.

5.4. Microscopy

5.4.1. Whole substrate scans

Images of stained substrates were taken using an Epson Perfection V500 Photo high resolution scanner at 16 bit grayscale scanning quality and 6400 DPI resolution. Analysis of levels of cell adhesion on substrates was done using ImageJ software.

5.4.2. Polarised light microscopy

When we examined our histologically stained PEEK samples under the microscope we observed a highly coloured surface where it was difficult to pick out exactly what was stained, and an image which bore very little resemblance to what standard examples of histological staining are meant to look like. As a result, it was difficult for us to tell if there was positive staining present and secondly, if we had carried out the staining process correctly.

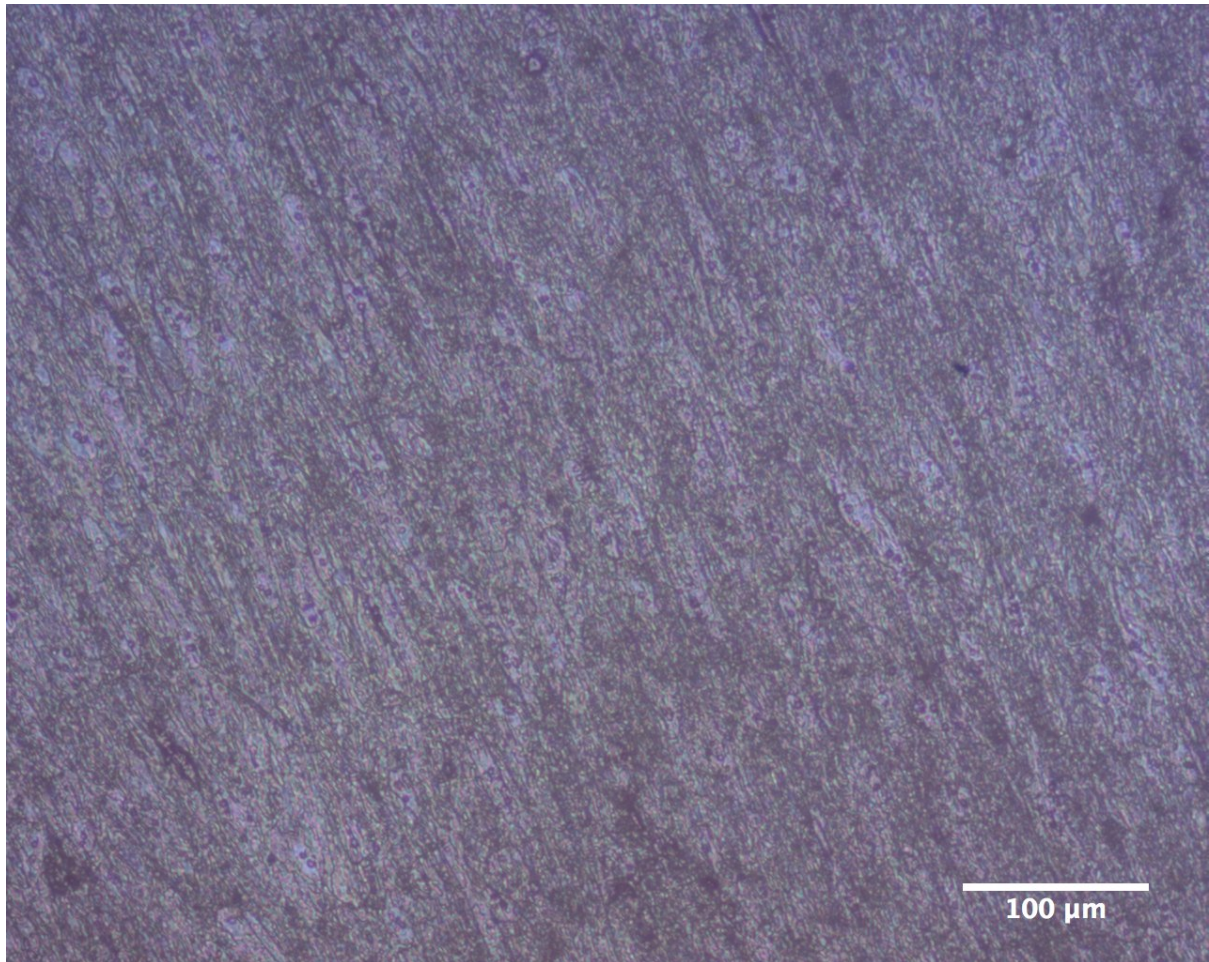


Figure 15 Example of von Kossa staining of osteoprogenitor cells on PEEK viewed via reflected light microscopy without the use of polarized light.

We believed that this was down to our samples exhibiting birefringence, a phenomenon where two components of light pass through or are refracted from the surface being observed, and do so at different speeds. As a result, they experience different refractive indices and interfere with each other, leading to what we see with histologically stained samples on PEEK viewed with reflected light microscopy.

To address this we opted to use polarised light microscopy. Polarised light microscopy is a method for enhancing the contrast, and by extension, the quality of the image produced for birefringent materials compared to that which would be produced by other forms of microscopy. It works by recombining the different light components that have become out of phase due to the birefringence of the material being observed. Only the components of the two beams that are travelling in the same direction and vibrating in the same plane are re-combined .

The polarisation filter ensures that the beams have the same amplitude when they are re-combined to provide maximum contrast.

The use of polarized light had a marked effect on the images generated from our surfaces. It allowed us to clearly and unambiguously identify the different stained components on the surfaces.

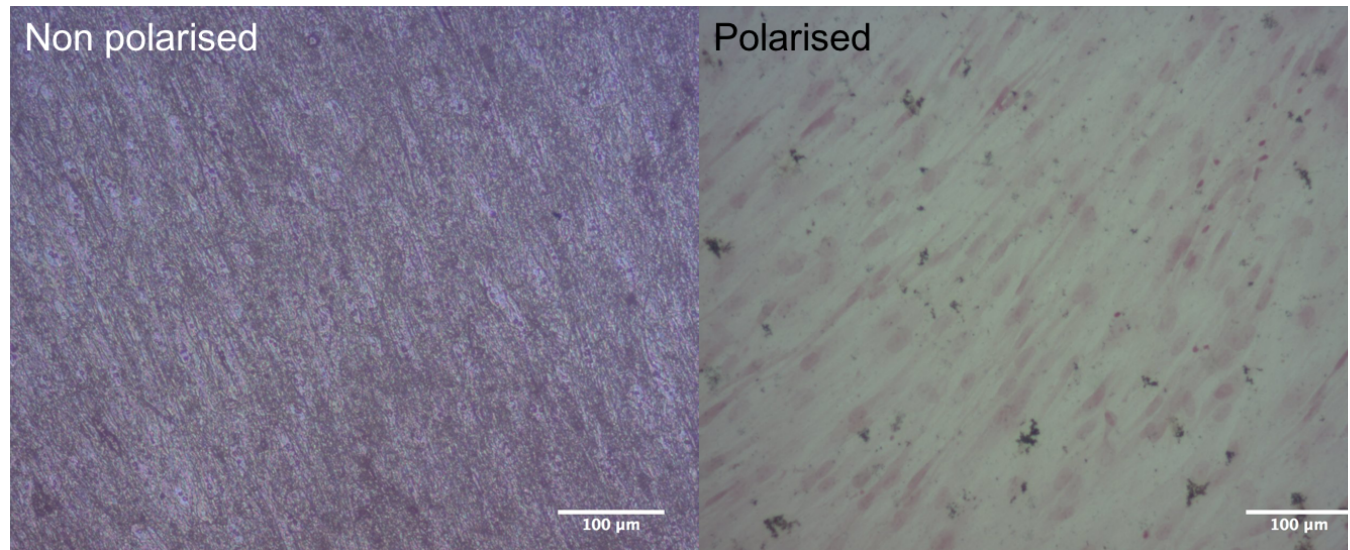


Figure 16 Comparison of the same cell prolifer pipeline processing the same area of the surface of a von Kossa stained sample without, and then with polarised light filters. Scale bar = 100um

As we can see, the use of polarized light microscopy allows us to clearly differentiate between unstained background, cell nuclei that have been stained pink/red, and phosphate containing material that have been stained black.

The use of polarized light microscopy produces images with clear enough definition between stained and unstained areas on the images to allow us to use Cell Profiler to measure the stained material.

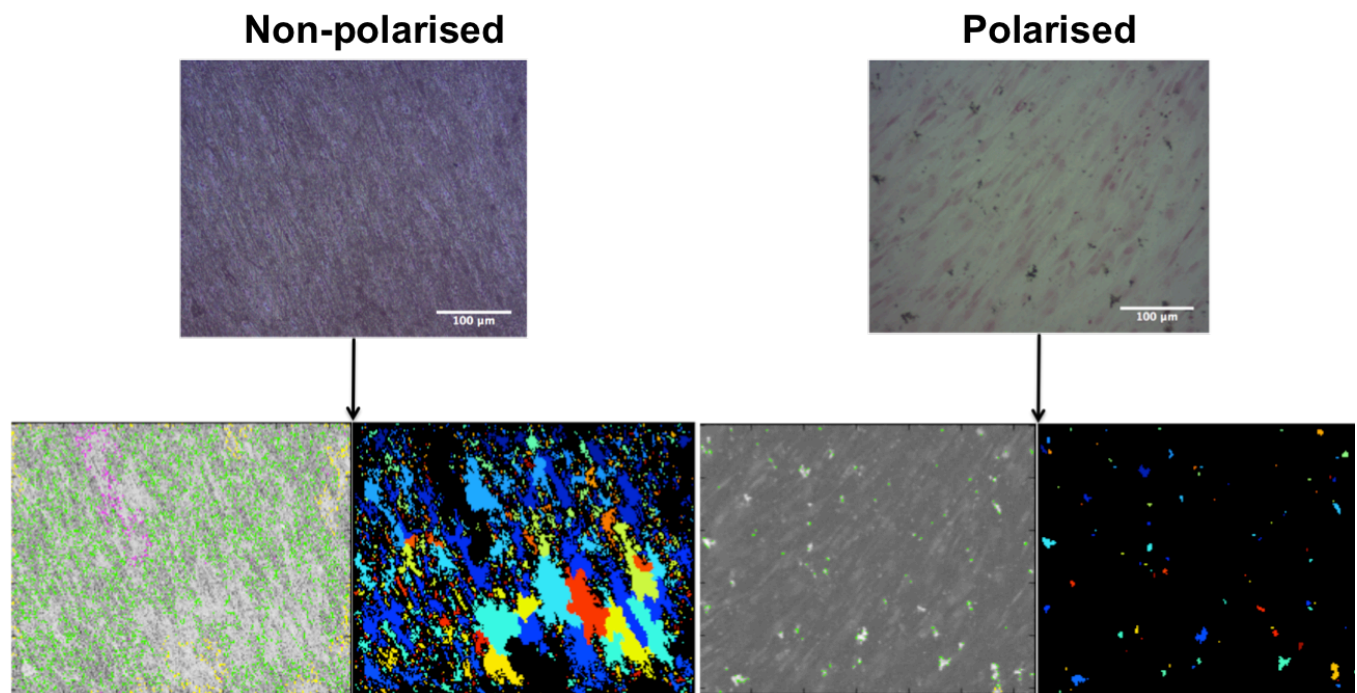


Figure 17 Comparison of the same cell prolifer pipeline processing the same area of the surface of a von Kossa stained sample without and then with polarised light filters. As we can clearly see the use of polarised light filter allows the accurate identification of only stained mineral (black objects) and not background material or stained cell bodies (pink objects). Scale bar = 100um.

5.4.3. Scanning Electron Microcopy (S.E.M)

Images were taken using a Hitachi S-4700 Field emission scanning electron microscope.

S.E.M Sample preparation

Samples were rinsed in 0.1M PIPES pH 7.4 for 2 minutes then fixed in 2.5% gluteraldehyde in 0.1M PIPES pH 7.4 for 5 minutes. They were then rinsed with 0.1M PIPES pH 7.4 for a total of 5 minutes (one 2 minute rinse and a subsequent 3 minute rinse). The samples were then post fixed in 1% Osmium Tetroxide in 0.1M PIPES pH 6.8 for 60 minutes. They were then rinsed in MilliQ water for a total of 5 minutes (one 2 minute rinse and a subsequent 3 minute rinse), and finally dehydrated with an alcohol series 50%, 60%, 70%, 80%, 96% and 100% for 5 minutes each. The samples were then transferred to the critical point dryer in ethanol where they were dried prior to sputter coating.

5.5. Image analysis/quantification

Cell Profiler is image analysis software that was designed to identify and quantify cell phenotypes. Originally developed to work in conjunction with samples that had been fluorescently immunostained, the analysis programme works by measuring the intensity and localisation of each of the fluorescently labelled objects present. The programme delivers information on the number, size and shape of these objects.

The major advantage which Cell Profiler has over competing image analysis software such as imageJ, is its capacity for handling very large data sets (it is capable of handling up to the order of hundreds of thousands of images) in an automated fashion, permitting a high throughput screening approach for experiments that use different forms of histology.

Cell Profiler uses a series of sequential operations (referred to as modules) to identify and measure objects present in images. These operations are grouped into pipelines. Once a pipeline has been established a large number of images can be loaded into Cell Profiler, which can then independently run each of these images through the specified pipeline, and once finished, can present the researcher with the results for the full set of images.

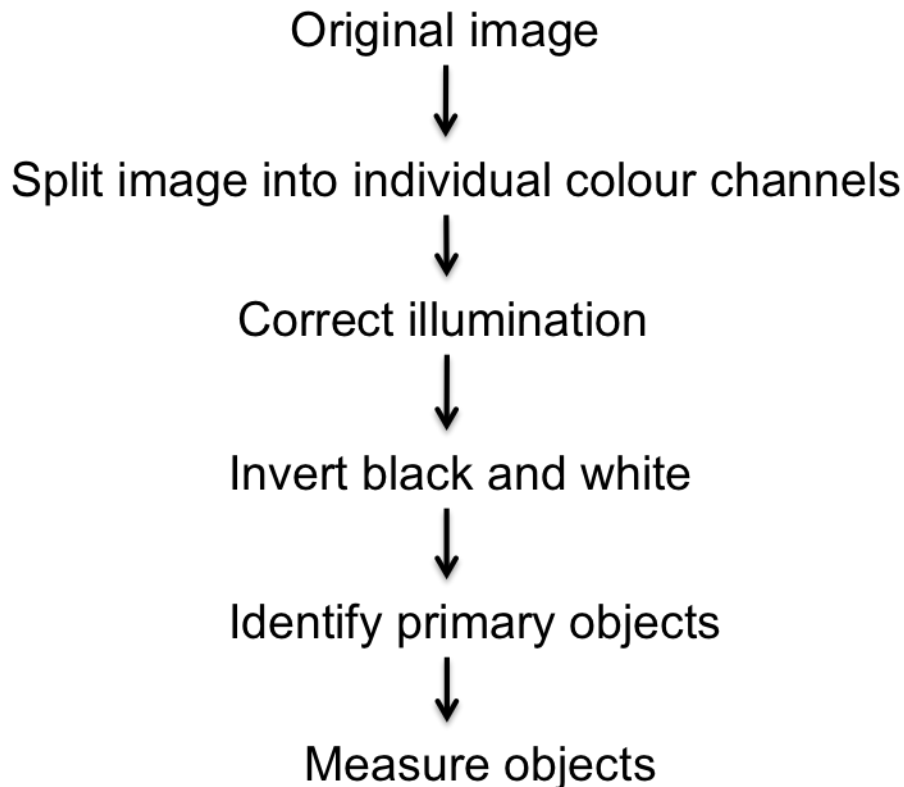


Figure 18 Schematic diagram of the stages involved in a Cell Profiler pipeline. Each different stage has differing numbers of operations involved with them. For example “Invert black and white” only has one operation, while “Identify primary objects” has a large number of different parameters to be adjusted in order to correctly identify stained material.

The modules involved in any given pipeline can be divided into three main categories; *Image processing* including illumination correction, *cell identification* and then *measurement and data analysis*.

If we were to use Cell Profiler to identify, and then measure the stained material in microscope images of von Kossa staining, the image would pass through the different modules outlined in figure 1. Firstly it is worth noting that in the microscope image, the von Kossa staining process has identified both material containing phosphate (stained black) and SAOS-2 cell nuclei (stained red/pink by nuclear fast red). This provides an extra challenge for Cell Profiler, as we want it to only identify the black stained material and nothing else. After the image has been loaded into the pipeline the next step is to split the colour microscope image into one colour channel, which will be the image used through the rest of the pipeline. In each instance, the colour channel chosen is the one that offers the greatest degree of contrast, in the case of von Kossa staining this is the green channel.

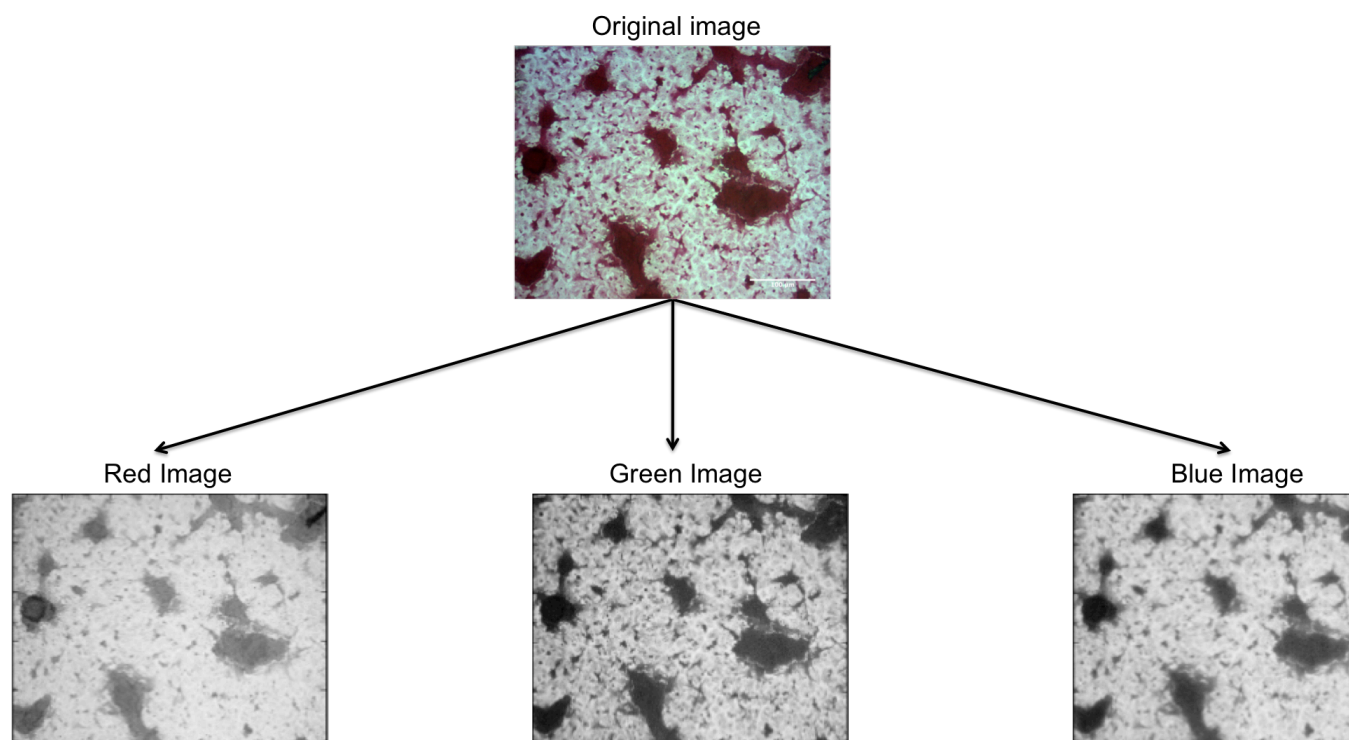


Figure 19 Demonstration of the channel splitting stage in a Cell Profiler pipeline. As Cell Profiler cannot process colour images the original image, in this case an example of von Kossa staining, is split into its constituent colour channels. As each colour channel has a differing degree of contrast, the operator must decide which image is clearest in order to generate the most accurate results further down the pipeline.

The next step after this is to correct the illumination of the image. As all the images that we analysed with Cell Profiler were taken with reflected light microscopy, the illumination across the surface was not uniform, and the images tended to be significantly brighter around the edges. If this was left unaddressed, it would cause the pipeline to be unable to accurately identify objects in these areas. As Cell Profiler was originally intended to analyse fluorescently stained samples (where by default the only bright objects are those that are fluorescing), the pipeline now has to invert black and white in the image in order for the pipeline to be able to correctly identify the stained material. At this point the pipeline can now identify and measure the stained material present in the image.

While Cell Profiler pipelines do follow a consistent sequence of actions, each individual pipeline requires considerable modification by the operator to ensure

that it accurately measures the stained material present in the images being analysed.

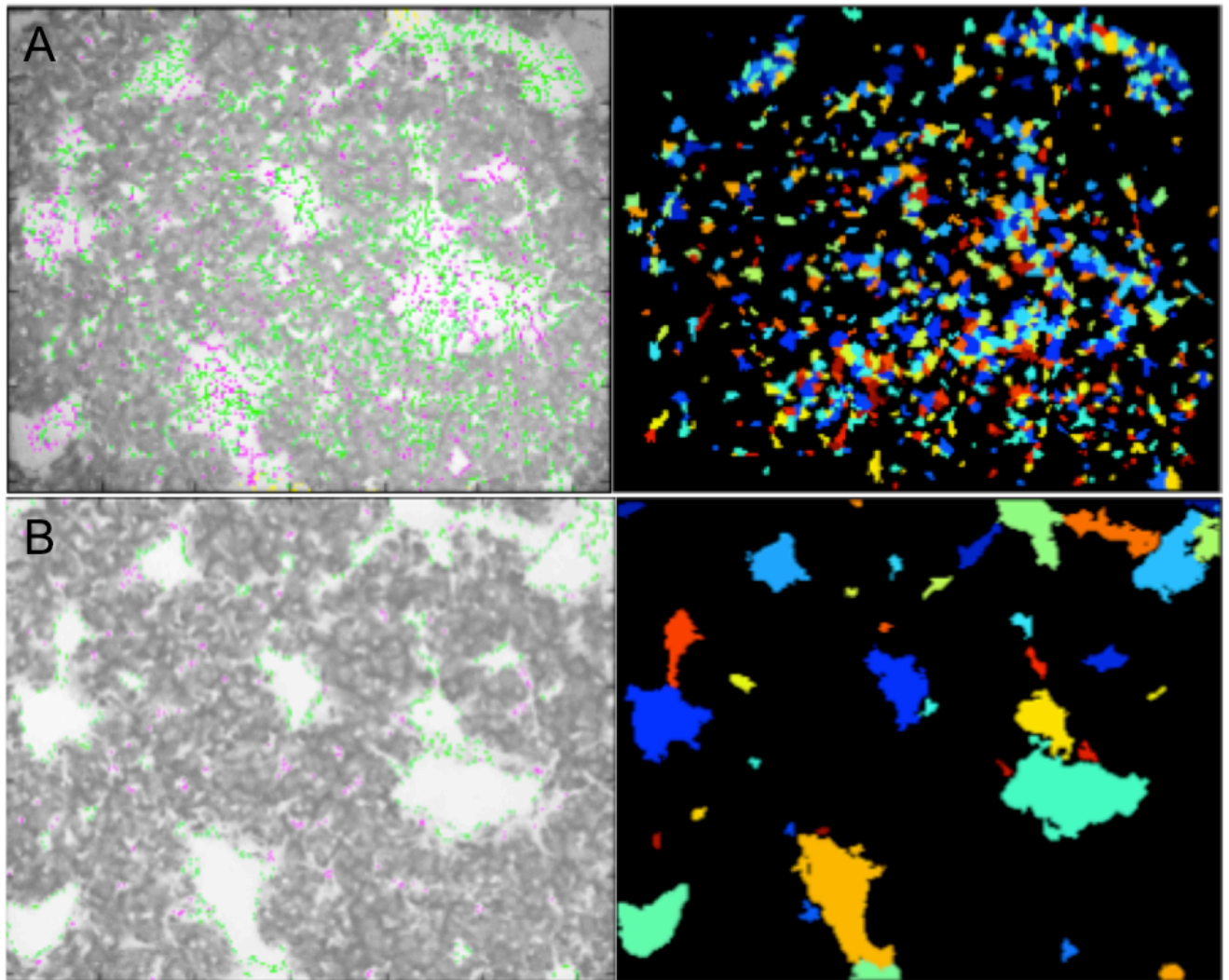


Figure 20 Example of the effect that alterations to identification and analysis parameters have on the identification of stained material. Image A has had no modification of the identification parameters in its pipeline outside of what it required to move the image through the pipeline, whereas image B has had extensive modification in order to accurately identify only stained material in the image.

If we use an image of von Kossa staining as an example, we can see that at the primary objects identification stage the identification parameters have to be closely tailored to ensure that only the stained material is being picked up by the programme. This is a stage where it is essential that the designer of the pipeline has a clear idea of what material in the image should and should not be marked out. As we can see in figure 3, alterations in the different parameters used in the pipeline strongly effects how much material is included as being marked or not. When we look at the original staining microscope images we can clearly see the large black coloured areas that indicate the presence of phosphate (which is the

type of staining we want to count), and we can also see small areas dotted around the image where the pink/red nuclear fast red cell nuclei is a little darker.

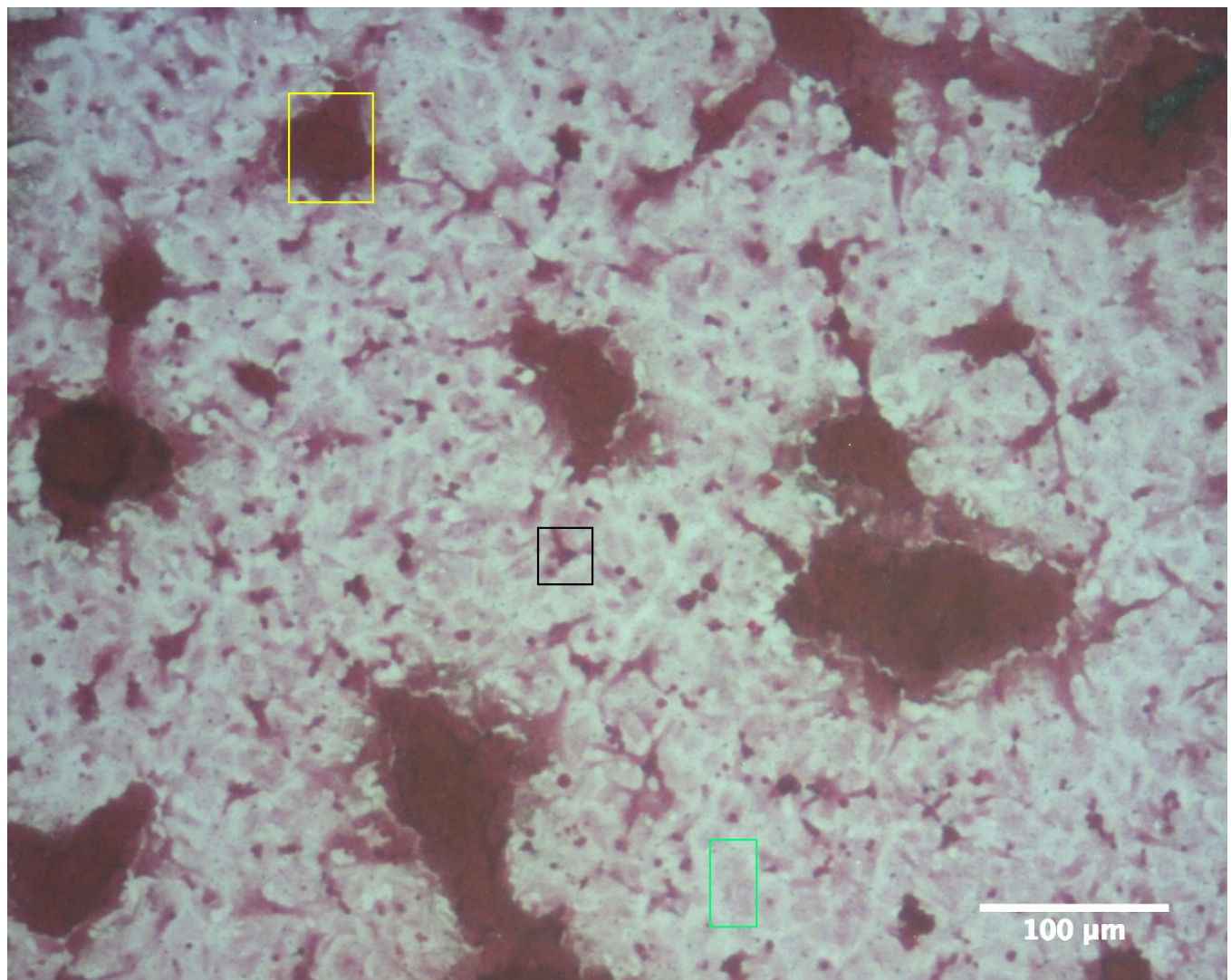


Figure 21 Example of different features present on a microscope image analysed by Cell Profiler. The pipeline should be designed to count objects that have been stained black (yellow box) indicating the presence of material containing phosphate. It should not count cell nuclei stained pink/red (green box). This is complicated by the presence of denser areas of nuclear fast red staining which can look black (black box).

To satisfy our requirements for what we wish Cell Profiler to do, we require the pipeline to mark out the large black areas, but not the small darker areas of nuclear fast red staining. By selecting the appropriate set of pipeline identification parameters, we are able to achieve this (fig4 A). However, by altering the pipelines parameters we can achieve a higher (B, D and E) or lower (C) level of recognized objects.

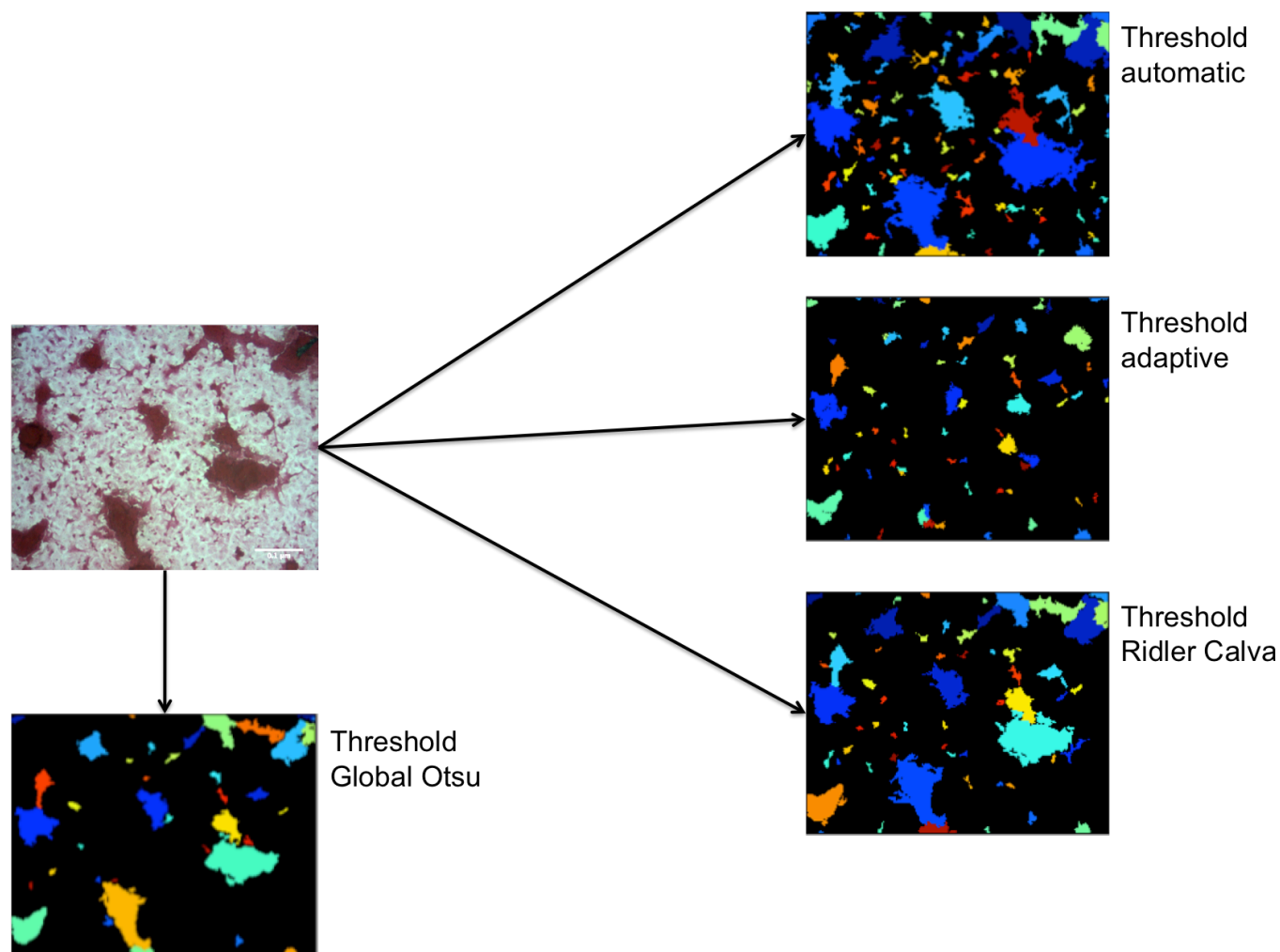


Figure 22 Comparison of how different analysis algorithms in the “identify primary objects” module of a pipeline can affect how much material on an image is counted as being stained. In each example all of the variables in the pipeline are identical, apart from the method used for thresholding. Global Otsu was the method that we felt gave the best representation of the stained material present in the original image.

As well as alterations to the parameters that govern the identification of the primary objects, other modules in a Cell Profiler pipeline can have strong effects on the ability of the pipeline to quantifying the staining present in a given image.

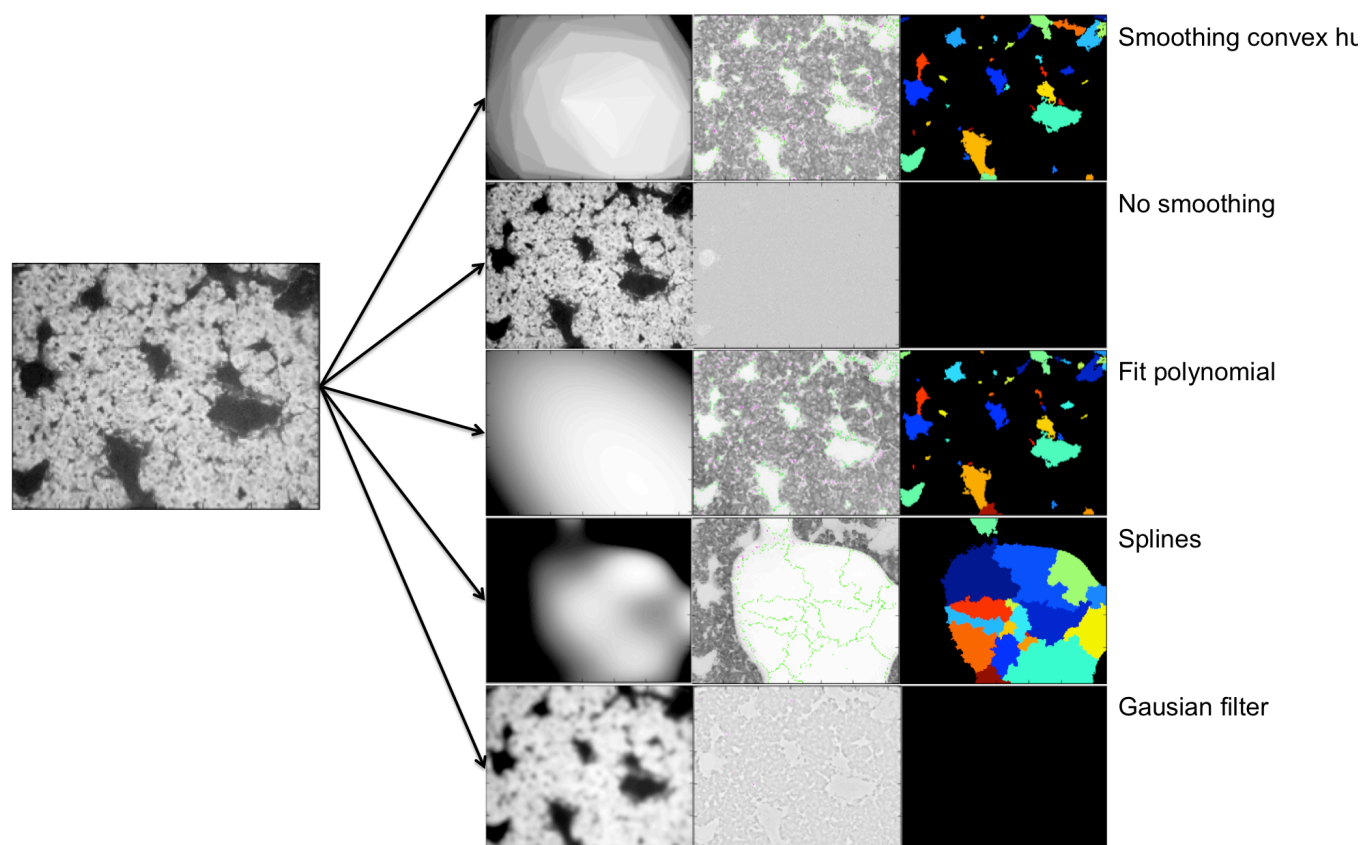


Figure 23 The impact of different methods for correcting illumination in an image, on the pipelines ability to identify stained material.

For example alterations to the smoothing filter that the pipeline uses to correct the illumination across an image can have significant downstream effects on the ability of a pipeline to accurately identify stained material in the image.

While different pipelines were established for different experiments, within an experiment all the images are run through the same pipeline to ensure that there is consistency in how different surfaces are compared to each other.

5.6. Plasma treatment

Oxygen plasma treatment was carried out using a Gala instruments plasmaprep 5 asher using Oxygen as gas. All samples were treated at 0.2 mbarr of pressure and at a time and power as described in the appropriate figure legend. Substrates treated with the Gala instruments plasmaprep 5 asher are from here on referred to as being Oxygen plasma treated

5.7. AFM

The AFM work included in this thesis was kindly performed for the author by Dr John Stormonth-Darling. The readings themselves were taken with a Veeco Dimension 3100 Atomic Force Microscope with a sharpened tetrahedral tip that has

a radius of 7nm. The readings were taken in “tapping” or intermittent contact mode, where the AFM tip rapidly oscillates over the sample, only making contact with the surface at the lower part of the oscillatory. This is preferred to a continuous dragging of the tip across the surface, as it both reduces wearing to the AFM tip and the possibility of particles from the material surface collecting on the tip. To assess etching of the PEEK surface due to plasma treatment, average roughness (R_a) was measured. Average roughness is described by the following equation

$$R_a = \frac{1}{L} \int_0^L |Z(x)| dx$$

Where $Z(x)$ is the function that describes the surface profile analysed in terms of height (Z) and position (x) of the sample over the evaluation length “ L ”. As a result R_a is the arithmetic mean of the absolute values of the height of the surface profile⁹⁵

5.8. Sessile drop water contact angle measurement

Water contact angle was measured using Kruss G10 contact angle measuring instrument. Three different measurements were taken per sample and an average of the three readings was expressed as the water contact angle for a surface.

5.9. X-ray photoelectron spectroscopy

X-ray photoelectron spectroscopy (XPS) has been applied to measure the elemental composition of chemically modified surfaces. It is a surface specific method as its probing depth is about 5-10 nm. An X-ray source illuminates the investigated surface. As a result photoelectrons are emitted with a kinetic energy specific for the individual elements. Subtraction of the measured electron kinetic energies from the energy of the impinging X-ray photons produces a spectrum of electron binding energies. The measured intensities are proportional to the elemental composition. A Specs Sage 100 instrument equipped with a non-monochromatised AlK α or MgK α X-ray source at a power of 300 W was used. Elements were identified and quantified from survey spectra (0-1100 eV, 100 eV pass energy). All of the samples were measured with a take-off angle of 90°.

5.10. Statistical analysis

T-Tests were used to probe for significant differences in experimental results. In each instance the results from the experimental surface (either the NSQ or SQ nanotopographies) were compared to the results from the control surface (the planar surface). The threshold for results being considered significant was set at 0.05 and highly significant at 0.001. Biological replicated were carried out in triplicate and an average taken of the results. In each relevant experiment the overall number of replicates used N, and the number of each different topography used is listed in the figure legend.

6. Use of plasma treatment to address poor cell response to PEEK

6.1. Introduction

6.1.1. Requirements for PEEK surface modification for use in biomaterials applications

While PEEK has a range of material properties that make it an extremely promising option for use in a number of biomaterial applications⁶⁴ it also displays a low level of initial cellular adhesion and growth of cells seeded on to it⁶⁵. This is problematic for two reasons. From the perspective of using PEEK in biomaterial applications and in particular in orthopaedic implant devices, a failure to generate a layer of adherent cells on the implants surface leads to a risk of the fibrous encapsulation occurring, preventing the formation of the desired strong interface between the implant and the patients tissue⁶.

Additionally, given that we are trying to investigate how cells respond to the nanotopography at the PEEK surface, if we can not get cells to adhere to the surface it is hard to look at how their behaviour is altered by the presence of nanotopography at the surface.

6.1.2. Oxygen plasma treatment for improved biomaterials

Oxygen plasma treatment is a method of modifying a material to increase surface energy by supplying energy to a gas (in our case oxygen) causing it to become ionized, whereby electrons are disassociated from their atoms with the gas forming a plasma⁸⁵. Under low temperature/low pressure conditions the ionized region of the gas includes ions, high energy photons, electrons, radicals and other excited species⁸⁵. These components react with the surface of the material altering the chemical environment through the incorporation of reactive species at the material surface. This has been demonstrated to improve the cytocompatibillity of polymers⁹⁶ including PEEK⁹⁷ without altering the bulk properties of the material.

It is worth noting that oxygen plasma treatment has been demonstrated to cause etching to the materials it is applied to⁸⁵. Since our surfaces have a specific

nanopattern incorporated into their surface, it would defeat the purpose of the investigation to use a surface modification method that completely removed or substantially damaged the nanotopography. And as such, the relationship between plasma treatment and degree of etching on the nanoscale needed to be investigated.

6.1.3. Alternative approaches to modifying the PEEK surface

As poor surface cellular adhesion is an issue for any researchers working with PEEK, there have been a number of different approaches to modifying the surface of the material in order to address this. These can be split into two broad approaches; either modifying the PEEK surface via chemical treatment or deposition of a more bioactive material onto the surface, or by producing a PEEK composite material.

Due to our use of injection moulding to produce our experimental surfaces we were not interested in employing PEEK composites, as this would have required substantial work around the optimisation of the parameters of the injection moulding process, which was not within the scope of this particular PhD project. Adding a layer of bioactive material (such as hydroxyapatite), or a metal such as titanium would run the risk of obscuring the nanotopography present. It may be possible to add a layer of such materials while not altering the desired dimensions of the nanofeatures, by investigating the deposition behaviour of the chosen coating material and then producing nanofeatures where the dimensions took into account this behaviour. For example, if it was found that a layer of titanium 50nm thick could be consistently deposited, and nanopits of 200nm were desired, then producing PEEK nanopits of 250nm depth would still be 200nm deep after titanium deposition. However, investigating deposition and designing new nanotopographies was not within the scope of this particular PhD project.

In terms of other chemical treatments based on the literature, plasma treatment using oxygen gas looked be the best of the previously used methods, but testing different chemical treatment would have moved us further away from our goal of testing the impact of nanotopographies in PEEK on cellular response.

6.1.4. Aims of the chapter

With these experiments our aim was primarily to investigate whether or not oxygen plasma treatment could be used successfully to address poor cellular adhesion and proliferation at the PEEK surface. In particular, we wanted to see if we could find an oxygen plasma treatment that would address the problems we were having with poor cytocompatibility at the PEEK surface, without causing unacceptable etching damage to our nanotopographies.

6.1.5. Experimental outline

In light of this, our experiments in this area can be split into two broad groups. Firstly experiments to investigate if oxygen plasma treatment can address PEEK's innate cytophobicity to the point where we can culture a sufficient number of cells on our surfaces to see if the presence of the topography is having a significant impact on the cells behaviour. To do this we initially seeded cell line cells (H-TERT and LE2 cells) on nanopatterned PEEK surfaces that had been treated with atmospheric plasma, and after a period of culture, stained the cells with coomassie blue to gauge the level of cell growth. We then moved onto treating the surfaces with oxygen plasma, and using SEM and alamar blue proliferation measurement to observe the changes in cell response to these treated surfaces.

Secondly, given the understanding that the oxygen plasma treatment could etch the surface and as a result disrupt the nanotopography present at the surface, we wanted to investigate how the topography of the surface was altered in response to the treatment, as well as generate as much information as we could on other physical/chemical changes the surface has undergone as a result of the treatment. AFM was used to investigate changes in nanotopography of the surfaces over a range of different plasma treatments in order to assess what morphological changes had taken place as a result of the treatment. We also took water contact angle measurements and XPS readings to further investigate alterations to the PEEK surface as a result of the plasma treatment.

Finally, we wanted to check if a plasma treatment that we felt had not caused unacceptable damage to the nanotopography, would be sufficient to allow enough

primary osteoprogenitor cells to develop. This was achieved by culturing primary osteoprogenitor cells on PEEK surfaces that had been given plasma treatments that we did not think would cause significant etch damage to the nanotopography, and then staining with coomassie blue to see if the plasma treated would lead to a sufficient layer of cells being formed.

6.2. Results

6.2.1. Oxygen plasma treatment of PEEK

In order to try to alter PEEK's intense cytophobicity we decided to try treating the material with oxygen plasma, as previously published work had reported that both oxygen and nitrogen based plasma treatment proved effective in improving cellular response to PEEK. To measure cell response to our treated PEEK surfaces we decided to use SEM to look at cellular attachment to the PEEK, which allows us to visualise individual cells on the PEEK surfaces and compare both the number of cell present and the degree of cell spreading on the different surfaces.

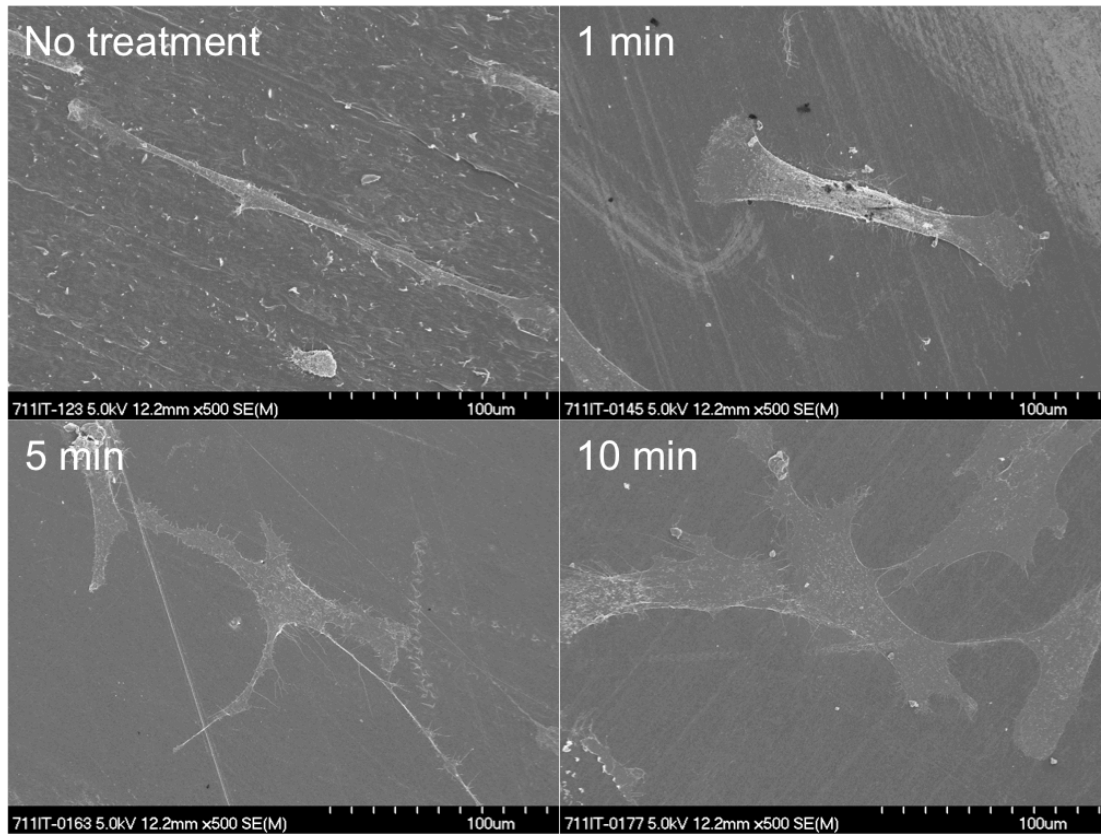


Figure 24 SEM images of h-TERT cells cultured on different durations of oxygen plasma treatment between 0 and 10 minutes and cultured for 3 days. The images show that with increasing energy of plasma treatment we observe an increase in cell spreading and in cell number.

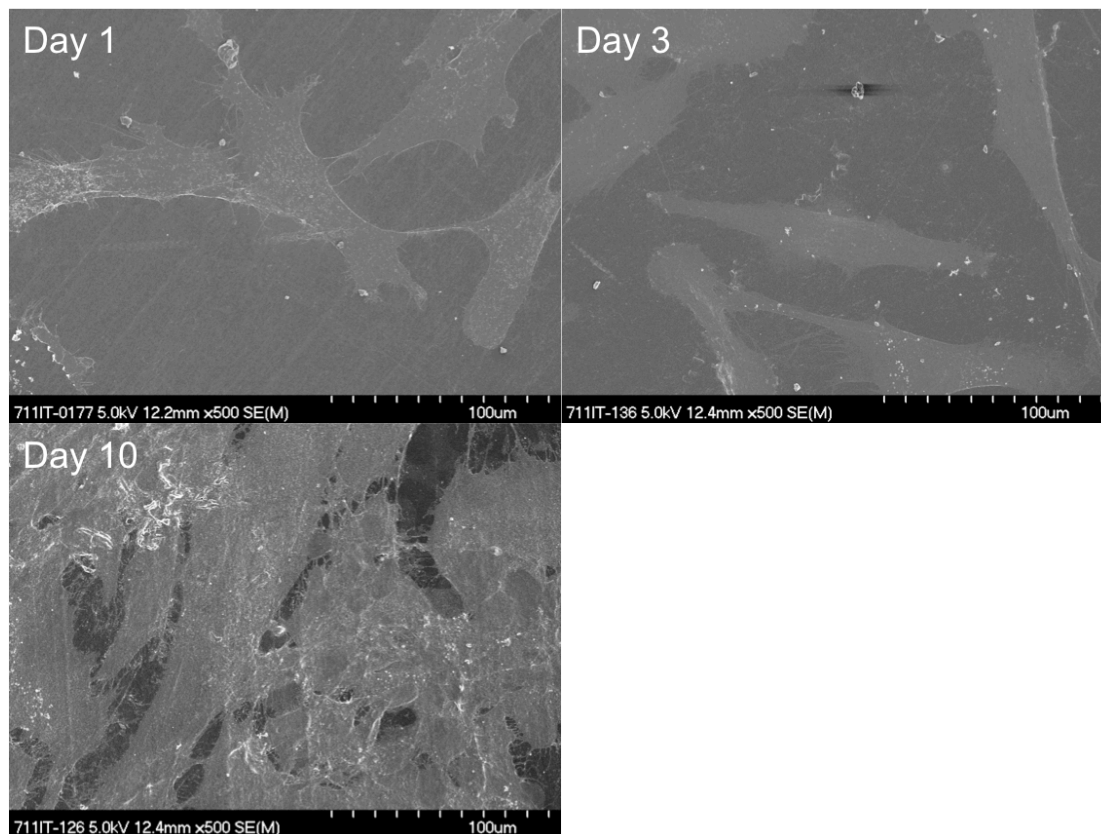


Figure 25 SEM images of h-TERT cells culture on machined PEEK surfaces that had benn plasma treated at 200W for 10 minutes after three different time points day 1, day 3 and day 10. These images demonstrate that the plasma treatment is suficient to produce an almost complete layer of cells on the PEEK surface by 10 days on culture.

As we can see from the results the oxygen plasma treatment has had a strongly positive effect on cell attachment to the PEEK surface, and the use of SEM has afforded us an effective look at what is happening at a cellular level on the PEEK surface.

As we can be seen from the results, the presence of oxygen plasma increases the number of cells on the surface proportional to the duration of the treatment. Additionally, when we look at the morphology of the cells, they also appear to have spread on the surface in proportion to the duration of plasma treatment (given the state of the cell we can see on the untreated surface in particular, that it is extremely stellate in shape. We believe that this cell may be dead. and has simply remained stuck to the surface during the fixation process for SEM). This suggests that the oxygen plasma treatment has accomplished what we needed it to, namely made PEEK a material that permits significant cell adhesion at its surface.

Additionally, we can see that the presence of oxygen plasma treatment cells do not only adhere, but are capable of proliferating to form a monolayer that covers the material surface. This is a positive result for using oxygen plasma treatment with PEEK, both in terms of our immediate in vitro work (as it generates a confluent monolayer of cells which would then permit us to use qPCR to look at the gene expression profile of cell cultured on our nanopatterned PEEK surfaces, which was the goal of these experiments at the time) but also for a future PEEK orthopaedic device, as they would require a monolayer of cell on each of its surfaces to prevent a fibrous encapsulation response (and associated poor device performance) from the patient.

Despite the positive biological results in terms of altering the ability of cells to adhere and proliferate on the surface from the oxygen plasma experiments, we did have some concerns about the effect of the treatment on the material itself. It is well established that oxygen plasma treatment etches material surfaces (and as a consequence is used in some lithographic processes) and we believed that we could see some surface damage taking place after the longer plasma treatment times we used in our experiments. Since these experiments were carried out on machined PEEK surfaces, and we could see pitting taking place on the surfaces via SEM, we had obvious concerns about the potential effect the oxygen plasma treatment could have on our nanotopographies. To investigate how oxygen plasma treatment would affect our topographies we decided to look at the impact of the longest duration of plasma treatment we had worked with (10 minutes) on one of our nanotopographies via SEM. Our reasoning was that if there was a trivial amount of alteration to the topography after treatment we could be satisfied that our topography was not adversely effected by the treatment, and it would not then be necessary to carry out a larger study on the relationship between oxygen plasma treatment and degree of surface etch with PEEK. However, if the results did show a concerning level of damage to the topography we could then go on to carry out a full investigation using AFM, as this would give more detailed information about the state of the topography.

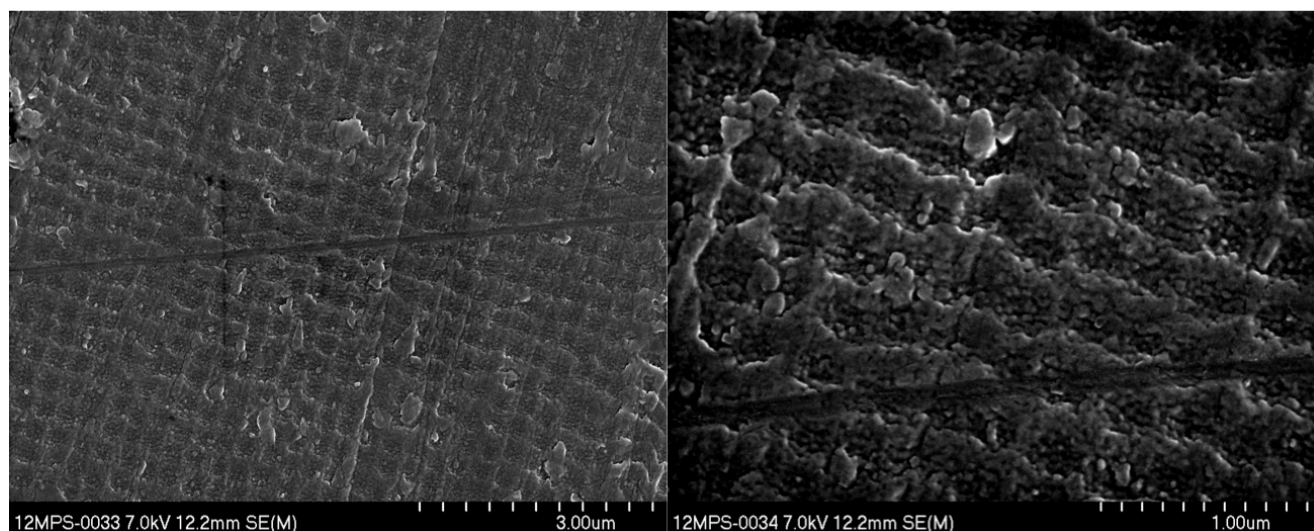
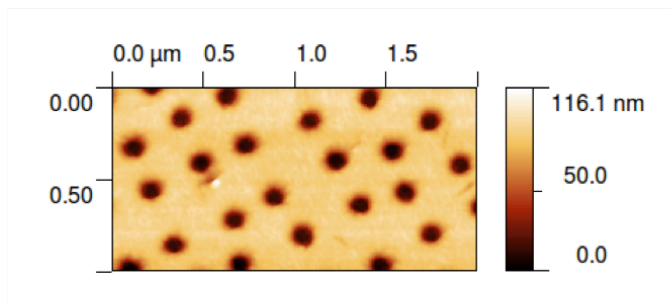


Figure 26 SEM images of PEEK nanotopographies that have been treated with plasma treatment for 7 minutes at 200W. The damage to the nanotopography can be clearly seen.

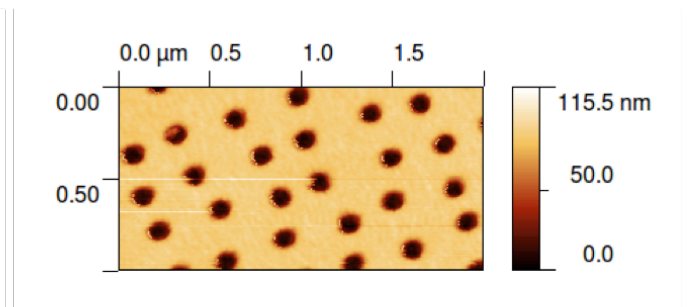
We discovered that after 10 minutes of oxygen plasma treatment there was a high degree of damage done to the topography, to the extent where we did not think it would be possible to still refer to it as a distinct topography.

In order to try to find the duration of oxygen plasma treatment which would be sufficient to address the materials innate cytophobicity, but would not cause an unacceptable level of damage to the nanotopography, we decided to analyze a range of PEEK nanotopographies that had been oxygen plasma treated for between 1 and 10 minutes via AFM. After the PEEK topographies were plasma treated, the AFM readings were kindly performed for the author by Dr John Stormonth-Darling.

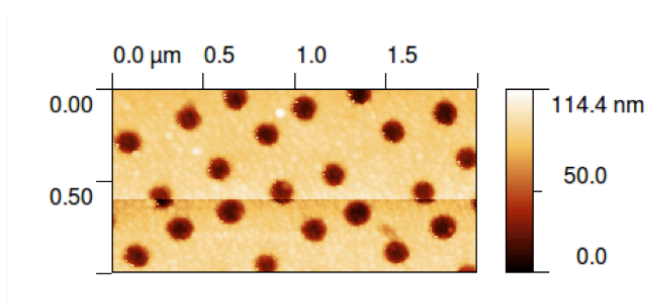
0 min



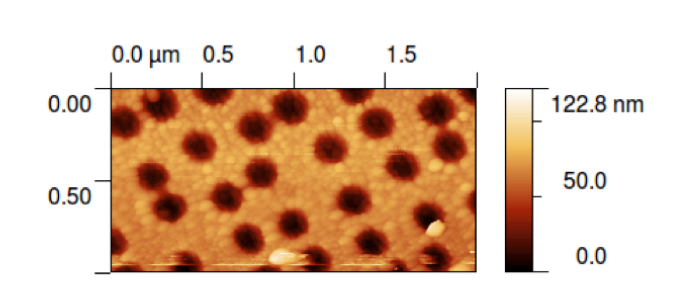
1min



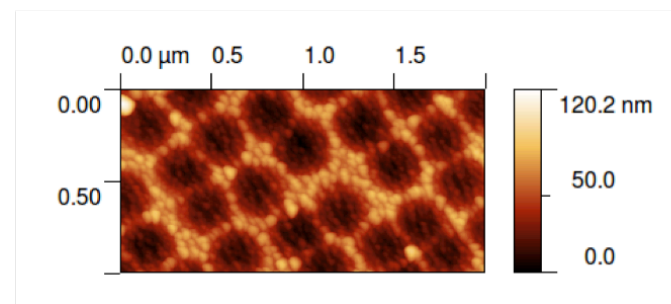
2min



5min



7min



10min

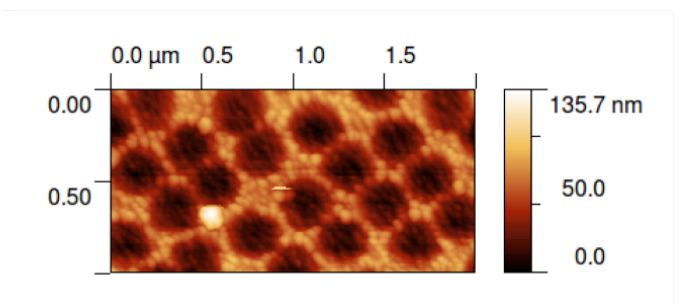


Figure 27 AFM readings of PEEK NSQ nanotopographies that have been treated with 200W of plasma for a range of durations (0, 1, 2, 5, 7, and 10 minutes). These results illustrate that with increasing time of plasma treatment, we see an increase in nanopit diameter and a decrease in nanopit depth.

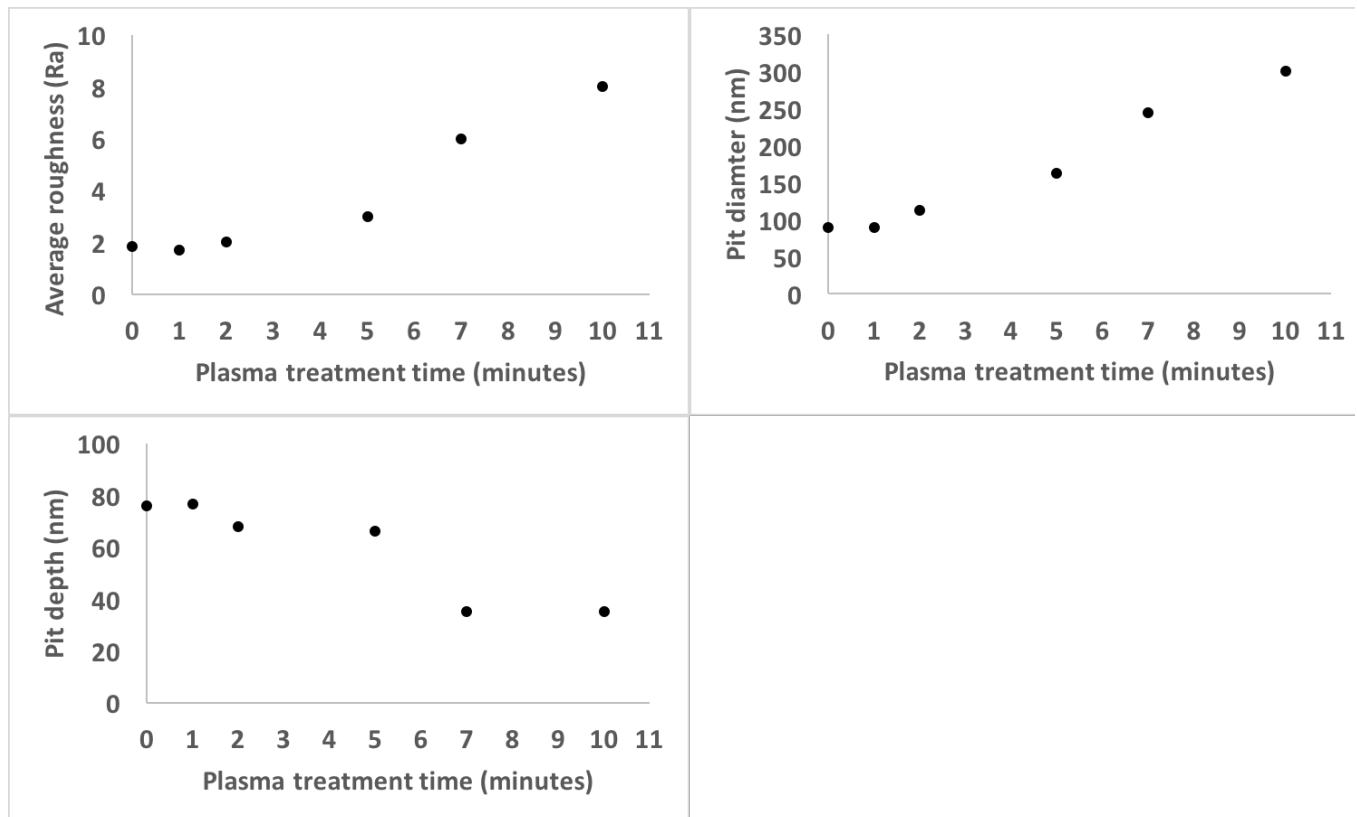


Figure 28 AFM measurements of area between nanopits, nanopit depth and diameter at increasing durations of 200W plasma treatments. The results show that as duration of plasma treatment increases, pit diameter and the average roughness of the interpit areas increases and pit depth decreases.

The cellular adhesion experiments had demonstrated that we needed to plasma treat our PEEK surfaces in order for the material to permit cells to adhere to it. However, the SEM and AFM experiments demonstrated that this plasma treatment etches the PEEK surface damaging the nanotopography present. These two results left us in the position of needing to find a plasma treatment that would maximise cellular adhesion to the PEEK surface, while also minimising as far as possible, damage to the nanotopography.

The three aspects of the nanotopography that we measured (the average roughness of the inter-pit areas, the depth of the nanopits and the diameter of the nanopits) built a picture of how the surface was altered on the nanoscale, by increasing duration of plasma treatment. For each of the elements measured the amount of change to the topography over time was not linear, and rises sharply after five minutes of plasma treatment. The average roughness of the interpit areas shows an increase of 50% between 2 minutes and five minutes and a 100%

increase between 5 minutes and 7 minutes. The measurement of pit depth showed a loss of 2nm of depth between 2 minutes and 5 minutes of plasma treatment, compared to a 31nm loss of depth between 5 minutes and 7 minutes. Finally, the pit diameter measurements demonstrated a 50nm widening of the pits between 2 and 5 minutes, and a 82nm widening between 5 and 7 minutes. When we look at all three measurements together we can see that there is a pronounced increase in the rate of damage to the nanotopography after five minutes of plasma treatment. Consequently we took five minutes of plasma treatment as the limit of how much plasma we should deliver to our surfaces, due to the sharp increase in damage after this point. While there is an increase in damage between two and five minutes of treatment, it was not as pronounced as was observed after five minutes, so we thought plasma treatments of under five minutes should be the starting point for biological experiments. While we could not be sure that the damage that had been done to the nanotopography by plasma treatments of up to five minutes would impact on how cells respond, the only way we could confirm this would be to carry out biological experiments with the plasma treated surfaces but given the strong increase in damage to the topography after five minutes of plasma treatment, we felt comfortable discounting these treatments.

6.2.2. Wettability

We also decided to investigate how oxygen plasma treatment impacted on the wettability of our PEEK nanotopographies. We plasma treated PEEK NSQ nanotopographies with a range of different oxygen plasma treatments, running from no treatment up to 2 minutes of 200W. We then measured the sessile drop water contact angle of each, and compared them.

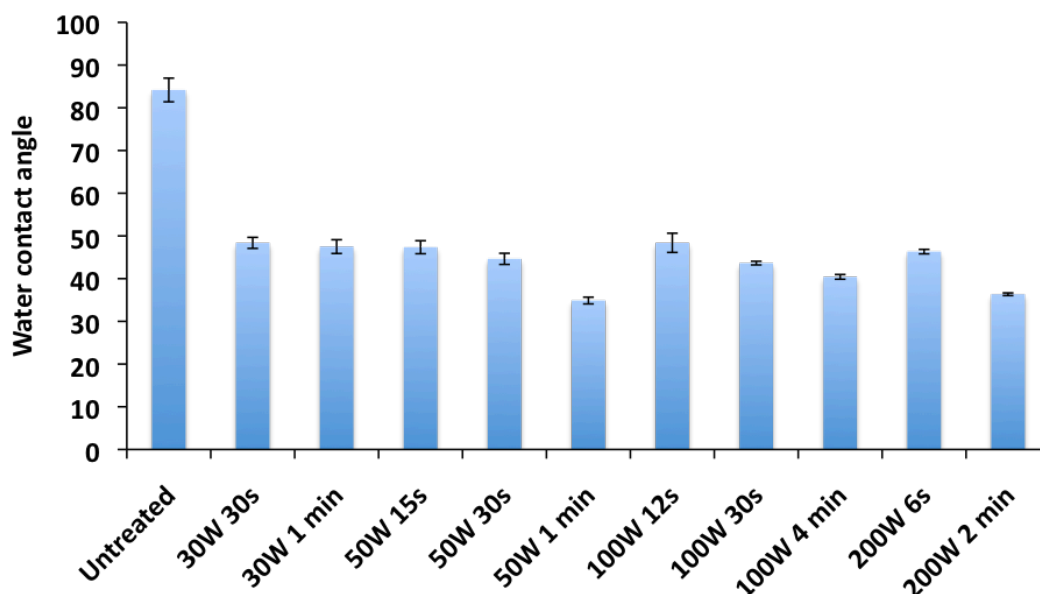


Figure 29 Sesile drop water contact angle measurements of PEEK surfaces that have been exposed to a range of different plasma treatments.

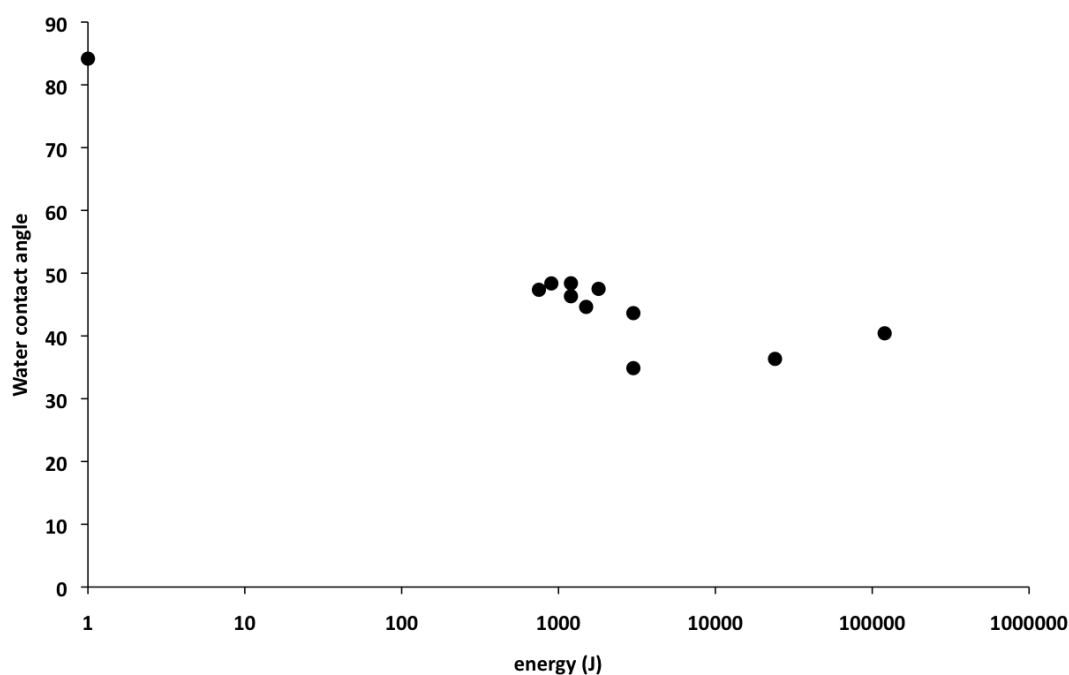


Figure 30 Water contact angle plotted against the energy of the different plasma treatments used.

As we can see from the results there is a strong decrease in water contact angle at 30W 30s compared to the untreated surface. It is interesting however, that further increases in the duration and strength of the plasma treatment do not lead to such strong reduction the in water contact angle. Given the demonstrated

relationship between oxygen plasma treatment and cell response up to this point, the strong decrease in water contact angle would explain the marked improvement in cell adhesion observed after oxygen plasma treatment. Given that we tend to see this improve with strong treatment regimes, it is interesting to note that this is not accompanied by similarly strong changes in wettability.

6.2.3. Surface chemistry

In order to look at how the plasma treatment altered the chemical environment of the PEEK surface, XPS readings were taken of the PEEK surface after increasing durations of plasma treatment. We were assisted in this by Dr Rasmus Pedersen who kindly took the XPS readings.

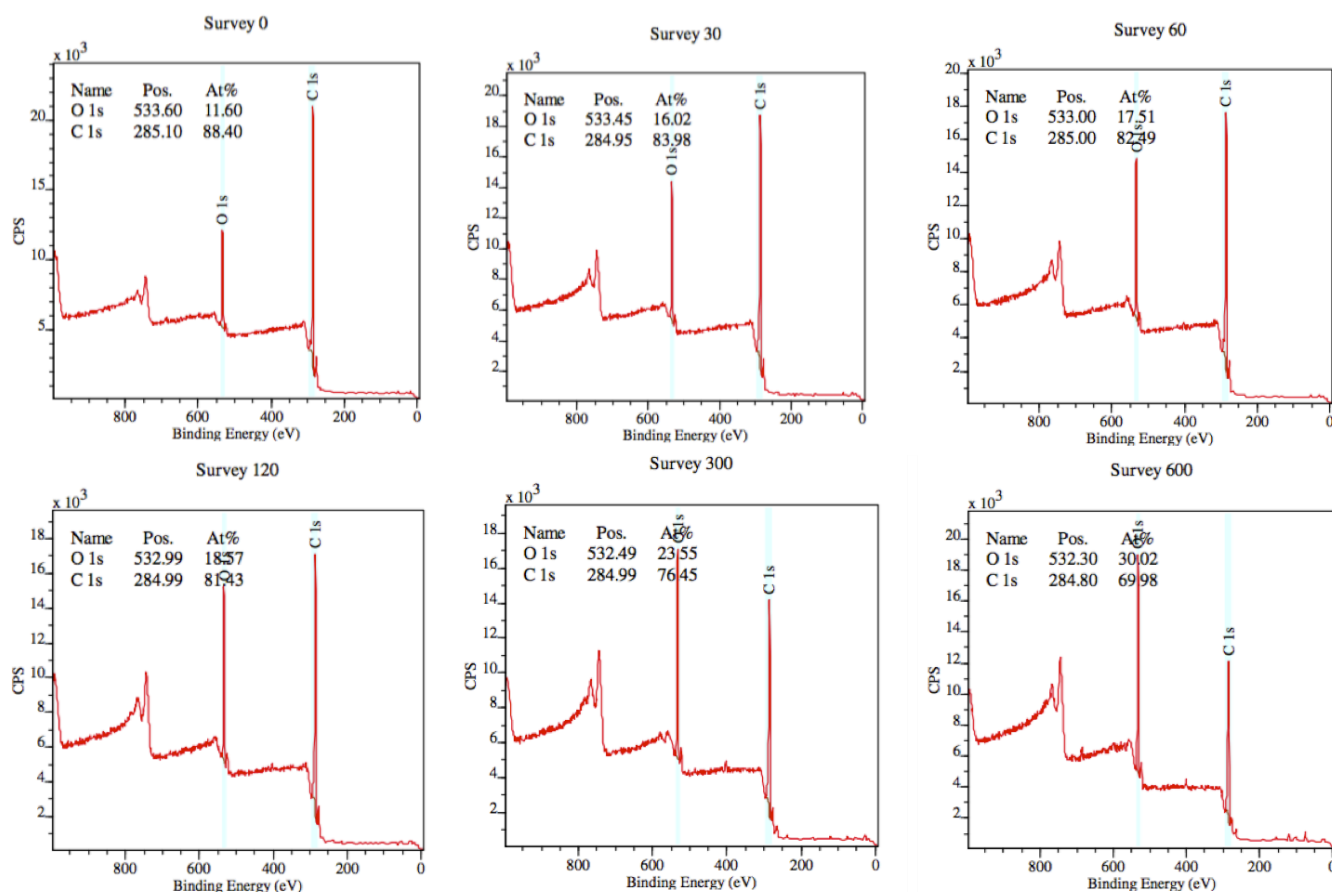


Figure 31 XPS spectra results from PEEK surfaces that had been oxygen plasma treated at 200W between 0 and 600 seconds.

Duration of plasma treatment (s)	% of the surface carbon	% of the surface oxygen
0	88.40	11.60
30	83.98	16.02
60	82.49	17.51
120	81.43	18.57
300	76.45	23.55
600	69.98	30.02

Figure 32 Table summarising the changes in surface chemistry in terms of oxygen and carbon content at the surface after different durations of oxygen plasma treatment . As plasma treatment time increases the percentage carbon falls while the percentage oxygen increases.

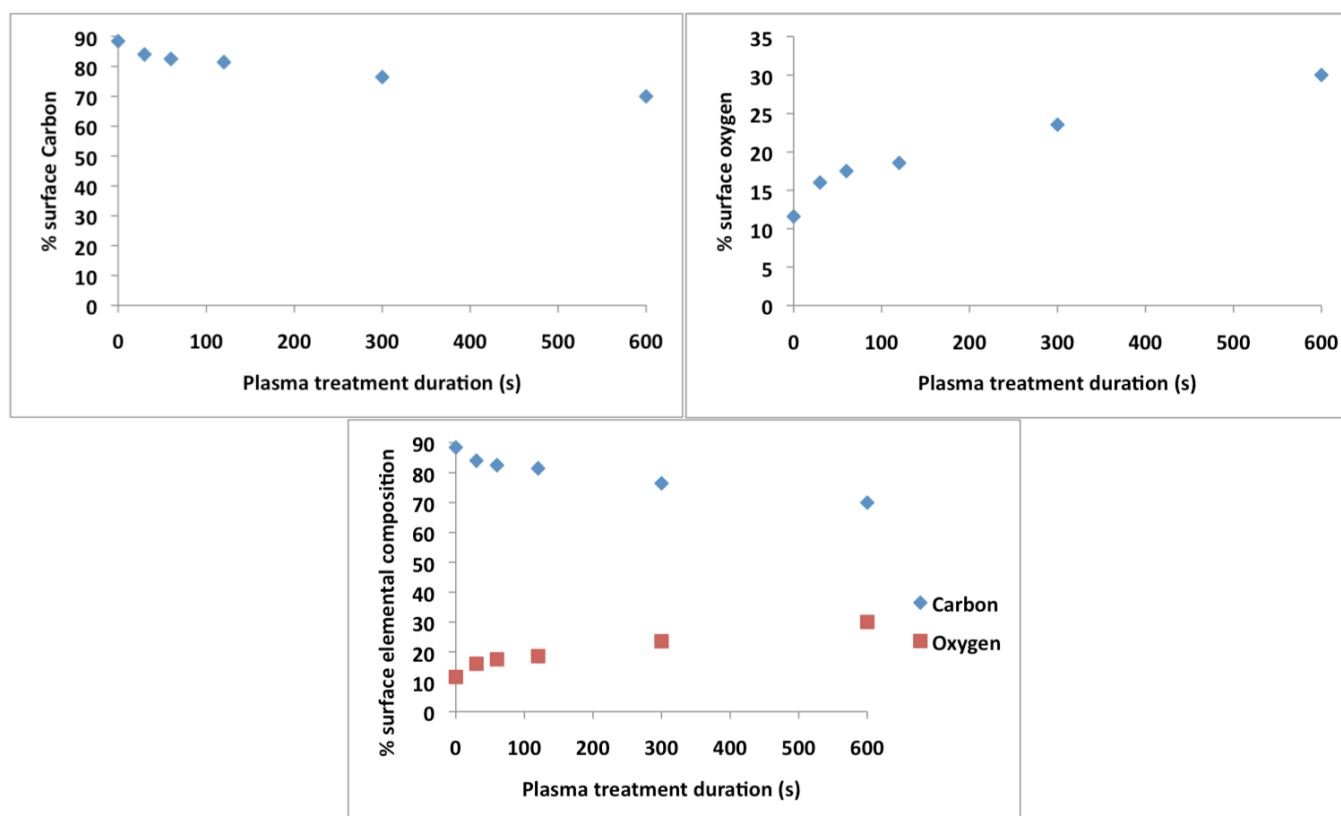


Figure 33 XPS results for carbon and oxygen at the surface plotted against duration of plasma treatment in seconds.

We can see from the XPS results that as the duration of plasma treatment increases the amount of carbon present at the surface decreases, as the amount of oxygen increases. This is not entirely surprising, given that the gas being used in the plasma treatment is oxygen. The increase in oxygen at the surface also correlates with our observed decrease in water contact angle resulting from the

plasma treatment. We also expected this increase in wettability to lead to an increase in cell adhesion⁸⁵.

6.2.4. Impact of the plasma treatment on osteoprogenitor cells

As a consequence of the work we had carried out up to this point we now had a technique that allowed us to circumvent PEEK's cytophobicity, which we also felt gave us a good understanding of its impact at the material as well as biological level. However, at this point we had only demonstrated that oxygen plasma treatment facilitated the adhesion and proliferation of cells from a cell line. Given that our interest was in investigating the response of primary human osteoprogenitors (given the interest in PEEK's use in orthopaedic implant devices these cells would offer the best insight into the *in vivo* response to the surface while still remaining in an *in vitro* environment) to our PEEK surfaces, and that the cell line cells that we had used up to this point are more robust in terms of adhesion and proliferation, we felt it was necessary to look directly at the relationship between these osteoprogenitors and oxygen plasma treatment on the PEEK surface. To do so we seeded primary human osteoprogenitors on PEEK NSQ nanotopographies that had been oxygen plasma treated between 0 and 10 minutes, cultured the cells for 11 days, then fixed the cells and stained them with coomassie. We then used polarised light microscopy and cell profiler analysis to measure the percentage of the surface with adherent cells.

0 min

2 min

5 min

10 min

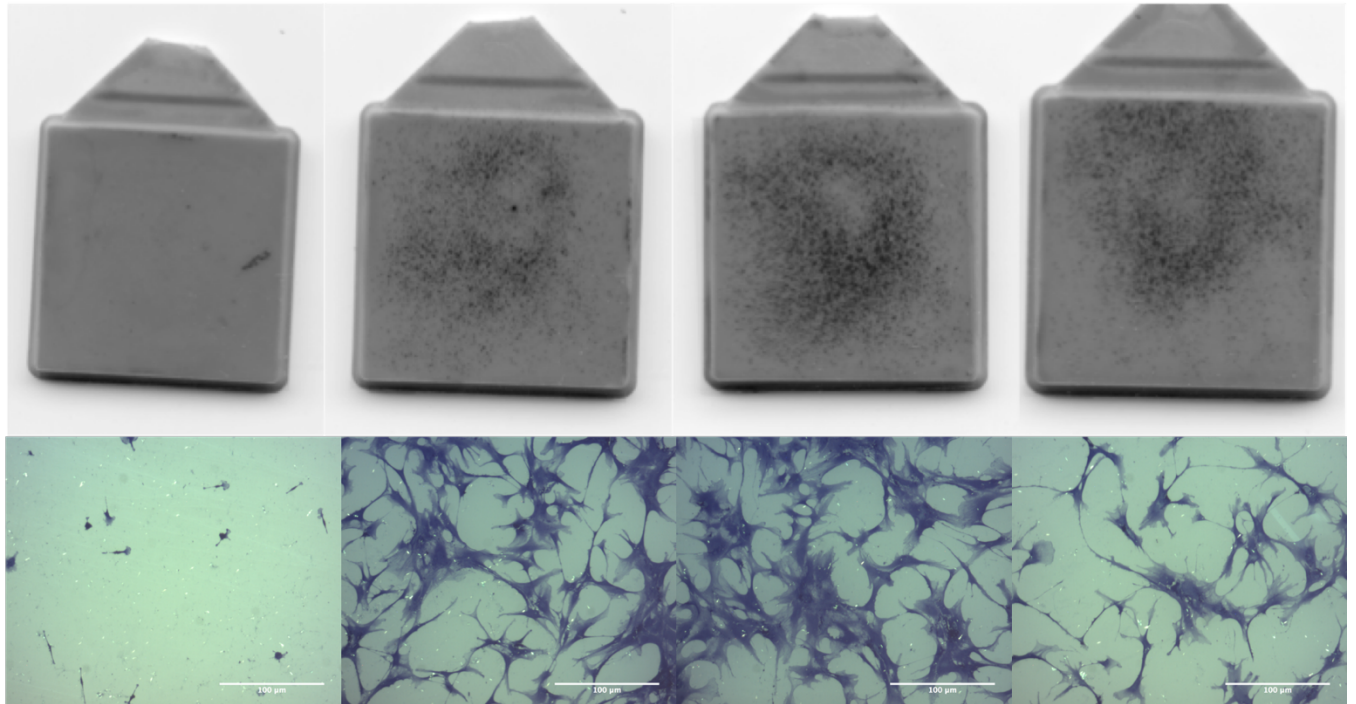


Figure 34 Coomassie blue staining of primary human osteoprogenitor cells cultured for 11 days on PEEK NSQ nanotopographies that have been plasma treated at 200W over a range of different times (0, 2, 5 and 10 minutes). The pattern of staining indicates a definite increase in cells present at 2 and 5 minutes compared to 0 minutes and a possible decrease at 10 minutes compared to 5. Scale bar = 100 μ m.

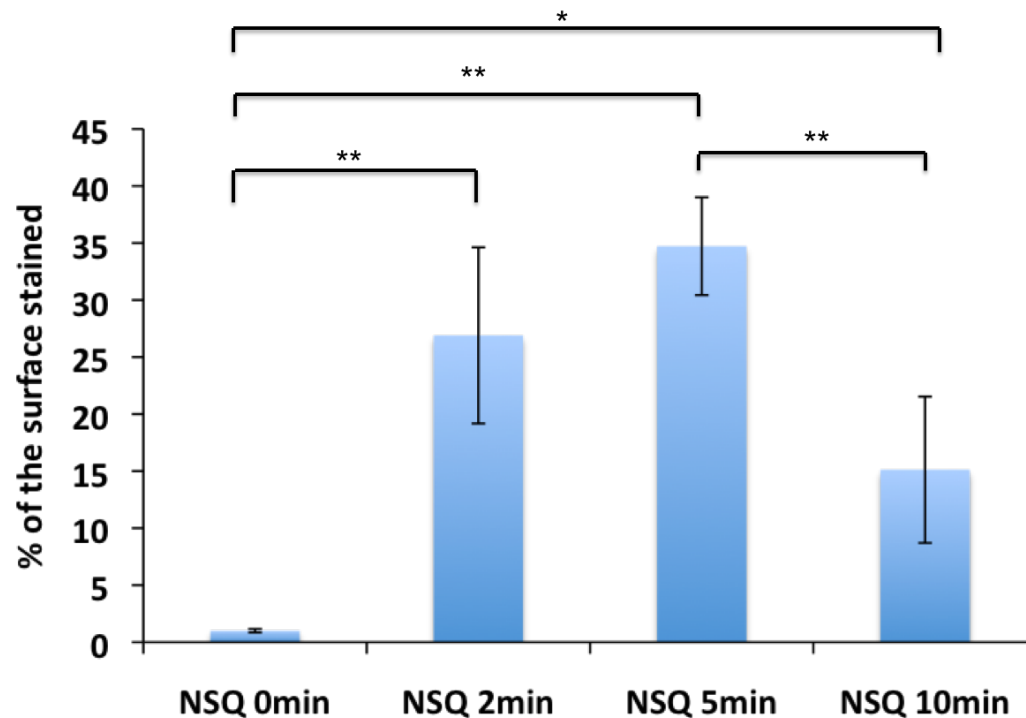


Figure 35 Cell profiler results for the percentage of the surface with stained material . All three durations of plasma treatment result in a statistically significant increase in staining. However 10 minutes is lower than 5 minutes to a highly statistically significant degree.

As we can clearly see from the results, the cellular impact of oxygen plasma treatment of PEEK is conserved between cell line cells and primary human osteoprogenitors, that is to say that it has a strong positive effect on cell response to the PEEK surface. The non-treated PEEK surface has almost no cells present (If we look closer at the morphology of the cells that are attached to the surface (*Figure 31*), given how rounded the cells appear it is certainly possible that cells are dead and have remained stuck to the surface through the fixation process). There is a strong increase after 2 minutes of treatment and a further increase on top of that at 5 minutes. It is interesting that there are fewer cells present on the 10 minute treated surface compared to either the 2 minute or 5 minute treated surfaces.

6.3. Discussion

Our use of oxygen plasma treatment has shown itself to be an effective method for reversing the poor cellular adhesion and proliferation seen on bare PEEK. Our findings were in line with other groups working with oxygen plasma treatment and PEEK in vitro⁸⁵. Our experiments with h-TERT cells on plasma treated machined (but not nanopatterned) PEEK surfaces showed a relationship between increasing duration of plasma treatment and resulting increased cell adhesion and subsequent proliferation. These results demonstrated to us that PEEK was a viable method for generating the required number of cells on our nanotopographies and allow us to investigate if the nanotopographies were directing cell behaviour. Our results indicated that by increasing the plasma treatment we could effectively increase the number of cells present on the surface, the question of which plasma treatment would be most appropriate now presented itself. As we were aware that plasma treatment can etch the surface of the material being treated, this introduced another factor into our consideration of what it is the ideal plasma treatment. What we were now looking for was the maximum amount of plasma treatment we could give our surfaces without causing unacceptable damage to the nanotopography present. Our first look into the effects of the plasma treatment on the condition of the nanotopography through SEM showed that by 7 minutes of treatment with 200W of plasma there was heavy damage to the surface nanotopography (*Figure 26*). This demonstrated that we needed to better understand the relationship between plasma treatment and degree of surface etching. To pursue this we treated PEEK NSQ nanotopographies with a range of durations of plasma treatment (0, 1, 2, 5, 7 and 10 minutes investigated), and used AFM to determine changes to the topography. The results illustrated an overall trend i.e. as plasma duration increases there is an associated increase in the roughness of the interpit areas and in pit diameter and a decrease in pit depth. We felt overall that five minutes indicated a point at which both the increase in pit diameter and decrease in pit depth became unacceptable.

After this we looked at the relationship between plasma treatment and water contact angle. Here we can see the largest single change in water contact angle is between the untreated PEEK surface and the lowest amount of plasma treatment used (30W 30s), where the water contact angle drops from 84° to 47°. Plotting the water contact angle against the power of the plasma treatment used demonstrates that the majority of the different plasma treatments are clustered around the high forties in terms of water contact angle. However, the three strongest treatments used (50W 1min, 200W 2min and 100W 4 min) showed a trend where the water contact angle drops down to 34° and then recovers back to 40°.

As the initial goal of our use of plasma treatment was to be able to culture enough stem cells on our nanotopographies to be able to investigate if the presence of the topography could alter their behaviour, we wanted to check that the plasma treatment would affect them in the same fashion as it did to the h-TERT cells. To investigate this, we cultured primary human osteoprogenitors on surfaces treated for a range of durations of plasma treatment (0, 2, 5 and 10 minutes of 200W plasma treatment was used) for 11 days, then stained the cells with coomassie and analysed the degree of staining with Cell Profiler. As we felt that based on the AFM results five minutes was the maximum duration of plasma treatment we wanted to expose our nanotopographies to, we used this as well as 2 minutes, under the reasoning that we wanted to cause as little change to the PEEK surface to allow us to get our desired results, and as there was little difference in cell response between two and five minutes of plasma treatment, we would use the shorter length of treatments. We also included 10 minutes as an insurance policy in case the two or five minute treatments yielded little cells, so we could tell if the lack of cells was down to insufficient degree of plasma treatment or down to the fact that these cells do not respond to the plasma treatment in the same fashion as the h-TERT cells. While this treatment would not be usable, due to the damage that it was demonstrated to deliver to the surface, it would demonstrate that plasma treatment would work with these cells.

The experimental results demonstrated that two and five minutes produced statistically highly significantly more staining than the untreated PEEK surface, and the ten minute treated surface produced statistically significantly more staining

than the untreated surface. This points toward the interesting trend that was displayed, that the level of staining increased with increasing plasma treatment up to 5 minutes, and after 10 minutes of treatment the level of staining had fallen at a highly statistically significant degree compared to the surface that had been treated for 5 minutes. This would suggest that at some point between five and ten minutes of treatment the level of staining reaches a maximum and begins to fall, however, due to the lack of time points between five and ten minutes we cannot say exactly where this is. The data does not provide a clear answer as to why the amount of staining (and therefore number of cells) does not continue to rise after five minutes and indeed falls to a highly statistically significant degree by ten minutes. Given the high degree of damage experienced by the nanotopography after ten minutes of plasma treatment, it is possible that the nanotopography in the state that it is in acts to discourage and disrupt the ability of cells to proliferate at the material surface.

6.4. Conclusions

Overall our results show that plasma treatment is an effective method for addressing the cytophobic nature of PEEK. Both h-TERT and primary human osteoprogenitors were demonstrated to respond positively to the treatment, with marked improvements in the ability of cells to adhere to and subsequently proliferate at the PEEK surface. While the plasma treatment did etch our surfaces and consequently cause damage to our surface topography, we felt, based on our AFM results that we could treat our surfaces up to 5 minutes at 200W without causing what we view as unacceptable levels of damage to our nanotopographies.

7. Interaction between SAOS-2 osteoblast like cells and oxygen plasma treated PEEK nanotopographies

7.1. Introduction

7.1.1. The role of SAOS-2 cells in *in vitro* PEEK tissue engineering research

Primary osteoprogenitors, the mononuclear fraction of cells derived from human bone marrow (see the methods section for further details on their extraction) are the closest model in terms of *in vitro* work we have to the cells that will interact with the surface of an orthopaedic implant. However, these cells are very slow growing and relatively few are harvested from the aspirate taken from a joint replacement. Immortalised cells taken from a cell line, while not offering the same level of fidelity of behaviour to that experienced by the implant surface (both in terms of the activity of the individual cells as well as the fact that osteoprogenitors are a heterogeneous population), offer us a much larger and faster replenishing pool of cells with which to work. They also share properties such as mineralization, which relate to the type of work we are doing. As a result of this it is possible to perform larger screening type experiments which we would be hard pressed to carry out with primary osteoprogenitors.

7.1.2. SAOS-2 cell line

We opted for SAOS-2 cells in our experiments working with cell line cells. SAOS-2 cells are cells from a cell line that is originally derived from a primary human osteosarcoma. As such these cells, due to the mutations that they accumulated, proliferate faster, generate an unlimited number of cells and are easier to culture than primary cells. However, due to these mutations the cells now behave significantly differently compared to primary cells. As there is continuing debate around how significant the differences are in behaviour between primary cells and

cell line cells, we felt that based on reviews of the published literature⁹⁸, and direct comparison between different cell lines and primary osteoblasts⁹⁹, that SAOS-2 cells were closest in behaviour to primary osteoblast cells of the different osteoblast cell lines available. The authors directly compared three more commonly used osteoblast cell lines SAOS-2, MG63 and MC3T3-E1 to human osteoblasts over a range of osteogenic behaviours. They found that SAOS-2 cells were the closest match to human osteoblasts in terms of mineralisation, which is of primary interest for this investigation.

7.1.3. Our objectives in working with SAOS-2 cells

As mature osteoblast cells play a role in the formation of the interface between an orthopaedic implant and the host tissue¹⁰⁰¹⁰¹ we thought it would be relevant to look at how cells from a mature osteoblast cell line responded to both the presence of nanoscale topography and oxygen plasma treatment at the PEEK surface. Additionally, given the abundance of SAOS-2 cell compared to primary osteoprogenitors, we were interested in exploring the synergistic relationship between plasma treatment and nano-topography. In particular, we had an interest in seeing if the plasma treatment could compete with the topography in terms of influencing cell activity. We believed that the type of experiments required to investigate this area would need a large number of cells and as such, would be difficult to carry out with primary human osteoprogenitors. As a comparison, an experiment where we compared the NSQ and SQ nanotopographies to the planar surface with a single plasma treatment and a single period of culture would require 270,000 cells, and a screening type experiment where we compared six different plasma treatments using the NSQ, SQ and planar surfaces would require 1,620,000 cells. A single aspirate from a hip replacement operation would yield two t75 flasks which in our experience would give on average 300,000 cells and it would take in our experience, a month and half to two months to generate this many cell (Since each aspirate is taken from a different patient we found variation in the number of cells and speed of proliferation between different aspirates). SAOS-2 cells on the other hand yielded on average two million cells per t75 flask and it takes around a week to generate this number of cells. Additionally, when

splitting a flask of SAOS-2 cells, multiple new flasks can be set up. As a consequence, using cells from a cell line was a logical choice.

7.1.4. Experimental outline

The intention with these experiments was primarily to see if SAOS-2 cells, cultured on plasma treated nano-patterned PEEK surfaces, had their osteogenic behaviour modulated by different nanotopographies.

The scope of this investigation widened into investigating whether the duration of culture of the cells on these surfaces impacted on the cellular response. In other words, we were interested in the possibility that the presence of topography may have affected the level of osteogenic response either earlier or later than the usual four week time point at which mineralization response is normally assessed , and as a consequence, would either not be seen or obscured by later events on the surface. Additionally, we became interested in how the presence of the oxygen plasma treatment at the PEEK surface impacts on the response of the cells. To investigate this we cultured cells on a range of different plasma treatments which were under the threshold at which we thought significant etching damage had occurred to the nanotopography.

7.2. Results

7.2.1. SAOS-2 culture duration experiments

Given we had decided on an osteoblast cell model we thought the most appropriate place to start with our investigation into osteoblast response to PEEK nanotopographies would be to look at mineralisation response to our PEEK surfaces at 28 days using von Kossa staining. We opted to culture the cells for 28 days, as it was the most common time course for mineralisation staining in the literature, and used von Kossa staining, as we thought it would offer greater contrast compared to alizarin red.

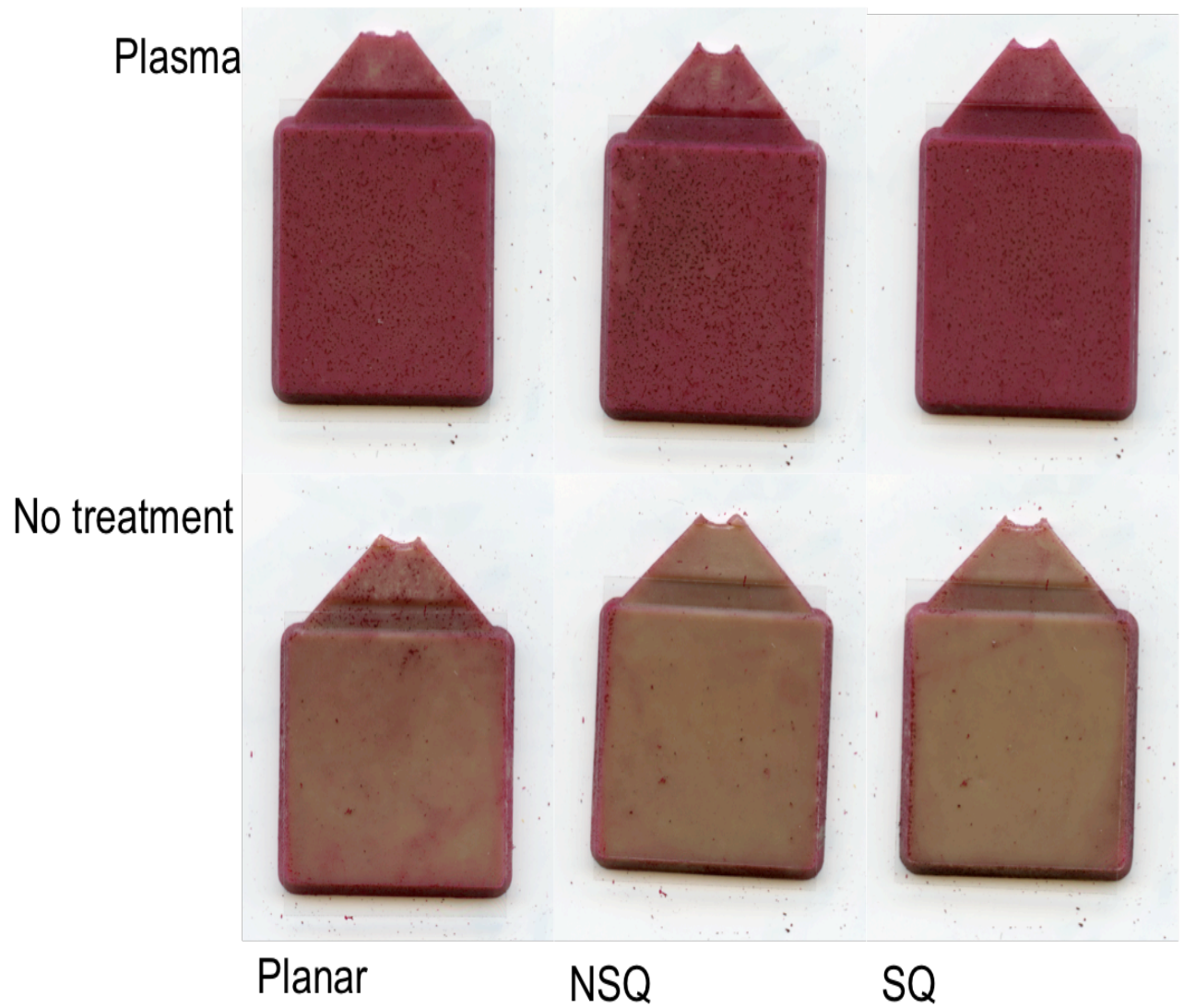


Figure 36 Representative full substrate high resolution scans of Von Kossa staining of SAOS-2 cells cultured for 28 days on PEEK nanotopographies that had been oxygen plasma treated for 2 minutes at 200W and those which had not receive any treatment. Red staining indicates the presence of cells and black staining indicates the presence of phosphate. Total number of replicates =18: 6 Planar, 6 NSQ, 6 SQ.

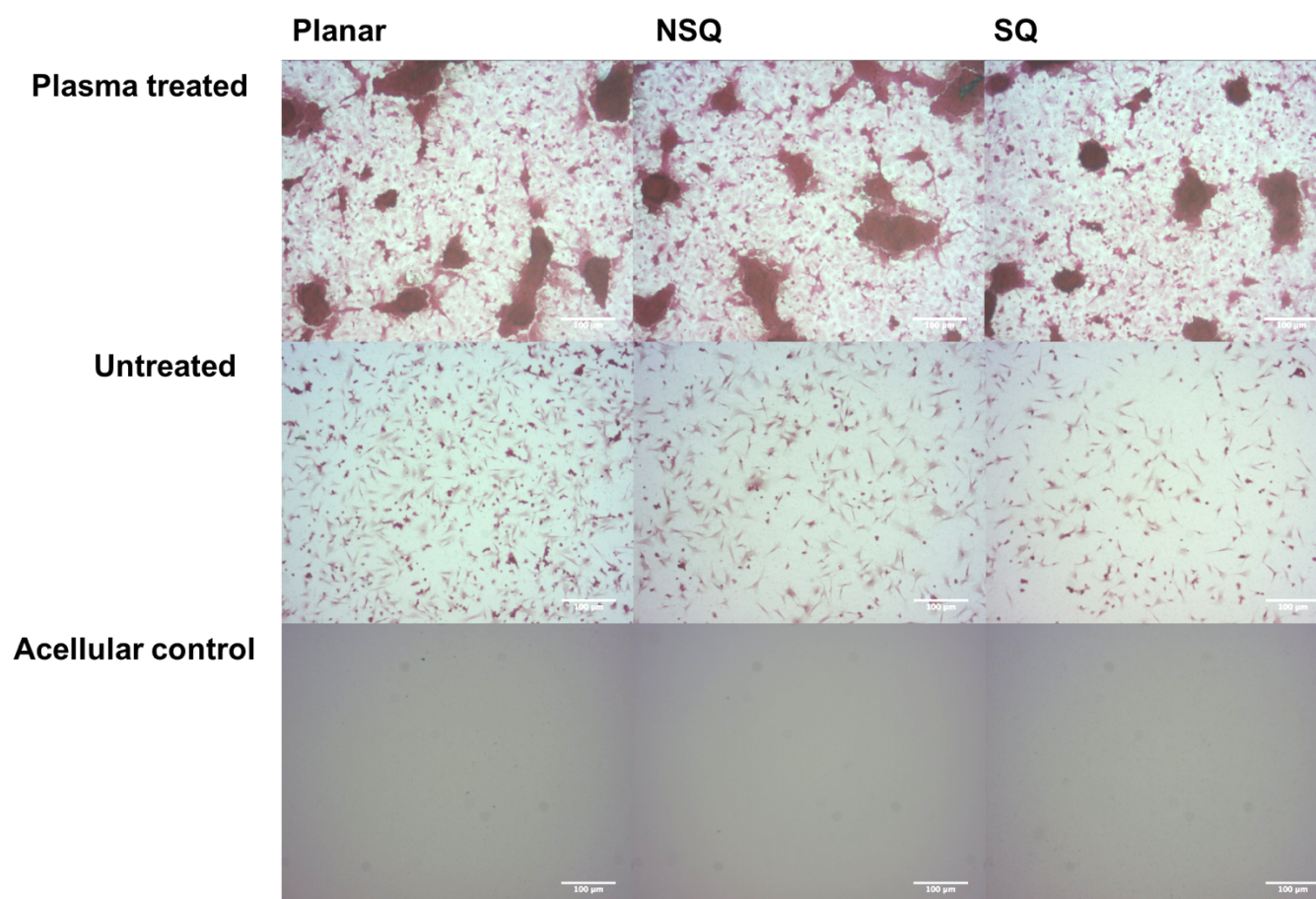


Figure 37 Polarised light microscope images of Von Kossa staining of SAOS-2 cells cultured for 28 days on PEEK nanotopographies which were treated with oxygen plasma for 2 minutes at 200W. Total number of replicates N=18: 6 Planar, 6 NSQ, 6 SQ. Scale bar = 100 μ m.

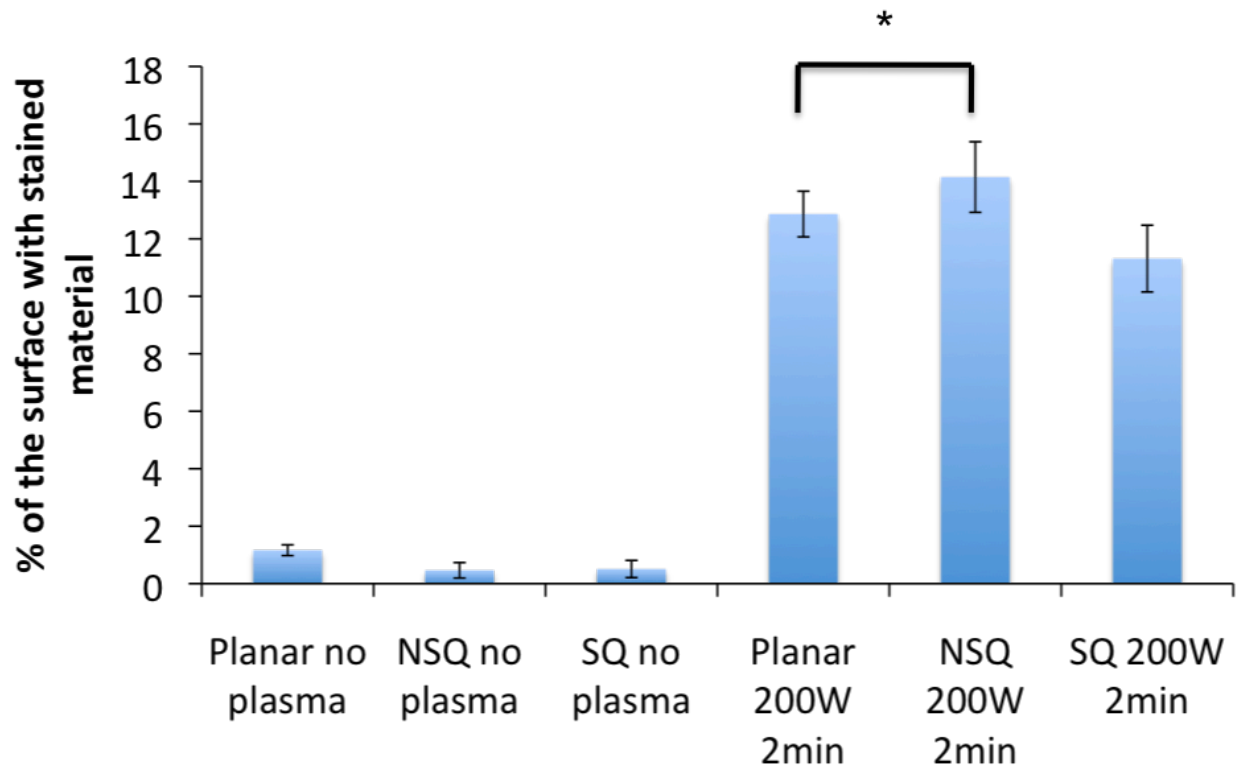


Figure 38 Cell Profiler analysis of polarised light microscope images of von Kossa staining of SAOS-2 cells cultured on PEEK substrates that had been oxygen plasma treated for 2 minutes at 200W. The presence of oxygen plasma has produced a strong increase in the level of phosphate produced on the surfaces. Additionally the percentage of the surface with stained material is significantly higher on the NSQ nanotopography compared to the planar surface. Total number of replicates =18: 6 Planar, 6 NSQ, 6 SQ.

	Times increase	Fold increase
Planar	11.059	1.043
NSQ	30.468	1.483
SQ	22.175	1.345

Figure 39 Table summarizing both the times increase and fold increase of the percentage of the surface stained via von Kossa, between untreated and plasma treated PEEK nanotopographies.

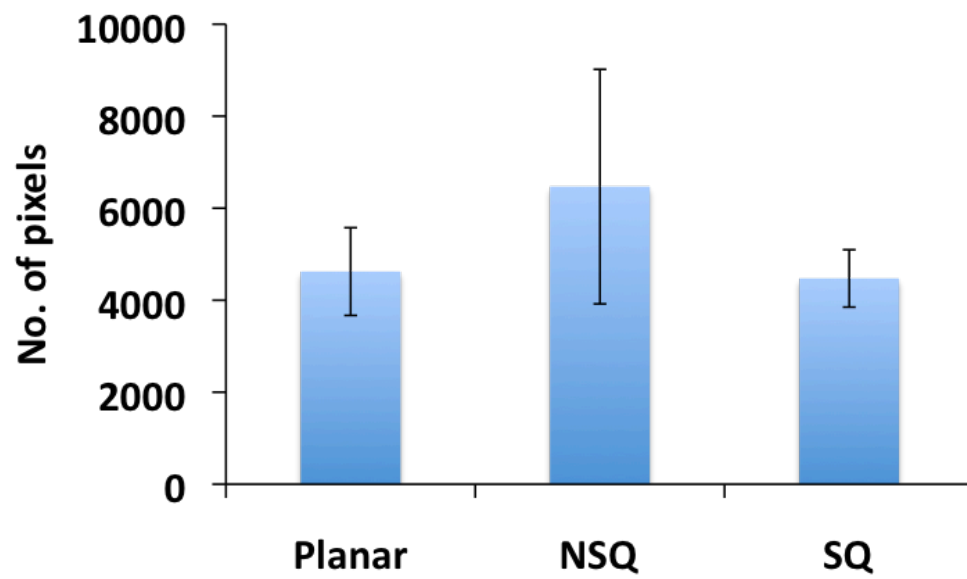


Figure 40 Average area of identified areas of staining calculated by Cell Profiler analysis of von Kossa staining of SAOS-2 cells cultured on PEEK substrates that had been oxygen plasma treated for 2 minutes at 200W. Total number of replicates N=18: 6 Planar, 6 NSQ, 6 SQ.

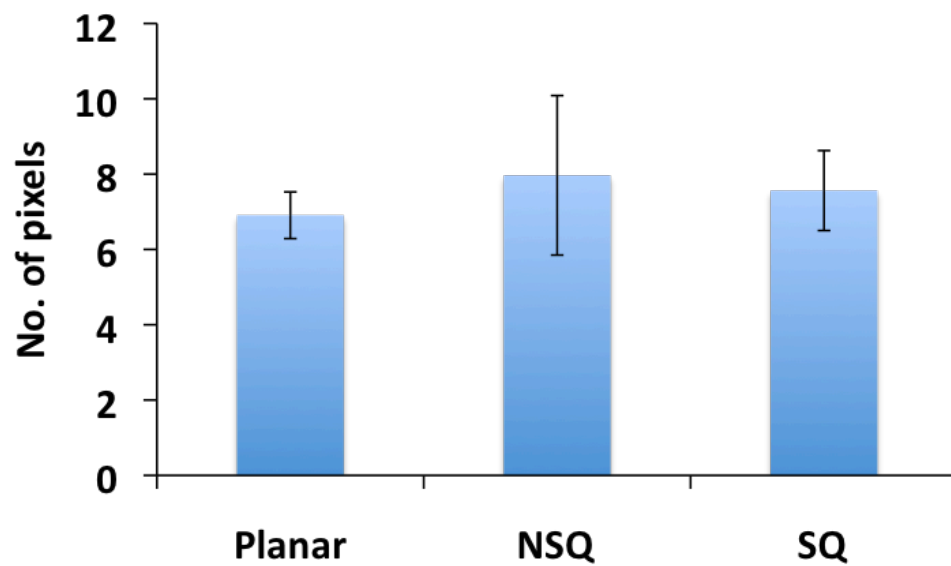


Figure 41 Mean radius of identified areas of staining calculated by Cell Profiler analysis of von Kossa staining of SAOS-2 cells cultured on PEEK substrates that had been oxygen plasma treated for 2 minutes at 200W. Total number of replicates N=18: 6 Planar, 6 NSQ, 6 SQ.

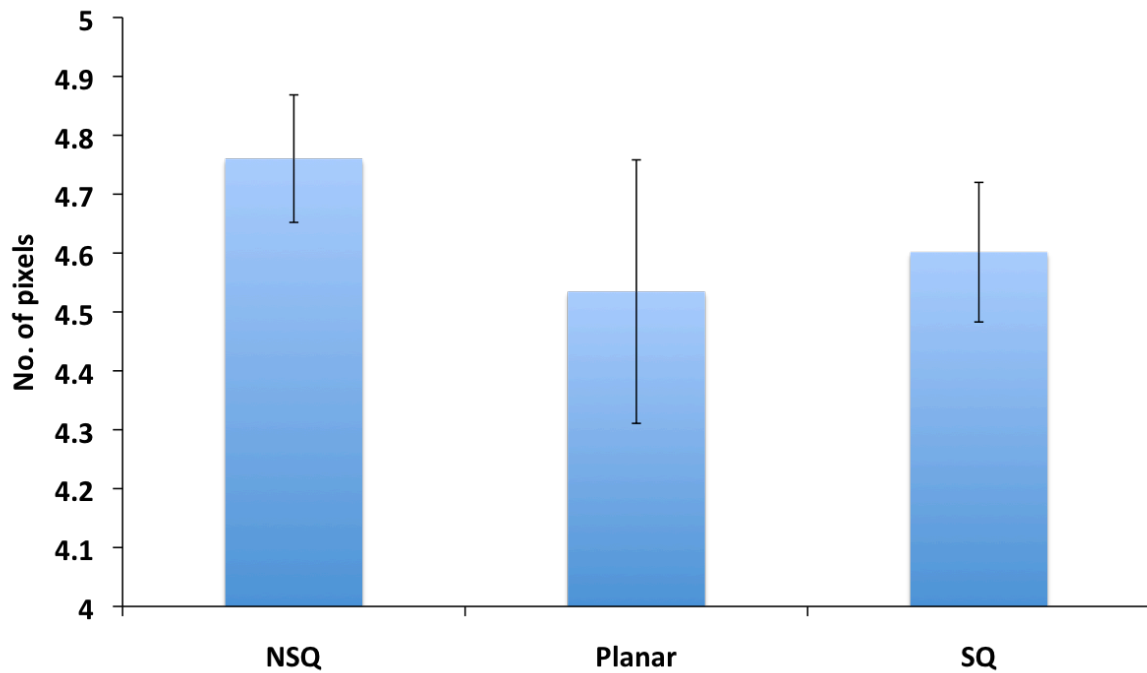


Figure 42 Median radius of identified areas of staining calculated by Cell Profiler analysis of von Kossa staining of SAOS-2 cells cultured on PEEK substrates that had been oxygen plasma treated for 2 minutes at 200W. Total number of replicates N=18: 6 Planar, 6 NSQ, 6 SQ.

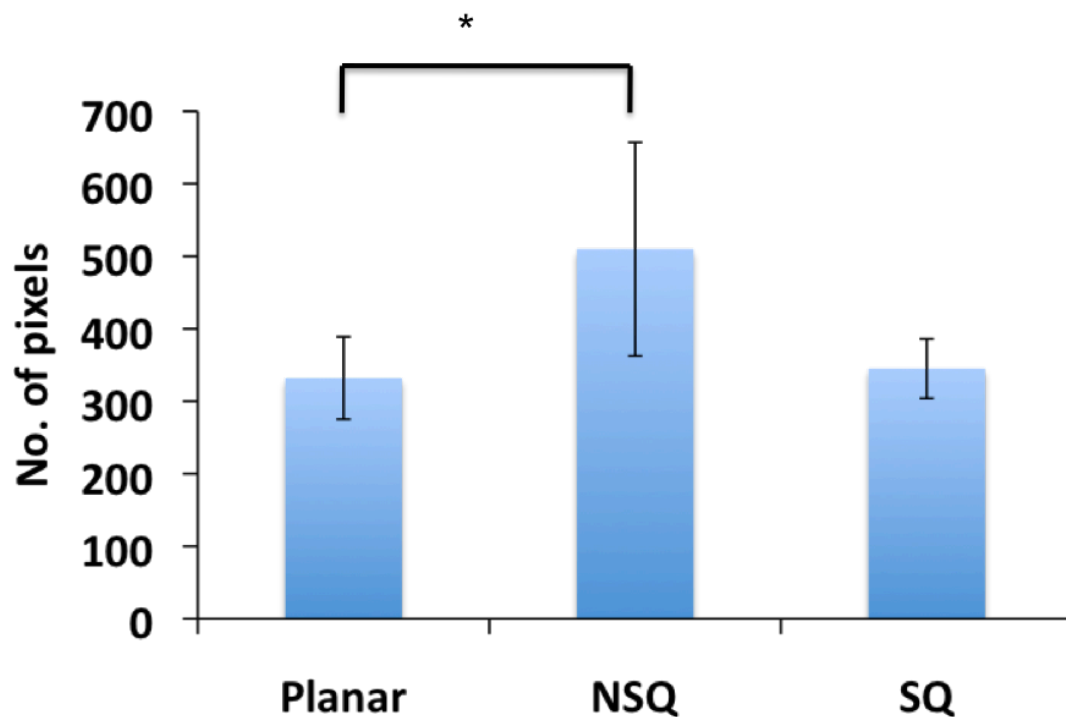


Figure 43 Average perimeter of identified areas of staining calculated by Cell Profiler analysis of von Kossa staining of SAOS-2 cells cultured on PEEK substrates that had been oxygen plasma treated for 2 minutes at 200W. Cells on the NSQ nanotopography displayed a statistically significant higher average perimeter compared to the planar surface Total number of replicates N =18: 6 Planar, 6 NSQ, 6 SQ.

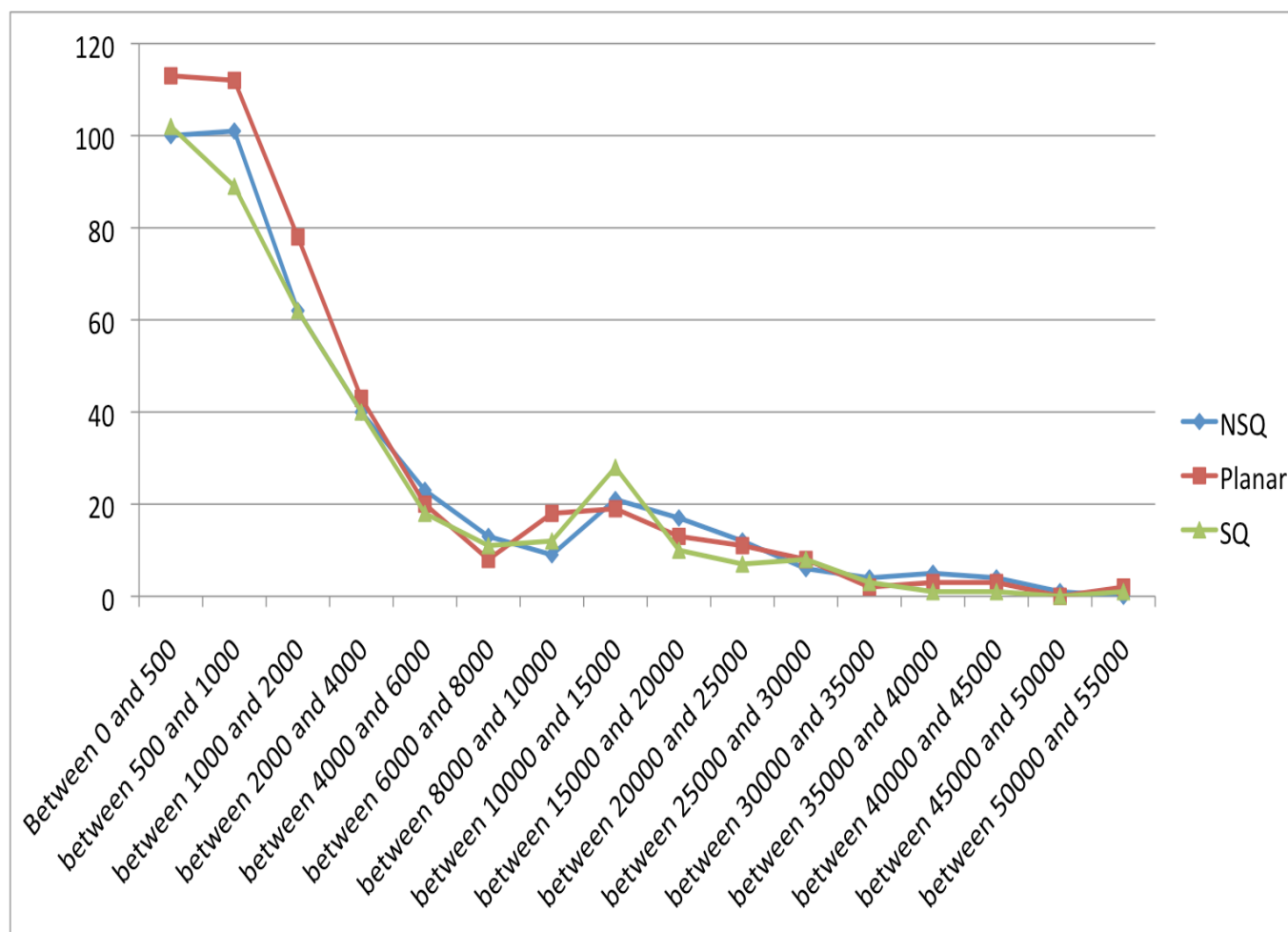


Figure 44 A size distribution analysis of the areas of the discrete objects identified by Cell Profiler analysis of SAOS-2 cells cultured for four weeks on PEEK nanopatternographies and stained with von Kossa. Total number of replicates N=18: 6 Planar, 6 NSQ, 6 SQ.

The results clearly showed that the SAOS-2 cells responded strongly to the oxygen plasma treatment. In the absence of the plasma treatment a small number of cells adhere to the surface but by 28 days they have failed to form a confluent monolayer across the surface and have not produced significant deposits of mineralised material, whereas after 2 minutes of 200W oxygen plasma treatment the cells have completely covered the surface and have produced large well defined mineralised deposits.

Cell Profiler allows us to measure a wide range of different properties of the stained areas which it has identified. We decided to take advantage of this to see if the presence of the nanopatternography had any impact on the size and shape of the mineralised deposits formed. We investigated; mean radius, average perimeter, average area and median radius. Additionally, we analysed the distribution of the

area of the discrete identified stained regions. We thought that when it came to the area of stained material, taking an average size might miss significance differences in cell behaviour on the different nanotopographies. We analysed the distribution of the area of the individual stained particle, as we thought that there was the possibility that for one of the nanotopographies the distribution may have been skewed significantly towards larger or smaller particles compared to the planar surface, which again may not have been picked up by looking at the average areas of identified particles for each of the topographies.

The results demonstrate that there is a significantly higher degree of von Kossa staining present on NSQ surface compared to the planar control. In addition to this, SAOS-2 cells on the NSQ nanotopography also exhibit areas of staining with significantly larger average perimeters than those of cells on the planar control. Cells on the SQ nanotopography did not display any behaviour in any of the investigated areas which were shown to be statistically significant, compared to the planar control surface. Although it is worth noting that in percentage of the surface with stained material, average perimeter and average area it displayed a trend towards being lower than the planar samples, albeit one that was not shown to be statistically significant.

The distribution analysis of the area of identified stained material did not show a clear difference in behaviour between the nanotopographies (*Figure 44*).

Given that there exists the possibility of von Kossa staining which does not indicate the presence of cell deposited apatite (effectively a false positive result)¹⁰², we decided to carry out alizarin red staining in an attempt to reinforce our von Kossa result. Given that von Kossa stains for the presence of phosphate and alizarin red stains for the presence of calcium, as long as we saw a similar pattern of staining with both techniques we would have a good degree of confidence that the staining we were seeing was down to mineralisation by the cells.

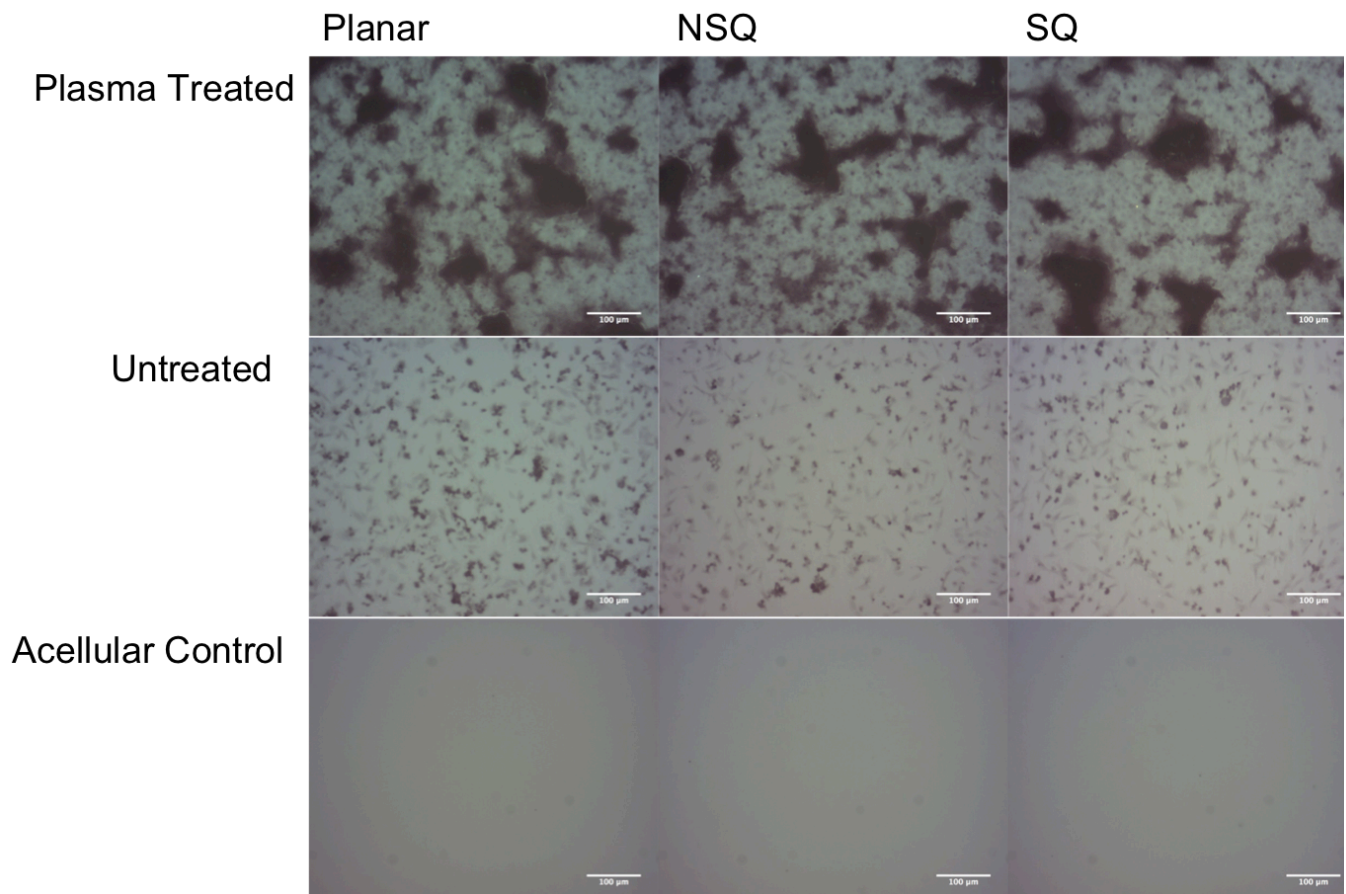


Figure 45 Polarised light microscope images of Alizarin red staining of SAOS-2 cells cultured for 28 days on PEEK nanotopographies which were treated with oxygen plasma for 2 minutes at 200W. Total number of replicates N=18: 6 Planar, 6 NSQ, 6 SQ. Scale bar = 100 μ m.

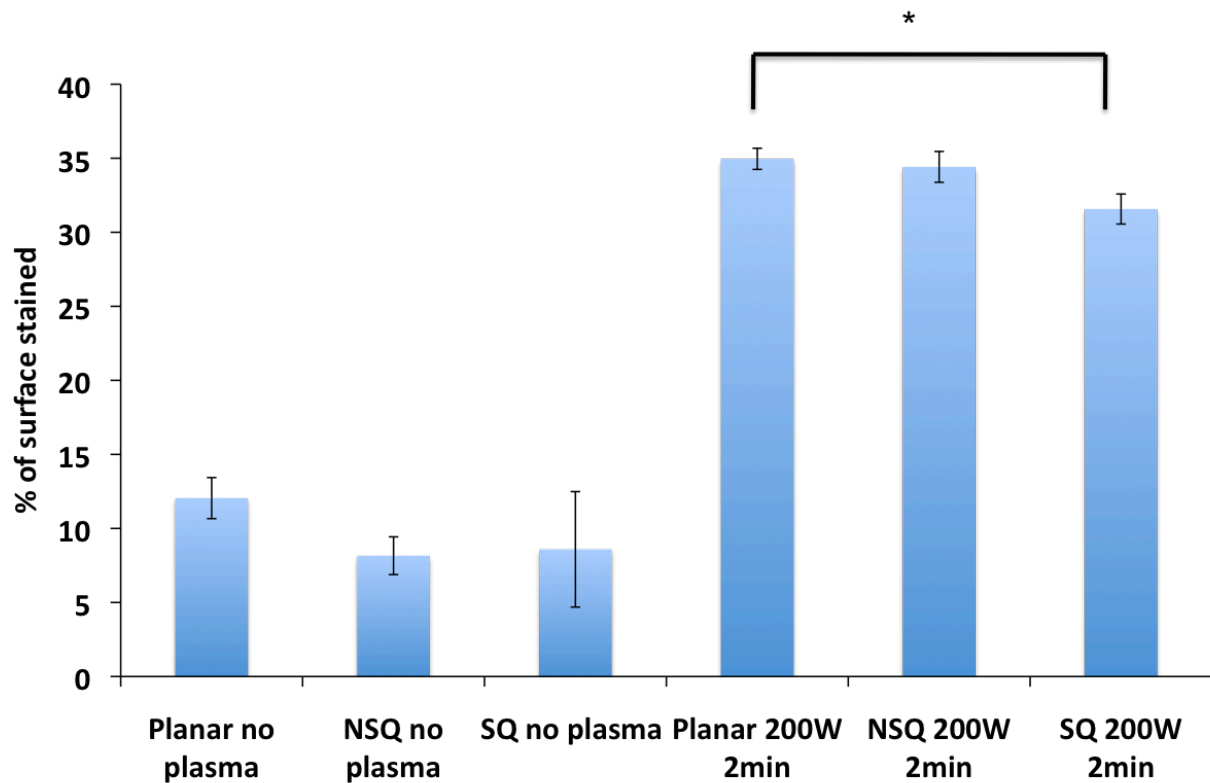


Figure 46 Cell Profiler analysis of polarised light microscope images of alizarin red staining of SAOS-2 cells cultured on PEEK substrates that had been oxygen plasma treated for 2 minutes at 200W. The presence of oxygen plasma has produced a strong increase in the level of phosphate produced on the surfaces. Additionally the percentage of the surface is significantly lower on the SQ nanotopography compared to the planar surface. Total number of replicates N=18: 6 Planar, 6 NSQ, 6 SQ.

	Times increase	Fold increase
Planar	2.704	0.432
NSQ	4.727	0.674
SQ	4.388	0.642

Figure 47 Table summarizing both the times increase and fold increase of the percentage of the surface stained via Alizarin between untreated and plasma treated PEEK nanotopographies.

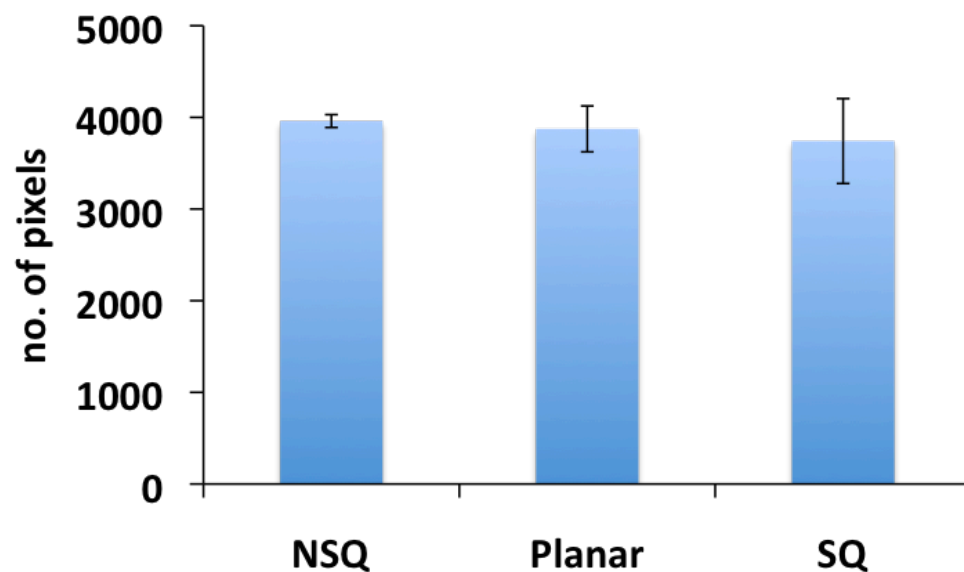


Figure 48 Average area of identified areas of staining calculated by Cell Profiler analysis of Alizarin red staining of SAOS-2 cells cultured on PEEK substrates that had been oxygen plasma treated for 2 minutes at 200W. Total number of replicates N=18: 6 Planar, 6 NSQ, 6 SQ.

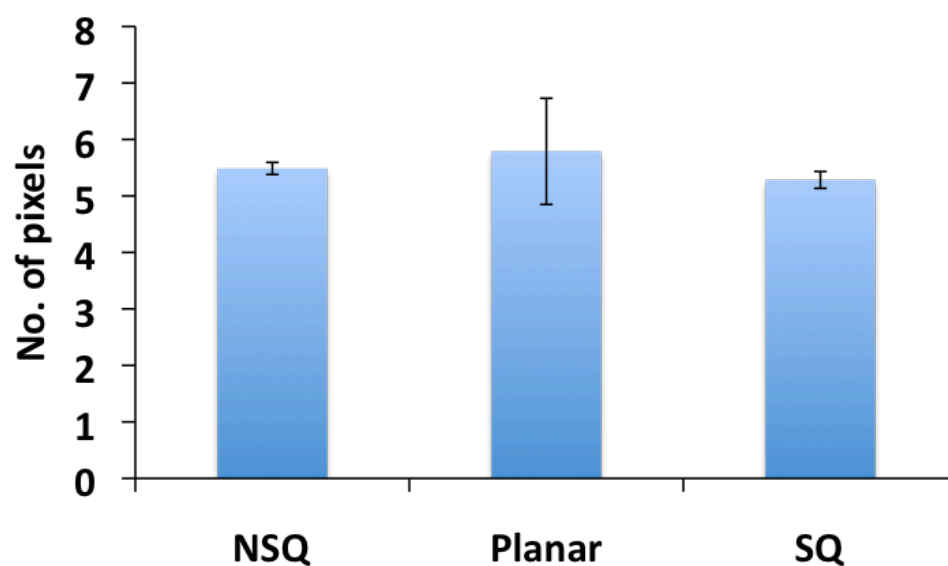


Figure 49 Mean radius of identified areas of staining calculated by Cell Profiler analysis of Alizarin red staining of SAOS-2 cells cultured on PEEK substrates that had been oxygen plasma treated for 2 minutes at 200W. Total number of replicates N=18: 6 Planar, 6 NSQ, 6 SQ.

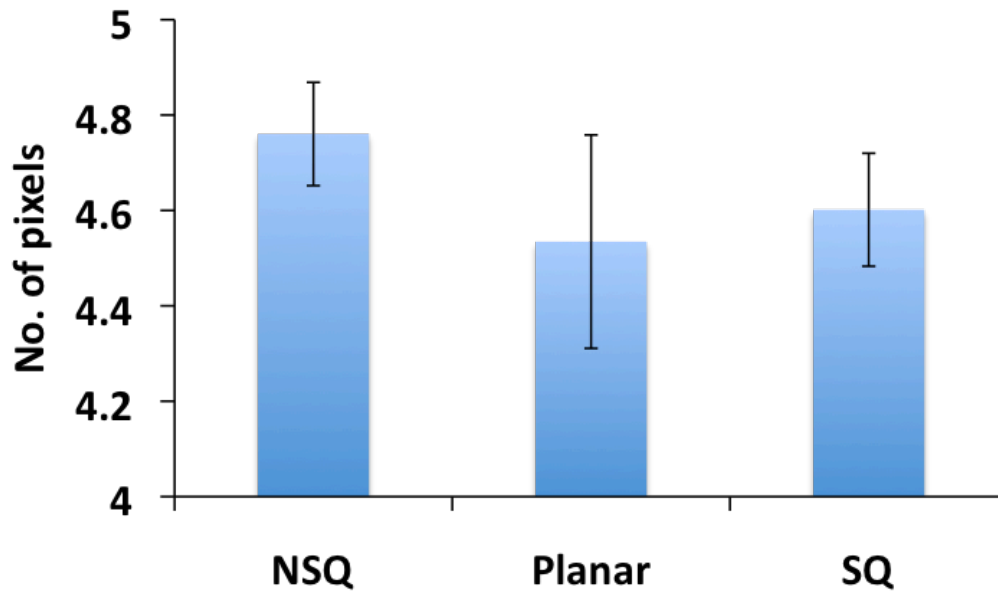


Figure 50 Median radius of identified areas of staining calculated by Cell Profiler analysis of Alizarin red staining of SAOS-2 cells cultured on PEEK substrates that had been oxygen plasma treated for 2 minutes at 200W. Total number of replicates N=18: 6 Planar, 6 NSQ, 6 SQ.

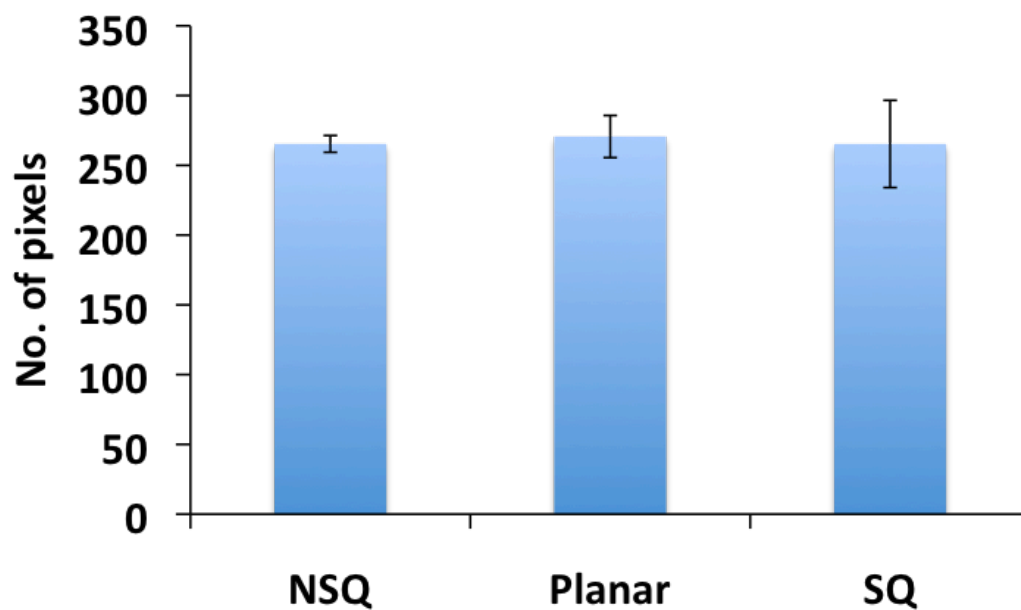


Figure 51 Average perimeter of identified areas of staining calculated by Cell Profiler analysis of Alizarin red staining of SAOS-2 cells cultured on PEEK substrates that had been oxygen plasma treated for 2 minutes at 200W. Total number of replicates N=18: 6 Planar, 6 NSQ, 6 SQ.

By comparing the results generated by the two different staining techniques, we can draw a number of conclusions. First of all, by comparing the two percentage of surface stained figures we can see that alizarin demonstrates an overall higher level of staining compared to von Kossa, both in the presence and absence of

plasma treatment. We believe that this suggests that there is a greater amount of calcium produced by the cells (alizarin red staining detects the presence of calcium) compared to phosphate (detected by von Kossa) and as a consequence, we see better definition in the von Kossa results. It is also worth noting that in our opinion Cell Profiler can better detect the border between stained and unstained regions with von Kossa stained samples compared to alizarin stained samples. Both techniques demonstrate a highly significant increase in the degree of staining on plasma treated compared to untreated surfaces across the different nanotopographies. The two techniques both show a nanotopography that has a significant difference in the percentage of the surface with stained material, compared to the planar surface. However, it is a different nanotopography with each different stain, with NSQ having a significantly higher result with von Kossa and SQ having a significantly lower result with alizarin. Additionally, NSQ displayed a significantly larger average perimeter of identified areas of staining compared to the planar surface.

We also considered the possibility that the presence of the topography may have exerted an effect on the cells that was stronger, or at least more visible, at an earlier time-point. In other words, cells on a topography may have mineralised faster or slower compared to the planar surface earlier in their time on the surfaces, but by 28 days the rate of mineralisation may have slowed or stopped on some surfaces and sped up on others, leading to less differences in the level of mineralisation between these surfaces. In order to test this we decided to stain the cells for von Kossa and alizarin red at 21 days. We decided not to include non-plasma treated surfaces as we felt that the previous experiment had established that we would not see significant cell adhesion, and as a consequence mineralisation, so would not contribute any useful data.

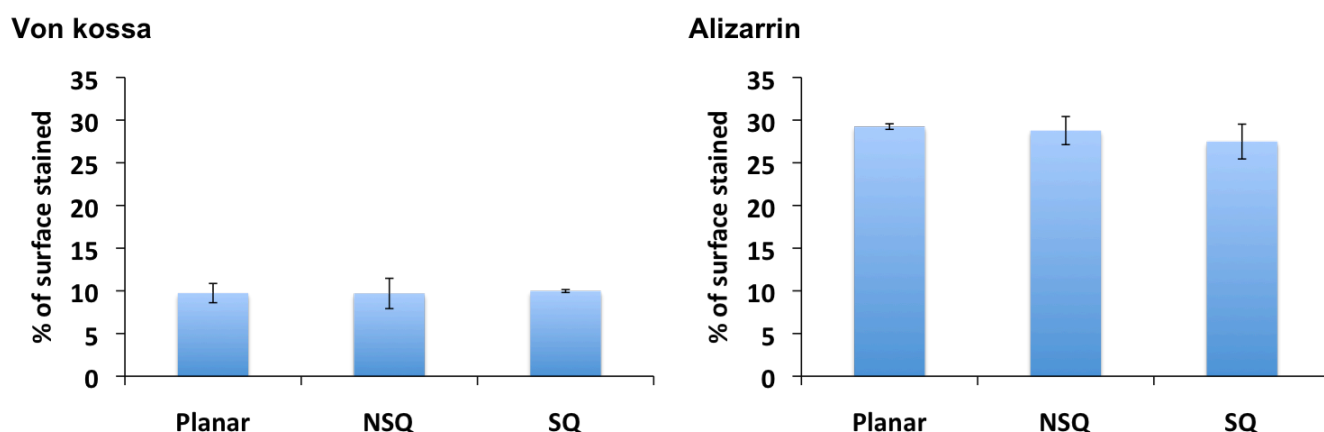


Figure 52 Cell Profiler analysis of polarised light microscope images of von Kossa and alizarin red staining of SAOS-2 cells cultured on PEEK substrates that had been oxygen plasma treated for 2 minutes at 200W and cultured for 3 weeks. Total number of replicates N=18: 6 Planar, 6 NSQ, 6 SQ.

The results of this experiment showed no statistically significant differences for either of the two nanotopographies with either of the two staining methods.

7.2.2. SAOS-2 plasma duration screen

We considered the role of the plasma treatment in our cells behaviour. As previous work with these nanotopographies had been carried out with other polymers³⁵³⁶ which did not require such radical surface treatment to allow cellular adhesion, we were unsure if the plasma treatment itself might have disrupted the topographies ability to influence cellular behaviour. It is also worth noting that this was the first work done with these nanotopographies fabricated from any material with these particular cells, so we were not entirely sure if they were capable of responding to the topography. However, given the possibility that Oxygen plasma treatment had the potential to negatively impact on the ability of the topography to influence the behaviour of osteoprogenitor cells (a cell type we knew had the capacity to respond to nanotopographies fabricated from other polymers), due to previously published work³⁵³⁶ we thought it would be worthwhile to test a range of different plasma treatments that gradually reduced the strength of the treatment from the 200W for two minutes that we used in the previous culture length experiments. We wanted to see if by decreasing the plasma treatment and therefore the degree of change in wettability we could find a “sweet spot”, where the plasma treatment was sufficient to permit an acceptable level of cell adhesion, but not so great as to interfere with the topographies ability to influence cellular behaviour, which we believed was

happening at 2 minutes of 200W plasma. While we were not certain that the SAOS-2 cells would be capable of responding to the presence of nanotopography in a similar fashion to that reported of osteoprogenitors, the SAOS-2 cells gave us the opportunity to screen a larger number of different plasma treatments in a shorter period of time, than would be possible with primary cells. Additionally, given the interest that an osteoblast like cell response would have for an eventual nanopatterned PEEK orthopaedic implant, it was thought worthwhile to screen different oxygen plasma treatments with SAOS-2 cells.

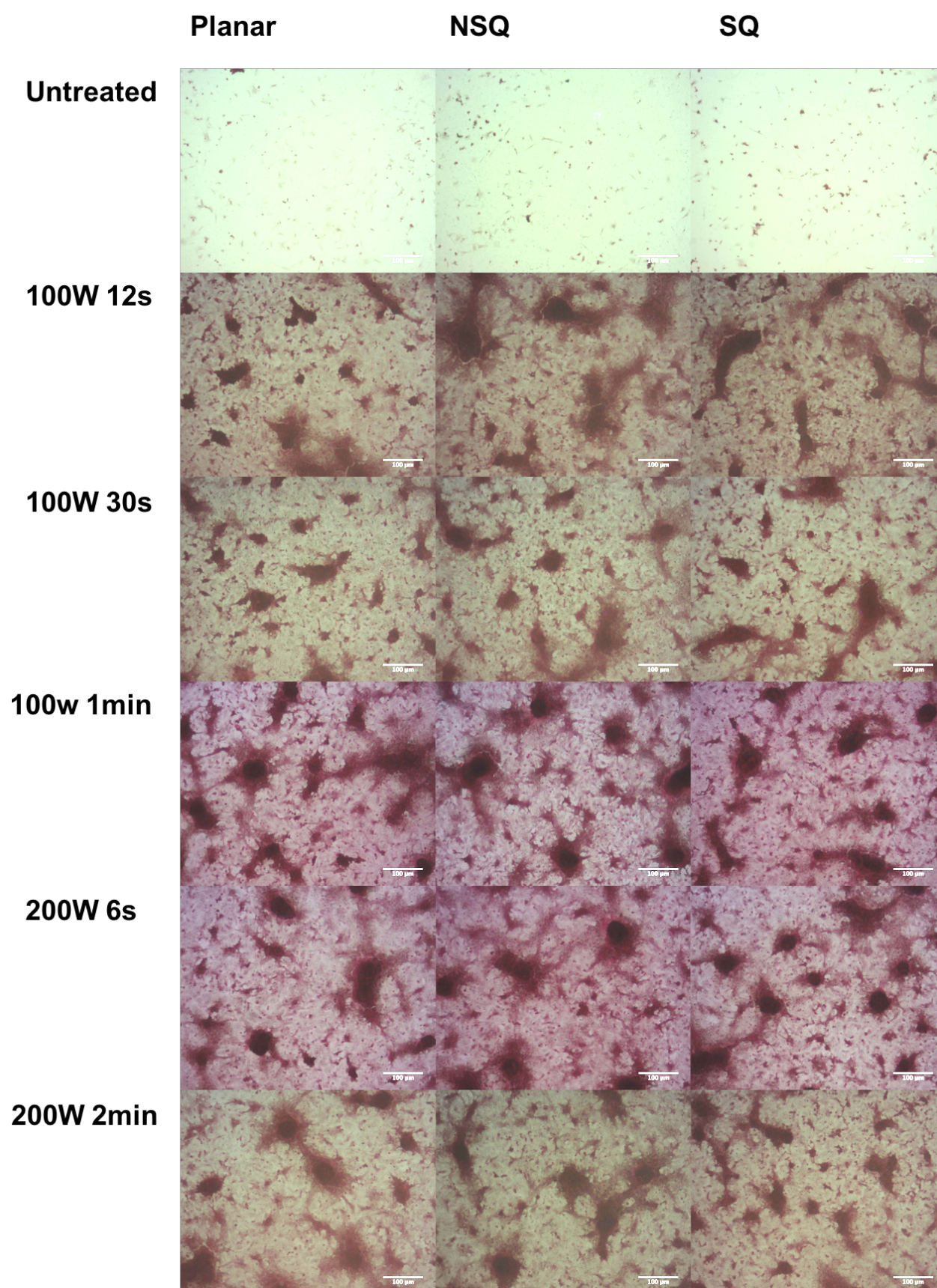


Figure 53 Polarised light microscope images of Von Kossa staining of SAOS-2 cells cultured for 21 days on PEEK nanoscale topographies that had received varying degrees of plasma treatment. Total number of replicates N=54: 18 Planar, 18 NSQ, 18 SQ. Scale bar = 100μm.

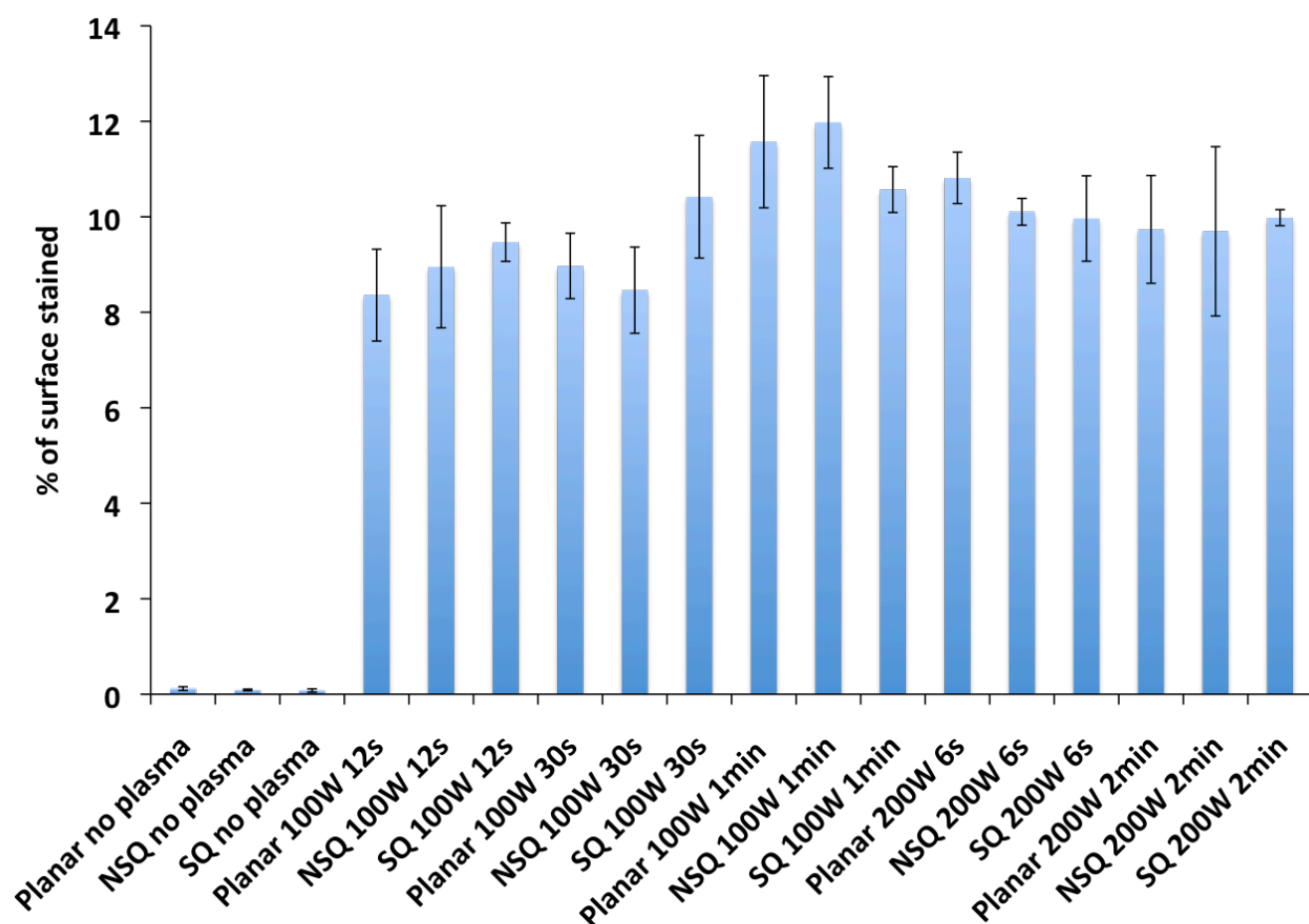


Figure 54 Collected cell percentage of the surface stained results from each of the Oxygen plasma treatments used. The Cell Profiler results were generated from polarised light microscope image of Von Kossa stained SAOS-2 cells. While there is little difference between individual nanotopographies at any of the different plasma treatments, there is however a strong difference in the level of mineralisation between the untreated surfaces and any of the plasma treatments. Total number of replicates N=54: 18 Planar, 18 NSQ, 18 SQ.

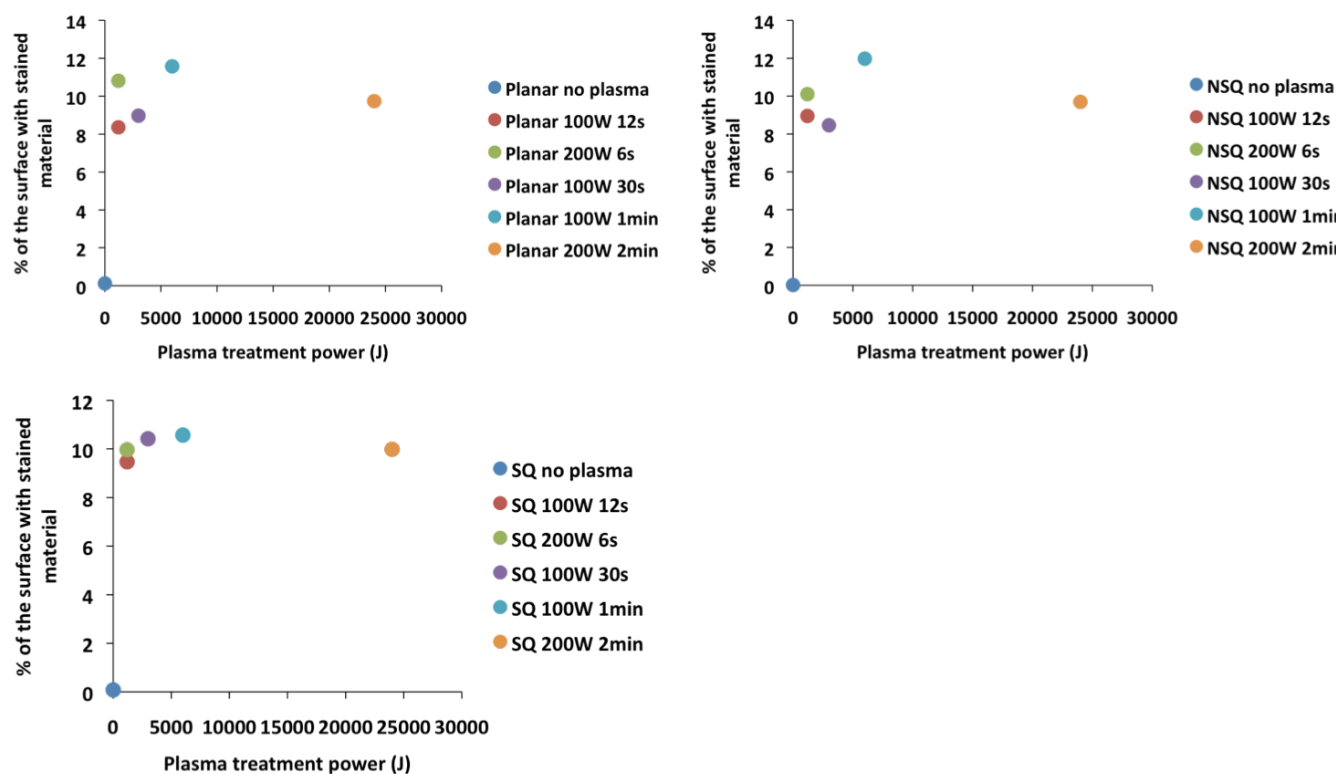


Figure 55 Percentage of the surface stained results plotted against the power in Watts of the plasma treatment used. Total number of replicates N=54: 18 Planar, 18 NSQ, 18 SQ.

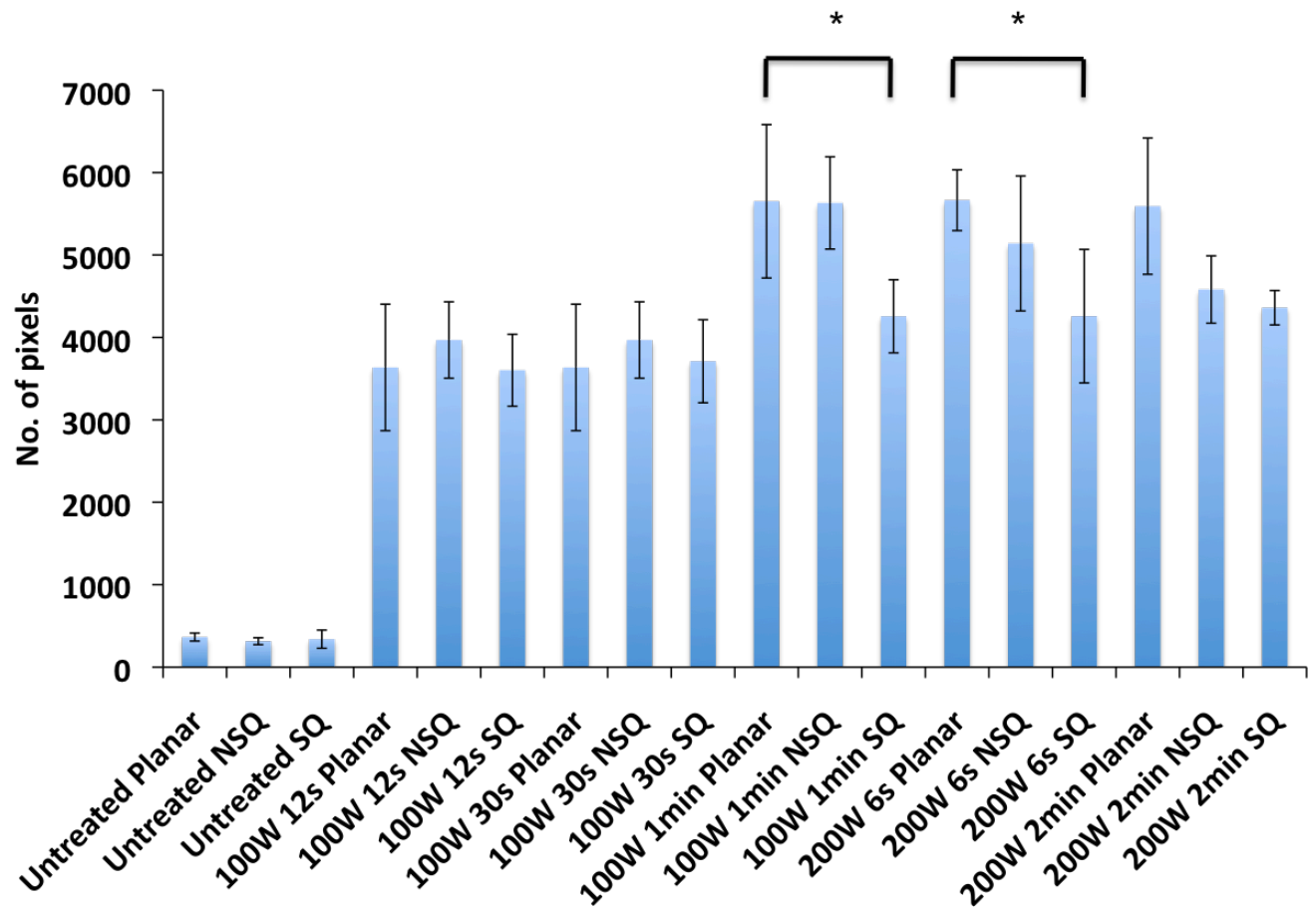


Figure 56 Collected average area of identified stained material from each of the Oxygen plasma treatments used The Cell Profiler results were generated from polarised light microscope image of Von Kossa stained SAOS-2 cells. The average area of the SQ nanotopography is statistically significantly lower than the planar surface at both 100W 1min and 200W 6s. Total number of replicates N=54: 18 Planar, 18 NSQ, 18 SQ.

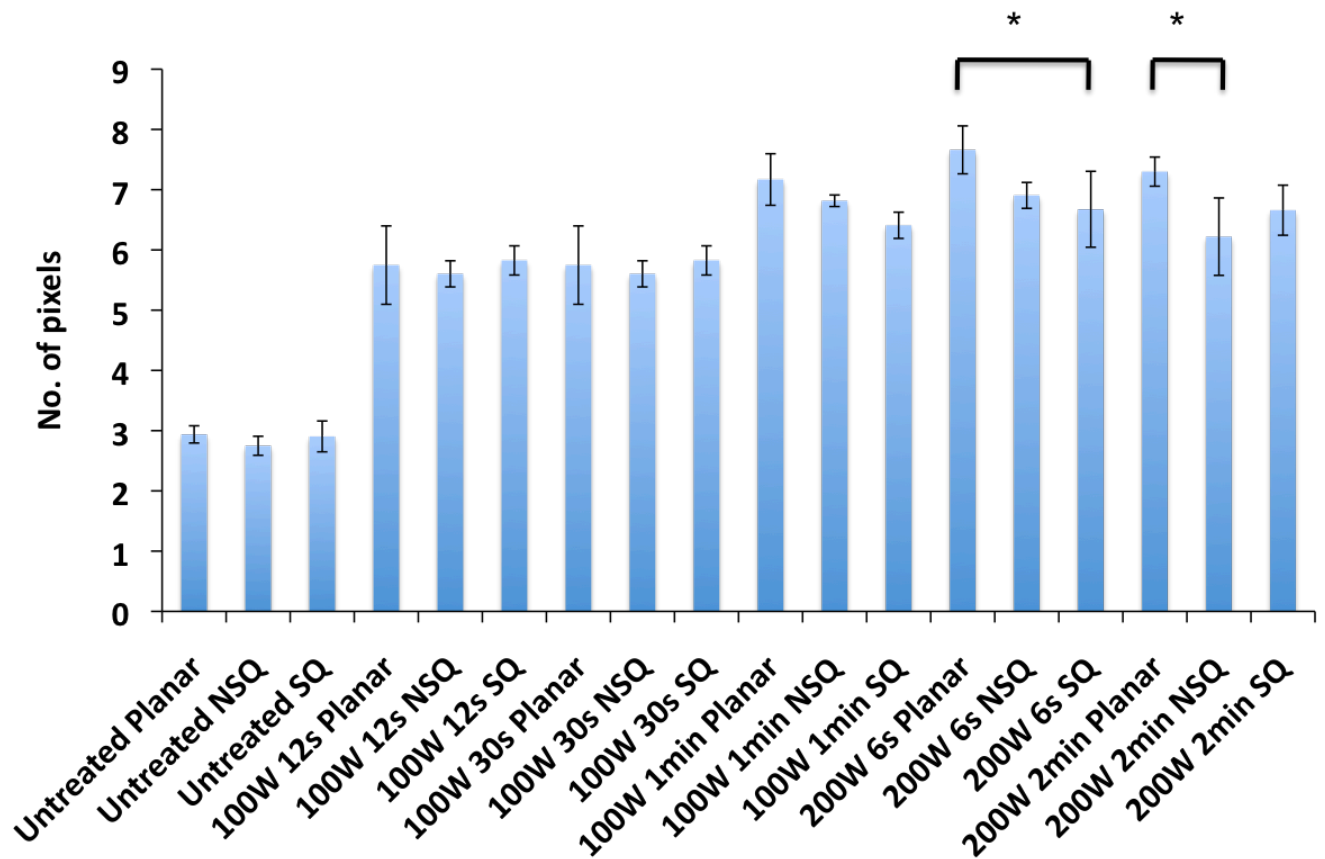


Figure 57 Collected mean radius of identified stained material from each of the Oxygen plasma treatments used. The Cell Profiler results were generated from polarised light microscope images of Von Kossa stained SAOS-2 cells. The mean radius of the SQ nanotopography was statistically significantly lower than that of planar surface at 200W 6s and the mean radius of the NSQ nanotopography was also statistically significantly lower than that of the planar surface at 200W 2min. Total number of replicates N=54: 18 Planar, 18 NSQ, 18 SQ.

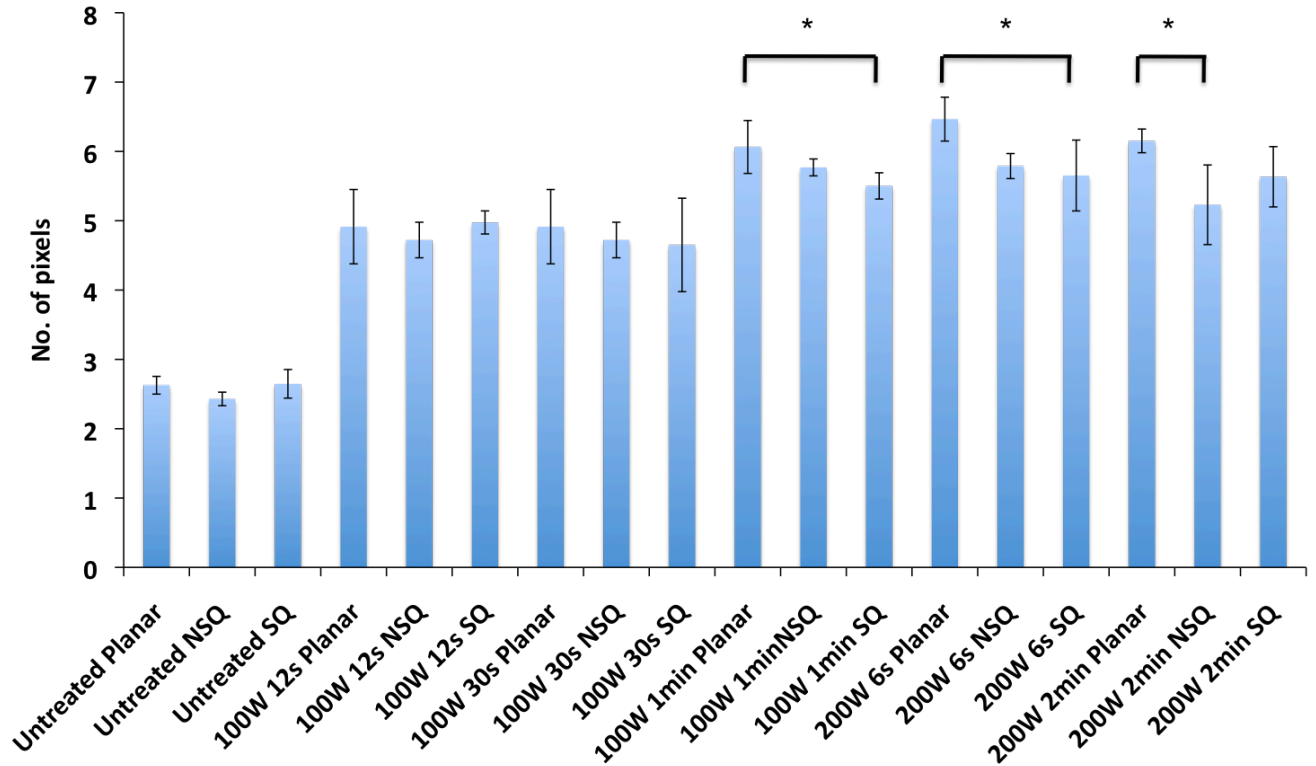


Figure 58 Collected median radius of identified stained material from each of the Oxygen plasma treatments used The Cell Profiler results were generated from polarised light microscope images of Von Kossa stained SAOS-2 cells. The median radius of the SQ nanotopography was statistically significantly lower than that of the planar surface at both 100W 1min and 200W 6s. Additionally the median radius of the NSQ nanotopography was statistically significantly lower than that of the planar surface at 200W 2min. Total number of replicates N=54: 18 Planar, 18 NSQ, 18 SQ.

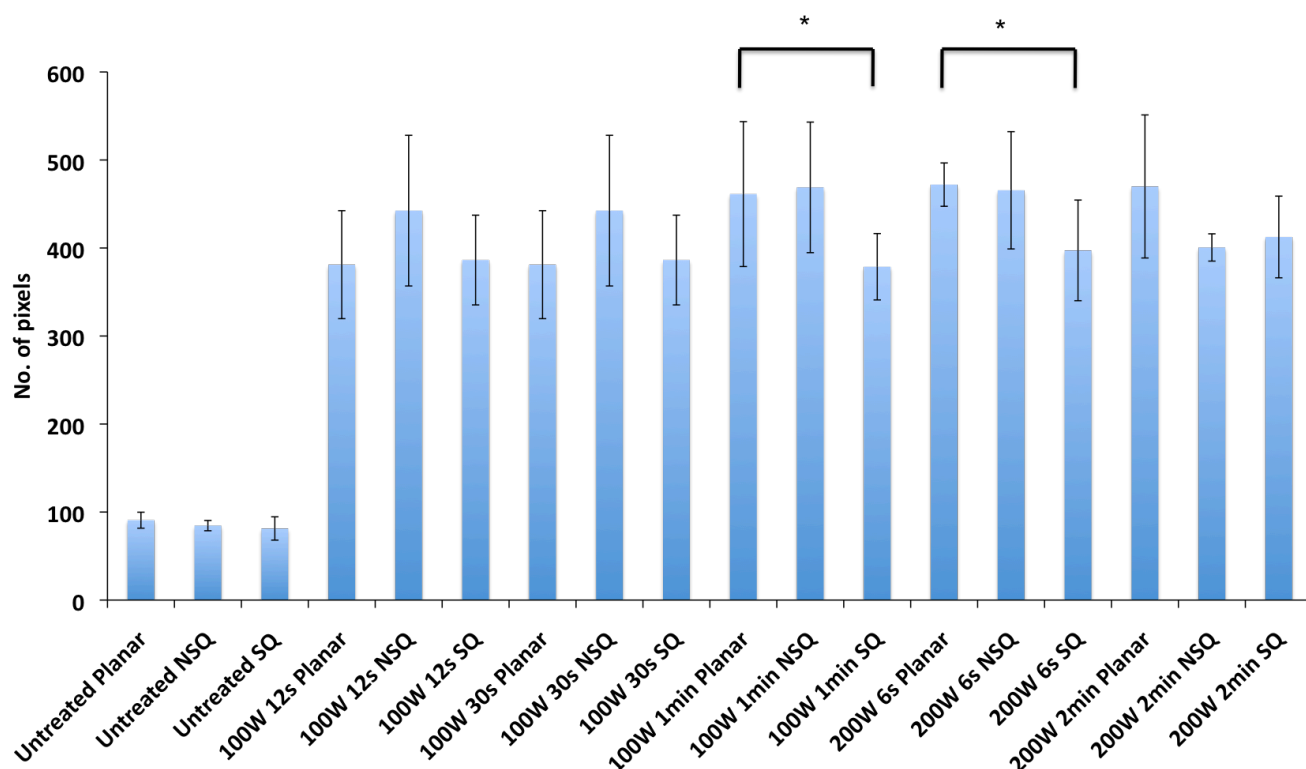


Figure 59 Collected average perimeter of identified stained material from each of the Oxygen plasma treatments used. The Cell Profiler results were generated from polarised light microscope images of Von Kossa stained SAOS-2 cells. The average perimeter of the SQ nanotopography was statistically significantly lower than that of the planar surface at both 100W 1min and 200W 6s. Total number of replicates N=54: 18 Planar, 18 NSQ, 18 SQ.

To analyze the results of this experiment we used Cell Profiler in order to look at a number of different properties of the von Kossa staining. Firstly we compared the overall percentage of the microscope image with stained material between the different plasma treatment regimes. We then plotted the percentage of the surface stained results against the power of the plasma treatment used in each case. We then investigated specific other properties of the individual stained objects i.e. the average area, mean radius, median radius and average perimeter between the different plasma treatments used.

The results demonstrate that there was no significant difference in the percentage of the surface with stained material between the nanotopographies at any of the different plasma treatments.

The relationship between the power of plasma treatment and the resulting percentage of the surface with stained material showed that overall, the level of staining increased with the power of plasma treatment. This trend was consistent

across the nanotopographies, although there were some slight variations between them. Each increase in power on the SQ surface was met with a subsequent increase in the percentage of the surface with stained material, whereas the 100W 30s NSQ and planar surfaces had a lower amount of staining than the preceding surfaces. In addition, the 200W 6s surfaces had a lower level of staining with both NSQ and Planar, than their preceding treatment.

More in depth analysis of the pattern of staining showed further significant differences between the nanotopographies. At 2 minutes of 200W plasma treatment the NSQ nanotopography had both a mean radius and a median radius that is significantly lower than that of the planar surface. At 1 minute of 100W plasma treatment both the median radius and perimeter of the SQ nanotopography were significantly lower than that of planar surface. At 30s of 100W plasma treatment the mean radius of the SQ nanotopography was significantly higher than that of the planar surface. Finally, at 6s of 200W treatment the median radius and average perimeter of the SQ nanotopography were significantly lower than those of planar surface.

7.3. Discussion

7.3.1. Behaviour of SAOS-2 cells on PEEK nanotopographies

Our results show that SAOS-2 cells are capable of having their osteogenic behaviour modulated by the presence of nanotopography in PEEK. Von Kossa staining of nanotopographies which had been plasma treated for 2 minutes at 200W using SAOS-2 cells that had been cultured for 28 days, showed that there was significantly more von Kossa staining on the NSQ nanotopography compared to the planar surface. The same experiment, using alizarin red instead of von Kossa showed the SQ nanotopography produced a lower level of mineralization compared to the planar surface.

These results are of particular interest as they shows a similar trend to that observed with these topographies on other polymers^{35,36,60}. It is worth pointing out these results were generated using stem cells, so it is interesting that we see a similarity in overall behaviour with fully differentiated cells. However the two staining techniques show two different results i.e. there is no significant

difference in behaviour between the SQ nanotopography and planar in the von Kossa staining and there is no significant difference between the NSQ nanotopography and planar in the alizarin staining. Our interpretation of this lack of consistency in results between the two staining techniques is that they overall show similar trends, but with von Kossa the SQ result isn't quite low enough to clear the threshold for significance, and with alizarin the NSQ result is not high enough to qualify as significant. While this indicates the behavioural cue delivered by the presence of these particular nanotopographies are not as strong as they could be, we believe that the behavioural signal delivered to the cells by the nanotopography is not as strong as the one delivered by the same nanotopography fabricated from one of the previously tested polymers e.g. polycarbonate. While we believe that it is eminently possible that a different nanotopography could be capable of delivering a stronger behavioural stimulus, it is evident that the presence of nanotopography at the PEEK surface is capable of modulating the osteogenic behaviour of these cells.

As mature osteoblasts make up an appreciable fraction of the cells that adhere to the surface of an orthopaedic implant, our finding that a specific nanotopography at the PEEK surface can modulate the behaviour of SAOS-2 (cells which have been shown experimentally to show a good degree of fidelity in behaviour to primary osteoblasts) could have significance for the use of PEEK in biomaterial applications as a whole. However, we believe that the results suggest that our topographies may not represent the most effective arrangement of features for inducing particular activity in these cells. Further testing of the relationship between cells and specific nanofeatures fabricated from this material could reveal arrangements that could produce stronger osteogenic responses from the cells.

7.3.2. Influence of the energy of plasma treatment on the SAOS-2 cells

The relationship between plasma treatment and SAOS-2 response is not entirely straightforward. The overall percentage of the surface stained data does not show a significant statistical difference between any of the nanotopographies, at any of the plasma treatments. This does run contrary to our earlier results from the stand alone SAOS-2 cultured for four weeks on surfaces treated at 200W for 2 minutes, where the NSQ nanotopography displayed a statistically significantly

higher result compared to the planar surface. The difference in the two results would suggest both, that there can be variability between individual surfaces and that the difference present between the NSQ and planar surfaces in the von Kossa 200W 2 minute four weeks of culture experiment, is just enough to cross the significance threshold, and it is possible that a second set of triplicates could provide a set of results that are on the other side of the significance threshold.

We can see that increasing the energy of plasma treatment in turn leads to an increase in the overall percentage of staining. There are exceptions to this, in particular the highest energy used (24000J) was lower than second highest energy setting employed (6000J). In addition to this, for the NSQ and planar surfaces the 3000J treatment was lower than the 1200J treatment. It is difficult to gauge the exact significance of these variations, and it is probably of more interest that all three surfaces appear to show a decrease in the percentage of the surface with staining at the highest power used (24000J), compared to the second highest (6000J). Given the large difference in the amount of power used, it seems plausible that at that some point between 6000J and 24000J there is a point at which the percentage of the surface stained stopped increasing, and by 24000J had already started to decline. The average difference between 24000J and 6000J for the three surfaces is 13.4% (planar = 15.6%, NSQ = 19.04% and SQ = 5.5%) so the decrease is not inconsiderable, and suggests that the plasma treatment which would deliver the highest mineralization response lies somewhere above 6000J and below 24000J.

7.4. Conclusions

Overall our results demonstrate that the presence of nanotopography on the surface of PEEK is capable of influencing the mineralisation behaviour of SAOS-2 cells. While we do not necessarily believe that the nanotopographies that we have tested here represent the most effective topographical features for guiding the behaviour of osteoblast like cells on PEEK, we do believe that the results indicated the presence of nanotopography at the PEEK surface which can influence the behaviour of these cells and as such provides evidence that, in our opinion, it is

worthwhile to continue exploring topographical alteration to the PEEK surface to guide osteoblast cells to desired behavioural responses.

The relationship between plasma treatment and the response of osteoblast like cells to our PEEK nanotopographies shows a general trend for increasing osteogenic response along with increasing power of treatment up to 6000J, whereafter it appears to decline. It is worth noting that the gap in power of plasma treatment between the highest power tested (24000J) and the second highest (6000J) where there is average 13.4% decline in mineralisation is large and as a result we are unable to say for certain at which point osteogenic response peaks. Further experiments of the type carried out here exploring the osteogenic response of treatments between 6000J and 24000J are required to identify the treatment which would deliver the strongest osteogenic response from these cells on PEEK.

8. Impact of defined nanotopography and controlled surface chemistry in PEEK on the osteogenic behaviour of primary human stem cells

8.1. Introduction

8.1.1. Ability of nanotopography to effect cell activity.

There are a number of examples of specific nanoscale topography being incorporated at a material surface and this topography directing differentiation behaviour of the cells cultured upon it^{26,27,30,35,58-60}.

Our work draws from earlier work performed at Glasgow with these topographies fabricated from other polymers, which demonstrated both that cells could interact with topographical features at the material surface, and that these interactions could direct a cells developmental behaviour^{35,36,60}

8.1.2. Aims of working with nanotopography

PEEK is in many respects an excellent choice for use in orthopaedic implants, as it displays a range of material properties such as a natural radiolucency and MRI compatibility, as well as good chemical and sterilization resistance⁶⁴. It has been demonstrated to have mechanical characteristics such as stiffness and modulus, which match those of bone better than competing biomaterials. It has an FDA master file and as a result has undergone extensive studies on intracutaneous toxicity and intramuscular implantation, sensitization and gene toxicity⁷¹⁻⁷⁵. Finally, as PEEK is a polymer, it is possible to utilise plastics technologies which enable us to manufacture devices from it, which in turn offers a range of different methods for the mass production of PEEK substrates. The material also has a reproducible, pure and traceable supply route

However, *in vivo* the material displays poor tissue to implant contact^{64,82,83} which leads to a weak interface between host tissue and the implant, which in turn leads to poor implant performance⁶. As nanotopography incorporated into the surface of other polymers has been demonstrated to lead to stem cells that came into contact with it differentiating down the osteogenic lineage³⁵, we believed that a

nanopatterned PEEK surface could display similar results, and in turn a nanopatterned PEEK implant would form a tighter interface with the host tissue, resulting in a better performing orthopaedic implant.

8.1.3. Structure of the experiments

An additional issue that arises from working with PEEK is that the material is strongly autofluorescent⁷⁴. As a consequence, it is not possible to use standard fluorescence based immunostaining to investigate the osteogenic behaviour of the cells cultured on our nanotopographies. This complication is significant, as fluorescence based immunostaining was one of the principle techniques used to investigate the response of stem cells to nanotopography in previous work carried out with these topographies fabricated from other polymers^{35,36}.

To address, this we have utilised a number of different histological techniques which, coupled with Cell Profiler analysis, allows us to quantitatively analysis a number of different stages of the osteogenic process between different nanotopographies, in order to give us the best chance of spotting any significant differences in cell response between the different nanotopographies.

8.1.4. Potential impact of plasma treatment on the activity of the nanotopography

In order to address the underlying issues of PEEK having poor cell adhesion and growth⁸⁴ we treated our PEEK nanotopographies with oxygen plasma. While we took a range of measurements to gauge how the treatment had altered the surface, we were conscious that the oxygen plasma treatment may have altered the surface in a way which could have disrupted the ability of the topography to direct the behaviour of the cells cultured on it.

8.2. Results

Our previous work with oxygen plasma treatment had demonstrated that it could address PEEK's innate and well-documented cytophobicity, while still maintaining the integrity of our nanotopography. Still there is an underlying question of

whether the presence of specific nanotopography can direct stem cell behaviour when incorporated into PEEK, in a similar fashion to that seen with other polymers^{35,36,60}, and indeed if this possible activity is disrupted by the presence of the oxygen plasma treatment. To address this we decided to look at different facets of the osteogenic response of osteoprogenitor cells on PEEK nanotopographies, to see if they were capable of modulating the behaviour of the cells cultured upon them.

Initially in order to assess if the presence of the nanotopography affected the osteogenic activity of the progenitor cells cultured on it, we used quantitative PCR to analyse the expression of osteogenesis related genes. Based on the expression pattern displayed by progenitor cells on the same nanotopographies fabricated from other materials observed by our colleagues, we employed a culture period of eleven days, then harvested the cells from the surfaces and analysed their transcriptional behaviour.

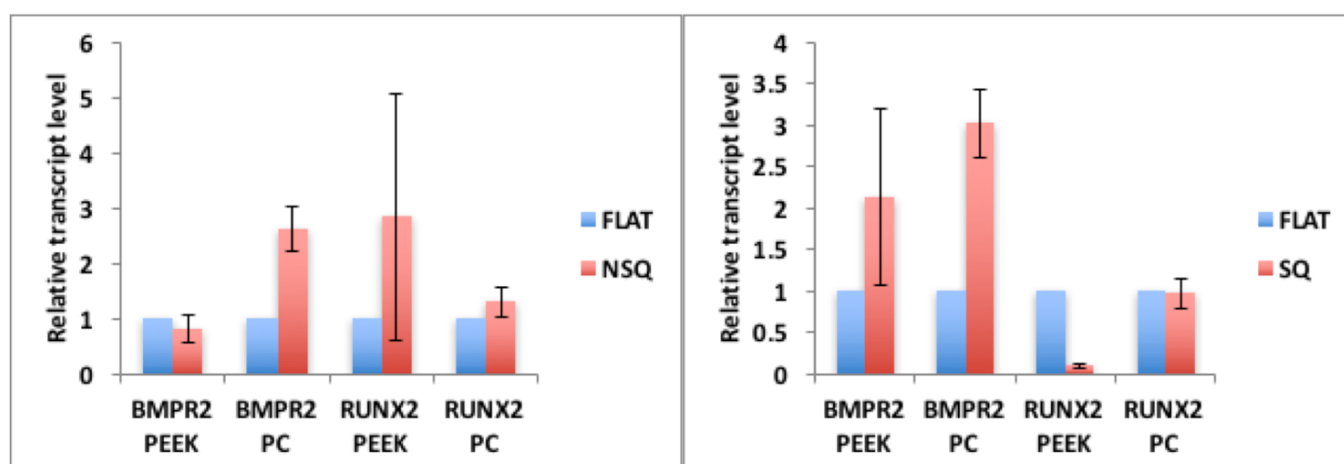


Figure 60 qPCR experiments measuring the expression of the osteogenesis related genes BMPR2 and RUNX2 by osteoprogenitor cells on PEEK and poly carbonate nanotopographies after 11 days of culture. Expression of both genes was normalised to the expression of GAPDH. For each gene N=81 Planar 27, NSQ 27, SQ 27.

The results did not demonstrate a clear statistically significant difference in gene transcription between the planar and experimental surfaces. In spite of this we can see some interesting trends in results. For the polycarbonate results we see the expected trend (transcript level being higher than that seen on flat for the NSQ surface and lower than that seen on the flat for the SQ surface) for the NSQ surface for both BMPR2 and RUNX2.

Upon consideration, we concluded that there were several possible reasons why we did not see significant differences in cell response between the flat and nanopatterned surfaces. It could be possible that the nanotopography did not have the same effect as observed in other polymers when fabricated from PEEK. It was also possible that the presence of the oxygen plasma treatment had disrupted the effect of the nanotopography, either through physical alteration to the topography itself or alteration to the surface chemistry. In addition, it was also possible that the nanotopography had, or does have the ability to cause the cells to express the genes being investigated differently, but at a time either before or after the eleven days. As we could not be sure why we saw the experimental results that we did, we decided not to repeat the experiment because of the large number of cells required and the associated period of time it would take to generate this number of progenitor cell. From that point onwards, we felt it would be more effective to look at osteogenic behaviour through histologically based means.

*Lian and Stein*¹⁰³ demonstrated that osteogenesis takes place in a number of distinct stages in a consistent manner, namely; they proliferate to reach confluence on the surface present, produce an extra cellular matrix, mature the produced matrix and then form mineralised nodules. Through the different biological assays that we had adapted to work with PEEK, we decided to look at the effect of the nanotopographies on the progenitor cells at each of the different stages of the osteogenic process. We did this for two main reasons. Firstly, we believed it was possible that the impact of the nanotopography on the progenitor cells may not have been uniform across the processes different stages, in other words, it may have been possible that the presence of the topography may have led to a change in adhesion and proliferation or ALP activity, but not in mineralisation behaviour. This still could be significant for the use of the topography in a future implant, but would be missed by only looking at mineralisation behaviour. Secondly, given that in vitro work is an imperfect model for the response to an implant in vivo, we felt that being able to demonstrate that the cells were passing through the established steps in osteogenesis would give us

more confidence that the nanotopography was leading to an alteration in osteogenic behaviour in a physiologically relevant manner, rather than say the staining techniques picking up phosphate or calcium that had precipitated onto the surface during the time the surfaces were cultured.

To investigate osteogenic behaviour on our PEEK surfaces we used alamar blue to track cell number (and by extension track proliferation), both histological staining (and Cell Profiler quantification) of alkaline phosphatase and an analysis of enzymatic activity, followed by von Kossa and alizarin red staining to look at mineralisation, by staining the phosphate and calcium aspects of hydroxyapatite respectively.

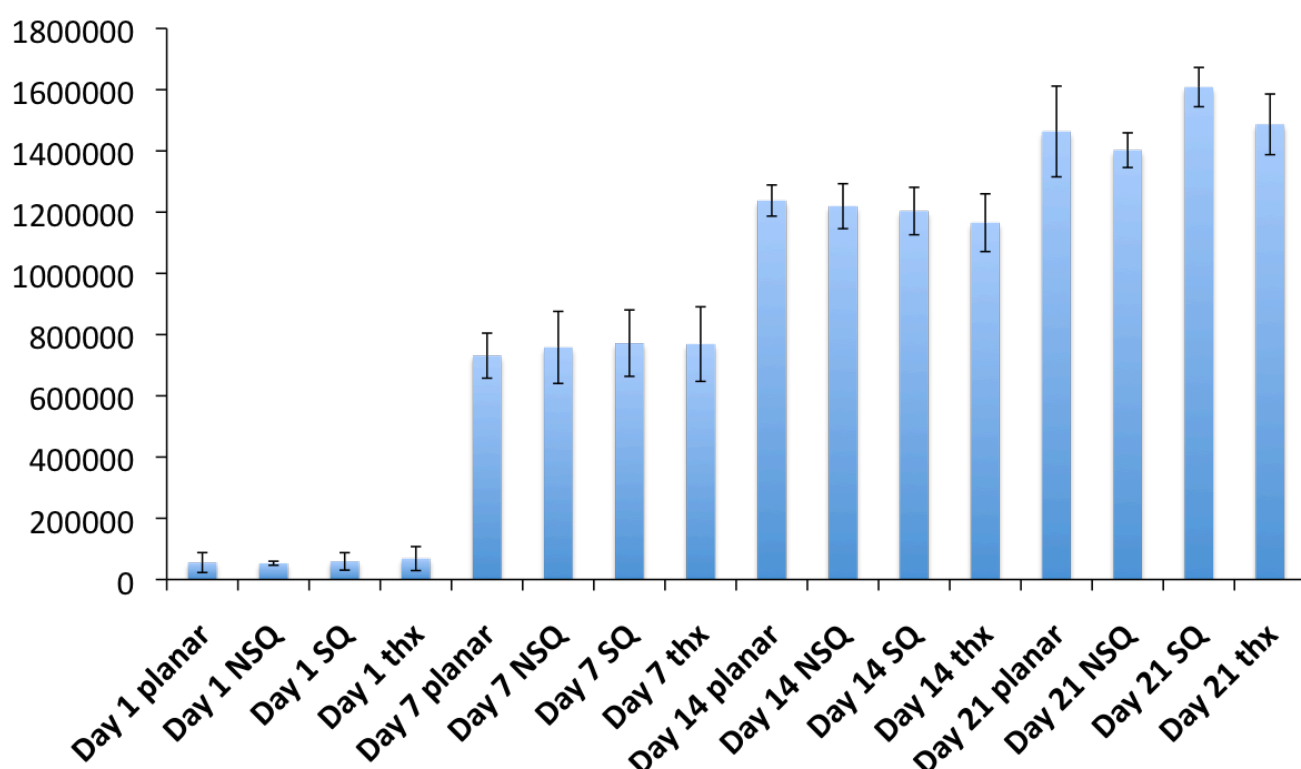


Figure 61 Alamar blue measurement of cell density on oxygen plasma treated PEEK nanotopographies with thermanox used as a positive control. We can see the cells rate of proliferation is at its highest between 1 and 7 days and to a lesser extent between 7 and 14 days as there is no statistically significant difference between any of the surfaces.

The Alamar blue results demonstrate that with the oxygen plasma treatment there is no significant difference in cell density between any of the different PEEK nanotopographies compared to the thermanox control surface at any of the time-

points tested. This shows that the effect of the oxygen plasma treatment is consistent with our previous experiments in that it has addressed PEEK's underlying poor cell adhesion at the materials surface, but it is interesting to note that despite the presence of significant nanofeatures on their surfaces there is no significant difference in cell density on these surfaces compared to the featureless planar and thermanox surfaces. This stands in contrast to the experiences of our colleagues working with the same nanotopographies fabricated from different polymers^{35,36,60}, where on the nanopatterned surfaces (particularly on ordered square SQ) there are routinely observed significantly less cells than on the planar surface. This may indicate that the oxygen plasma treatment has led to the cells being unable to sense a difference between the different surfaces.

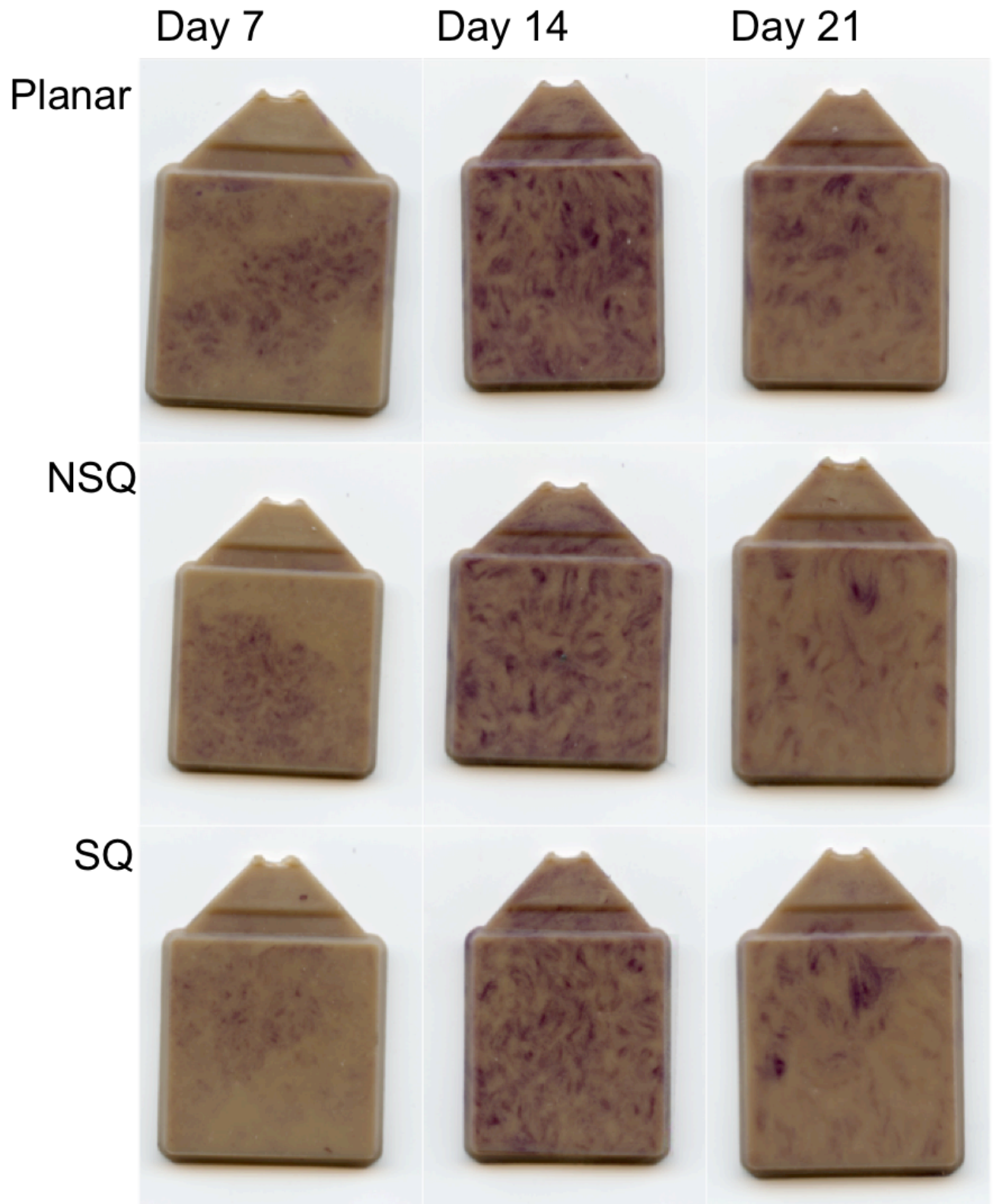


Figure 62 Representative whole substrate scans that have been histologically stained for alkaline phosphate at 1, 14 and 21 days. In each instance ALP level increases at day 14 compared to day 1 and then declines by day 21 compared to day 14. Total number of replicates N=9 3 Planar, 3 NSQ, 3 SQ.

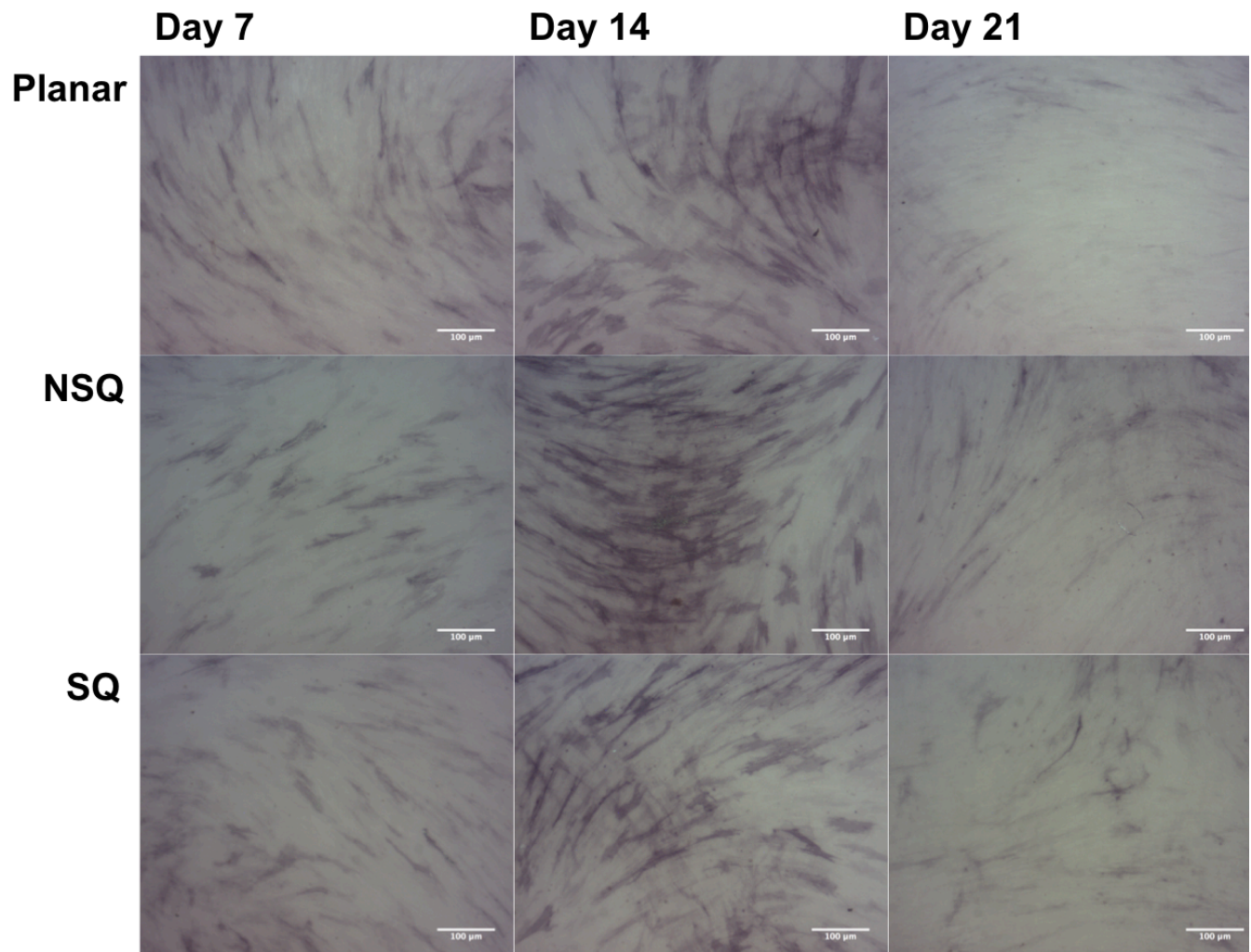


Figure 63 Representative polarised light microscope images of histological staining for alkaline phosphatase at 7, 14 and 21 days. In each instance ALP level increases at day 14 compared to day 7 and then declines by day 21 compared to day 14. Total number of replicates N=9 3 Planar, 3 NSQ, 3 SQ. Scale bar = 100 μ m

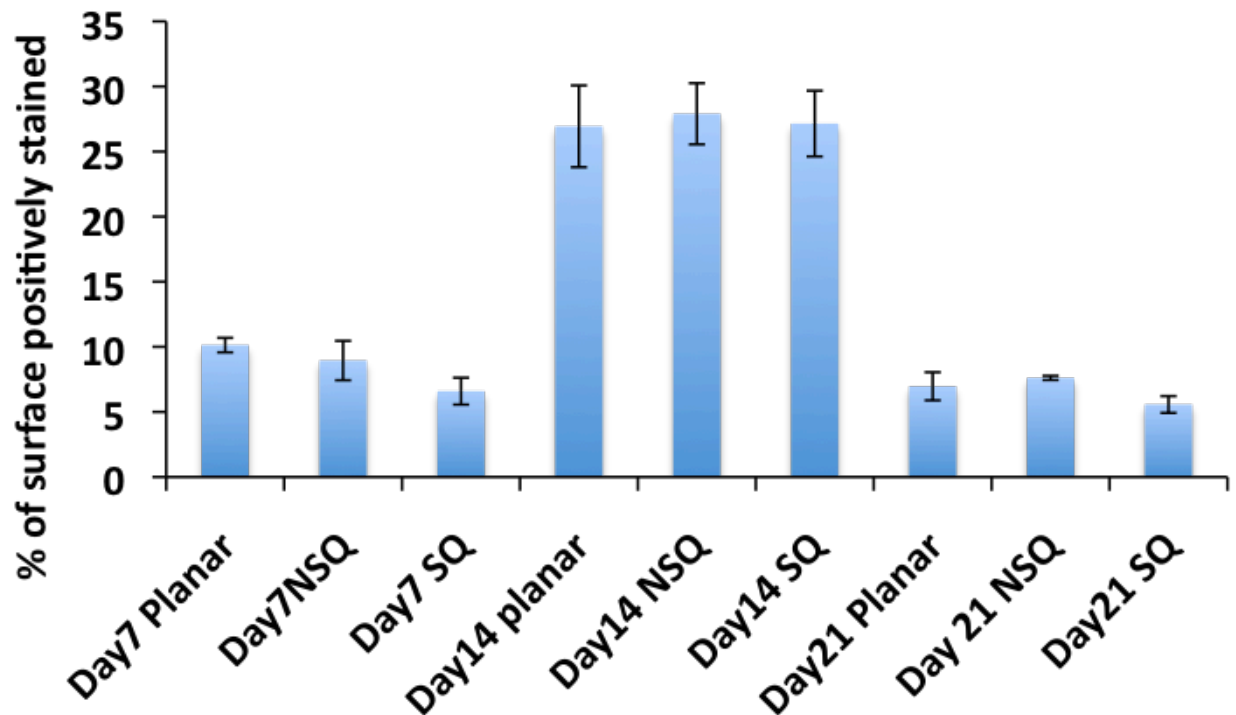


Figure 64 Cell Profiler analysis of the percentage of the surface with ALP staining at 7, 14 and 21 days. The results show that in line with the microscope images, ALP level rise at 14 days and decrease again at 21 days. There was no statistically significant differences in ALP activity between the surfaces at any of the time points. Total number of replicates N=9 3 Planar, 3 NSQ, 3 SQ.

The alkaline phosphate results demonstrate that the cells cultured on our surfaces produce ALP in a physiologically relevant manner, and is shown to be most abundant, and demonstrates the highest enzymatic activity at 14 days. Additionally, both abundance and activity has dropped significantly by 21 days. However this behaviour is uniform across the surfaces with no significant difference in either the amount of ALP produced, or the level of enzymatic activity between any of the topographies.

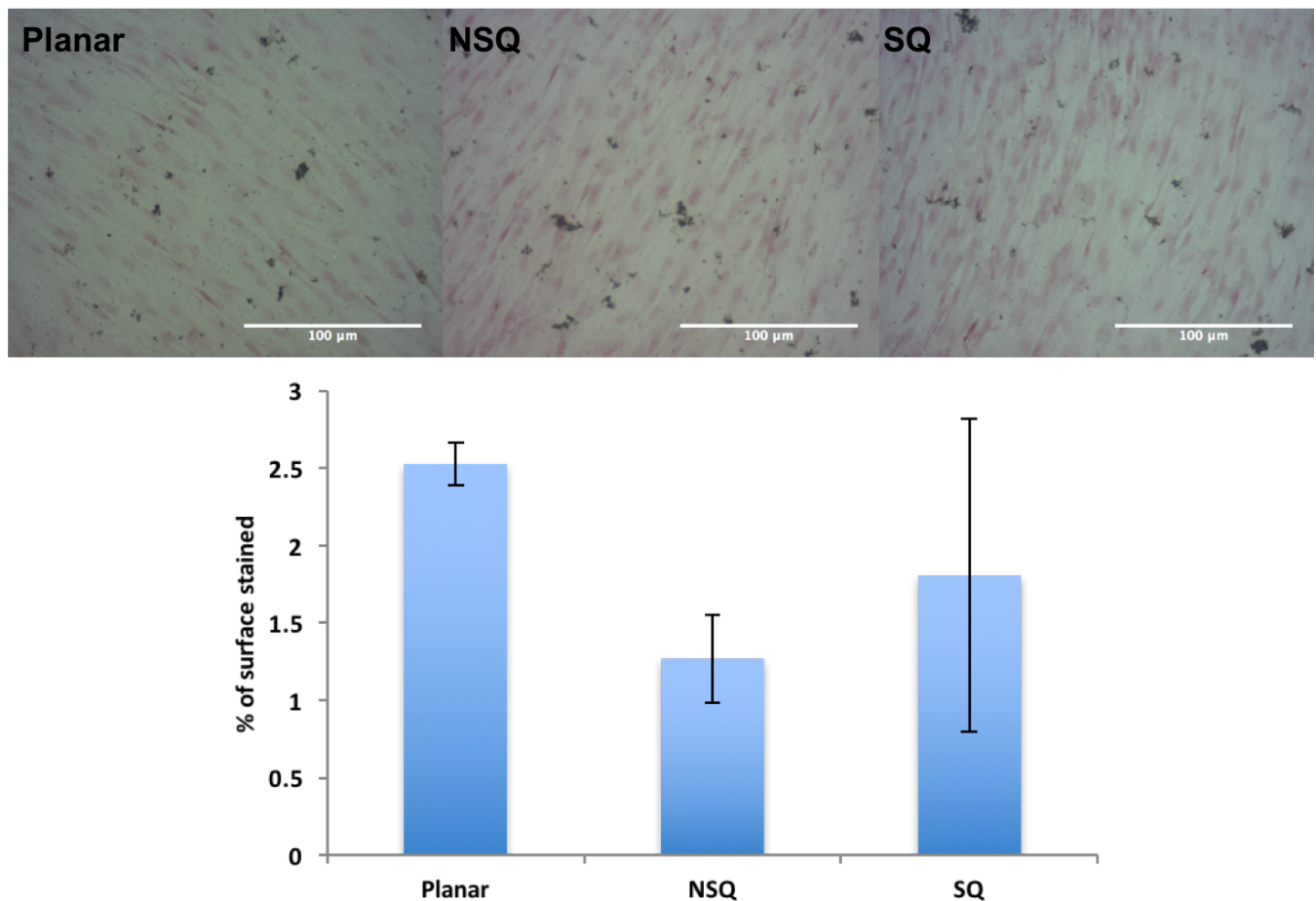


Figure 65 von Kossa staining and Cell Profiler analysis of the percentage of the surface with stained material of primary osteoprogenitor cells cultured for 21 days. Total number of replicates N =9, 3 Planar, 3 NSQ, 3 SQ. Scale bar = 100μm.

The von Kossa staining results show that mineralization has occurred by 21 days with evidence of phosphate containing material on all three different surfaces. The Cell Profiler analysis of this staining indicates that the degree of mineralization is highest on the planar surface with the level of mineralization being lower on both of the nanopatterned surfaces. Interestingly, the mineralization does appear to be slightly higher on the SQ surfaces compared to NSQ, which is the exact opposite of the results of other work done with these topographies fabricated from alternative polymers. However, neither of these differences were shown to exhibit statistical significance, and as a result should be view as similar to both the alamar blue and ALP experiments i.e. there being a lack of significantly different response by the cells between nanotopographies

The alizarin red staining results overall show a similar pattern to the von Kossa results where there is little (when standard deviation is taken into account) difference between the different topographies that have been plasma treated. It is worth noting that the oxygen plasma treatment has led to the level of alizarin staining on the PEEK surfaces comparable to that seen on the tissue culture plastic ware, which illustrates how effective oxygen plasma is at improving cell adhesion and proliferation on PEEK surfaces.

8.2.1. Plasma treatment screen

In the context of these results we considered the possibility that the use of oxygen plasma treatment is effectively “masking” the ability of the topography to direct stem cell differentiation behaviour. This is complicated by the fact that due to PEEK’s inherent cytophobicity we are unable to culture stem cells on non-surface modified PEEK nanotopographies. As a result, we could not be completely certain if the PEEK nanotopographies themselves were capable of influencing stem cell behaviour, and if so, does the presence of the plasma treatment disrupt this ability, or does PEEK’s chemistry interfere with the action of the nanotopography in a different way to the chemistry of the other polymers these nanotopography have been previously fabricated on.

In order to try and better understand the relationship between plasma treatment and stem cell response we decided to screen a range of plasma treatments of different strengths and duration, to see if there was a treatment where we could see a significant difference between planar and NSQ surfaces. We also included the same two surfaces fabricated from polycarbonate to ensure the cells we were using were indeed capable of responding to the topography.

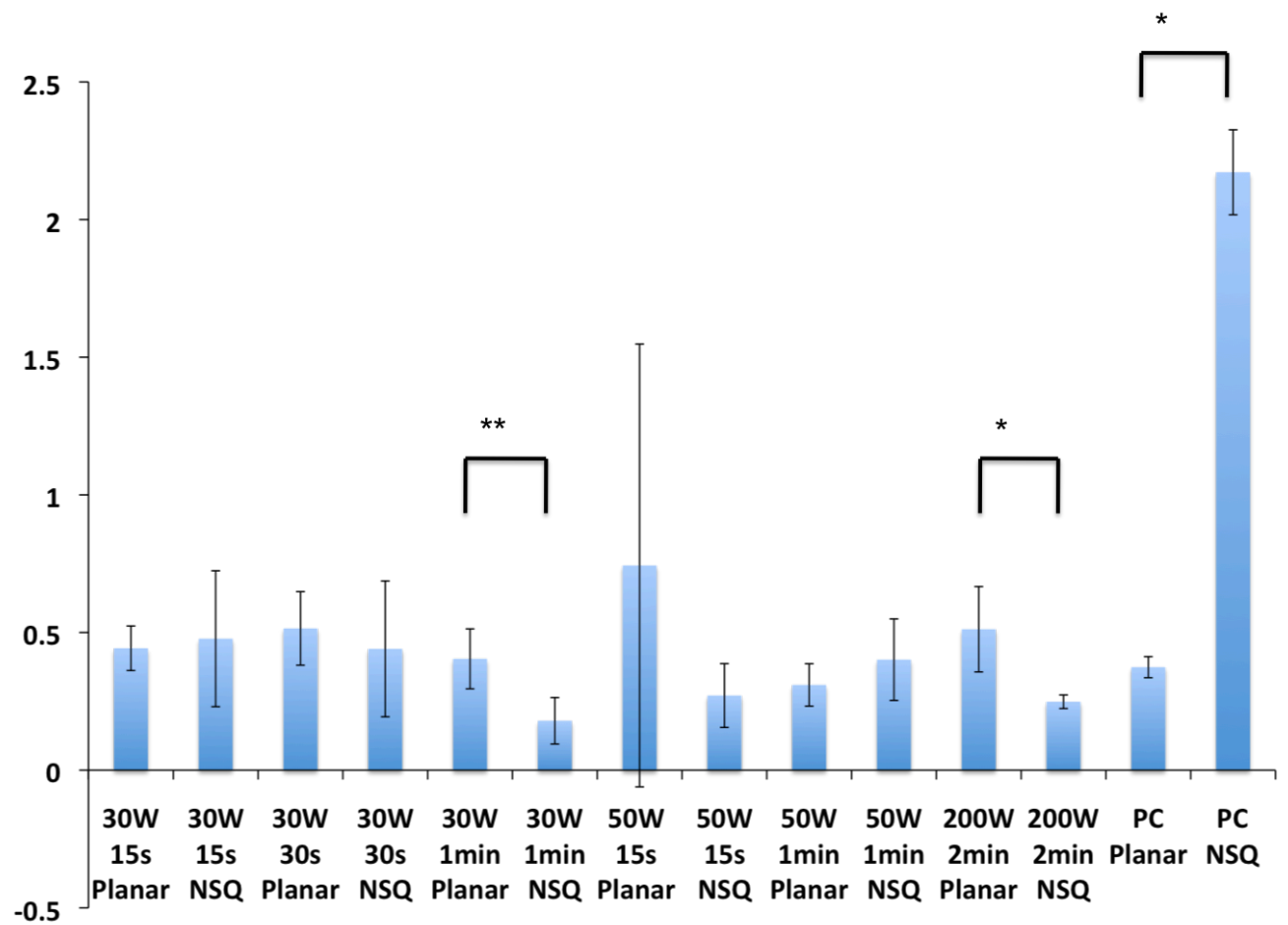


Figure 66 Total percentage of the microscope image, with stained material analysis of the Cell Profiler results for the experiment. We can see that at 30W 1min and 200W 2min NSQ is statistically significantly lower than the planar control.

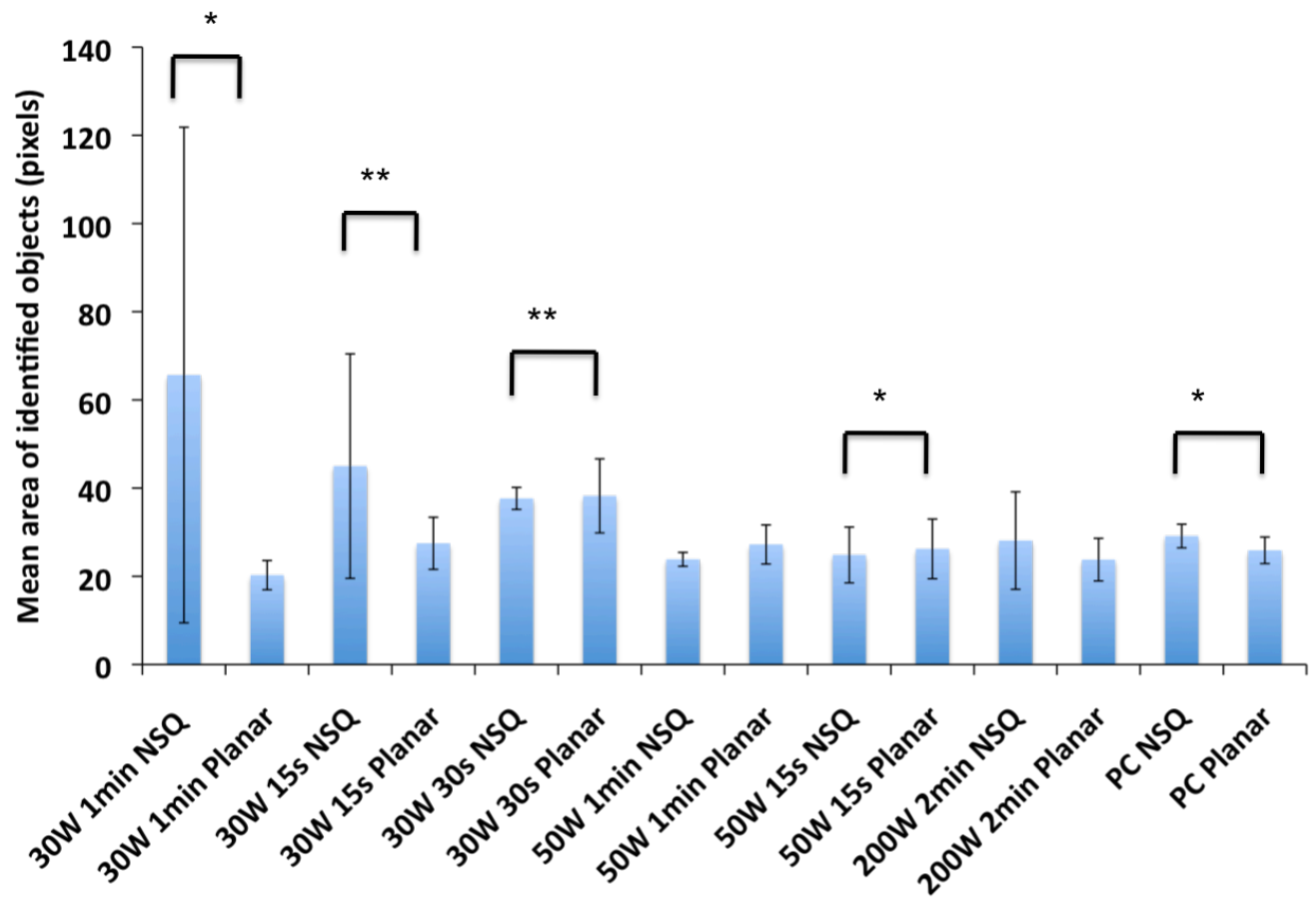


Figure 67 Average area of identified objects analys, of the Cell Profiler results for the experiment. At 30W 1 min and 30W 15s NSQ is statistically significantly higher than the planar control while at 30W 30s and 50W 15s NSQ is statistically significantly lower than the planar control.

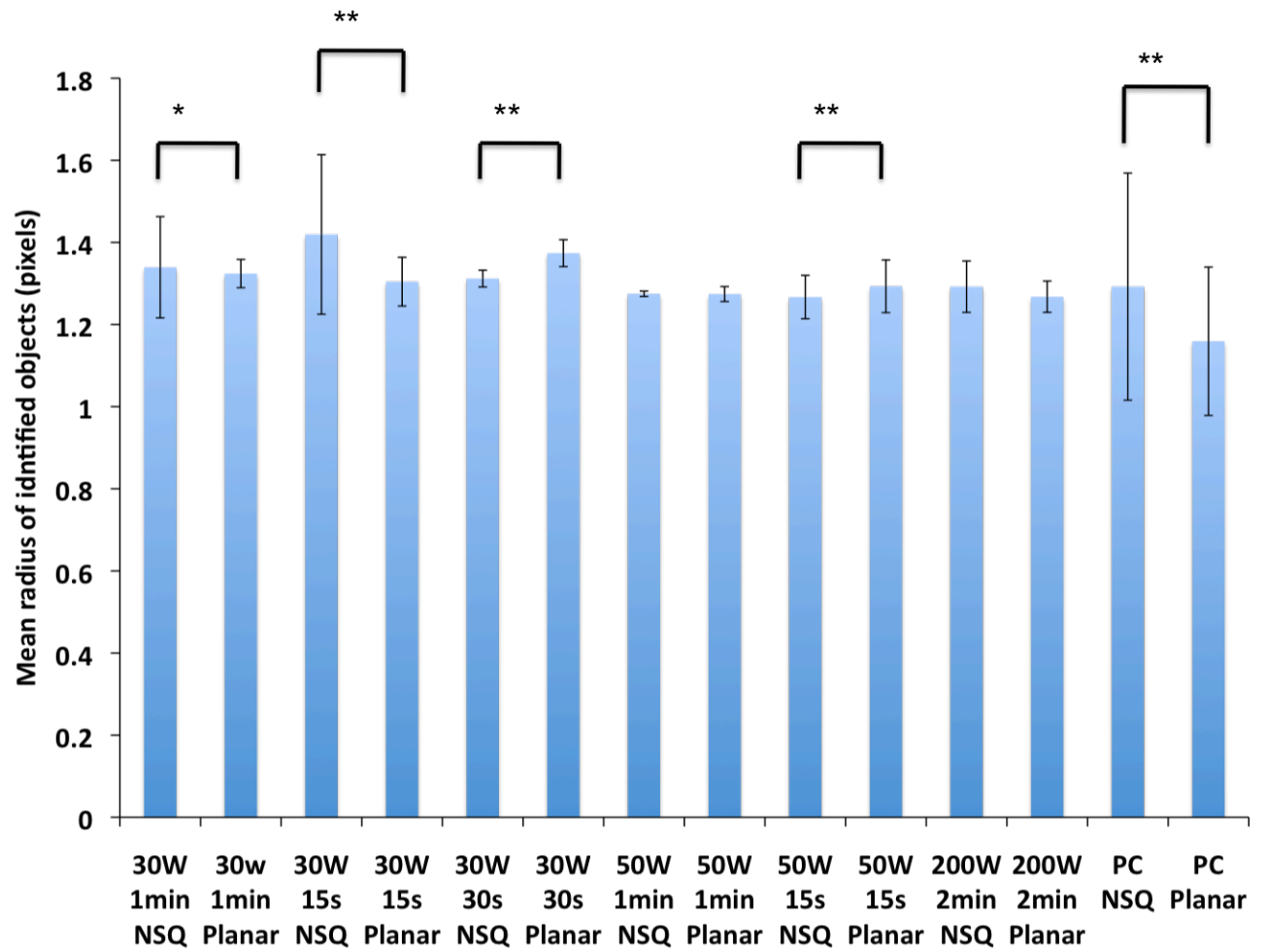


Figure 68 Mean diameter of identified objects analysis of the Cell Profiler results for the experiment. 30W 1 min and 30W 15s NSQ was statistically significantly higher than the planar control while 30W 30s and 50W 15s NSQ was lower than the planar control.

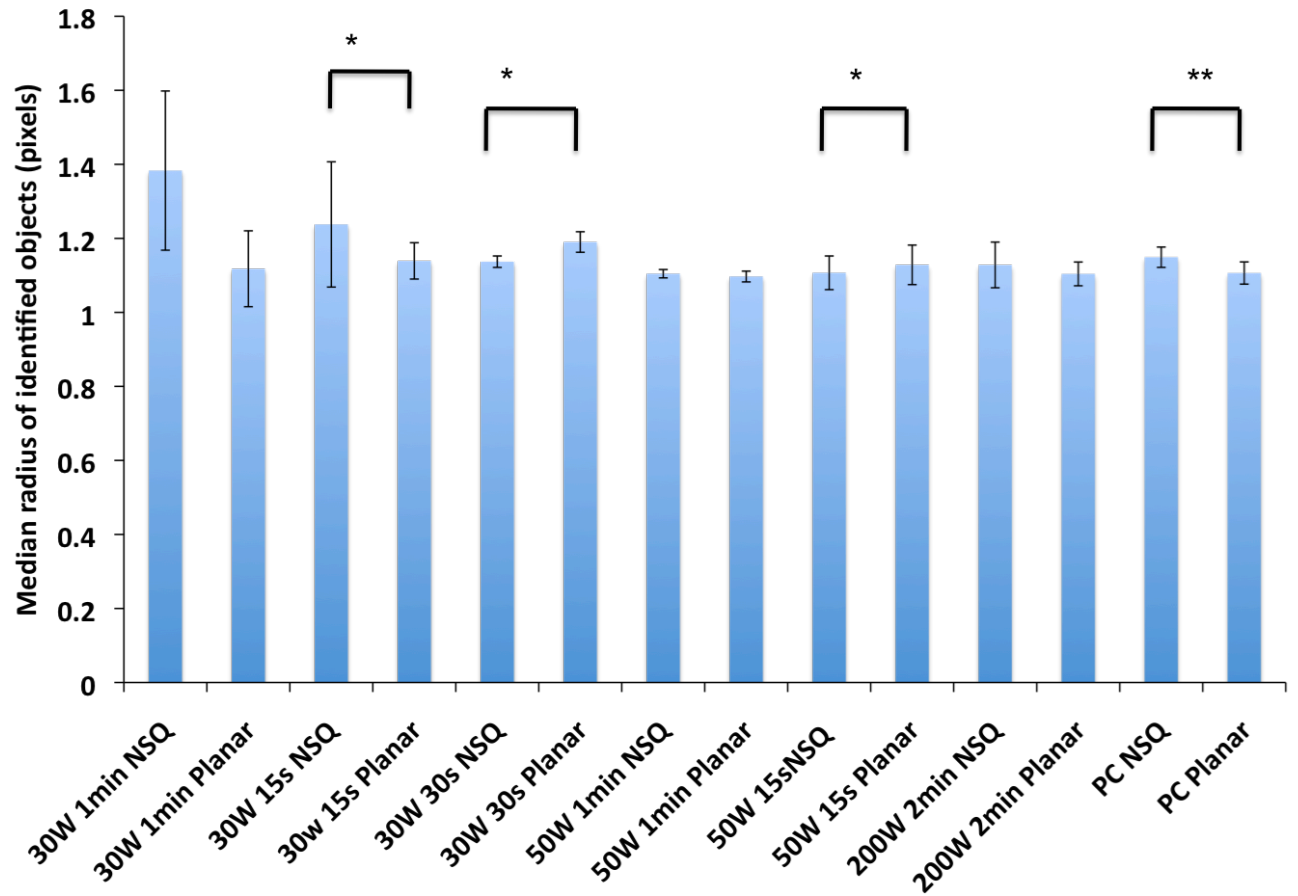


Figure 69 Median diameter of identified objects analysis of the Cell Profiler results for the experiment. 30W 15s NSQ was statistically significantly higher than the planar control while 30W 30s and 50W 15s NSQ was statistically significantly lower than the planar control.

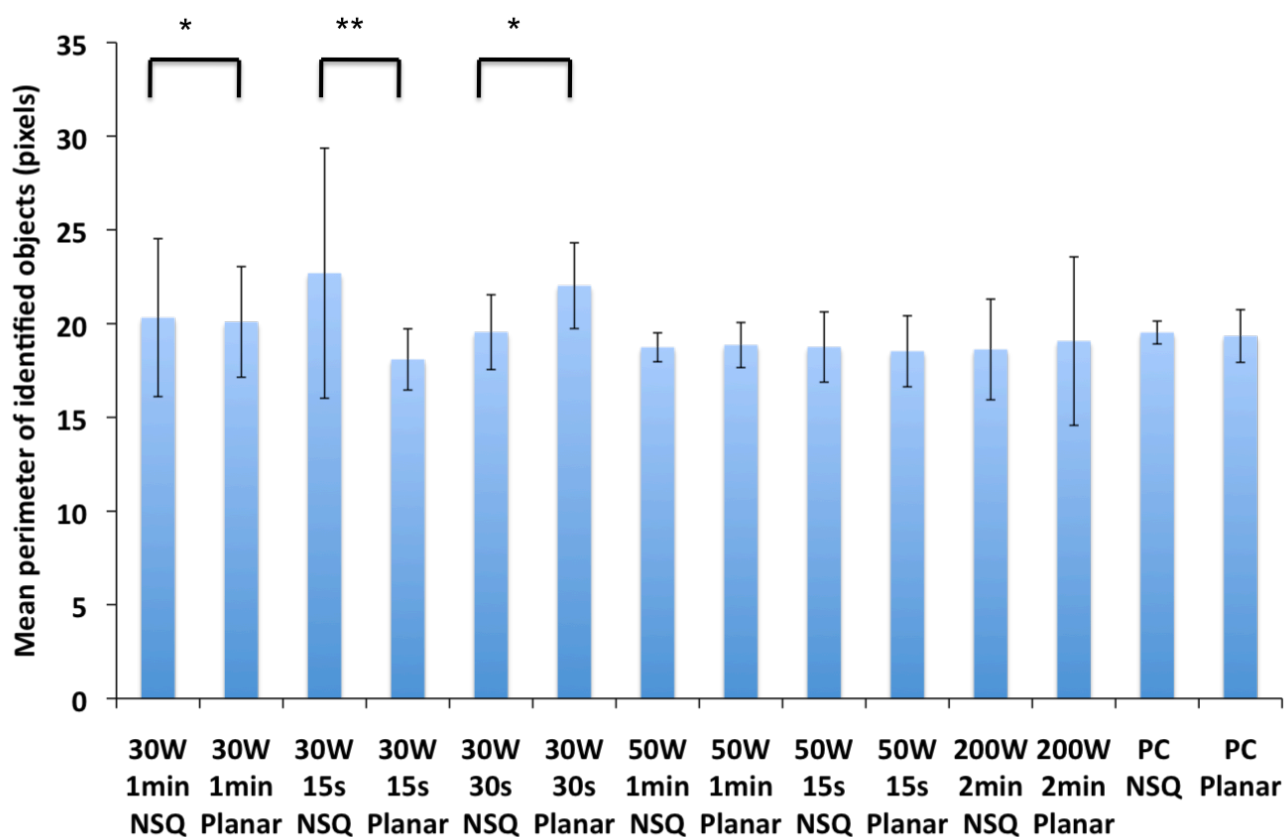


Figure 70 Mean perimeter of identified objects analysis of the Cell Profiler results for the experiment. 30W 1min and 30W 15s NSQ was statistically significantly higher than the planar control while 30W 30s NSQ was statistically significantly lower than the planar control.

When looking at the percentage of the surface stained result (*Figure 65*) can see that the polycarbonate samples display the trend we would expect to see based on previous work done with the nanotopographies i.e. mineralization is statistically significantly higher on the NSQ nanopattern compared to the planar surface. For the PEEK surfaces we observe the opposite trend, with the NSQ nanotopography having a statistically significantly lower amount of mineralization compared to the planar surface at the 200W 2min and 30W 1min plasma treatments, and a lack of statistically significant difference between the two at the other treatments.

The average area of identified objects results demonstrates that two plasma treatments lead to PEEK substrates where the NSQ nanotopography produces a higher average area of identified objects compared to the planar surface i.e. 30W 15s and 30W 1min. However, two of the plasma treatments also produced the opposite trend where the average area of identified objects on the NSQ

nanotopography are statistically significantly lower than the planar surface i.e. 30W 30s and 50W 30s. In addition, the polycarbonate NSQ nanotopography has an average area of identified objects that is statistically significantly higher than that of the planar surface.

The mean radius results are similar to the average area of identified objects results in that they both have two treatments where the mean radius of identified objects is statistically significantly higher on the NSQ nanotopography compared to the planar surface i.e. 30W 15s and 30W 1min, and two treatments where the average area of identified objects are statistically significantly lower on the NSQ nanotopography compared to the planar surface i.e. 30W 30s and 50W 30s. Also, similar to the average area of identified objects results, the polycarbonate NSQ nanotopography has an average area of identified objects that is statistically highly significantly higher than that of the planar surface.

The median radius of identified object results demonstrate one plasma treatments that delivers PEEK substrates where the median radius of identified objects is statistically significantly higher on the NSQ nanotopography compared to the planar surface i.e. 30W 15s and two treatments where the average area of identified objects are statistically significantly lower on the NSQ nanotopography compared to the planar surface i.e. 30W 30s and 50W 30s. Once again the polycarbonate NSQ nanotopography has a median radius of identified objects that is statistically highly significantly higher than that of the planar surface.

The average perimeter of identified objects results demonstrates one plasma treatments that delivers PEEK substrates where the average perimeter of identified objects is statistically highly significantly higher on the NSQ nanotopography compared to the planar surface i.e. 30W 15s, and one plasma treatment where the average perimeter of identified objects is significantly higher than the planar surface i.e. 30W 1min. There was one plasma treatment where the average perimeter was statistically significantly lower on the NSQ nanotopography compared to the planar surface i.e. 30W 30s.

Taken as a whole, these results show some general trends. Firstly, the polycarbonate surfaces show a consistent pattern of higher results on the NSQ nanotopography. This would suggest the polycarbonate substrates are acting in a consistent fashion to observations in previous publications. For the PEEK substrates the opposite trend is observed, albeit not for all of the treatment across all of the properties investigated. It is also noticeable that where there are statistically significant differences on the PEEK substrates they tend to be clustered around the lower energy plasma treatments which could suggest that the plasma treatment is in fact disrupting a function of the nanotopography which is why, as the energy increases, we see less statistically significant differences between the NSQ nanotopography and the planar surface.

Perhaps the strongest conclusion we can draw from these results is that, in itself the material from which defined nanotopographies is fabricated is not irrelevant to how the cells respond to them. However, drawing a definite conclusion in this matter is complicated by the fact that we are unable, due to the materials innate cytophobia, to look at the cellular response to non-surface modified PEEK, so were unable to tell if the difference in response by the OPGs to the PEEK topographies compared to the polycarbonate is down to the chemistry of the PEEK itself, or as an unintended consequence of the oxygen plasma treatment.

8.3. Discussion

8.3.1. Effect of the presence of defined nanoscale topography on stem cell behaviour

Overall the results are mixed. Our experiments which were designed to look at the stages in osteogenesis in turn showed a lack of statistically significant differences between the surfaces studied. However, our experiments which varied the plasma treatment delivered to the surfaces, showed the NSQ topography was capable of causing cells cultured on it to behave significantly differently when compared to the planar surface. These differences are not entirely straightforward. Firstly, the overall trend, namely the results are lower on the NSQ topography compared to the planar surface, is the opposite of what has been observed with this particular nanotopography in the past. Secondly, different treatments have given

different statistically significant results, for example for average area of identified objects 30W 15s and 30W 1min delivered NSQ nanotopographies results that are higher than the planar surface, while 30W 30s and 50W 30s delivered NSQ nanotopographies results that were lower than the planar surface. There are no readily apparent answers for why we observe either of these phenomena. The fact that the polycarbonate substrates that were used as a seeding control consistently delivered results that were statistically significantly higher for the NSQ nanotopography compared to the planar surface would suggest that the results from the PEEK surfaces were an accurate reflection of reality (in other words that these results are not artefacts arising from errors in stem cell isolation, cell seeding on the substrates or any part of the staining or fixation process).

8.3.2. The relationship between oxygen plasma treatment and stem cell response.

The relationship between oxygen plasma treatment and cellular response to the nanotopography is a complex one. In the experiments where we investigated different stages in osteogenesis, and all of the surfaces were treated for 2 minutes at 200W of plasma, there is total lack of significant difference in cell response between the surfaces. When we start to vary the plasma treatment we observe statistically significant differences between the NSQ nanotopography and the planar surface. These differences are also clustered down at the lower end of the energies of plasma treatment investigated. This may indicate that the plasma treatment is in fact disrupting a function of the nanotopography which is why, as the energy increases, we see less statistically significant differences between the NSQ nanotopography and the planar surface. However, this does not explain why plasma treatments which have small differences in energy between them can produce opposite results which show statistical significance, for example looking at average area of identified objects at 30W 15s and 30W 30s. These two plasma treatments, which have a difference in energy between them of 450J, show opposite behaviour compared to 30W 15s treatment producing a NSQ nanotopography which is statistically significantly higher than the planar surface, and the 30W 30s treatment producing a NSQ nanotopography which has an average

area statistically significantly lower than that of the planar surface. This is further complicated by the fact that the 30W 1 min surface (a treatment that has energy of treatment that is 1350J higher than the 30W 15s treatment) also produces an NSQ nanotopography that has an average area that is statistically significantly higher than that of the planar surface.

8.3.3. Potential reasons for diversity in the response of stem cells to the same nanotopography in different polymers.

This is an interesting question and in many respects addressing it could provide key insights into some of the mechanics driving stem/progenitor cells initial response to implanted orthopaedic materials. Additionally, it could potentially offer interesting insights into how proteins are altered by interaction with different surfaces, and in turn, how these interactions affect the stem cell response.

When cells encounter a material surface (in our case PEEK) they do not interact with the bare material. Instead, as soon as a biomaterial is placed in an environment containing cells, very quickly (in the order of nanoseconds), water molecules interact with it and are adsorbed onto its surface. Water molecules have been demonstrated to interact differently with surfaces dependant on their material properties. The orientation of these polar water molecules at the surface impacts on subsequently adsorbed proteins, in terms of alteration to the protein structure (e.g. if the proteins denature or not), its orientation and coverage¹⁰⁴. It is with these adsorbed proteins that the stem/progenitor cells interact with when they adhere to the surface of materials.

It is our theory that by applying oxygen plasma treatment we have altered the behaviour of the adsorbed proteins at the PEEK nanotopography surface in such a way that we see a uniform stem cell/progenitor response between different nanotopographies. It is also possible that the innate chemistry of PEEK itself may also be responsible for the protein adsorption behaviour, which leads to this result. Since we are unable to culture enough cells on untreated PEEK to investigate, we cannot be certain. In either case, this would suggest that it may be the presence of a specific nanotopography alone which produces specific stem cell/progenitor developmental responses. We however believe that the results show that some

aspect of the surface chemistry also plays a role, although based on our current work we can not be sure what that is. We can however make a reasonable argument that it is not as simple as an absolute water contact angle requirement (i.e. the material simply has to have a water contact angle of say 55° and it will have an impact of the behaviour of the cells cultured on it), given that none of the range of different plasma treatments we screened, and as a consequence different water contact angles, had a significant effect on the ability of the nanopatterned surface to induce mineralisation, compared to the planar surface. Instead, we think that in order for the nanotopography to have the effect that it does on stem/progenitor cell behaviour, the chemistry of the material plays a role in influencing the behaviour of the proteins that are absorbed at the surface. We believe that because of the surface chemistry of PEEK, and the further alterations we have made to it with oxygen plasma treatment, may cause a change in how proteins adsorbed at the material surface interact with receptors at the cell surface compared to the way they do at the surface of other polymers which have these nanotopographies on them. Alterations in how integrins at the cell surface interact with adsorbed proteins at the material surface would lead to changes in focal adhesion behaviour. As the activity of these structures has been identified as one of the mechanisms of action in how changes in topography lead to changes in cell behaviour¹⁸, this would provide a credible explanation for the differences in cell response for the same nanotopography when it is made from PEEK, compared to other polymers. It could also explain why there were observed differences in mineralisation behaviour when the energy of plasma treatment was varied, this could have led to alteration in the adsorption behaviour at the material surface. It is worth noting however that this is speculation as our data does not offer any specific insight into protein behaviour at the surface of our PEEK surfaces, although focal adhesion behaviour in response to different energies of plasma treatment and in comparison to the same nanotopography in other polymers could provide a fruitful avenue for further research.

8.4. Conclusions

In summary we wanted to see if the two nanotopographies we were working with NSQ and SQ were capable of directing the behaviour of human stem cells in a

similar fashion to that demonstrated in previous publications^{35,36,60}. We found that when the PEEK substrates were treated with 24000J of oxygen plasma (2min at 200W) there was a lack of any statistically significant differences between the surfaces for any of the different aspects of osteogenic activity investigated. We then decided to compare the osteogenic response of cells on a PEEK surfaces treated with a range of different plasma treatments to see if the energy of plasma treatment significantly altered the cellular response. We found that there were a number of statistically significant differences in mineralization behaviour between the NSQ and planar surfaces at different plasma treatments. These statistically significant differences on the PEEK substrates tended to be clustered around the lower energy plasma treatments, which could suggest that that the plasma treatment is in fact disrupting a function of the nanotopography which is why, as the energy increases, we see less statistically significant differences between the NSQ nanotopography and the planar surface.

9. The adaptation of chromatic based Immunohistochemistry for use in stem cell research with PEEK

9.1. Introduction

9.1.1. The role of existing fluorescence based immunohistochemistry in biomaterials research

Fluorescence based immunostaining (also referred to as immunohistochemistry or IHC) is a well-established and widely used laboratory technique, used commonly in many different areas of biological research, as well as in pathology and diagnostic medicine. Based on the breakthrough work of Coons and Kaplan^{105,106}, IHC works by taking an antibody that was raised against the antigen of interest (antigen choice is limited only by the availability of an appropriate antibody and currently a wide range of monoclonal primary antibodies are commercially available), and then adding a fluorescent label. This antibody then binds either directly or indirectly to the antigen of interest, which allows the antigen to be detected. This technique is able to both demonstrate the presence and spatial location of the antigen of interest (via fluorescence or confocal microscopy) and allow quantification of the level of antigen of interest present in the sample (via flow cytometry or automated imaging instrument)¹⁰⁷.

This technique allows the researcher using it to investigate almost any biological system (the only limiting factor is that the system of interest has to have an observable marker, and that a monoclonal antibody raised against this marker can be obtained) in both an accurate (the ultimate accuracy of the process is dependent on how accurately a given antibody binds exclusively to the antigen it was raised against), and sensitive fashion. It is also worth noting that, as the primary antibody will bind to the antigen it was raised against (in most instances a mature functional protein), so a positive staining result is an indication of the presence of the target antigen being present in, if you like, a “finished” state.

This is a significant advantage this technique has over qPCR which, while more sensitive (but additionally more expensive, more demanding technically to perform and requires the use of significantly more cells in order to obtain a sufficient yield of RNA), measures the number of gene transcripts present in the sample. There is no absolute guarantee of the exact translation between the number of transcripts and how much functional protein it will yield. In a field such as the orthopaedic application of tissue engineering, where there is a good understanding of the biological behaviour that leads to a positive end result e.g. stem cells differentiating into osteoblasts, osteoblast producing Osteopontin, Osteocalcin and RUNX2 and the production of mineralised deposits, Immunostaining for these markers/behaviours is probably of more use when it comes to trying to work out how effective a given technology will be at directing osteogenic behaviour in vivo, than an analysis of gene transcript levels.

An example of the important role this technique can play in tissue engineering is the initial experiments done in Glasgow with early versions of the nano-topographies used in research³⁵. By using immunostaining, the researchers were able to investigate the ability of the topography to influence a number of different aspects of stem cell behaviour (different topographies could indeed induce osteogenesis, or maintain the cells in an undifferentiated state). The technique allowed researchers to compare cellular response across a series of topographies with both different features, and then gradually increasing feature spacing. This enabled them to look at both the effect the features themselves had on cell behaviour and, once this had been established, find the optimum spacing of these features in order to produce the desired effect. The use of Immunostaining in these experiments allowed them to directly compare a number of different surfaces for two very distinct types of stem cell behaviour, in a sensitive and consistent manner. Trying to carry out this type of investigation primarily using quantitative PCR would require the researchers to effectively guess the temporal transcription window of the gene of interest, or failing that, investigate transcription behaviour at a number of different time points, which would make the experiment extremely hard to carry out with stem cells as cell number is at a premium in these type of experiments.

Factors leading to the incompatibility of PEEK with existing fluorescence based immunohistochemistry and the associated impact on the materials use in biomaterials research

Based upon this the natural place to start working with the same nanotopographies fabricated from PEEK, would be to fluorescently immunostain stem cells cultured on them for osteogenic markers. However, as we discovered, PEEK is in fact intensely auto-fluorescent. This is due to the chemical structure of the polymer and as such is an inherent property of the material. In other words we have to accept that auto fluorescence much like the material being non-transparent, is simply a part of the material and so experimental strategies must be designed to take this into account. Other research groups working with PEEK have also observed this behaviour¹⁰⁸, and as a consequence it is not possible to use the established Immunofluorescent staining techniques that one would expect, with competing biomaterials. In the opinion of the author, the inability to use this type of technique is one of the major reasons why titanium may be more attractive than PEEK in biomaterial research, alongside of course PEEK's relative youth in terms of both biomaterials research and application compared to more established materials, such as stainless steel and titanium, and the materials not undeserved reputation as being difficult to work with in research circles. When designing a research strategy to look into osteogenic behaviour using a non- autofluorescent biomaterial, fluorescence based immunostaining plays a crucial role. A researcher would be able to perform an initial experiment to look at cellular response to the material in terms of both adhesion and proliferation to ensure that the material and or the experimental treatment is cytocompatible. They would then be able to follow this up with an immunostaining experiment which looked specifically at elements of osteogenesis (commonly utilised specific markers include osteopontin, osteocalcin and RUNX2). Based on these results von Kossa or alizarin red (or better still both) staining could be used to demonstrate that increased levels of osteogenic markers does indeed lead to the formation of fully mineralised deposits. Additionally, alkaline phosphatase could also be looked at, both in terms of its gross production and enzymatic activity, if more evidence was required to demonstrate osteogenesis proceeding in as a physiological like manner as possible. Regardless of whether or not the researcher chooses to include a mineralisation

and/or alkaline phosphatase experiments after performing the immunostaining , they would have enough data to publish the study. Subsequently, further experiments could be carried out utilising more expensive but more precise techniques such as quantitative PCR or metabolomic or proteomic based approaches that would generate more in depth data about the interactions between the cells and the experimental surfaces being investigated. Furthermore, the previous immunostaining experiment would give invaluable information for the planning of these experiments, for example qPCR requires a good understanding of when you would expect to see certain genes begin to be transcribed. On different materials, cells will proliferate at different rates and as a consequence will begin to transcribe genes after different periods of culture. In other words, if you were to directly compare the osteogenic behaviour of stem cells via qPCR on titanium and PEEK at 21 days, in all probability the level of osteogenesis related markers would be raised on titanium compared to PEEK. However, this is not to say that the cells on PEEK are not capable of transcribing those genes, but more likely, that given how much slower cells proliferate on PEEK compared to titanium, they simply have not had enough time to do so. In other words, it is essential to have a good understanding of the underlying behaviour of cells on the experimental material before it is possible to use a number of the more advanced, and by extension, expensive techniques for further analysing cell behaviour. So in summary, Immunostaining is an important component in the toolbox of tissue engineering, as it can provide a vital bridge between older more low-tech, low cost but useful techniques (such as counting cell number by hand after coomassie staining, using alamar blue to generate a growth curve, histological staining of alkaline phosphatase and identification of mineralised deposits via von Kossa and alizarin red), and more modern, more sensitive and by extension, more expensive techniques (such as qPCR, metabolomics and proteomics), which require a greater understanding of the behaviour of cells on the experimental surfaces in question. The incompatibility of fluorescent immunostaining with PEEK unfortunately means researchers working with it have to jump straight from the older, more low-tech and less sensitive but lower cost and less technically demanding techniques, into the more modern, more sensitive but more expensive and technically demanding techniques. This is a major contributing factor to the fact that published research

work on PEEK often falls into two categories; firstly, where the main focus of the work has been on a development in the material itself (whether surface topography or chemistry or by an alteration to the structure of the material e.g. production of a composite), and the biological aspect of the paper is either absent or is limited solely, to an assessment of the ability of cells to adhere and proliferate on this new surface, and secondly the other type(albeit somewhat less common), where the focus is entirely on the biological response to the material, where ability to include an immunostaining experiment would help to either lend more weight to the works conclusions (in papers where the primary means of investigation has a potential alternate explanation for the observed phenomena e.g. von Kossa and alizarin red staining only for the presence of phosphate and calcium respectively not necessarily the presence of cell deposited hydroxyapatite), or where the results from an immunostaining experiment may have helped to focus the use of expensive modern techniques into a smaller number of experiments, where more directed work may have yielded more coherent results.

9.1.2. Alternate approaches for immunohistochemistry on PEEK surfaces

As a consequence of not being able to employ fluorescence based immunostaining as a technique to interrogate stem cell response to our PEEK nanotopographies, we effectively looked backwards in order to go forwards, and examined older histological methods that had been either superseded or supplanted entirely by fluorescence based immunostaining. We were able to effectively utilise von Kossa, alizarin red and alkaline phosphatase staining to interrogate different aspects of osteogenesis on PEEK, as well as utilising a number of stains primarily developed in the nineteenth century, originally used to identify parasites and other microorganisms, to investigate changes in cell morphology in response to changes in the chemistry and/or topography of the material surface. Additionally, our use of polarised light microscopy enabled us to easily distinguish between stained material and their background when using reflected light microscopy. The images generated with this process were of sufficient quality to allow us to use Cell Profiler to analyse them in a quantitative fashion. While this was not an inconsiderable accomplishment (in our opinion this did demonstrate a significant

improvement in the methods for biological investigation compatible with PEEK compared to the state of the field when this work commenced), the development, or at least refinement of these techniques did not fully compensate for the inability to employ fluorescence based immunostaining. Von Kossa and alizarin red stain for the presence of phosphate and calcium respectively, so there is the possibility for false or at least misleading results from these stains. In their 2003 paper Bonewald *et al*¹⁰² used Fourier transform infrared spectroscopy (FTIR) to compare structures which stained positively for von Kossa from rat calvarial cells and two cell lines, to that of the spectra generated from the *in vivo* mineral of rat calvarial bone. Their results indicated that it was possible for cells cultured *in vitro* to test positive for von Kossa whilst failing to form apatite due to the stain reacting with calcium or phosphate that was present on the surfaces, but not produced by the cells. In their opinion the positive staining indicates the presence of “dystrophic mineralization of unknown origin”. This finding does not invalidate the use of von Kossa staining as a technique, but the demonstrable capacity for false or at least misleading positive results highlights the need for subsequent assays to support results generated by the use of Von Kossa staining. As the authors themselves point out, “Therefore, when examining mineralization in new osteoblast cultures or even using well established cell lines, it is important to perform techniques other than von Kossa staining, such as EM or FTIR, to verify that one is quantifying calcium phosphate as a marker of bone formation *in vitro*”. While it is possible to reinforce results obtained with von Kossa using alizarin red which stains for calcium, another component of the apatite deposited by cells, it is worth noting that in a similar fashion to von Kossa, alizarin red can stain calcium binding proteins and proteoglycans generating a non-apatite based positive result in a similar fashion to von Kossa. This does highlight that, in the absence of being able to immunostain and demonstrate the presence of markers that are involved in the production of mineral in a physiological like manner, it is significantly harder to generate an utterly conclusive positive result, and while research science often does not provide answers beyond any shadow of a doubt, and instead is a question of both relative certainties and the judgement of the researcher, the inability to demonstrate osteogenesis occurring in a fully physiological like manner (which for example, the ability to immunostain for osteocalcin would definitively

demonstrate), is a source of frustration in the use of PEEK as a biomaterial. There remains a question of the overall sensitivity of techniques such as von Kossa and alizarin red when compared to fluorescent based immunostaining. While we have not been able thus far to directly investigate the relative levels of sensitivity of these techniques, it remained a source of concern that potentially there may have been significant differences between PEEK topographies in their ability to induce an osteogenic response from the cells cultured on them, but von Kossa and alizarin red were not sensitive enough to detect them. Whereas, had we been able to use fluoro based immunostaining, any differences would have been apparent. While it is not possible to fully answer this question without being able to compare the respective techniques on PEEK (which is of course not possible due to PEEKs inherent auto fluorescence), it does raise an interesting question about the level of cellular response to our surfaces which should be considered significant. Given that the ultimate goal in this particular area of biomaterials research is to produce an implant device that is not only an improvement over existing implants, but also enough of an improvement to justify the commitment of adjusting surgical practices to compensate for the use of a new implant.

Finally, the inability to employ antibody based immunostaining restricts the scope of cell behaviour we are able to investigate on PEEK. While our histological techniques, von Kossa, alizarin and ALP staining give us a solid view of the osteogenic response to our surfaces by stem cells, they are unable to tell us anything else about the behaviour of the cells. If we wanted to look at cell response to the presence of a topography on our surfaces the most straightforward way would be by seeding cells on the surfaces, culture the cells for a short period of time (in the order of days) and then stain them with DAPI and phalloidin. This would allow you to quickly and relatively easily look at changes to the architecture of the cytoskeleton (phalloidin stains the cells actin filaments). We could then see if a given change in shape gives a consistent response by different cells on the same surface, and if this behaviour was significantly different to that of the same cells on a different topography. Additionally it would then be relatively straightforward to look at the number, distribution and maturity of the focal adhesions made by the cells (it would only require the experiment being rerun with a primary antibody directed against a known component of the focal adhesion

complex), which could provide further information about the interaction between the cells and the surface. As is apparent, it is not possible to do any of this on PEEK, and is also not possible to investigate this type of cell behaviour on a PEEK surface. While we did go on to perform a number of experiments to try to adapt a number of different histological stains to allow us to mark out the shape of the cell these methods do not produce the same accuracy and specificity as DAPI and phalloidin, nor is there a direct histological replacement to look at focal adhesion behaviour. Of course immunostaining is not limited to only investigating cell morphological behaviour. Due to the wide range of primary antibodies available, any biologic process that has an identifiable antigenic marker can be investigated in this fashion, and clearly there is not a technique that can provide equivalent results.

9.1.3. Horse radish peroxidase based immunohistochemistry

While we were able to develop a number of histologically based techniques that allowed us to look at the osteogenic response of stem cells on PEEK, due to the above mentioned reasons we still felt that the inability to immunostain continued to hindered our work, and as a consequence we continued to look for ways to adapt this type of assay for use with PEEK. While there are examples of researchers who have been able to use scanning laser fluorescence imaging to generate usable data from fluorescence based immunostaining on PEEK^{68,92} these results do appear to have a number of caveats. In one of the investigations the researchers⁹² only used the technique to generate a discrete number of images in order to demonstrate the presence of adherent cell on the PEEK surface, which does seem to suggest that the technique is not a 'like for like' replacement. The work done by *Schroder et al*⁶⁸ did however include a quantitative analysis of two types of β integrins expressed by cells cultured on plasma treated PEEK surfaces. This work was however carried out with what they describe as PEEK films, so it is not clear if this method would be applicable with a substantially thicker PEEK surface, which is more commonly used in biomaterials research.

While these results were interesting, it is worth bearing in mind that the equipment required to carry out this type of work is prohibitively expensive unless the researchers institution already had the equipment *in situ*, and imaging surfaces

with it is far more technically difficult and time consuming than more widely use fluorescence microscopy (this is based on the our conversations with one of the researchers who used laser scanning fluorescence microscopy to image cells on PEEK). So while laser scanning confocal microscopy maybe a viable technique for use with PEEK it was not available to us, and given that it is available to a very small number of researchers, there would be interest from other researchers working with PEEK in a more easily accessible method for immunostaining the material.

We became aware of the possibility of being able to stain for a primary antibody raised against a specific antigen, without the need for fluorescence based microscopy.

Horse radish peroxidase based immunostaining (or HRP) is a method of staining for the presence of a particular antigen of interest, that shares much in common with fluorescence based immunostaining, with the key difference being that the presence of the antigen is indicated not by the presence of a fluorophore, but the enzymatic reaction of HRP and the substrate with the resulting deposition of an insoluble reaction product at the site where the primary antibody is bound. The development of enzymes as antibody labels came roughly 30 years after the development of fluorescent tags for antibodies and quickly became popular within the field of pathology, due to the fact that it allowed the operator to look at both antigen of interest localisation and tissue morphology, at the same time. Over time fluorescence based immunostaining has become the more widely used technique, at least within the field of tissue engineering, although there was a time when it was suggested that the use of fluorescence in immunostaining would be made obsolete by enzyme labelled secondary antibodies. That fluorescence based immunostaining has come to be the more widely used technique is most likely down to the fact that the images produced are more easily interpreted (particularly in the case of modern computer based analytical methods), than those produced through enzyme based immunostaining. This is largely due to the fact that with fluorescence microscopy the only material that is visible is that which has fluorescently labelled antibodies bound to it, whereas an enzyme based

approach requires more circumspection, as well as the inclusion of specific controls in the experiment, on what is and is not stained material. Additionally, fluorescence based immunostaining does not have any issue around the presence of endogenous enzymatic activity leading to false positive results. While this is taken into account in modern HRP based immunostaining protocols with the inclusion of an endogenous enzyme-blocking step, it is still a potential source of false positive results.

Despite this, it is worth noting that there is no inherent reason for fluorescence based and enzyme based immunostaining to give significantly different results¹⁰⁹. Enzyme based immunostaining very much comes into its own when fluorescence microscopy is not available to the researcher either due to the researcher not having ready access to a fluorescence microscope or the material being worked with is inherently autofluorescent.

9.2. Results

9.2.1. Initial testing of the technique

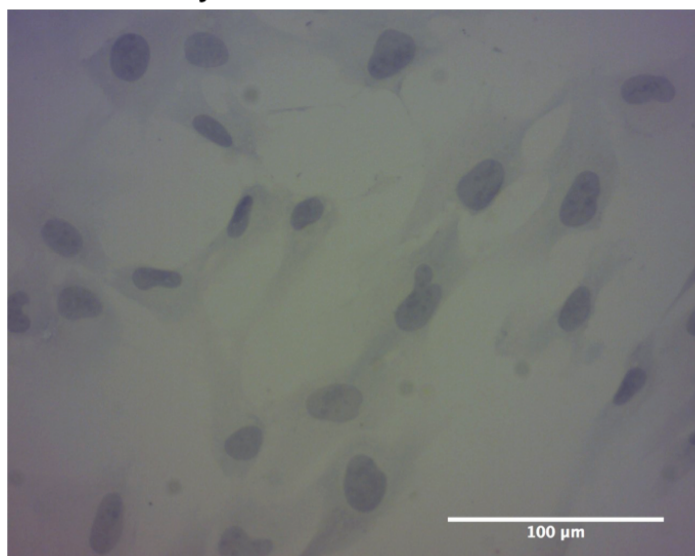
We had identified that HRP based immunostaining was a technique that could allow us to immunostain cells cultured on PEEK surfaces for various osteogenic markers. However, as we could not find any examples of this technique being used with PEEK in the literature, we were unsure as to the best way to proceed, both in terms of the reagents to use and their optimal usage.

We decided to try an initial small-scale experiment to test out if the technique would work at all. To this end we opted to stain for β tubulin in h-tert cells, as these cells would quickly provide a large number of adherent cells on our surface and β tubulin is a widely expressed antigen, which would, if the technique worked correctly, give us a large amount of positive staining. What we were very much trying to avoid was a situation where the technique would work correctly but there would be so little antigen present that we would wrongly interpret this as indicating that the technique had failed to work (this was a serious concern at the time, as we did not know how HRP stained cells would look against a non-transparent background using reflected light microscopy). The examples of this type of staining in the literature which we could find, involved cells on either glass

or a range of tissue culture plasticware, taken using transmission light microscopy).

We decided to use haematoxylin counter staining in this experiment for two reasons. Firstly we had an outstanding interest in finding a technique that would allow us to specifically mark out both the nucleus and the cell shape, which would permit us to use Cell Profiler to accurately measure how cell shape is altered in response to changes in topography and chemistry (on materials that are not auto fluorescent this is done by staining with DAPI and phalloidin). It was hoped that the haematoxylin would give us the nucleus, and the β tubulin as it is distributed throughout the cytoplasm would give the cell shape. Additionally, since the two stains should produce two distinct colours (haematoxylin stains blue/black and the HRP immunostaining would produce a red reaction product as we were using AEC with it), we were interested to see if we saw two distinct, discrete types of staining on the PEEK surface. Secondly, by including haematoxylin in the absence of HRP staining, we wanted to check that there was a layer of cell present on the surface so if there was an absence of HRP staining, we could be sure that it was down to the technique not having worked versus there having been an issue with the cell seeding on the surfaces, and as a consequence there not being any cells present on the surfaces.

Haematoxylin



Haematoxylin + β Tubulin AB

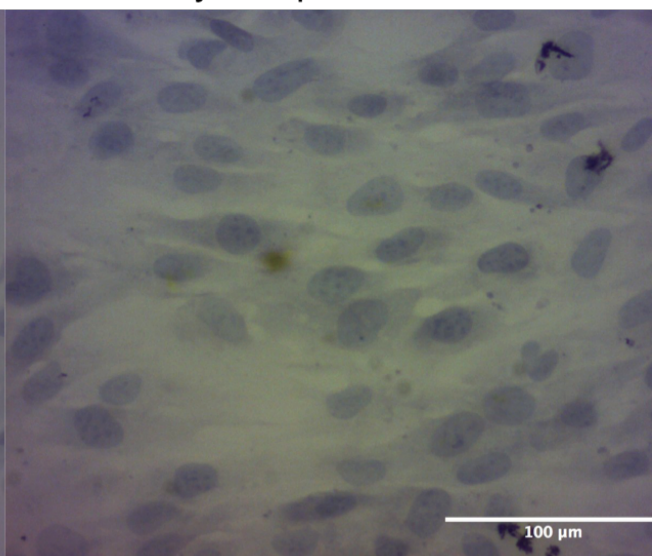


Figure 71 Microscope images taken with polarised light microscopy of h-tert cells stained with either HRP based immunostaining against β tubulin using Santa Cruz biotech secondary antibodies and haematoxylin or only haematoxylin. In both cases cells were cultured on machined PEEK discs for 3

days. Note the absence of significant additional staining in the presence of the HRP conjugated secondary antibodies compared to the haematoxylin only samples. Scale bar =100µm

As we can see from the results of the experiment, there is no discernible additional staining in the presence of HRP immunostaining compared to only haematoxylin, demonstrating that no HRP based staining has taken place. The reasons for this are not immediately apparent. Our suspicion is that the secondary antibody concentration suggested by the manufacturer (1 in 500) while sufficient for western blotting, is however not sufficiently high to produce visible immunostaining. It is also possible that the secondary antibody failed to bind to the primary antibody (we viewed this as less likely as the primary antibody was raised in a mouse and the secondary antibody is targeted against mouse antibodies) or that the haematoxylin staining had obscured the HRP staining which may have been present.

But what we did learn unequivocally from this experiment was that in the presence of a large amount of the target antigen (the haematoxylin staining demonstrated that there was an appreciable number of cells on the surfaces, and h-tert cells as an aspect of their underlying biology, have β tubulin present hence our assertion that there is a plentiful amount of target antigen present to potentially be stained), HRP based immunostaining failed to produce any visible staining.

At this juncture the evidence that we had available suggested that HRP based immunostaining was not a viable technique for use with PEEK. Additionally our experimental evidence did not definitively demonstrate why the technique had not worked, and this made making a decision on whether to continue working with the technique to see if we could adapt it to work with PEEK much more complicated, as we were not sure if the failure of the technique was due to an easily rectified parameter, such as having used the incorrect dilution of secondary antibody, or something more complex, such as the reaction product does not stand out well against the PEEK background or our method of microscopy (we have to use reflected light microscopy with a polarised light filter or PEEK is non-transparent) either struggles to, or is unable to detect the reaction product. In other words we were left with the real possibility that continuing to try to adapt this technique to work with PEEK would be throwing good money after bad.

Ultimately, for the reasons mentioned earlier in the chapter we felt that the potential benefits of having a functional method for immunostaining on PEEK outweighed the financial costs associated with this method.

9.2.2. Switch to use of Dako EnVision staining procedure

In order to give ourselves the best possible chance of getting the technique to work we opted to use a kit based HRP immunostaining approach. While this was more expensive than buying separate reagents and diluting them ourselves, the kit was developed to be used “straight out of the box” and as such, we felt that if the technique still didn’t work, we could have confidence in eliminating issues with the reagents themselves being the cause.

We opted to repeat the previous experiment with the new Dako immunostaining kit, namely staining h-TERT cells on machined PEEK surfaces for the presence of β tubulin. However due to a problem with the delivery of the new staining kit we ended up having to culture the cells for 14 days, rather than the 3 days the cells were cultured for in the previous experiment. We decided not to include haematoxylin staining this time due to a combination of concerns i.e. that the haematoxylin could potentially mask the result of the HRP staining, as well as the fact that since the cells being used in the experiment proliferate quickly and had been cultured for 14 days, we had some concerns about adherent cells being present, or in sufficient numbers to provide easily visible staining.

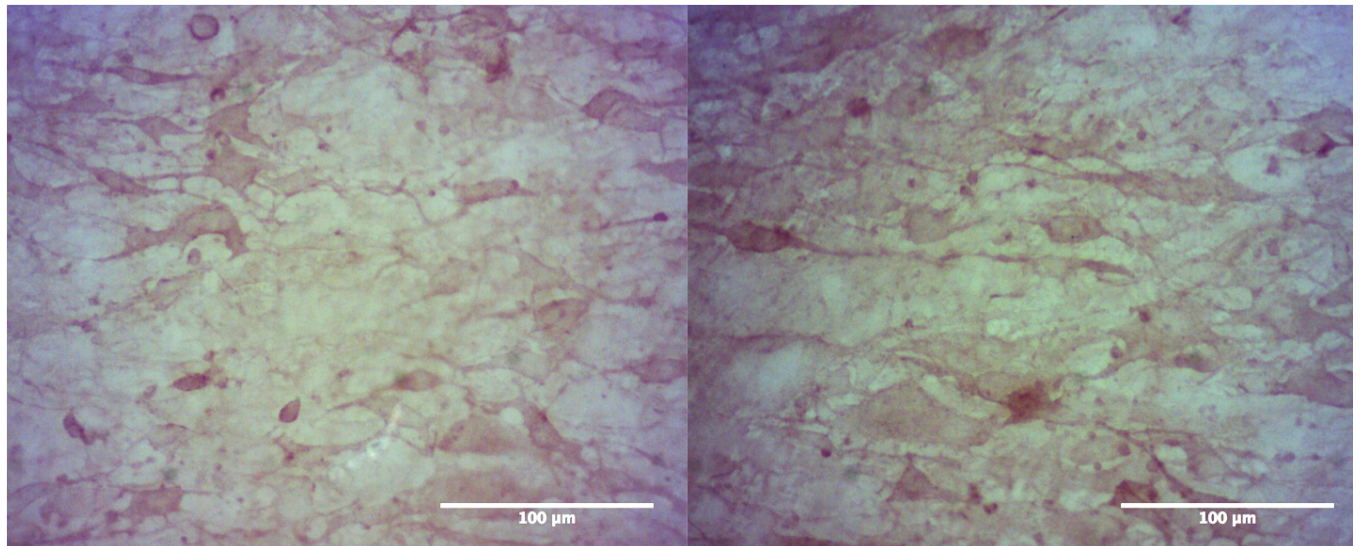


Figure 72 Polarised light microscope images of h-tert cells cultured on machined PEEK surfaces for 14 days and then stained for β tubulin via HRP immunostaining. While it is readily apparent that there is staining present on both of the samples it is hard to say if β tubulin has been specifically stained. Scale bar = 100 μ m

The experimental results were initially difficult to interpret. While it was apparent that staining had indeed taken place, shown by the presence of red stain across the surface, it did not look like the sort of the well-defined regular repeating structures we had expected to see if the staining technique had specifically stained β tubulin. However, we considered that since we could not find any examples of HRP immunostained β tubulin on a transparent background, it was hard to tell if the staining had been “successful” or not.

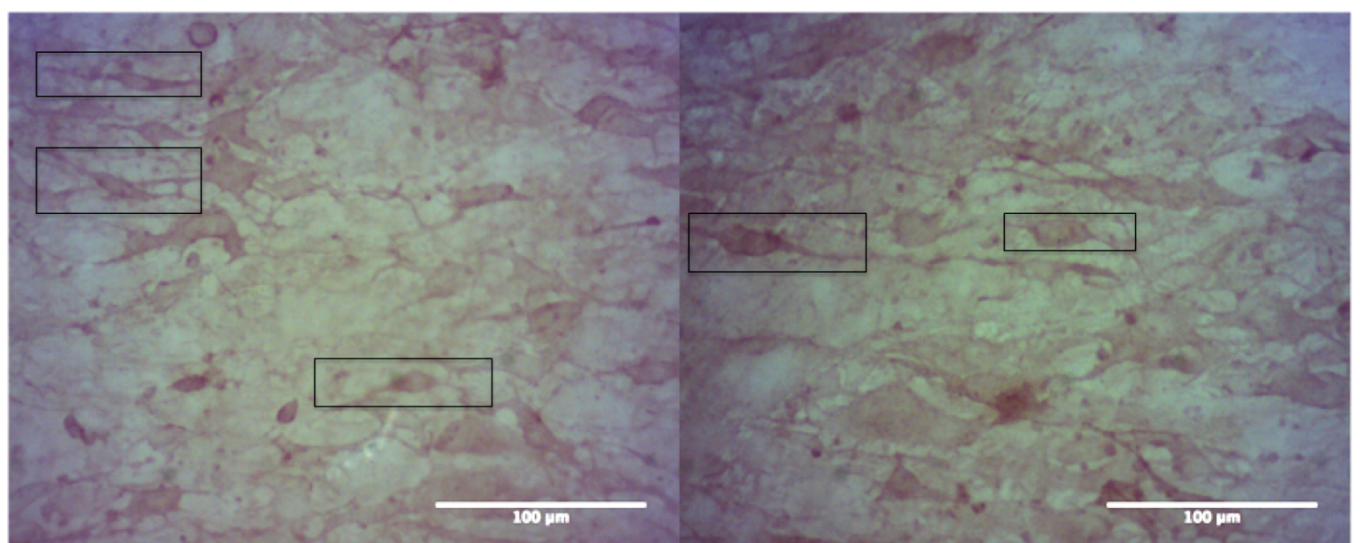


Figure 73 Polarised light microscope images at x20 magnification of h-tert cells cultured on machined PEEK surfaces for 14 days and then stained for β tubulin via HRP immunostaining. Objects enclosed in black rectangles are consistent objects that we believed demonstrated specific staining of β tubulin. Scale bar = 100 μ m.

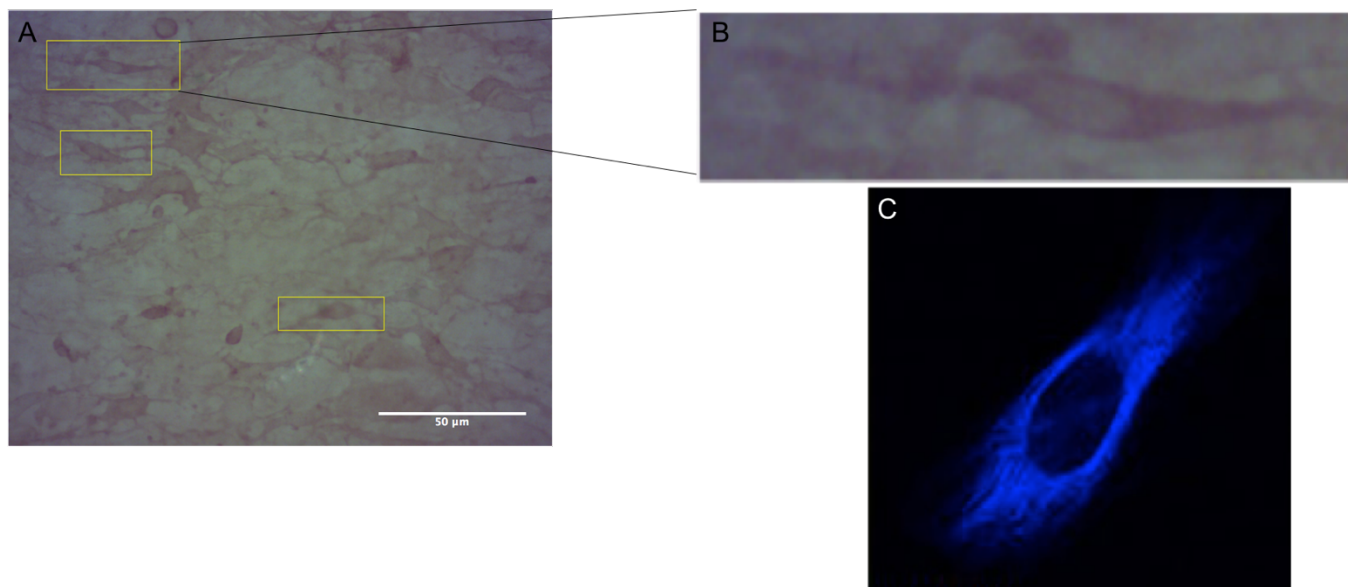


Figure 74 A closer look at staining of β tubulin by HRP based immunostaining. A = microscope image of HRP based immunostaining of h-tert cells on PEEK with what we believed to be an example of stained β tubulin enclosed in a yellow rectangle. B = enlarged view of the object. C = example of β tubulin staining using fluorescence based immunostaining. When comparing B and C note the similar shape of the stained area and the round non-stained area in the middle of both (the nucleus).

Furthermore when you look at the higher magnification images of the surfaces you begin to notice the recurrence of multiple oval shapes with what appear to be tapering ends which stand out slightly against the other staining. Also a number of these shapes appear to have a pale round “hole” in the middle. If we take this pale region as being an area with less or no staining, then the overall pattern of staining is consistent with what you would expect to see given the physiological role of the target antigen (β tubulin along with α tubulin are the major components of microtubules). These structures, as part of the cytoskeleton help to define the shape of the cell (as well as playing a major role in cell motility) and do not extend into the cell nucleus.

Based on this our conclusion was that the immunostaining had in fact worked to a certain extent, and was staining β tubulin. Due to the fact that we had cultured the cells on the surfaces for 14 days, and based on our observation of the proliferation behaviour of these cells, we believed that at the time of staining there were multiple layers of cells present on the surfaces.

This density of cells is why we see so much staining, and is acting to obscure some of the finer detail of the staining, which we are still able to see some examples of.

Effectively what we think is happening, is staining from the layer(s) of cells below the top layer of cells is shining through and obscuring the staining present in the top layer of cells. We think that had we been able to culture the cells for 3 days as we had originally intended, we are confident that we would have seen a single layer of somewhat spaced out cells, where the cells are stained in a similar fashion to the example included in the figure. We were also aware of the possibility that the actual staining component of HRP based immunostaining may not in fact be all that specific, particularly when compared to fluorescence based immunostaining. It is possible that the mass of staining we see is simply down to the HRP reaction product not being specifically deposited at the site where the antibody complex is bound to the antigen of interest, but instead produced a non area-specific smear of stain.

While we felt on balance that this experiment did provide evidence that the technique was working, the initial results were not fully conclusive. Additionally there was an alternate explanation for the results we observed, namely that the staining that we see is not specifically staining of β tubulin, which could indicate that the technique does not work in the manner we would require if it was to be useful in our research.

In light of this, we decided to conduct another experiment to conclusively answer whether or not HRP based immunostaining was a viable technique or not. To do this we decided to culture SAOS-2 cells on polycarbonate substrates for 28 days, then stain half of the samples for osteopontin using fluorescence based immunostaining, and half with HRP based immunostaining.

Our reasoning was that to definitively show that HRP staining was working, we would need an example of immunostaining for the same target antigen where we were sure it had worked, and the only way we could think of doing this would be to immunostain using fluorescence. Of course, in order to do this we could not use PEEK, so instead we opted to use polycarbonate substrates (which do not have PEEK's issues with autofluorescence). We felt, based on the previous experiment that there should not be a problem in being able to detect HRP staining on PEEK via microscopy. We were also aware that we were using a transparent material in

place of an opaque one and that this would impact on how we set up the Cell Profiler analysis of what is, and is not, stained material.

We then intended to use Cell Profiler to quantify, and then compare, the amount of staining generated by the two different methods of immunostaining. We were hoping to see roughly similar results from the two different approaches given that they were being used to measure the behaviour of the same type of cells, on the same material, seeded at the same time, by the same scientist. We were willing to accept some diversity between the two methods, however if HRP immunostaining showed much higher or much lower levels of staining compared to fluorescence based immunostaining we would have to consider whether or not HRP based immunostaining is accurate enough to be able to effectively measure stem cell response to our PEEK nanotopographies.

Additionally, directly comparing the pattern of staining between fluorescence and HRP based immunostaining would offer us some answers on how accurate the deposition of the HRP reaction product is to the site of the bound antibody complex. Given that fluorescence based immunostaining is held to be generally geographically accurate (by dint of the fluorescent molecule being conjugated to the antibody complex that is bound to the antigen, and the fluorescence signal indicates where the antigen is found on the surface), then similarities in the general patterns of staining, particularly when looking at the samples at lower magnifications, could give us an idea on how accurate the localisation HRP reaction product is to the site of the bound antibody complex.

We opted to use SAOS-2 cells in the experiment, as they were a source of a large number of cells in short period of time, and are capable of expressing the osteogenic markers we would be interested in when looking at stem cells cultured on PEEK. Since SAOS-2 proliferate quickly we were also confident that there would be a large amount of target antigen present, so we were confident we would see a good amount of staining present on the samples at 28 days, which would make it easier to compare the levels of staining using Cell Profiler.

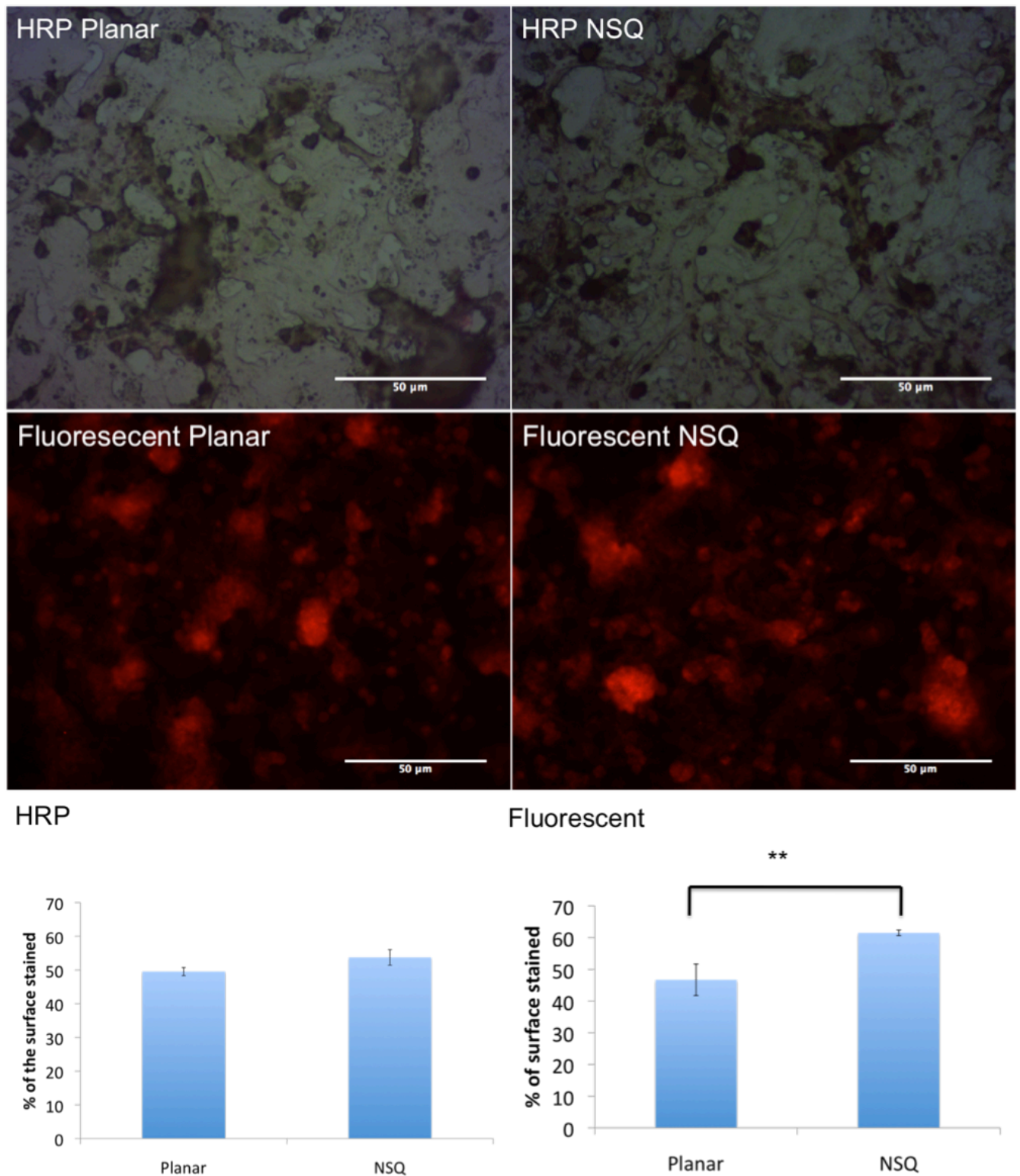


Figure 75 Examples of fluorescent and HRP based immunostaining of osteopontin in SAOS-2 cells cultured on polycarbonate substrates for 21 days. While the staining is not identical between different types of immunostaining we can see similarities in the overall pattern of staining. Comparison of the immunostaining results generated by two different types of secondary antibody staining for Osteopontin in SAOS-2 cells cultured for 21 days on poly carbonate substrates. In each instance there is a representative example of the type of microscopy used (fluorescence and light respectively) and then a

graph generated from the Cell Profiler results based on measuring the percentage of the microscope image containing stained material fluorescence based immunostaining HRP based immunostaining. Cell Profiler analysis of the fluorescent staining indicates that the results for the NSQ nanotopography is highly statistically significant compared to the planar surface. Scale bar = 50µm

The results of the immunostaining comparison experiment were on the whole very encouraging. If we visually compare the two different methods of immunostaining we see the same general pattern of staining in both, namely strongly stained regions (bright red with fluorescence and black regions with HRP) fading towards the edges, and with spaces with no stained material spread across the surfaces. These patterns match with what we have seen when we stain SAOS-2 cells with alizarin and von Kossa to investigate mineralisation, and given osteopontins role in binding calcium-phosphate during the process of mineralisation, this is not surprising.

The Cell Profiler analysis indicated that for the fluorescently stained samples the staining present on the NSQ nanotopography was highly statistically significantly higher than that of the planar surface. The HRP samples showed the same trend but this was not found to have statistical significance. These results confirm that fluorescence based immunostaining is more sensitive than HRP based immunostaining and produces greater contrast between stained and non-stained material but as the two methods generate the same trend it would suggest that HRP based immunostaining is able to accurately identify and stain the target.

As we were, at this point, confident that HRP immunostaining was a technique that would allow us to accurately measure the osteogenic response of stem cells, we were ready to carry out a large scale experiment to look at the osteogenic response of stem cells to our different PEEK nanotopographies. We opted to look at the osteocalcin and osteopontin response of osteoprogenitors and the osteocalcin response of 271⁺ mesenchymal stem cells to PEEK planar, NSQ and SQ

nanotopographies after 28 days of culture. After microscopy we then analysed the results using Cell Profiler.

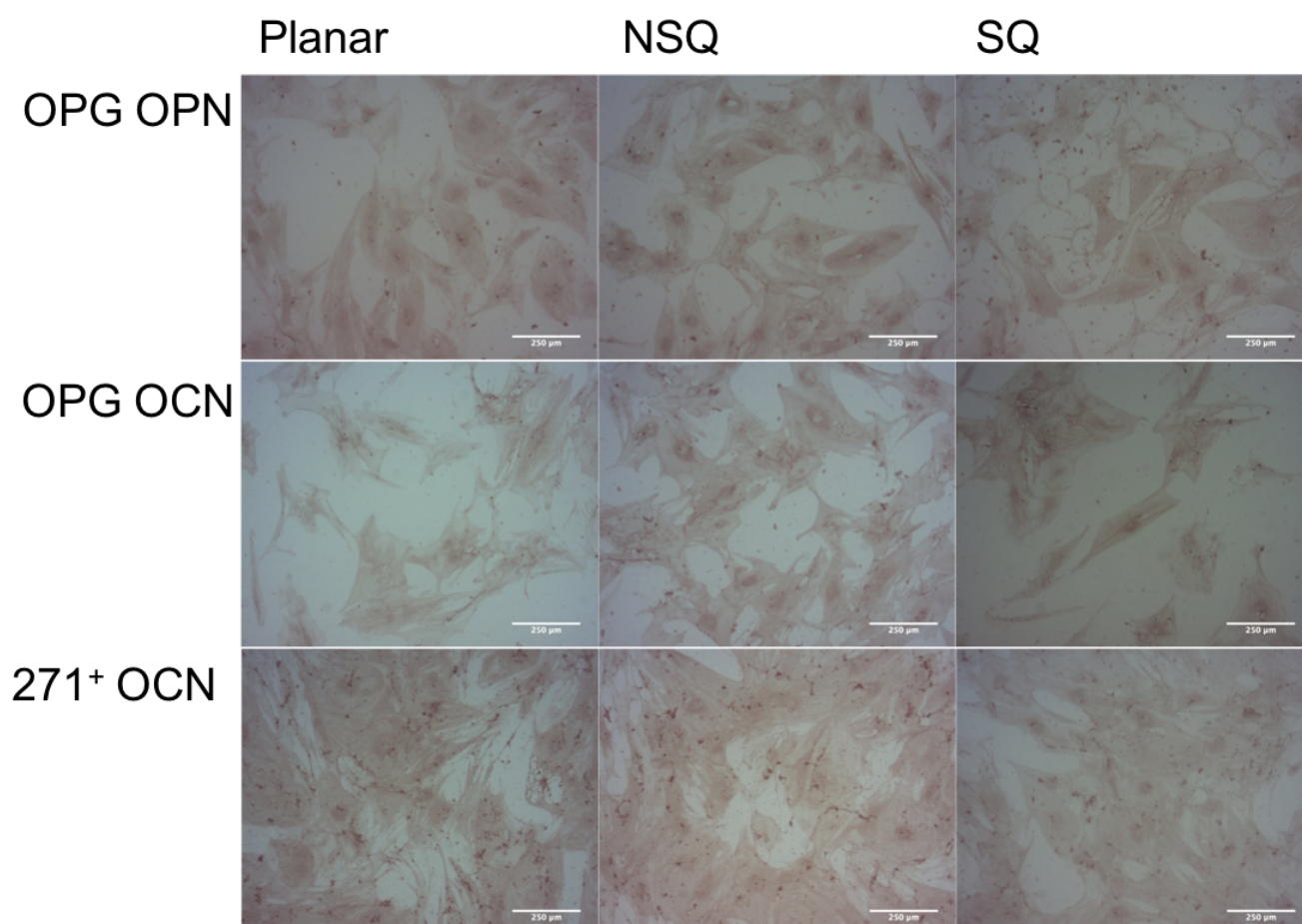


Figure 76 Representative images generated by polarised light microscopy of HRP based immunostaining of stem cells (osteoprogenitors (OPG) and 271⁺ MSC (271⁺)) stained for either Osteocalcin or Osteopontin markers cultured on various PEEK nanotopographies for 28 days. In each instance the scale bar is equal to Total number of replicates N=9 Planar=3, NSQ=3, SQ=3. Scale bar =250 μ m.

We can see a number of things from the initial microscopy of the experiment. In each instance the cells have adhered to the surfaces, proliferated and then progressed through the osteogenic pathway, producing a late stage osteogenic marker (either osteopontin or osteocalcin). This lends credence to our previous results that show positive results for mineralisation having occurred in a physiologically relevant manner as opposed to being due to the presence of either calcium or phosphate being accumulated on the surface through some other process. In each instance, the acellular control demonstrates that there is almost no background staining of the material, which would indicate that the staining we are seeing on the sample is as a downstream result of binding to the primary

antigen by the primary antibody. The level of staining looks uniform across surfaces in the 271+ MSC experiment, while in the osteoprogenitor experiments there does look to be less staining present on the SQ surfaces particularly in the osteopontin experiment.

We then took the microscopy data and used Cell Profiler to measure the amount of staining present on each of the surfaces. We used this data to compare the percentage of the surface that has stained material on it for each of the samples.

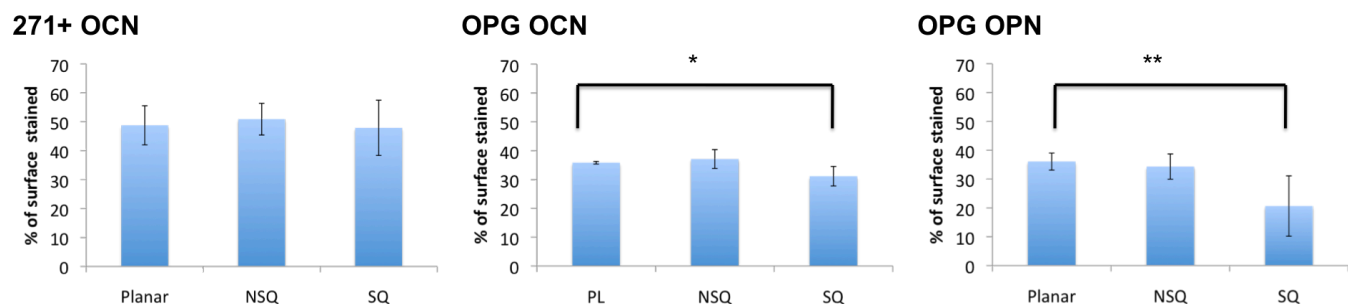


Figure 77 Total percentage of the microscope image with stained material analysis of the Cell Profiler results for the experiment. The osteoprogenitors on the SQ nanotopography produces statistically significantly lower results compared to the planar surface for OCN and highly statistically significantly lower for OPN Total number of replicates N=9 Planar=3, NSQ=3, SQ=3.

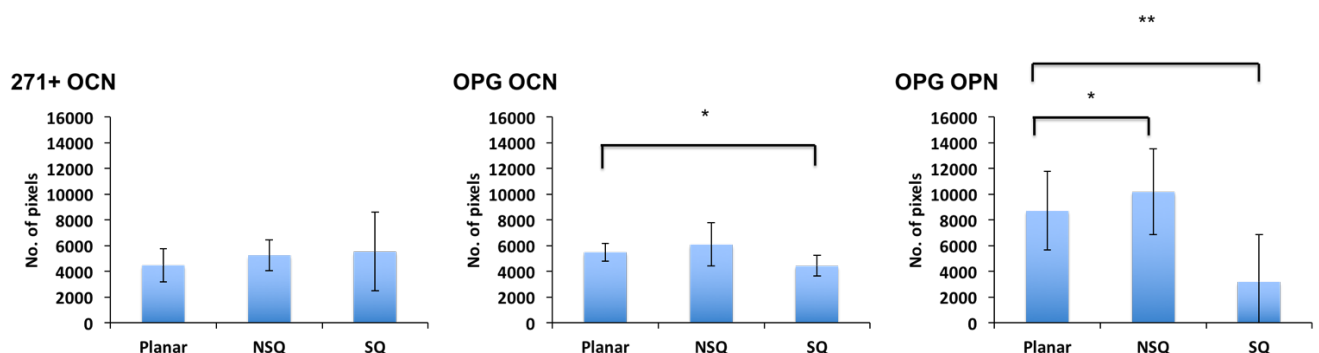


Figure 78 Average area of identified objects present on the microscope images as generated by Cell Profiler analysis. The osteoprogenitors on the SQ nanotopography produces statistically significantly lower results compared to the planar surface for OCN and highly statistically significantly lower for OPN. These same cells produce statistically significantly higher results for OPN on NSQ. Total number of replicates N=9 Planar=3, NSQ=3, SQ=3.

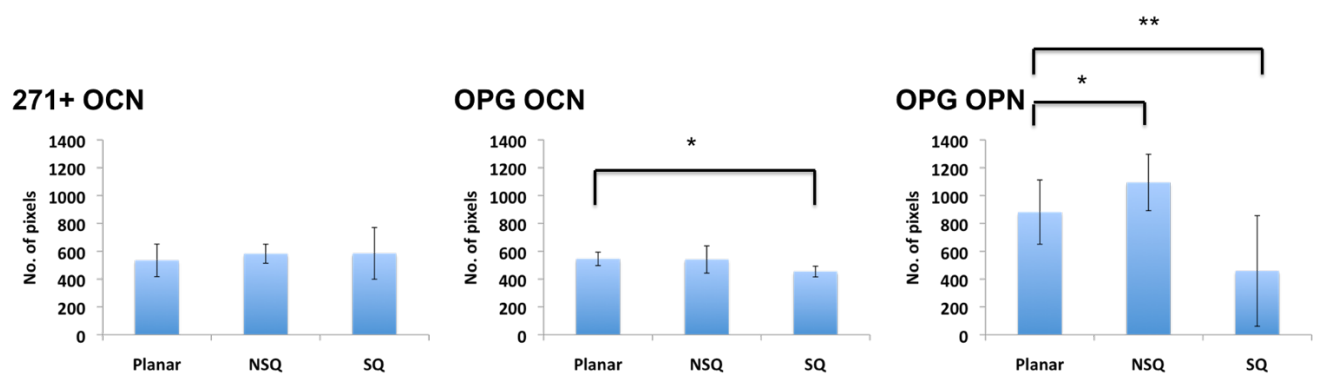


Figure 79 Average perimeter of identified objects present on the microscope images as generated by Cell Profiler analysis. The osteoprogenitors on the SQ nanotopography produced statistically significantly lower results compared to the planar surface for OCN and highly statistically significantly lower for OPN. These same cells produce statistically significantly higher results for OPN on NSQ. Total number of replicates N=9 Planar=3, NSQ=3, SQ=3.

The Cell Profiler analysis in many respects validates our initial conclusions from looking at the stained images, namely that for the osteoprogenitor cells there is less staining present on the SQ nanotopography compared to the planar surface and the 271⁺ MSC's staining levels do not vary significantly between the surfaces tested. For the osteoprogenitors stained for osteocalcin the SQ nanotopography had a total percentage of the surface with stained material, average area and average perimeter which were all statistically significantly lower than the planar surface. For the osteoprogenitors that were stained for osteopontin the SQ nanotopography had a total percentage of the surface with stained material, average area and average perimeter which were all highly statistically significantly lower than those of the planar surface. Additionally the NSQ nanotopography had average areas and average perimeters that were highly significantly higher than those of the planar surface. There were no significant differences for any of the values investigated for the 271⁺ MSC's.

These results would indicate that the osteoprogenitor cells are much more sensitive to the surface topography compared to the 271⁺ MSC's. They also show that the production of osteopontin is more sensitive to modulation by the presence of the topography compared to that of osteocalcin (it is worth noting that osteopontin is generally expressed at a higher level than osteocalcin as it can be involved in other cellular events other than osteogenesis unlike osteocalcin which is only involved in osteogenesis). As such it is possible osteocalcin may be expressed at a level low enough that the HRP immunostaining may have struggled

to measure it. It would have been interesting to see if carrying out this experiment with fluorescence based immunostaining to see if it would have delivered different results for osteocalcin staining. The SQ nanotopography consistently reduces both markers relative to the planar surface in terms of percentage of the surface with stained material, average area of identified stained areas and average perimeter of identified stained areas. This has similarities to work previously done with this nanotopography fabricated from polycarbonate where MSC's were found to continue expressing markers associated with pluripotency when cultured on the SQ nanotopography. Here we cannot say for certain that there has been a significant maintenance of pluripotency, but we can see there has been a reduction in osteogenesis compared to the absence of nanotopography (the planar surface) which could be evidence that the topography is encouraging the osteoprogenitor cells not to differentiate. However since we have only stained for osteogenic markers we can't tell if the cells are expressing other markers, so the only thing we can say for certain is that the SQ nanotopography is discouraging the osteoprogenitor cells from expressing osteopontin and osteocalcin. It is interesting that the 271⁺ MSC's have not responded in terms of expression of either marker to either of the nanotopographies tested. Osteoprogenitors are a heterogeneous mix of cells including mature osteoblasts, pre-osteoblasts and mesenchymal stem cells, whereas the 271⁺ MSC's used in this experiment were extracted from a population of osteoprogenitors via magnetic purification and as such is a monoculture of cells that are in an undifferentiated state, with the capacity to differentiate down multiple lineages. Despite this, these cells have shown a lack of significant difference in osteogenic marker activity between the topographies. Based on our data we cannot draw any concrete conclusions as to why this is.

9.3. Discussion

9.3.1. Effectiveness of horse radish peroxidase based immunostaining as a technique for investigating cell behaviour on PEEK.

Overall we believe that HRP based immunohistochemistry is an extremely effective technique that has the capacity to positively impact on the field of *in vitro* cell work with PEEK. This is not to say that the technique is without its own difficulties. The main problem with chromatic based immunohistochemistry boils down to being able to unequivocally identify what is stained material and what is background and/or artefact (a problem not encountered in fluorescence based immunohistochemistry where the only visible objects are ones which fluoresce, and as long as the technique has been carried out correctly the only fluorescing objects will be ones that have a fluorescently labelled secondary antibody bound to them. This is, in our minds at least, the major advantage of fluorescence based immunohistochemistry over chromatic immunohistochemistry). This was a major source of difficulty in our initial experiments with the technique. However, these drawbacks can be addressed by the appropriate design of controls. Employing both an acellular control, a control using cells that cannot express the antigen and a control that uses only the primary anti-antigen antibody would conclusively demonstrate if there was any non specific staining taking place (if indeed any is taking place), and would allow the researcher to subtract this value from their experimental results, and thus have a greater degree of confidence in their experimental results. Used in conjunction with Cell Profiler the technique enables quantitative measurement of the level of staining both in terms of the amount of stain present and also the displacement and size/shape of the stained objects.

Given the crucial role played by immunohistochemistry in modern tissue engineering we believe that our development of an accurate quantitative method for identifying specific markers produced by cells cultured on PEEK would be of great interest to other researchers working with this material, and could make a significant contribution to the field of tissue engineering with PEEK.

9.3.2. Ability of nanotopography at the PEEK surface to influence the osteogenic activity of stem cells.

Our experiments, comparing the levels of osteocalcin and osteopontin produced by 271⁺ mesenchymal cells and osteoprogenitor cells cultured on oxygen plasma treated PEEK nanotopographies showed that certain nanotopographies in particular the SQ nanotopography were capable of directing the osteogenic behaviour of stem cells, and that the osteoprogenitors are significantly more sensitive to these topographies than the 271⁺ MSCs. The SQ nanotopography lead to a statistically significant decrease in the total percentage of the surface with stained material, average area and average perimeter when stained for both osteocalcin and osteopontin compared to the planar surface, while the NSQ nanotopography induced average areas and average perimeters that were highly significantly higher than those of the planar surface when stained for osteopontin, but not osteocalcin. There were no statistically significant differences detected on the 271⁺ MSC cells. Given the sensitivity of this technique and the fact that it stains for the presence of the protein target itself and not the presence of an indicative chemical (.e.g von Kossa staining for the presence of phosphate not hydroxyapatite itself) we feel that these results offers definitive evidence that these topographies fabricated from PEEK have the capacity to influence osteogenic behaviour. It is worth noting that this capacity is not as clear as that observed previously with these topographies fabricated from different materials^{35,36,60}. We believe that this demonstrates that the impact of the surface topography on the cells does not operate entirely independently of the surface chemistry and potentially indicates that different materials may need slightly different arrangements of nanoscale features to produce a desired effect.

This raises an interesting question: why do we see statistically significant differences with the osteoprogenitors but not the 271⁺ MSCs? The answer may be as simple as that due to the number of 271⁺ MSCs we had available at the time of this experiment we only investigated for osteocalcin activity and not for osteopontin as well, which we did with the osteoprogenitors. As there is a higher

overall level of osteopontin expression compared to that of osteocalcin it may have been possible to have detected a statistically significant difference between the surfaces with osteopontin. However, it is also possible that the 271⁺ MSCs do not respond in a statistically significant manner to these surfaces and the significant results we see in the osteoprogenitor experiments are down to a non-MSC fraction of the heterogeneous osteoprogenitor mix responding to the PEEK surface. Another possibility is that there is a potentially significant response by the 271⁺ MSCs but HRP immunostaining is not sensitive enough to detect it.

9.4. Conclusions

In summary we sought to find an alternate method which would allow us to use immunohistochemistry with PEEK, as due to its innate autofluorescence we were unable to use the widely available and commonly used fluorescence based immunohistochemistry.

To do this we opted to use horse radish peroxidase based immunohistochemistry, a process where the reaction product of the enzyme marks the presence of the bound primary antibody. Adapting this process required several experiments as well as the use of polarized light microscopy in order to differentiate between stained and background material.

Our direct comparisons between HRP and fluorescence based immunostaining showed that while the fluorescence based approach is more sensitive, the two techniques demonstrated the same trend. This demonstrated to our satisfaction that it was possible for HRP based immunostaining to generate the same type of data as we would have expected had we been able to use a more conventional immunostaining approach with this material. We believe that this approach (using HRP based immunostaining along with polarized light microscopy and then using Cell Profiler to quantify the results) could be of great use to other researchers working with PEEK, as the inability to harness immunohistochemistry in biological studies using this material looks to have been a serious impediment to the proliferation of PEEK as a material of interest in research.

The use of HRP based immunostaining on human stem cells cultured on our PEEK nanotopographies demonstrated that there were statistically significant differences in cell response to the different surfaces. The SQ nanotopography

produced total percentage of the surface with stained material, average area of identified objects and average perimeter of identified objects that were all significantly lower than the planar surface. In addition the NSQ nanotopography produced average area of identified objects and average perimeter of identified objects that were both significantly higher than the planar surface when stained for osteopontin.

10. Discussion

10.1. How did our experimental data address the key aims of the project

10.1.1. Alteration of the PEEK surface both in terms of the topography and chemistry to improve the osteogenic response of cells that come into contact with it.

Nanotopography

Thanks to the continuing excellence of nanofabrication at the University of Glasgow our colleagues were able to supply us with perfect copies in PEEK of the nanotopographies previously used, to guide stem cell differentiation behaviour^{35,36,60}. So, as producing highly ordered nanofeatures on PEEK was not something we had to accomplish, our challenge was to see if the presence of this nanoscale topography could direct stem cell differentiation in a way previously observed in other polymers. Overall, our results demonstrated that they did not.

We looked at a number of different aspects of the osteogenic process (our primary interest was in producing a surface that would encourage osteogenic behaviour as PEEK is best suited for use in direct bone contact orthopaedic implants), as we thought that it was possible that the presence of the topography may have a significant impact on the speed and/or strength of one stage of osteogenic process, which could be missed by only focusing on the final stages of osteogenesis.

Our results showed that the presence of nanotopography is capable of influencing cell behaviour, but the overall picture of how this takes place is not as straightforward as that seen with other polymers. The SAOS-2 cells on PEEK surfaces that had been plasma treated for 2 minutes at 200W (24,000J) showed statistically significantly higher levels of von Kossa staining on the NSQ surface compared to the planar surface, and the same experiment employing alizarin red staining, showed a statistically significantly lower level of staining on the SQ

surface compared to the planar surface. Ideally we would want to see identical results generated by both staining techniques (the two stains stain different components of hydroxyapatite) and while we do see a similar trend between the two, there is not a significant difference for either of the staining techniques. We do not believe however that this indicates that the results are without merit, instead it is our opinion that with von Kossa the SQ result is not quite low enough to clear the threshold for significance, and with alizarin the NSQ result is not high enough to qualify as significant. We do believe that the behavioural signal delivered to the cells by the nanotopography is not as strong as the one delivered by the same nanotopography fabricated from one of the previously tested polymers e.g. polycarbonate. While we believe that it is eminently possible that a different nanotopography could be capable of delivering a stronger behavioural stimulus, it is evident that the presence of nanotopography at the PEEK surface is capable of modulating the osteogenic behaviour of these cells. In our experiments which employed primary osteoprogenitor cells and were designed to look into whether the presence of nanotopography effected primary osteoprogenitors, we found that each of the main stages of osteogenesis in turn demonstrated a lack of statistically significant difference between the surfaces studied for each of the behaviours investigated. By utilising HRP based immunostaining we were able to investigate, in a quantitative fashion, the production of the two osteogenic markers osteopontin and osteocalcin by primary osteoprogenitors, and the production of osteocalcin by primary 271⁺ MSCs. For the osteoprogenitors stained for osteocalcin, the SQ nanotopography had a total percentage of the surface with stained material, average area and average perimeter, all statistically significantly lower than the planar surface. For the osteoprogenitors that were stained for osteopontin the SQ nanotopography had a total percentage of the surface with stained material, average area and average perimeter all highly statistically significantly lower than those of the planar surface. Additionally the NSQ nanotopography had average areas and average perimeters that were highly significantly higher than those of the planar surface. There were no significantly significant differences for any of the values investigated for the 271⁺ MSCs. This demonstrates that the nanotopography once again is capable of directing the behaviour of cells cultured on it, and that these particular topographies are much

more effective at altering the behaviour of osteoprogenitor cells compared to the 271⁺ MSCs. Why this is so, is currently unclear. There are a number of different possibilities for why this could be. As osteoprogenitors are a heterogeneous mixture of cells, unlike the 271⁺ MSCs which were actively selected for the presence of the 271⁺ surface marker, it could suggest that the presence of the nanotopography has different effects on different mononuclear cells that are all found in human bone marrow. As MSCs are a component of osteoprogenitors, this could suggest that it is the other cell types present that are responding to the presence of topography. It is also possible that the 271⁺ MSCs respond in a different way to the presence of the chemical alteration to the PEEK surface due to the plasma treatment. The cells on both surfaces are expressing osteocalcin, which indicates that they have differentiated down the osteogenic lineage, but as there is no statistically significant difference between the planar surface and the NSQ nanotopography this could indicate that the plasma treatment caused the MSCs to differentiate down the osteogenic lineage, but then further to this the cells did not respond to nanotopography. It is also possible that the HRP based immunostaining is not sensitive enough to pick up significant differences in behaviour between the 271⁺ cells on the nanotopographies. When we directly compared fluorescence and HRP based immunostaining techniques, by using them both on SAOS-2 cells on polycarbonate surfaces, fluorescence was shown to be significantly more sensitive than HRP, so it is possible that there could have been a statistically significant difference between the 271⁺ MSCs on the nanotopographies that the HRP immunostaining was unable to detect. However it is worth noting that HRP based immunostaining was sensitive enough to detect statistically significant differences in marker behaviour by osteoprogenitor cells which would demonstrate that even if there was an undetected significant difference present with the 271⁺ it would still be orders of magnitude less than that observed in the osteoprogenitor cells. So regardless of overall sensitivity of our staining technique, osteoprogenitor cells are still more sensitive to the presence of our nanotopography.

Taken as a whole these results demonstrate that the presence of nanotopography at the PEEK surface is capable of modulating the osteogenic behaviour of cell cultured upon it, and as such suggests that nanotopography incorporated at the

surface is a viable technology for addressing PEEKs documented lack of biological activity.

Given that our experiments used two different nanotopographies (along with a planar surface that acted as a control surface), it is absolutely possible that other nanotopographies could be capable of producing stronger changes of cellular behaviour, and as such our results should not be viewed as the maximum extent of what can be achieved in terms of modulating cell behaviour with nanotopography, but instead a demonstration of the suitability of this technology as used with PEEK.

Chemistry (plasma treatment)

Our use of oxygen plasma treatment was successful in tackling PEEKs underlying problem with poor cellular adhesion and proliferation. Our findings were consistent with previous work done in this area⁸⁵.

Due to the capability of oxygen plasma treatment to etch surfaces that are exposed to it, we looked at the relationship between length of plasma treatment and alteration to the surface topography. Our AFM results illustrated an overall trend that as plasma duration increases there is an associated increase in the roughness of the interpit areas, in pit diameter and a decrease in pit depth. We felt that overall, five minutes indicated a point at which both the increase in pit diameter and decrease in pit depth became unacceptable.

The plasma treatment led to a strong reduction in the water contact angle, as measured by the sessile drop method. A comparison of the water contact angles of the different plasma treatments used throughout the project showed that there was a strong reduction in water contact angle between untreated PEEK and the lowest amount of plasma treatment used. There was however very little difference in water contact angle between any of the different strengths of treatment. This does correlate with the relationship between plasma treatment and cell adhesion/proliferation, where the strongest improvement is seen between an untreated PEEK surface and one with any duration of plasma treatment .

Variation in the duration and power of plasma treatment were shown to alter cellular response but not always in a straightforward manner. We cultured SAOS-2 cells on a range of PEEK nanotopographies that had been plasma treated between

12s and 2 minutes and 100 to 200W. In terms of the percentage of the surface with stained material, there was no significant difference for any of the different plasma treatments tested. There was a general trend for an increase in the level of staining with the power of plasma treatment. This trend was consistent across the nanotopographies, although there were some slight variations between them. More in depth analysis of this trend showed that there were further significant differences between the nanotopographies when properties other than percentage of the surface with stained material were considered. At 2 minutes of 200W plasma treatment, the NSQ nanotopography both had a mean radius and a median radius that is significantly lower than that of the planar surface. At 1 minute of 100W plasma treatment, both the median radius and perimeter of the SQ nanotopography was significantly lower than that of planar surface. At 30s of 100W plasma treatment the mean radius of the SQ nanotopography was significantly higher than that of the planar surface. Finally, at 6s of 200W treatment, the median radius and average perimeter of the SQ nanotopography were significantly lower than those of planar surface.

We can see from these results that increasing the energy of plasma treatment in turn leads to an increase in the overall percentage of staining. There are exceptions to this, in particular, the overall percentage staining for the highest energy used (24000J) was lower than that of the second highest energy setting employed (6000J). In addition to this, for the NSQ and planar surfaces the overall percentage staining of the 3000J treatment was lower than that of the 1200J treatment. Given the large difference in the amount of power used, it seems plausible that at that some point between 6000J and 24000J there is a point at which the percentage of the surface stained stopped increasing, and by 24000J had in fact already started to decline. The average difference between 24000J and 6000J for the three surfaces is 13.4% (planar = 15.6%, NSQ = 19.04% and SQ = 5.5%) so the decrease is not inconsiderable, and suggests that the plasma treatment which would deliver the highest mineralization response lies somewhere above 6000J and below 24000J.

We also carried out a similar experiment with stem cells isolated from human bone marrow cultured on a range of PEEK nanotopographies that had been plasma treated between 15s and 2 minutes, and between 30W and 200W. In addition we

included polycarbonate surfaces as a seeding control. In this experiment the percentage of the surface stained results showed that for polycarbonate surfaces mineralization is statistically significantly higher on the NSQ nanopattern compared to the planar surface, whereas on the PEEK surfaces we observe the opposite trend, with the NSQ nanotopography having a statistically significantly lower amount of mineralization compared to the planar surface at the 200W 2min and 30W 1min plasma treatments, as well as a lack of a statistically significant difference between the two at the other treatments. The mean radius results, in common with the percentage of the surface stained results, both have two treatments where the mean radius of identified objects is statistically significantly higher on the NSQ nanotopography compared to the planar surface i.e. 30W 15s and 30W 1min, and two treatments where the average area of identified objects are statistically significantly lower on the NSQ nanotopography compared to the planar surface i.e. 30W 30s and 50W 30s. Again in common with the percentage of surface stained results, the polycarbonate NSQ nanotopography had an average area of identified objects that is statistically significantly higher than that of the planar surface. The mean radius results are similar to the average area of identified objects results in that they both have two treatments where the mean radius of identified objects is statistically significantly higher on the NSQ nanotopography compared to the planar surface i.e. 30W 15s and 30W 1min, and two treatments where the average area of identified objects are statistically significantly lower on the NSQ nanotopography compared to the planar surface i.e. 30W 30s and 50W 30s. Also, similar to the average area of identified objects results, the polycarbonate NSQ nanotopography has an average area of identified objects that is statistically highly significantly higher than that of the planar surface. The median radius of identified object results demonstrates one plasma treatments that delivers PEEK substrates where the median radius of identified objects is statistically significantly higher on the NSQ nanotopography compared to the planar surface i.e 30W 15s, and two treatments where the average area of identified objects are statistically significantly lower on the NSQ nanotopography compared to the planar surface i.e. 30W 30s and 50W 30s. Once again the polycarbonate NSQ nanotopography has a median radius of identified objects that is statistically highly significantly higher than that of the planar surface. The

average perimeter of identified objects results demonstrates one plasma treatments that delivers PEEK substrates where the average perimeter of identified objects is statistically highly significantly higher on the NSQ nanotopography compared to the planar surface i.e. 30W 15s, and one plasma treatment where the average perimeter of identified objects is significantly higher than the planar surface i.e. 30W 1min. There was one plasma treatment where the average perimeter was statistically significantly lower on the NSQ nanotopography compared to the planar surface i.e. 30W 30s.

The experiment demonstrates that the polycarbonate control acts in consistent fashion, giving a pattern of higher results on the NSQ nanotopography compared to the planar surface. This would indicate that the variation in response between the different plasma treatments applied to the PEEK surfaces are not artefacts of the process of seeding, cell culture or staining. In our opinion, the standout trend from the PEEK results is that the statistically significant differences on the PEEK substrates are clustered around the lower energy plasma treatments, which could suggest that the plasma treatment is in fact disrupting a function of the nanotopography, which is why, as the energy increases, we see less statistically significant differences between the NSQ nanotopography and the planar surface. It is notable that our experiments carried out with HRP based immunostaining showed statistically significant results by osteoprogenitors and 271+ MSCs on surfaces that had been plasma treated for 2min at 200W. This could indicate that the von Kossa staining used here is not sensitive enough to pick up on small, but significant differences between the surfaces at the different plasma treatments. Equally it is possible that particular plasma treatment effects the production of the two different osteogenic markers differently.

Our interpretation of these results is that different plasma treatments have different effects on the cells cultured on the PEEK surfaces. However our results do not demonstrate a clear relationship that governs cell response i.e. increasing energy of plasma treatment leads to an increase in percentage of staining. We suspect that it is a property which is altered by the plasma treatment that we cannot currently quantify, such as alteration to the way in which proteins are absorbed by the material surface, that governs how the cells respond to our plasma treated surfaces.

10.1.2. Extent of fidelity of nanopattern effect in different polymers

Since the initial discovery that specific nanotopographies alone could effectively influence osteogenic behaviour in stem cells³⁵, there has been an understandable interest in translating this discovery into technology ready for use in clinics. Initially the main obstacle to this was the material which the topographies were fabricated from. Replication of the biological effect of the topography when fabricated from PC⁶⁰ opened up the possibility that the mechanism of action of the topography worked regardless of the material that the topography was constructed from. This opened up the possibility that a material like PEEK, that has excellent material properties for use in orthopaedic implant devices⁶⁴ but consistently displays a poor cellular response^{64,82,83}, could have a specific nanotopography incorporated into its surface which would significantly improve cell response without compromising any of the material qualities that made it of interest for use in implant devices in the first place.

However, our experimental results ultimately did not display the same consistency of biological effect when specific nanotopographies were fabricated from PEEK compared to when they were constructed from PC.

We screened a range of different oxygen plasma treated PEEK surfaces to look at the effect these different treatments had on the osteogenic response of osteoprogenitors as measured by von Kossa staining. As a control we included PC planar and NSQ surfaces to demonstrate if there were errors present in the execution of the cell seeding and culture, or in the isolation and culture of the stem cells used. Since the NSQ PC surface had been demonstrated to induce osteogenesis relative to the planar surface⁶⁰, if it failed to do so in this experiment it would demonstrate that there were problems with its execution. However, if the PC substrates did show the expected pattern it would demonstrate that the experiment had been performed correctly. Additionally, the inclusion of this

control would demonstrate if the previously reported osteogenic effect of the NSQ nanotopography was distinct enough to be picked up by von Kossa staining.

The experiment demonstrated that none of the different plasma treatments used led to a significant difference in the percentage of the surface stained result for the osteoprogenitors between the planar and NSQ surfaces (the different treatments used were designed to effectively cover the range of plasma treatments that had been demonstrated not to cause significant damage to the topography) whereas on the PC surfaces, we can see there is a large increase in osteogenic response on the NSQ topography compared to the planar surface.

The results of the experiment showed that the polycarbonate control acts in consistent fashion with pattern of higher results on the NSQ nanotopography compared to the planar surface. The PEEK results on the other hand demonstrated a pattern of lower results on the NSQ nanotopography compared to the planar surface, with an overall trend of statistically significant differences clustered around the lower energy plasma treatments

The question of why do we not see a conservation in stem cell response to the nanotopography when it is constructed from PEEK compared to when the same nanotopography is constructed from other polymers like PC or PCL, is a complex one. It is additionally complicated by the fact that at no time were we able to look at the cellular response to PEEK surfaces where the only modification is an alteration in topography. Due to the extremely poor level of cell adhesion and subsequent proliferation observed when cells were seeded on PEEK nanotopographies that had received no further surface modifications, we had to use oxygen plasma treatment to generate enough cells on our surfaces to be able to investigate cell behaviour. As a consequence of this all of our biological results reflect how the cells in question respond to a combination of the defined nanoscale topography present at the materials surface, as well as the alterations to the surface chemistry caused by the oxygen plasma treatment. While this is not ideal, it is worth noting that one of the major drivers for this research was to improve PEEK suitability for use in load bearing implants. Given the specifications for these types of devices (orthopaedic implants require that a layer of host cells

adhere and proliferate in order to cover the implant surface, otherwise there is a risk of fibrous encapsulation taking place), looking at cellular interactions with non-surface modified PEEK is of little practical interest. So while it would have been interesting from a purely intellectual perspective to be able to look at cellular interactions with the bare PEEK surface, from a functional biomaterials standpoint our inability to do so is not of critical concern.

Nevertheless the question of why we see a failure of replication of biological effect in nanotopographies fabricated from PEEK is an interesting one.

An intuitive place to start to unpick this question is to ask the perhaps self-evident question “what is the difference between our PEEK surfaces and the previously used polymer surfaces?”

The most readily apparent difference would be that we have to apply a fairly intense oxygen plasma treatment to our surfaces to obtain an acceptable number of cells on its surface. Is it possible that the presence of the plasma treatment acts to nullify the action of the nanotopography? While this is a possibility, and indeed may be the case, there is evidence that suggests that it may not be this straightforward. Our finding that plasma treatments of differing strengths all had the same effect on the osteogenic response of osteoprogenitor cells is interesting in this respect. If the surface treatment has the effect of causing the cells to ignore the nanotopography present, it does seem unusual that even the lowest plasma treatment possible on our asher has the same effect as the strongest plasma treatment which we identified as not causing an unacceptable level of damage to the nanotopography. While it is possible that this “weak” plasma treatment is still enough to “knock out” the effect of the topography, it is possible that it is instead, an innate property of the PEEK material that causes the nanotopography to not influence the cells in the same manner as it does in other materials.

10.1.3. Development of an approach that enables high quality analysis of cell response on PEEK that works around the materials specific difficulties

By utilizing a number of histological techniques along with polarized light microscopy and Cell Profiler analysis, we feel that we have developed a high quality system for analyzing the response of cells to PEEK surfaces.

One of the major problems that we encountered at the beginning of this work was the lack of established techniques for investigating the biological behaviour of stem cells cultured on PEEK surfaces. The standard technique for exploring the relationship between surface modifications and cellular response i.e. fluorescence based immunostaining, is incompatible with PEEK due to the materials auto fluorescence. qPCR is compatible with PEEK, however this technique requires an understanding of the timeframe in which you would expect target genes to be upregulated in order to get the most from it.

Our utilization of alizarin, von Kossa, ALP staining, coomassie blue and horse radish peroxidase based immunostaining has enabled us to investigate a number of different aspects of cell behaviour. While the reagents involved in the staining techniques mention do vary in price, overall they are much less expensive than qPCR. HRP based immunostaining would be roughly commensurate in price with fluorescence based immunostaining and the remaining techniques are relatively inexpensive. Additionally these staining techniques do not require any specialist equipment other than what you would expect to find in a standard biochemistry laboratory.

The use of polarised light microscopy allows us to image histologically stained PEEK samples with a high degree of contrast between different stains and the background material, facilitating easy identification of different material on the experimental surfaces. As PEEK is non-opaque, in order to image the material surface we have to use reflected light microscopy. A side effect of this is, due to the fact that PEEK is anisotropic it exhibits birefringence, and as a consequence of this, it is difficult to identify or differentiate between stained objects and the material surface. By employing polarized light microscopy we were able increase the contrast to a point where we can easily distinguish stained material, and

subsequently use Cell Profiler to quantify the staining present, and measure several different aspects of the observed staining.

10.2. Future research avenues with PEEK

10.2.1. Comparison between this work and other approaches to modifying the PEEK surface for use as a biomaterial

In general there are three principal approaches that have been taken to address poor cellular response to PEEK. These are; producing a PEEK composite material (usually with HA), coating the PEEK surface with metal and chemically altering the surface with plasma treatment. Using a combination of nanotopography along with plasma treatment compares reasonably well with these other approaches. While nanotopography that has been tested in this thesis does not deliver the type of standout results that have been observed previously³⁵ and may have been hoped for, it does offer encouragement that this technology is compatible with PEEK and different arrangements of nanotopography could offer stronger results.

10.2.2. Suggested next steps in PEEK research

There are a number of interesting follow up experiments to the work covered in this thesis that we believe could be carried out.

Given that focal adhesions have been demonstrated to play a central role in how nanotopography guides cell behaviour⁴¹, comparing the adhesion behaviour of cells on PEEK nanotopographies to nanotopographies fabricated from PC, PMMA or PCL. This is an avenue of research we would have explored, however until we successfully developed HRP based immunohistochemistry with PEEK (In previous work done with the nanotopographies with different polymers fluorescence based immunohistochemistry was used to look at focal adhesion activity, an approach that is incompatible with PEEK) we did not have the capability to do so. By the time we had this form of immunohistology available to us we did not have the time to carry out these experiments.

Comparing the size/maturity and distribution of focal adhesions formed by cells on a nanotopography fabricated from PEEK versus those on the same topography

fabricated from a polymer that has displayed the capacity to direct cell behaviour, could offer some interesting information. Firstly, if we see a significant difference in focal adhesion behaviour between different materials it would conclusively demonstrate that the PEEK nanotopographies do not act in the same way as the same topographies fabricated from other polymers. While this may seem like a question that has already been answered by the work done as part of this thesis, and given the fact that we could not use the same methods that had been used to investigate cell behaviour in these other polymers, there was always an underlying concern that by having to design a new set of methods for PEEK we had perhaps missed a subtle change of cell behaviour which may have been more apparent on other polymers. Differences in focal adhesion activity between different polymers would also indicate that topography is not the only factor involved in directing cell activity, and that it is instead modulated by the underlying properties of the material, which in our opinion is most likely to be the chemistry of the surface. While it is not of immediate assistance to the goal of producing a PEEK surface that displays an improved cell response, if we could identify what the difference(s) are between induced focal adhesion behaviour in a “successful” and “unsuccessful” nanotopography it could offer us an exemplar to aim for when screening new surface modifications to PEEK. If we knew which focal adhesion activity led to a given cell response, instead of investigating cells for an aspect of the mature behaviour (for example if we were looking for a surface that induced osteogenic activity, we would either be looking at a late stage protein marker such as osteopontin or osteocalcin, or use von Kossa or alizarin to stain for the presence of components of hydroxyapatite. Cells would have to be cultured for 21 and 28 days respectively for these markers to be expressed), we could instead culture cells for only a couple of days then investigate focal adhesion behaviour. Surfaces which demonstrated a similar pattern in adhesions to those on the surfaces that demonstrated the cellular activity that we are looking for, could then be investigated in more depth, to see if they do indeed display the activity. The advantage of using this type of approach, is that allows you to begin with a large pool of surfaces with small differences in the particular modification (if the modification being investigated was plasma treatment you would start with a range of surfaces with small regular increases in plasma treatment between them.

Alternately if you were investigating the influence of topographical features you would have a series of surfaces with regular alterations in feature size or spacing), and quickly identify promising candidates, and perhaps more usefully, discard surfaces which have little potential. This allows the researcher to focus time and resources on surfaces that are most likely to produce a positive result. It also permits the researcher to look at a wide range of variations on the factor of interest which strongly decreases the chance that they had found a factor that could positively influence their area of interest but miss the vital tipping point, due to being limited to the number of different variations of the modification they could investigate if they were, for example, looking into how topography impacts cell behaviour it is possible that a given structure is capable of altering cell behaviour only when the feature itself is a certain size, or the features themselves have a certain spacing between them. If the researchers library of variations does not cover this “tipping point” they would be under the impression that the feature is unable to influence cell behaviour. By expanding the pool of variations on the modification being investigated it reduces the chances of missing a type of surface that could produce an interesting cell response. Using Cell Profiler it could also be possible to do this by assessing the morphology of the cells on the different surfaces. This would potentially be similar, from a microscopy and Cell Profiler analysis point of view, compared to staining components of focal adhesions and possibly could be done with simple whole cell histological stains which are significantly cheaper and easier to use than HRP immunostaining. The difficulty with adopting this approach would lie in deciding which cellular morphology would indicate interesting behaviour by the cells.

This type of screening approach is in our opinion the best way to go in terms of trying to develop an improved PEEK surface for orthopaedic applications. As it appears from our results that nanotopographies that had consistent biological effects across different polymers do not have the same effect in PEEK.

This does not mean however that there are no nanotopographies which when fabricated from PEEK, can direct cell behaviour in exactly the manner in which we want it to. As the results in this thesis have demonstrated, cells are capable of responding to the presence of nanotopography present at the PEEK surface with

the caveat that they do not necessarily respond in the same way cells responded to the similar nanotopography fabricated from other polymers. Based on this we believe that the best way to identify topography that can direct cell behaviour in PEEK would be to effectively take a step back and fabricate a range of different topographical features from PEEK and look for initial relationships between surface features and cell response.

The original work developing the nanotopographies that are capable of directing cell response, followed this process by fabricating structures available to them given the technology and experience available at the time, and looking for relationships between these structures and cells. Once initial relationships had been identified, variations on size and spacing were tested to optimize the topographies for cellular function. Changes in technology has made it easier to produce libraries of different topographies compared to when the original nanotopography work was done in Glasgow, and as a consequence a much larger range of topographies can be produced for the same cost as would have been previously possible, giving the researcher access to a much larger pool of starting topographies. A practical way of doing this would be to produce a number of small patterned areas onto a larger, (compared to the substrates we had been using up to this point), PEEK surface. Adding wells on top the PEEK surface which would divide each of the patterned areas into their own separate environment, would allow the researcher to assess the impact of the different patterns present on the surface on cells. While due to there being multiple small pattern areas on the same piece of PEEK, this would lead to using significantly less PEEK cells and staining reagents. If any of the patterns were found to be of interest it would be possible to produce larger substrates with the just that pattern on it to carry out more in depth work on the effect of that particular pattern. This would require more fabrication work to produce full sized shims of the pattern of interest, but since the pattern would have already have shown evidence that it has an interesting effect on cells there would be less chance that the money invested in the fabrication of the larger scale pattern would be wasted

A slightly different approach which could yield interesting results would be to test the effects of micron scale topography on cells when incorporated into the PEEK surface. Given that a wide range of cell behaviours that have been demonstrated to be capable of being elicited by the presence of micron scale features¹⁹ investigating the ability of micron scale topography at the PEEK surface to direct cell behaviour could yield interesting results.

Another potential avenue that would be compatible with our work on nanopatterned PEEK would be to deposit a layer of metal on to the surface of the topography as an alternative to using plasma treatment, to address poor adhesion and proliferation of cells on bare PEEK. This approach has been demonstrated by a number of research groups to be effective⁹¹⁻⁹³. The challenge for adapting this type of approach to our work with nanotopographies would be to ensure that the deposited layer of metal did not cover over the nanotopography. It is worth noting that the interface between the deposited metal and the main PEEK material would be a point of weakness, with the possibility of the metal breaking away from the polymer. If this approach is to be carried on into the clinic, significant work would need to be undertaken to demonstrate that the interface is strong enough not to break off from the main bulk polymer when used *in vivo*. Modifying the surface with plasma does not have any of these issues.

10.2.3. Continuing relevance of Nanotopography a viable technology for further study with PEEK in the context of the results generated by plasma treatment

While plasma treatment was demonstrated to have a very clear and unambiguous effect on the ability of cells to adhere and proliferate on the PEEK surface it is not necessarily the best option for inducing osteogenic behaviour. An *in vivo* investigation into the effect of plasma treatment on the performance of PEEK implant devices in sheep⁷⁶ found a lack of statistically significant differences in bone to implant contact ratios (there was a trend for better results on the plasma treated compared to untreated but not to a statistically significant degree). This would suggest that plasma treatment alone is not enough to produce a PEEK implant device that can compete with other established.

10.3. Contribution of this thesis to the wider scientific community.

10.3.1. Histological/chromatic methods for investigating osteogenic response on PEEK.

PEEK's incompatibility with standard fluorescence based immunohistochemistry is a major complication to its use in *in vitro* bioengineering research, due to the crucial role played by fluorescence based immunostaining in the field. Immunostaining occupies an important niche among the different methods for investigating cell response *in vitro* where it is substantially cheaper and easier to generate consistent results when compared to quantitative PCR or modern proteomic methods, but crucially offers a significantly greater depth of information compared to older histology based methods such as von Kossa and alizarin red staining. In many respects if the techniques available to the researcher investigating material surfaces for suitability for use in orthopaedic implants are considered as a continuum of complexity/depth of data generated, immunostaining would sit almost exactly in the middle. As a consequence, immunostaining can fulfil an important role. It can be used to cap off a study that has used older less sensitive techniques i.e. being used to lend more weight when used with the most interesting result identified by the older less sensitive techniques. The immunostaining could demonstrate that the positive result is entirely due to the target being investigated (for example if the purpose of the study was to look at osteogenic response by cells the main "heavy lifting" of the investigation may have been done by older techniques such as von Kossa, alizarin or alkaline phosphate staining and by replicating the most interesting result found with these methods by immunostaining for say the presence of osteopontin or osteocalcin the research would be able to demonstrate clearly and unequivocally that the previous results reflected a biological reality and were not down to the stains reacting to substances that had become deposited on the material surface (Using a combination of the older histological techniques helps to avoid this but the HRP based immunostaining is still significantly different insofar as it is staining

the presence of a particular biological molecule not the presence of a chemical that could in theory be present on the surface due to other non- cellular means).

When it comes to screening a pool of different surfaces to look at the relationship between the surfaces and cell response, immunostaining is an excellent method to use. It allows the researcher to analyse a number of different surfaces for a wide range of different biological markers with a high degree of accuracy and an established mechanism for generating quantitative results from the stained images that are produced.

Our successful adaptation of horse radish peroxidase based staining we believe, opens up a range of new possibilities for researchers working with PEEK surfaces. A major advantage that immunostaining has is that it demonstrates the presence of antigen of interest (this is compared to say von Kossa which indicates the presence one component of hydroxyapatite not hydroxyapatite itself or qPCR which measures the number of gene transcripts of the target antigen not necessarily the level of protein that is produced). Coupled with polarized light microscopy and Cell Profiler analysis, we have a technique that permits the researcher, in a quantitative fashion, to assess the levels of their target antigen. Given that the choice of antigen is limited only by the availability of an appropriate antibody, there is a wide range of different biological processes that can be investigated using this approach. Additionally given that immunostaining is more sensitive than our other histological techniques, it may be possible to pick smaller but still statistically significant differences that would be missed using our other more commonly used histological techniques. These attributes make HRP immunostaining an excellent technique to use when screening an initial library for points of interest, as it enables the analysis of a large number of initial surfaces for a wide range of different biological markers with a high degree of accuracy, and an established mechanism for generating quantitative results from the staining results.

10.4. Main findings contained within this Thesis

10.4.1. Interaction between PEEK and nanotopography

Our results showed that nanotopography does not have the same effect on cells *regardless* of the material it is fabricated from. It was hoped that nanotopographies, which had previously shown to have effects on cell behaviour when fabricated from other polymers, would also show these effects when fabricated from PEEK. Our results showed that this is not the case, and we demonstrated that the material surface itself plays a synergistic role, along with topography in influencing cell behaviour.

10.4.2. Development of new approaches for investigating cell behaviour on PEEK.

In this thesis we were able to take histological staining techniques and couple them with polarized light microscopy and Cell Profiler which enabled quantitative measurement of cell responses on PEEK. This approach was shown to be more effective than existing approaches. As PEEK is strongly autofluorescent, it is not possible to use fluorescent based immunostaining to interrogate cell behaviour on the surface of the polymer. While fluorescence based immunostaining is not the only method for investigating cell behaviour, it is extremely useful in the type of biomaterials research we were engaged in. It produces quantitative results for any biological marker for which there is an antibody available, as well as demonstrating the localization of the antigen. Since this technique cannot be used in conjunction with PEEK, we were able to use histological techniques for interrogating different aspects of osteogenesis in order to investigate how PEEK nanotopographies effect the osteogenic behaviour of cells. By combining these techniques with polarized light microscopy and Cell Profiler analysis, we were able to produce quantitative results for a number of different aspects of the staining. In addition, we were also able to adapt horse radish peroxidase based

immunostaining for use with our PEEK nanotopographies, which allowed us a more sensitive technique for investigating the response of stem cells to our PEEK surfaces.

10.4.3. Nanotopography may still be a viable approach for modulating cell response to PEEK surfaces

While the nanotopographies tested did not have the same effects on cell behaviour when fabricated from PEEK, some of our results did suggest that the presence of nanotopography can still have an effect on cell behaviour. Our experiments with stem cells and HRP based immunostaining showed that there were significant differences in the results for the nanopatterned surfaces compared to the planar surfaces, which we did not see when investigating the same surfaces with other techniques, such as von Kossa staining. We believe that it is possible that the the nanopatterns we used in our work are influencing the behaviour of the cells, but the change in behaviour is very subtle, and is comparable to changes in behaviour observed by other researchers working with the same nanotopographies fabricated from different polymers. As a result, we believe that different arrangements of nanofeatures or indeed features on the micron scale could elicit much stronger cellular responses. If so this would make surface topography a competitor to other methods for improving PEEKs suitability for use in biomaterials applications, such as deposited coatings or composite blends.

10.4.4. Effects of plasma treatment on PEEK

Previous research with PEEK had demonstrated the ability of plasma treatment to improve cell adhesion on the polymer surface, which was consistent with our results. However the relationship between plasma treatment and osteogenic response is not entirely clear. In our experiments, where we varied the plasma treatment, we observed statistically significant differences in osteogenic response between the NSQ nanotopography and the planar surface. These differences are also clustered down at the lower end of the energies we used for plasma

treatment. This may indicate that the plasma treatment is in fact disrupting a function of the nanotopography which is why, as the energy increases, we see less statistically significant differences between the NSQ nanotopography and the planar surface. This suggests that the changes the plasma treatment makes to the chemistry of the PEEK surface must be thought of as working in concert with the surface topography, and should be borne in mind when designing a PEEK surface for biomaterials applications.

11. References

1. Bergmann, C. P. & Stumpf, A. Dental Ceramics. 9-14 (2013). doi:10.1007/978-3-642-38224-6
2. Hench, Larry L., and J. M. P. Third - generation biomedical materials. *Science* (80-.). (2002).
3. Agarwal, R. & García, A. J. Biomaterial strategies for engineering implants for enhanced osseointegration and bone repair. *Adv. Drug Deliv. Rev.* **94**, 53-62 (2015).
4. Huiskes, R., Weinans, H. & van Rietbergen, B. The relationship between stress shielding and bone resorption around total hip stems and the effects of flexible materials. *Clin. Orthop. Relat. Res.* 124-134 (1992). doi:10.1097/00003086-199201000-00014
5. Bauer, T. W. & Schils, J. The pathology of total joint arthroplasty. I. Mechanisms of implant fixation. *Skeletal Radiol.* **28**, 423-432 (1999).
6. Ramazanoglu, M. & Oshida, Y. Osseointegration and Bioscience of Implant Surfaces - Current Concepts at Bone-Implant Interface. *Dent. - A Rapidly Evol. Pract.* 57-80 (2011). doi:10.5772/16936
7. Benoit, D. S. W., Schwartz, M. P., Durney, A. R. & Anseth, K. S. Small functional groups for controlled differentiation of hydrogel-encapsulated human mesenchymal stem cells. *Nat. Mater.* **7**, 816-823 (2008).
8. Saha, K. *et al.* Surface-engineered substrates for improved human pluripotent stem cell culture under fully defined conditions. (2011). doi:10.1073/pnas.1114854108/- /DCSupplemental.www.pnas.org/cgi/doi/10.1073/pnas.1114854108
9. Lee, J., Abdeen, A. A., Zhang, D. & Kilian, K. A. Directing stem cell fate on hydrogel substrates by controlling cell geometry, matrix mechanics and adhesion ligand composition. *Biomaterials* **34**, 8140-8 (2013).
10. Engler, A. J., Sen, S., Sweeney, H. L. & Discher, D. E. Matrix Elasticity Directs Stem Cell Lineage Specification. 677-689 (2006). doi:10.1016/j.cell.2006.06.044
11. Anselme, K. Osteoblast adhesion on biomaterials. *Biomaterials* **21**, 667-81 (2000).
12. ANSELME, K. & BIGERELLE, M. Topography effects of pure titanium substrates on human osteoblast long-term adhesion. *Acta Biomater.* **1**, 211-222 (2005).
13. Novaes, A. B. *et al.* Influence of implant surfaces on osseointegration. *Braz. Dent. J.* **21**, 471-481 (2010).
14. Huebsch, N. *et al.* Harnessing traction-mediated manipulation of the cell/matrix interface to control stem-cell fate. *Nat. Mater.* **9**, 518-526 (2010).
15. Khetan, S. *et al.* Degradation-mediated cellular traction directs stem cell fate in covalently crosslinked three-dimensional hydrogels. *Nat. Mater.* **12**, 458-465 (2013).
16. Murphy, W. L., McDevitt, T. C. & Engler, A. J. Materials as stem cell

- regulators. *Nat. Mater.* **13**, 547-557 (2014).
17. Curtis, A. & Wilkinson, C. Topographical control of cells. *Biomaterials* **18**, 1573-1583 (1997).
 18. Kearns, V. R., McMurray, R. J. & Dalby, M. J. Biomaterial surface topography to control cellular response: technologies, cell behaviour and biomedical applications BT - Surface modification of biomaterials: Methods, analysis and applications. *Surf. Modif. Biomater. Methods, Anal. Appl.* 169-201 (2011). at <papers2://publication/uuid/E6F45936-DBCE-4C78-8371-8804A0071254>
 19. McNamara, L. E. *et al.* Nanotopographical Control of Stem Cell Differentiation. *J. Tissue Eng.* **1**, 120623-120623 (2010).
 20. Park, S. & Im, G.-I. Stem cell responses to nanotopography. *J. Biomed. Mater. Res. A* **1-8** (2014). doi:10.1002/jbm.a.35236
 21. C. Vieu, F. Carcenac, A. Pepin, Y. Chen, M. Mejias, A. Lebib, L. Manin-Ferlazzo, L. C. and H. L. Electron beam lithography - Resolution limits and applications. *Appl. Surf. Sci.* **111-117** (2000). doi:10.1016/0167-9317(95)00368-1
 22. Gadegaard, N. *et al.* Arrays of nano-dots for cellular engineering. *Microelectron. Eng.* **68**, 162-168 (2003).
 23. Hanarp, P., Sutherland, D. S., Gold, J. & Kasemo, B. Control of nanoparticle film structure for colloidal lithography. *Colloids Surfaces A Physicochem. Eng. Asp.* **214**, 23-36 (2003).
 24. Denis, F. A., Hanarp, P., Sutherland, D. S. & Dufrene, Y. F. Fabrication of nanostructured polymer surfaces using colloidal lithography and spin-coating. *Nano Lett.* **2**, 1419-1425 (2002).
 25. Krishnamoorthy, S. *et al.* Block copolymer micelles as switchable templates for nanofabrication. *Langmuir* **22**, 3450-2 (2006).
 26. Park, J., Bauer, S., von Der Mark, K. & Schmuki, P. Nanosize and vitality: TiO₂ nanotube diameter directs cell fate. *Nano Lett.* **7**, 1686-91 (2007).
 27. Oh, S. *et al.* Stem cell fate dictated solely by altered nanotube dimension. *Proc. Natl. Acad. Sci. U. S. A.* **106**, 2130-2135 (2009).
 28. Evelyn KF Yim, S. W. P. and K. W. L. Synthetic Nanostructures Inducing Differentiation of Human Mesenchymal Stem Cells into Neuronal Lineage. *Exp cell Res* **313**, 1820-1829 (2007).
 29. Kong, Y. P., Tu, C. H., Donovan, P. J. & Yee, A. F. Expression of Oct4 in human embryonic stem cells is dependent on nanotopographical configuration. *Acta Biomater.* **9**, 6369-80 (2013).
 30. Sjöström, T. *et al.* Fabrication of pillar-like titania nanostructures on titanium and their interactions with human skeletal stem cells. *Acta Biomater.* **5**, 1433-1441 (2009).
 31. Flemming, R. G., Murphy, C. J., Abrams, G. a., Goodman, S. L. & Nealey, P. F. Effects of synthetic micro- and nano-structured surfaces on cell behavior. *Biomaterials* **20**, 573-588 (1999).
 32. Watari, S. *et al.* Modulation of osteogenic differentiation in hMSCs cells by submicron topographically-patterned ridges and grooves. *Biomaterials* **33**, 128-136 (2012).
 33. Li, W. J., Laurencin, C. T., Caterson, E. J., Tuan, R. S. & Ko, F. K. Electrospun nanofibrous structure: A novel scaffold for tissue engineering. *J. Biomed. Mater. Res.* **60**, 613-621 (2002).
 34. Jang, J. H., Castano, O. & Kim, H. W. Electrospun materials as potential

- platforms for bone tissue engineering. *Adv. Drug Deliv. Rev.* **61**, 1065-1083 (2009).
35. Dalby, M. J. *et al.* The control of human mesenchymal cell differentiation using nanoscale symmetry and disorder. *Nat. Mater.* **6**, 997-1003 (2007).
 36. McMurray, R. J. *et al.* Nanoscale surfaces for the long-term maintenance of mesenchymal stem cell phenotype and multipotency. *Nat. Mater.* **10**, 637-644 (2011).
 37. Curran, J. M. *et al.* Introducing dip pen nanolithography as a tool for controlling stem cell behaviour: unlocking the potential of the next generation of smart materials in regenerative medicine. *Lab Chip* **10**, 1662 (2010).
 38. Curran, J. M., Chen, R. & Hunt, J. A. Controlling the phenotype and function of mesenchymal stem cells in vitro by adhesion to silane-modified clean glass surfaces. *Biomaterials* **26**, 7057-67 (2005).
 39. Curran, J. M., Chen, R. & Hunt, J. A. The guidance of human mesenchymal stem cell differentiation in vitro by controlled modifications to the cell substrate. *Biomaterials* **27**, 4783-93 (2006).
 40. Ren, Y.-J. *et al.* In vitro behavior of neural stem cells in response to different chemical functional groups. *Biomaterials* **30**, 1036-44 (2009).
 41. Dalby, M. J., Gadegaard, N. & Oreffo, R. O. C. Harnessing nanotopography and integrin-matrix interactions to influence stem cell fate. *Nat. Mater.* **13**, 558-69 (2014).
 42. M, C. A. and B. CULTIVATION IN VITRO OF MALIGNANT TUMORS. *J Exp Med* **12**, 571-5 (1911).
 43. Dunn, G. a & Brown, a F. Alignment of fibroblasts on grooved surfaces described by a simple geometric transformation. *J. Cell Sci.* **83**, 313-340 (1986).
 44. Clark, P., Connolly, P., Curtis, a S., Dow, J. a & Wilkinson, C. D. Topographical control of cell behaviour. I. Simple step cues. *Development* **99**, 439-448 (1987).
 45. Clarke, P. & Connolly, P. Topographical control of cell behaviour : 2. Multiple grooved substrata. **644**, 635-644 (1990).
 46. Clark, P., Connolly, P., Curtis, a S., Dow, J. a & Wilkinson, C. D. Cell guidance by ultrafine topography in vitro. *J. Cell Sci.* **99** (Pt 1), 73-77 (1991).
 47. Curtis, a S. & Varde, M. Control of Cell Behavior: Topological Factors. *J. Natl. Cancer Inst.* **33**, 15-26 (1964).
 48. Dalby, M. J., Riehle, M. O., Yarwood, S. J., Wilkinson, C. D. W. & Curtis, A. S. G. Nucleus alignment and cell signaling in fibroblasts: Response to a micro-grooved topography. *Exp. Cell Res.* **284**, 274-282 (2003).
 49. Wójciak-Stothard, B., Madeja, Z., Korohoda, W., Curtis, a & Wilkinson, C. Activation of macrophage-like cells by multiple grooved substrata. Topographical control of cell behaviour. *Cell Biol. Int.* **19**, 485-490 (1995).
 50. Rovinsky Yu. A. & Samoilov, V. I. Morphogenetic response of cultured normal and transformed fibroblasts, and epitheliocytes, to a cylindrical substratum surface. Possible role for the actin filament bundle pattern. *J. Cell Sci.* **107**, 1255-63 (1994).
 51. Curtis, Adam S G and Seehar, G. M. The control of cell division by tension or diffusion. *Nature* 52-53 (1978).
 52. Tsuruma, A., Tanaka, M., Yamamoto, S. & Shimomura, M. Control of neural

- stem cell differentiation on honeycomb films. *Colloids Surfaces A Physicochem. Eng. Asp.* **313-314**, 536-540 (2008).
53. Sanford K K, E. W. E. and L. G. D. The growth in vitro of single isolated tissue cells. *J Natl Cancer Inst* 229-246 (1948).
 54. Aebischer, P., Guénard, V. & Valentini, R. F. The morphology of regenerating peripheral nerves is modulated by the surface microgeometry of polymeric guidance channels. *Brain Res.* **531**, 211-218 (1990).
 55. Dalby, M. J., Riehle, M. O., Johnstone, H., Affrossman, S. & Curtis, A. S. G. Investigating the limits of filopodial sensing: a brief report using SEM to image the interaction between 10 nm high nano-topography and fibroblast filopodia. *Cell Biol. Int.* **28**, 229-36 (2004).
 56. Wilkinson, C. D. W., Riehle, M., Wood, M., Gallagher, J. & Curtis, a. S. G. The use of materials patterned on a nano- and micro-metric scale in cellular engineering. *Mater. Sci. Eng. C* **19**, 263-269 (2002).
 57. Gadegaard, N., Mosler, S. & Larsen, N. B. Biomimetic Polymer Nanostructures by Injection Molding. *Macromol. Mater. Eng.* **288**, 76-83 (2003).
 58. Gandhimathi, C. *et al.* Mimicking Nanofibrous Hybrid Bone Substitute for Mesenchymal Stem Cells Differentiation into Osteogenesis. *Macromol. Biosci.* **13**, 696-706 (2013).
 59. Zouani, O. F. *et al.* Altered nanofeature size dictates stem cell differentiation. *J. Cell Sci.* **125**, 1217-1224 (2012).
 60. Kingham, E., White, K., Gadegaard, N., Dalby, M. J. & Oreffo, R. O. C. Nanotopographical Cues Augment Mesenchymal Differentiation of Human Embryonic Stem Cells. *Small* 1-12 (2013). doi:10.1002/smll.201202340
 61. Dang, J. M. & Leong, K. W. Myogenic induction of aligned mesenchymal stem cell sheets by culture on thermally responsive electrospun nanofibers. *Adv. Mater.* **19**, 2775-2779 (2007).
 62. Li, W.-J. *et al.* A three-dimensional nanofibrous scaffold for cartilage tissue engineering using human mesenchymal stem cells. *Biomaterials* **26**, 599-609 (2005).
 63. Stormonth-Darling, J. M. Fabrication of difficult nanostructures by injection moulding. (2013). at <<http://theses.gla.ac.uk/4456/1/2013stormonth-darlingphd.pdf>>
 64. Kurtz, S. M. & Devine, J. N. PEEK biomaterials in trauma, orthopedic, and spinal implants. *Biomaterials* **28**, 4845-69 (2007).
 65. Sagomonyants, K. B., Jarman-Smith, M. L., Devine, J. N., Aronow, M. S. & Gronowicz, G. a. The in vitro response of human osteoblasts to polyetheretherketone (PEEK) substrates compared to commercially pure titanium. *Biomaterials* **29**, 1563-1572 (2008).
 66. Ponnappan, R. K. *et al.* Biomechanical evaluation and comparison of polyetheretherketone rod system to traditional titanium rod fixation. *Spine J.* **9**, 263-267 (2009).
 67. Green, S. in *PEEK Handbook 1st ed* 23-48 (2012).
 68. Schröder, K. *et al.* Similarities between Plasma Amino Functionalized PEEK and Titanium Surfaces Concerning Enhancement of Osteoblast Cell Adhesion. *J. Adhes. Sci. Technol.* **24**, 905-923 (2010).
 69. Skinner, H. B. Composite technology for total hip arthroplasty. *Clin. Orthop. Relat. Res.* 224-36 (1988). at <<http://www.ncbi.nlm.nih.gov/pubmed/3416528>>

70. Morrison, C. *et al.* In vitro biocompatibility testing of polymers for orthopaedic implants using cultured fibroblasts and osteoblasts. *Biomaterials* **16**, 987-992 (1995).
71. Katzer, a, Marquardt, H., Westendorf, J., Wening, J. V & von Foerster, G. Polyetheretherketone--cytotoxicity and mutagenicity in vitro. *Biomaterials* **23**, 1749-1759 (2002).
72. Wenz, L. M., Merritt, K., Brown, S. a, Moet, a & Steffee, a D. In vitro biocompatibility of polyetheretherketone and polysulfone composites. *J. Biomed. Mater. Res.* **24**, 207-215 (1990).
73. Lin, T. W., Corvelli, A. A., Frondoza, C. G., Roberts, J. C. & Hungerford, D. S. Glass peek composite promotes proliferation and osteocalcin production of human osteoblastic cells. *J. Biomed. Mater. Res.* **36**, 37-144 (1997).
74. Hunter, a., Archer, C. W., Walker, P. S. & Blunn, G. W. Attachment and proliferation of osteoblasts and fibroblasts on biomaterials for orthopaedic use. *Biomaterials* **16**, 287-295 (1995).
75. Petillo, O. *et al.* In vivo induction of macrophage Ia antigen (MHC class II) expression by biomedical polymers in the cage implant system. *J. Biomed. Mater. Res.* **28**, 635-646 (1994).
76. Poulsson, A. H. C. *et al.* Osseointegration of machined, injection moulded and oxygen plasma modified PEEK implants in a sheep model. *Biomaterials* **35**, 3717-3728 (2014).
77. Kulkarni, A. G., Hee, H. T. & Wong, H. K. Solis cage (PEEK) for anterior cervical fusion: preliminary radiological results with emphasis on fusion and subsidence. *Spine J.* **7**, 205-209 (2007).
78. Camarini, E. T., Tomeh, J. K., Dias, R. R. & da Silva, E. J. Reconstruction of frontal bone using specific implant polyether-ether-ketone. *J Craniofac Surg* **22**, 2205-7 (2011).
79. Brantigan John W, McAfee Paul C, Cunningham Bryan W, W. H. and O. C. M. INTERBODY LUMBAR FUSION USING A CARBON-FIBER CAGE IMPLANT VERSUS ALLOGRAFT BONE. *Spine J.* **19**, 1436-1444 (1994).
80. Videbaek, T. S. *et al.* Circumferential fusion improves outcome in comparison with instrumented posterolateral fusion: long-term results of a randomized clinical trial. *Spine (Phila. Pa. 1976).* **31**, 2875-2880 (2006).
81. Rivard, C. H., Rhalmi, S. & Coillard, C. In vivo biocompatibility testing of peek polymer for a spinal implant system: A study in rabbits. *J. Biomed. Mater. Res.* **62**, 488-498 (2002).
82. Brennan, W. J. Investigation of the ageing of plasma oxidized PEEK. *Polymer (Guildf).* **32**, 1527-1530 (1991).
83. Toth, J. M. *et al.* Polyetheretherketone as a biomaterial for spinal applications. *Biomaterials* **27**, 324-334 (2006).
84. Awaja, F., Bax, D. V., Zhang, S., James, N. & McKenzie, D. R. Cell adhesion to PEEK treated by plasma immersion ion implantation and deposition for active medical implants. *Plasma Process. Polym.* **9**, 355-362 (2012).
85. Poulsson AHC, R. R. in *PEEK Handbook 1st ed* 145-62 (2012).
86. Abu Bakar, M. S. *et al.* Tensile properties, tension-tension fatigue and biological response of polyetheretherketone-hydroxyapatite composites for load-bearing orthopedic implants. *Biomaterials* **24**, 2245-2250 (2003).
87. Wong, K. L. *et al.* Mechanical properties and in vitro response of strontium-containing hydroxyapatite/polyetheretherketone composites. *Biomaterials* **30**, 3810-3817 (2009).

88. Lee, J. H. *et al.* In vitro and in vivo evaluation of the bioactivity of hydroxyapatite-coated polyetheretherketone biocomposites created by cold spray technology. *Acta Biomater.* **9**, 6177-6187 (2013).
89. Briem, D. *et al.* Response of primary fibroblasts and osteoblasts to plasma treated polyetheretherketone (PEEK) surfaces. *J. Mater. Sci. Mater. Med.* **16**, 671-677 (2005).
90. Khoury, J. *et al.* Neutral atom beam technique enhances bioactivity of PEEK. *Nucl. Instruments Methods Phys. Res. Sect. B Beam Interact. with Mater. Atoms* **307**, 630-634 (2013).
91. Yao, C., Storey, D. & Webster, T. J. Nanostructured metal coatings on polymers increase osteoblast attachment. *Int. J. Nanomedicine* **2**, 487-492 (2007).
92. Han, C.-M. *et al.* The electron beam deposition of titanium on polyetheretherketone (PEEK) and the resulting enhanced biological properties. *Biomaterials* **31**, 3465-70 (2010).
93. Rust-dawicki, A. M. & Cook, S. D. Preliminary Evaluation of Titanium-Coated PEEK Implants. 75-77 (1995).
94. Barkarmo, S. *et al.* Nano-hydroxyapatite-coated PEEK implants: A pilot study in rabbit bone. *J. Biomed. Mater. Res. - Part A* **101 A**, 465-471 (2013).
95. Oliveira, R. R. L. De, Albuquerque, D. A. C. & Cruz, T. G. S. Measurement of the Nanoscale Roughness by Atomic Force Microscopy : Basic Principles and Applications.
96. Chu, P. Plasma-surface modification of biomaterials. *Mater. Sci. Eng. R Reports* **36**, 143-206 (2002).
97. Briem, D. *et al.* Response of primary fibroblasts and osteoblasts to plasma treated polyetheretherketone (PEEK) surfaces. *J. Mater. Sci. Mater. Med.* **16**, 671-7 (2005).
98. Czekanska, E. M., Stoddart, M. J., Richards, R. G. & Hayes, J. S. In search of an osteoblast cell model for in vitro research. *Eur. Cells Mater.* **24**, 1-17 (2012).
99. Czekanska, E. M., Stoddart, M. J., Ralphs, J. R., Richards, R. G. & Hayes, J. S. A phenotypic comparison of osteoblast cell lines versus human primary osteoblasts for biomaterials testing. *J. Biomed. Mater. Res. Part A* **102**, 2636-2643 (2014).
100. Jäger, M., Zilkens, C., Zanger, K. & Krauspe, R. Significance of nano- and microtopography for cell-surface interactions in orthopaedic implants. *J. Biomed. Biotechnol.* **2007**, 69036 (2007).
101. Marco, F., Milena, F., Gianluca, G. & Vittoria, O. Peri-implant osteogenesis in health and osteoporosis. *Micron* **36**, 630-44 (2005).
102. Bonewald, L. F. *et al.* von Kossa staining alone is not sufficient to confirm that mineralization in vitro represents bone formation. *Calcif. Tissue Int.* **72**, 537-47 (2003).
103. Lian, J. B. & Stein, G. S. in *Oral Biology & Medicine Concepts of Osteoblast Growth and Differentiation : Basis for Modulation of Bone Cell Development and Tissue Formation.* (1992). doi:10.1177/10454411920030030501
104. Kasemo, B. Biological surface science. *Surf. Sci.* **500**, 656-677 (2002).
105. Albert H. Coons, H. J. C. and R. N. J. Immunological Properties of an Antibody Containing a Fluorescent Group. *Proc Soc Exp Biol Med* **47**, 200-202 (1941).

106. Kaplan, A. H. C. and M. H. Localization of Antigen in Tissue Cells. *J. exp med* (1950).
107. Robinson, J. P., Bs, J. S. & Kumar, G. L. Chapter 10 | Immunofluorescence. 61-65
108. Hunter, a, Archer, C. W., Walker, P. S. & Blunn, G. W. Attachment and proliferation of osteoblasts and fibroblasts on biomaterials for orthopaedic use. *Biomaterials* **16**, 287-95 (1995).
109. Brandtzaeg, P. The increasing power of immunohistochemistry and immunocytochemistry. *J. Immunol. Methods* **216**, 49-67 (1998).